Application of Plasma Phenomena

Po-Yu Chang

Institute of Space and Plasma Sciences, National Cheng Kung University

Lecture 5

2024 spring semester

Tuesday 9:10-12:00

Materials:

https://capst.ncku.edu.tw/PGS/index.php/teaching/

Online courses:

https://nckucc.webex.com/nckucc/j.php?MTID=m4082f23c59af0571015416f6e58dd803

2024/3/25 updated

Plasma was generated during the starship re-entry

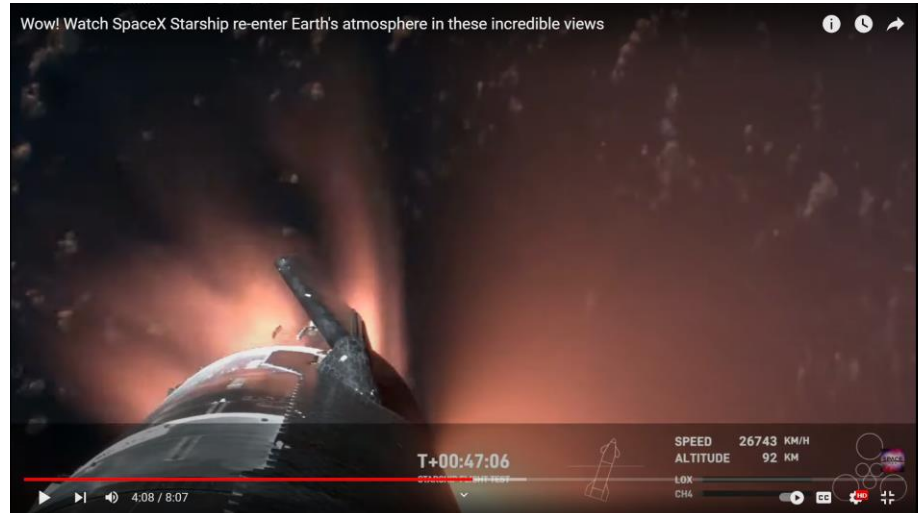

https://www.youtube.com/watch?v=PQfkvC6RASA

AC electrical discharges deliver energy to the plasma without contact between electrodes and the plasma

- **DC electrical discharge – a true current in the form of a flow of ions or electrons to the electrodes.**
- **AC electrical discharge – the power supply interacts with the plasma by displacement current.**
  - **Inductive radio frequency (RF) electrical discharges**
  - **Capacitive RF electrical discharges**
  - **Microwave electrical discharges**
  - **Dielectric-barrier discharges (DBDs)**
- **Other mechanism**
  - **Laser produced plasma**
  - **Pulsed-power generated plasma – it will be introduced later.**

RF can interact with plasma inductively or capacitively

Capacitively coupled

planar

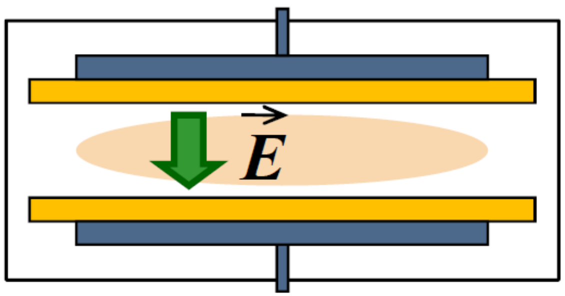

coaxial

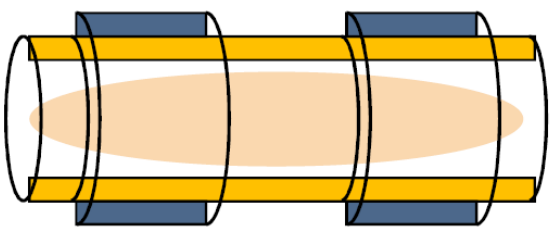

Inductively coupled

coaxial

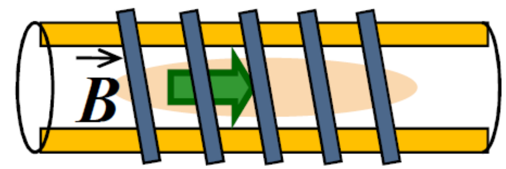

coil

spiral

planar

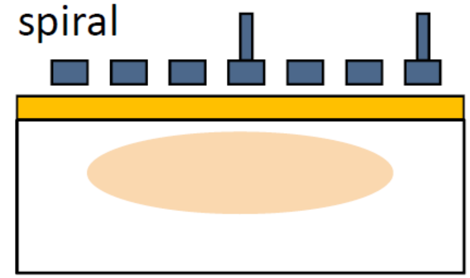

The plasma is generated by the induced electric field from the oscillating magnetic field

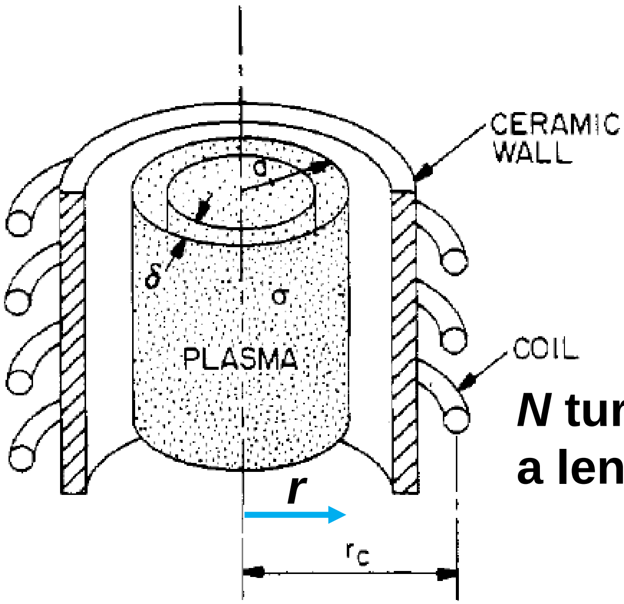

N **turn within a length of *l***

$$\nabla \times \vec{E} = -\frac{\partial \vec{B}}{\partial t}$$

$$\int (\nabla \times \vec{E})\, d\vec{A} = \int \left(-\frac{\partial \vec{B}}{\partial t}\right) d\vec{A}$$

$$2\pi r E = -\pi r^2 \frac{\partial B}{\partial t}$$

$$E = -\frac{r}{2}\frac{\partial B}{\partial t}$$

$$B \times l = \mu_o N I$$

$$E = -\frac{r}{2}\mu_o \frac{N}{l}\frac{\partial I}{\partial t}$$

$$|E| = \frac{r}{2}\mu_o \frac{N}{l}\omega I$$

RF energy is strongly absorbed within the skin depth if the frequency is below the electron plasma frequency

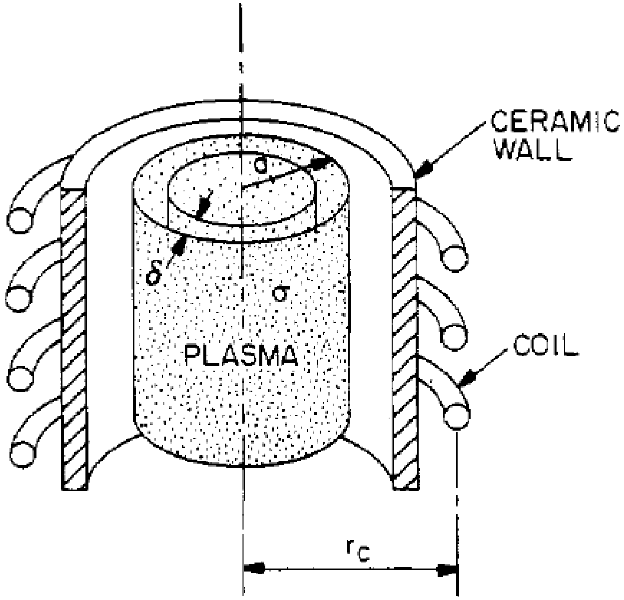

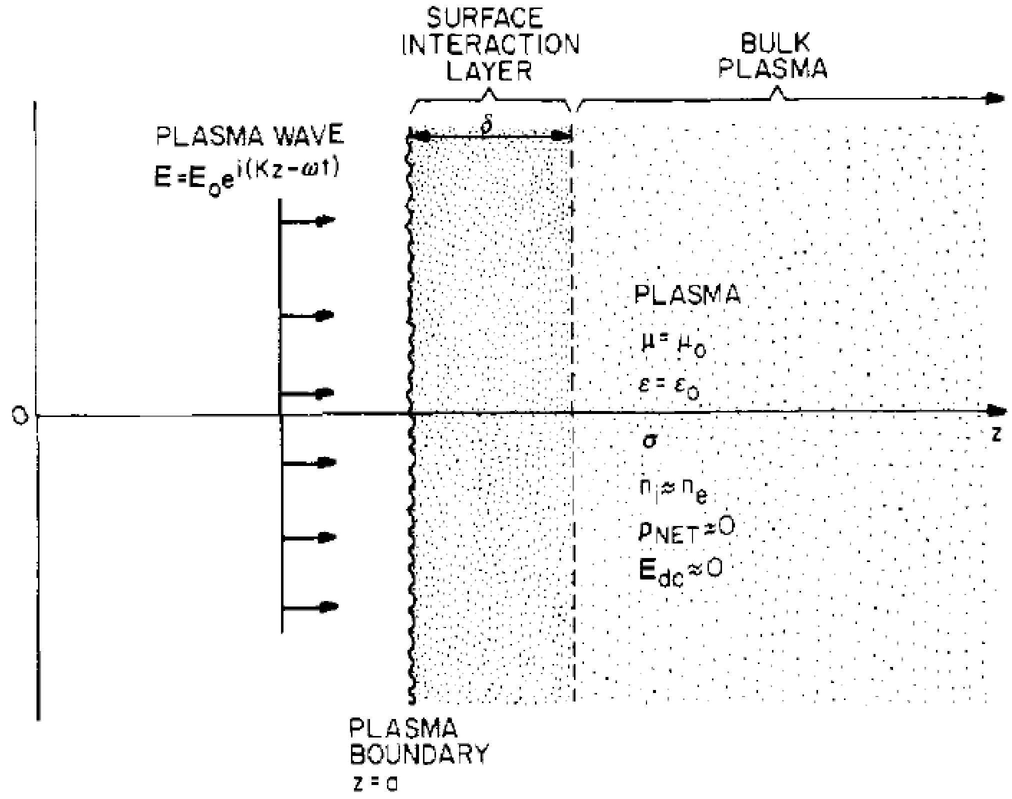

Capacitive RF coupling plasma without magnetic fields

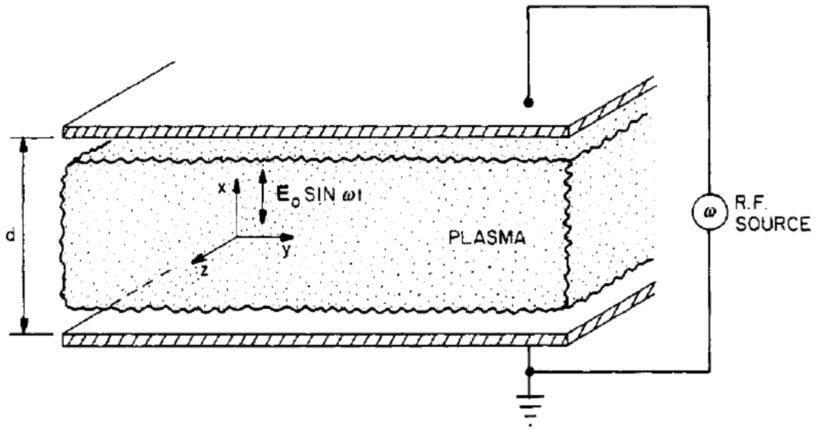

$$\vec{F} = m\,\vec{a} = -\nu_c m\,\vec{v} - e\,\vec{E}$$

$$m\frac{\mathrm{d}v_y}{\mathrm{dt}} + m\nu_c v_y = 0$$

$$v_y(t) = v_{y0}\exp(-\nu_c t)$$

$$m\frac{d^2x}{\mathrm{dt}^2} + m\nu_c\frac{dx}{\mathrm{dt}} = eE_0\sin(\omega t)$$

$$x = C_1\sin(\omega t) + C_2\cos(\omega t)$$

$$C_1 = -\frac{eE_0}{m}\frac{1}{\omega^2 + {\nu_c}^2}$$

$$C_2 = -\frac{\nu_c eE_0}{\omega m}\frac{1}{\omega^2 + {\nu_c}^2}$$

$$v_x(t) = -\frac{eE_0\omega}{m(\omega^2 + {\nu_c}^2)}\left[\cos(\omega t) - \frac{\nu_c}{\omega}\sin(\omega t)\right]$$

$$P = \frac{dW}{dt} = \mathrm{e}\mathrm{E}_0\sin(\omega t)v_x$$

$$\bar{P}_{\mathrm{tot}} = n_e\bar{P} = \frac{1}{4}\epsilon_0{E_0}^2\frac{2n_e e^2}{m\epsilon_0}\frac{\nu_c}{\omega^2 + {\nu_c}^2}$$

Empirical scaling of electrode voltage drop

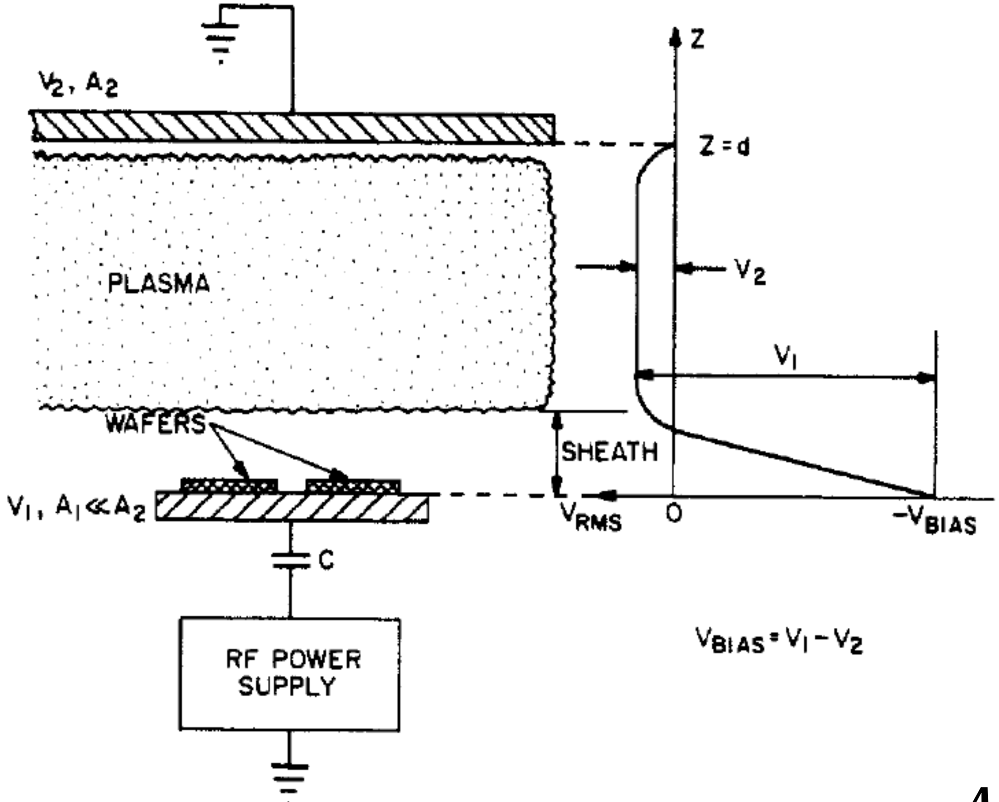

$$I_1 = A_1 J_1 = A_1 e n_{i1} \overline{v}_{i1}$$

$$I_2 = A_2 J_2 = A_2 e n_{i2} \overline{v}_{i2}$$

$$\overline{v}_{i1} = \sqrt{\left(\frac{2eV_1}{m_i}\right)}$$

$$\overline{v}_{i2} = \sqrt{\left(\frac{2eV_2}{m_i}\right)}$$

Assuming: $I_1 = I_2 \quad n_{i1} = n_{i2}$

$$A_1 e n_{i1} \sqrt{\left(\frac{2eV_1}{m_i}\right)} = A_2 e n_{i2} \sqrt{\left(\frac{2eV_2}{m_i}\right)}$$

$$\frac{V_1}{V_2} = \left(\frac{A_2}{A_1}\right)^2$$

$$\frac{V_1}{V_2} = \left(\frac{A_2}{A_1}\right)^q \text{ where } 1.0 \leq q \leq 2.5$$

Example of capacitively coupled RF plasma source 2

- **Plane parallel reactor**

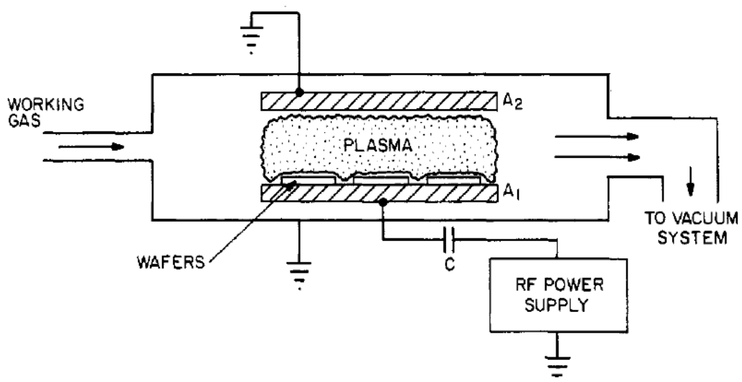

- **Multiple electrode system**

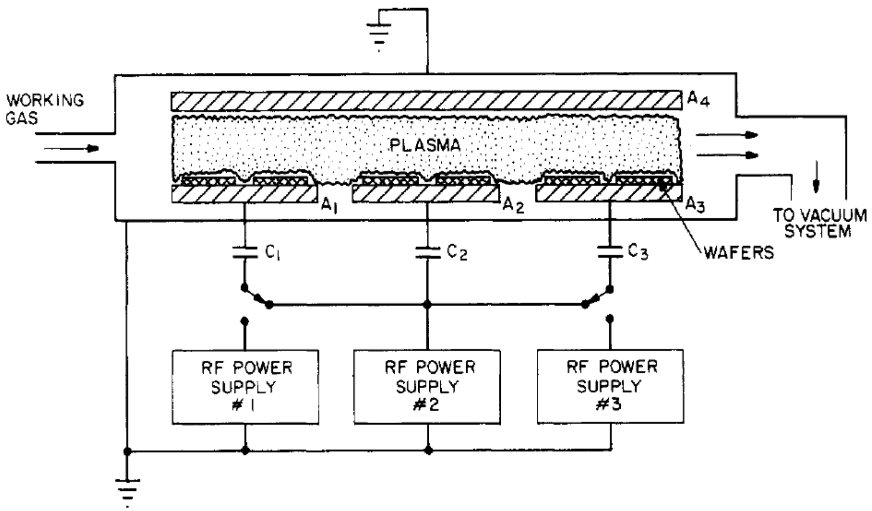

AC electrical discharges deliver energy to the plasma without contact between electrodes and the plasma

- DC electrical discharge – a true current in the form of a flow of ions or electrons to the electrodes.
- AC electrical discharge – the power supply interacts with the plasma by displacement current.
  - Inductive radio frequency (RF) electrical discharges
  - Capacitive RF electrical discharges
  - **Microwave electrical discharges**
  - Dielectric-barrier discharges (DBDs)
- Other mechanism
  - Laser produced plasma
  - Pulsed-power generated plasma

Advantage of using microwave electrical discharges

- The wavelength of the microwave is in centimeters range. In contract, the wavelength is 22 m for RF frequency f = 13.6 MHz.
- The electron number density can approach the critical number density. (7×10^{16} m^{-3}) at a frequency of 2.45 GHz.
- The plasma in microwave discharges is quasi-optical to microwave.
- Microwave-generated plasmas have a higher electron kinetic temperature (5 ~ 15 eV) than DC or low frequency RF-generated plasmas (1 or 2 eV).
- Capable of providing a higher fraction of ionization.
- Do not have a high voltage sheath.
- No internal electrodes.

Microwave frequency is determined for those used in communications and radar purposes

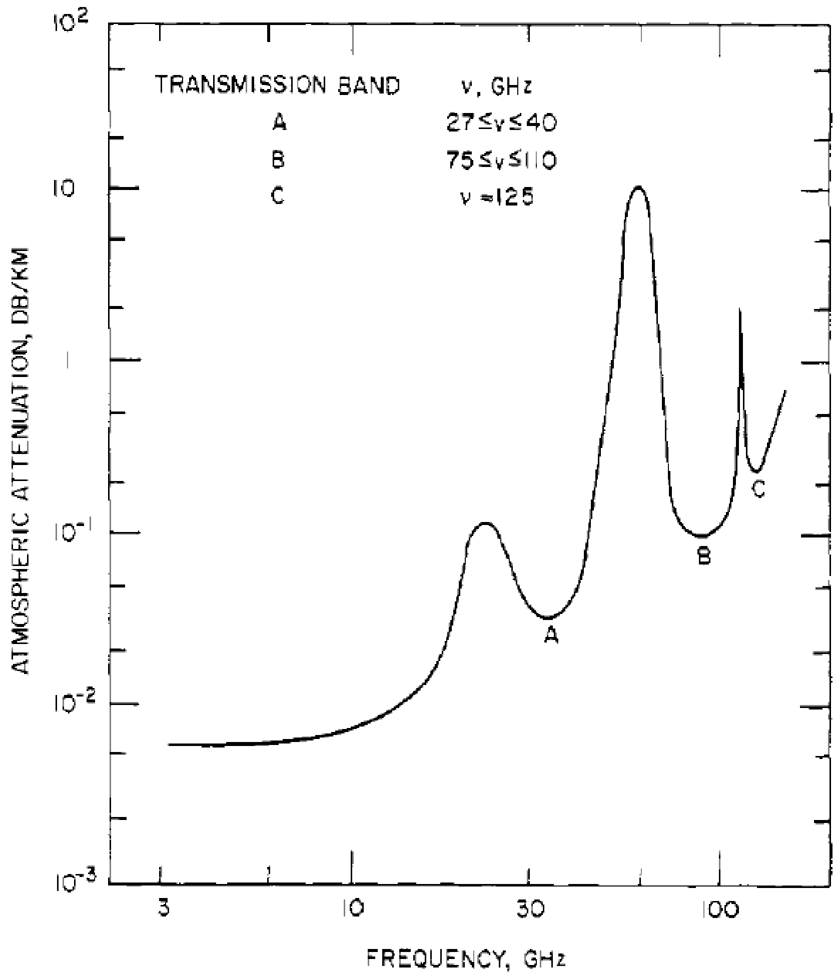

Internal of a magnetron

$$\omega_{\mathrm{LC}} = \frac{1}{\sqrt{LC}} \equiv 4\omega_{\mathrm{ce}}$$

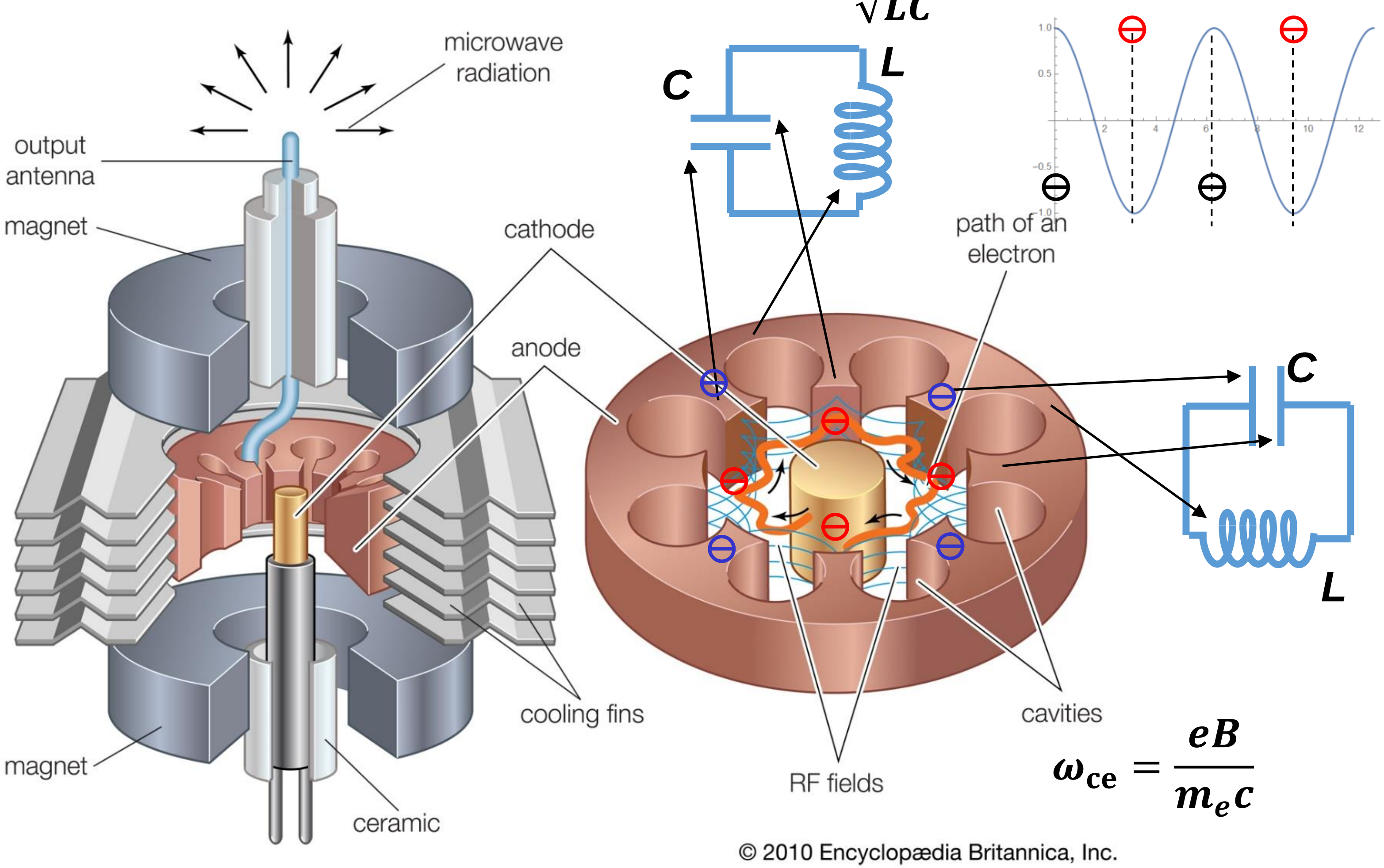

$$\omega_{\mathrm{ce}} = \frac{eB}{m_e c}$$

https://kids.britannica.com/students/article/electron-tube/106024/media?assemblyId=137

Internal of a magnetron

$$\omega_{LC} = \frac{1}{\sqrt{LC}} \equiv 4\omega_{ce}$$

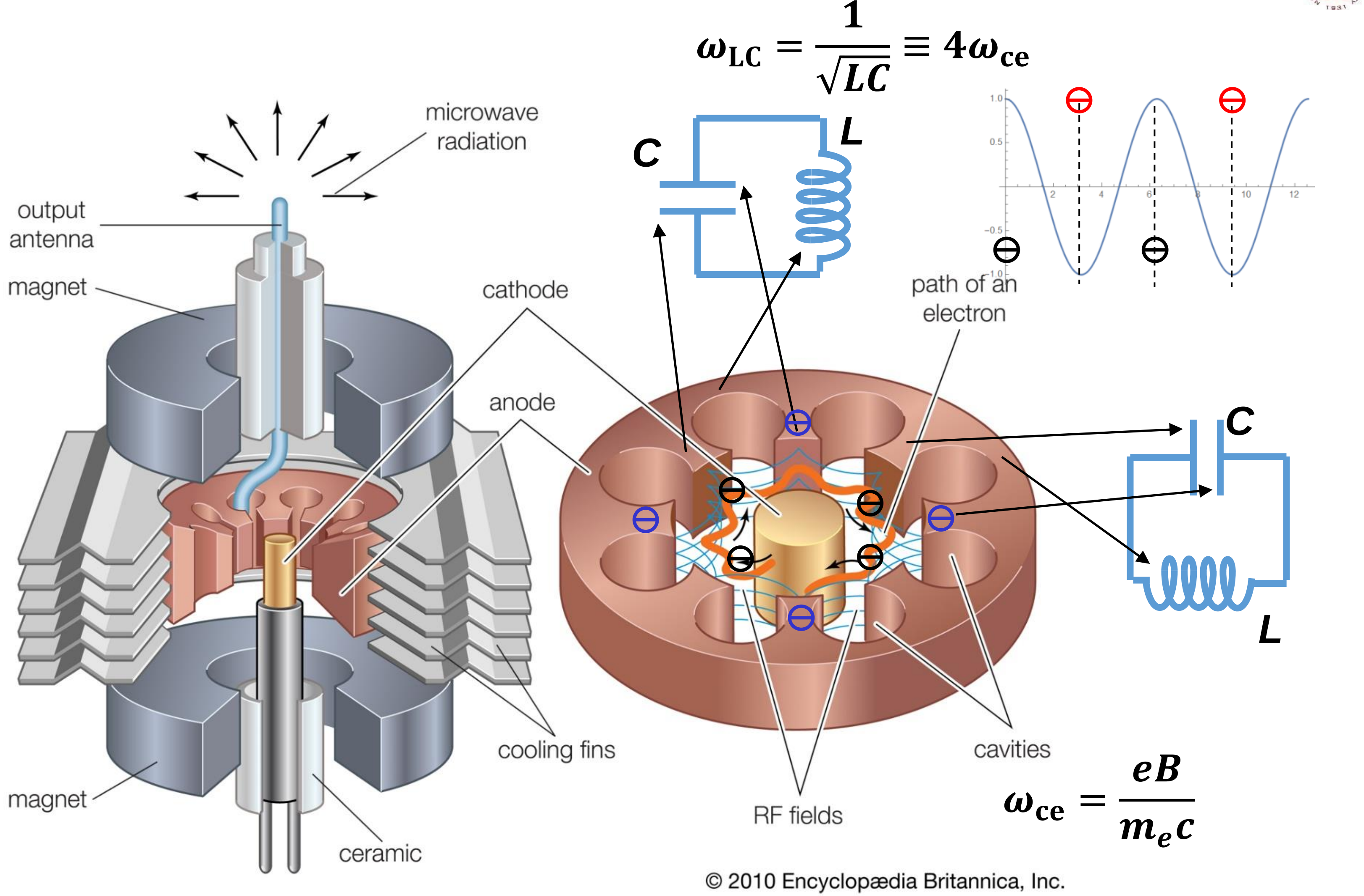

$$\omega_{ce} = \frac{eB}{m_e c}$$

https://kids.britannica.com/students/article/electron-tube/106024/media?assemblyId=137

Resonance in a magnetron

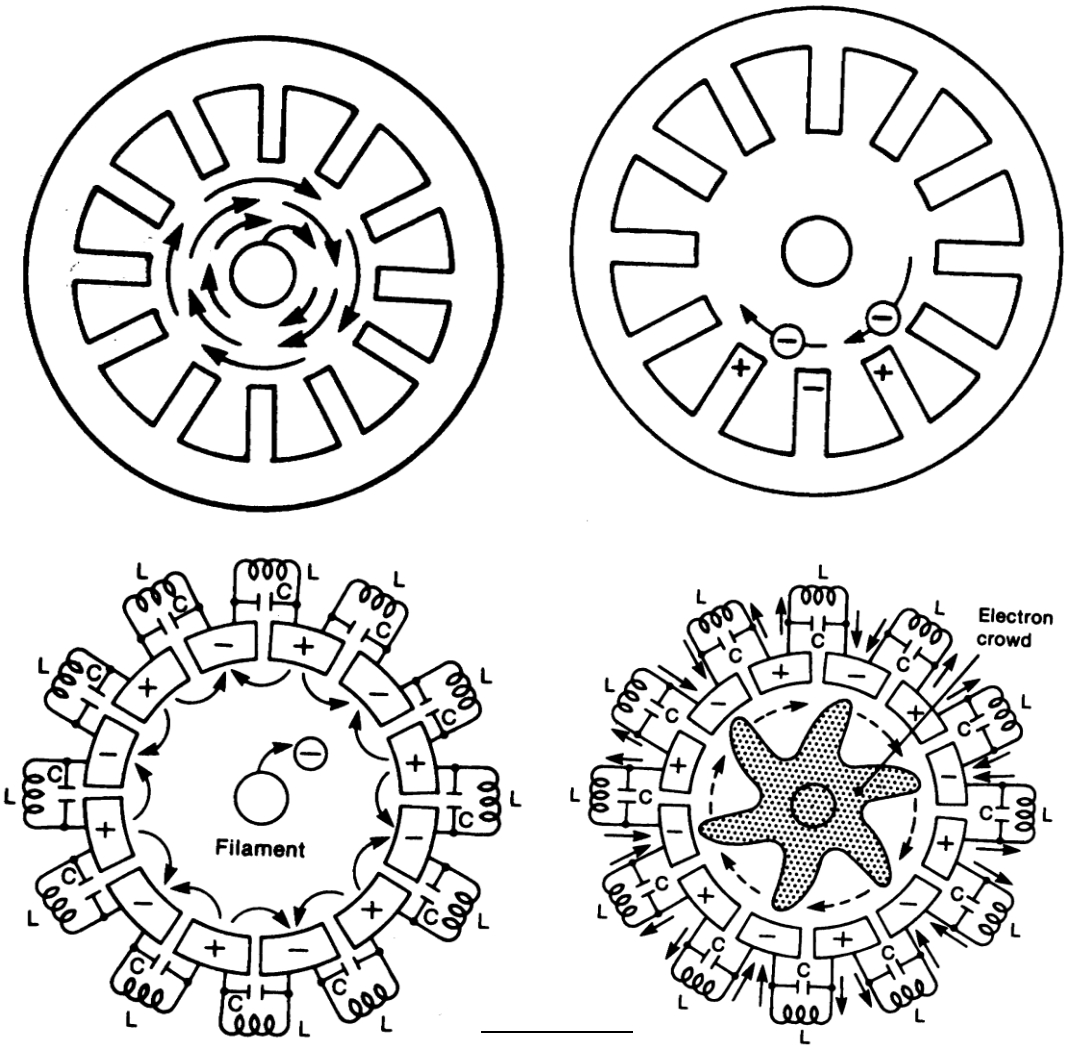

http://cdn.preterhuman.net/texts/government_information/intelligence_and_espionage/homebrew.military.and.espionage.electronics/servv89pn0aj.sn.sourcedns.com/_gbpprorg/mil/herf1/index.html

Magnetron schematic diagram

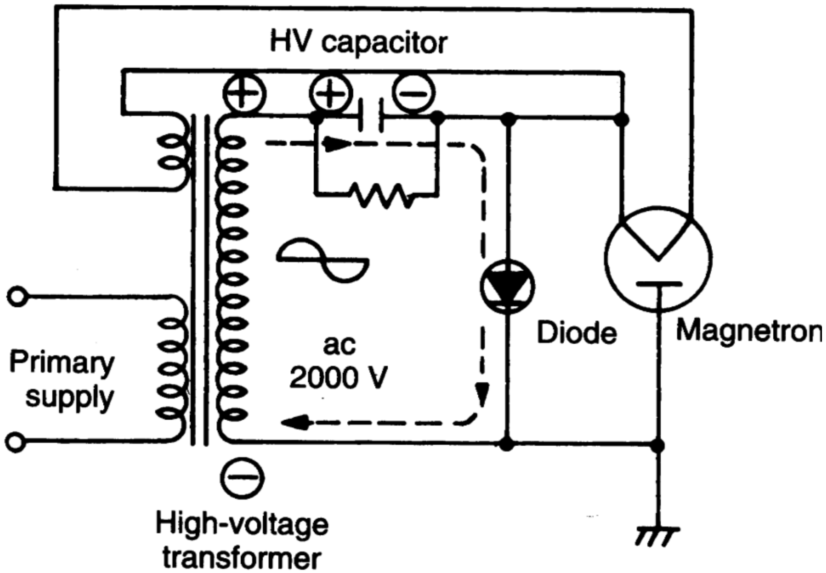

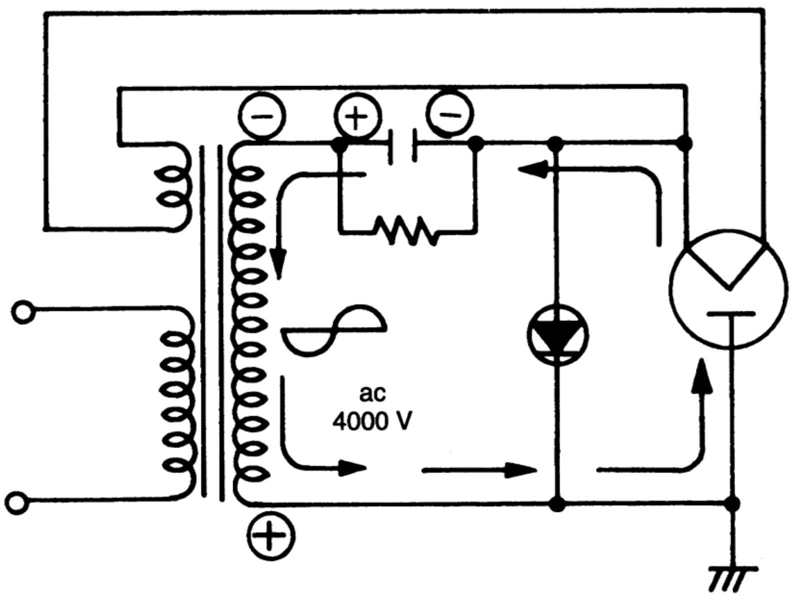

http://cdn.preterhuman.net/texts/government_information/intelligence_and_espionage/homebrew.military.and.espionage.electronics/servv89pn0aj.sn.sourcedns.com/_gbpprorg/mil/herf1/index.html

Strong absorption occurs when the frequency matches the electron cyclotron frequency

- **Electron cyclotron resonance (ECR) plasma reactor**

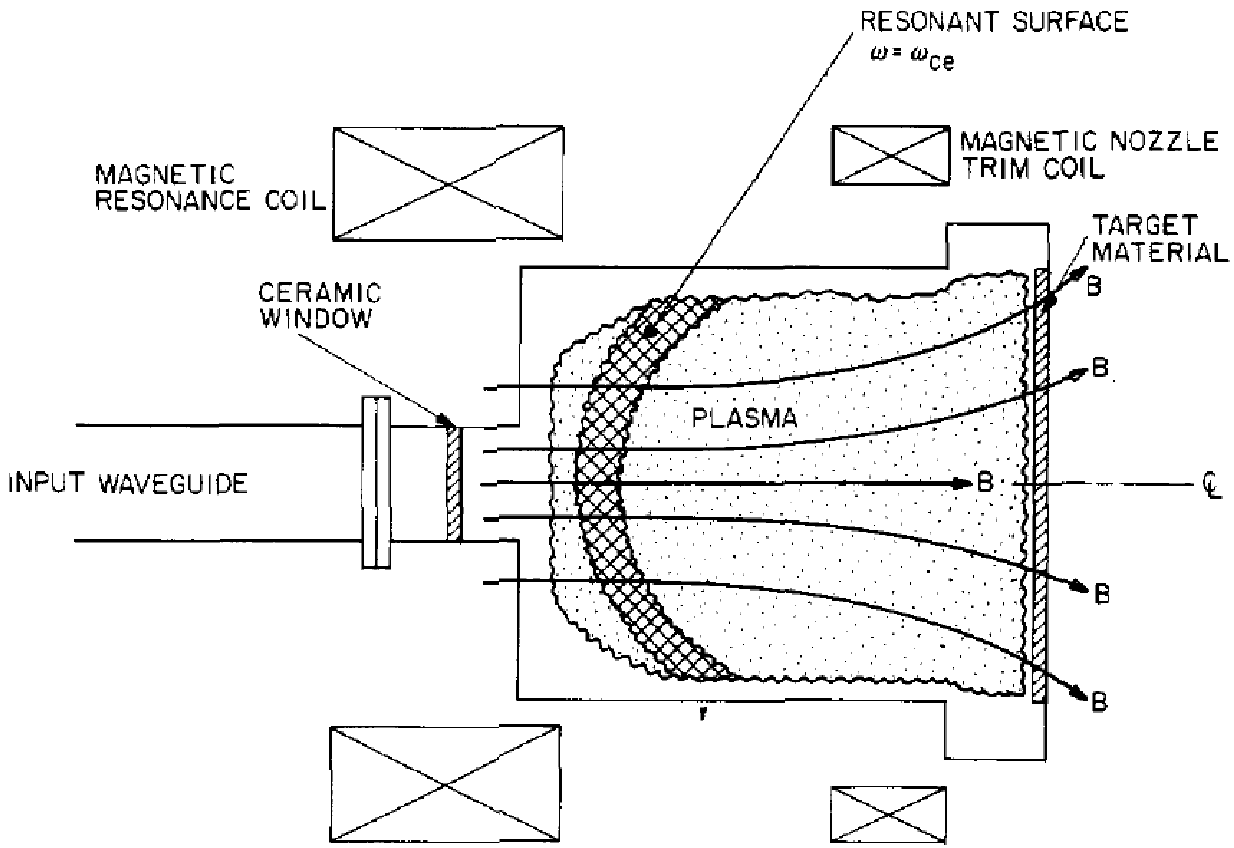

Electron cyclotron frequency depends on magnetic field only

$$m_e \frac{d\vec{v}}{\mathrm{dt}} = -\frac{e}{c}\,\vec{v} \times \vec{B}$$

- Assuming $\vec{B} = B\hat{z}$ and the electron oscillates in x-y plane

$$m_e \dot{v}_x = -\frac{e}{c} B v_y \qquad m_e \dot{v}_z = 0$$

$$m_e \dot{v}_y = \frac{e}{c} B v_x$$

$$\ddot{v}_x = -\frac{eB}{m_e c}\dot{v}_y = -\left(\frac{eB}{m_e c}\right)^2 v_x$$

$$\ddot{v}_y = -\frac{eB}{m_e c}\dot{v}_x = -\left(\frac{eB}{m_e c}\right)^2 v_y$$

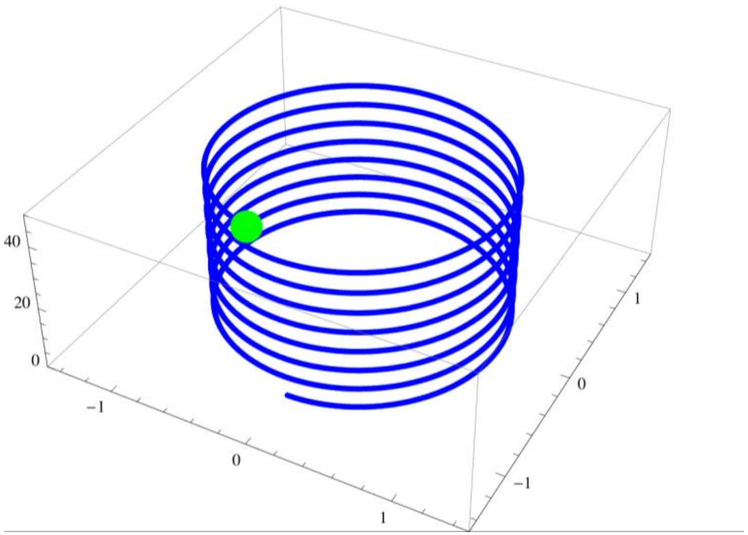

- Therefore

$$\omega_{\mathrm{ce}} = \frac{eB}{m_e c}$$

Electrons keep getting accelerated when a electric field rotates in electron's gyrofrequency

$$m_e \frac{d\vec{v}}{dt} = -\frac{e}{c}\vec{v}\times\vec{B} - e\vec{E} \qquad \vec{B} = B_0\hat{z} \qquad \vec{E} = E_0[\hat{x}\cos(\omega t) + \hat{y}\sin(\omega t)]$$

$$m_e\dot{v}_x = -\frac{e}{c}Bv_y + E_0\cos(\omega t) \qquad m_e\dot{v}_y = \frac{e}{c}Bv_x + E_0\cos(\omega t) \qquad m_e\dot{v}_z = 0$$

$$\ddot{v}_x = -\frac{eB}{m_e c}\dot{v}_y - \frac{E_0}{m_e}\omega\cos(\omega t) = -\omega_{ce}{}^2 v_x - \frac{E_0}{m_e}(\omega_{ce}+\omega)\cos(\omega t)$$

$$\ddot{v}_y = -\frac{eB}{m_e c}\dot{v}_x + \frac{E_0}{m_e}\omega\sin(\omega t) = -\omega_{ce}{}^2 v_y + \frac{E_0}{m_e}(\omega_{ce}+\omega)\sin(\omega t)$$

$$\omega_{ce} = \frac{eB}{m_e c}$$

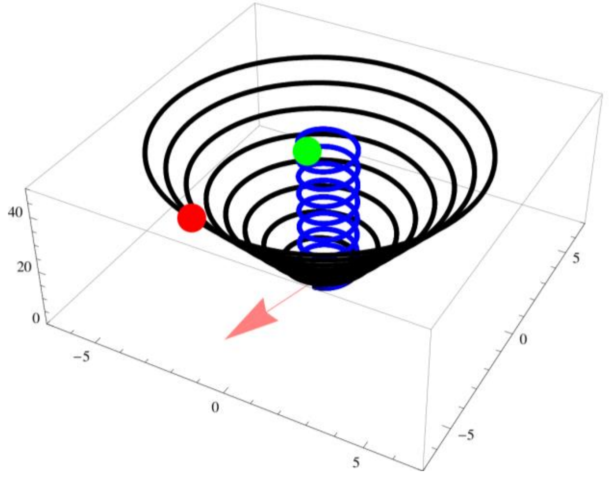

Electric field in a circular polarized electromagnetic wave keeps rotating as the wave propagates

- **Right-handed polarization**

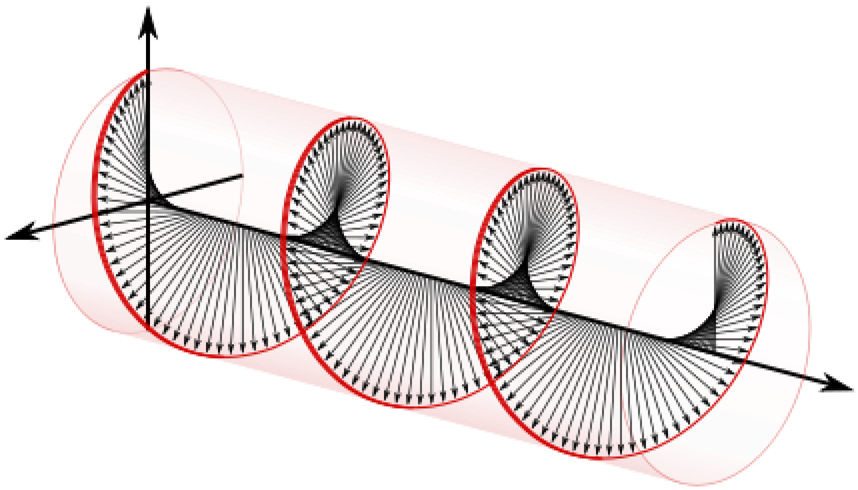

- **Left-handed polarization**

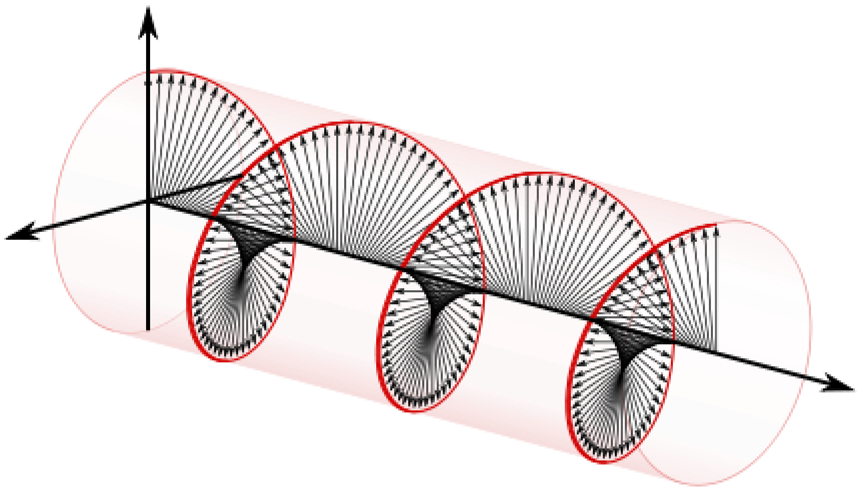

https://en.wikipedia.org/wiki/Circular_polarization

Only right-handed polarization can resonance with electron's gyromotion

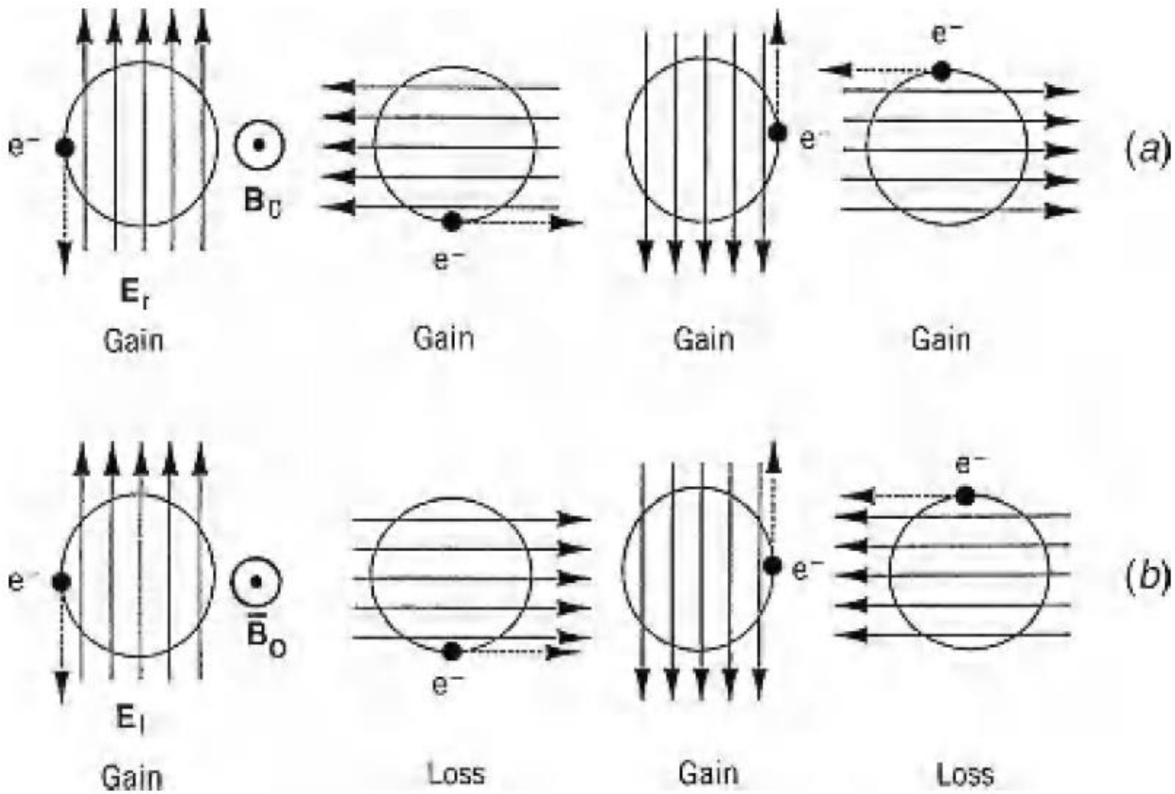

FIGURE 13.5. Basic principle of ECR heating: (*a*) continuous energy gain for right-hand polarization; (*b*) oscillating energy for left-hand polarization (after Lieberman and Gottscho, 1994).

Strong absorption occurs when the frequency matches the electron cyclotron frequency

- **Electron cyclotron resonance (ECR) plasma reactor**

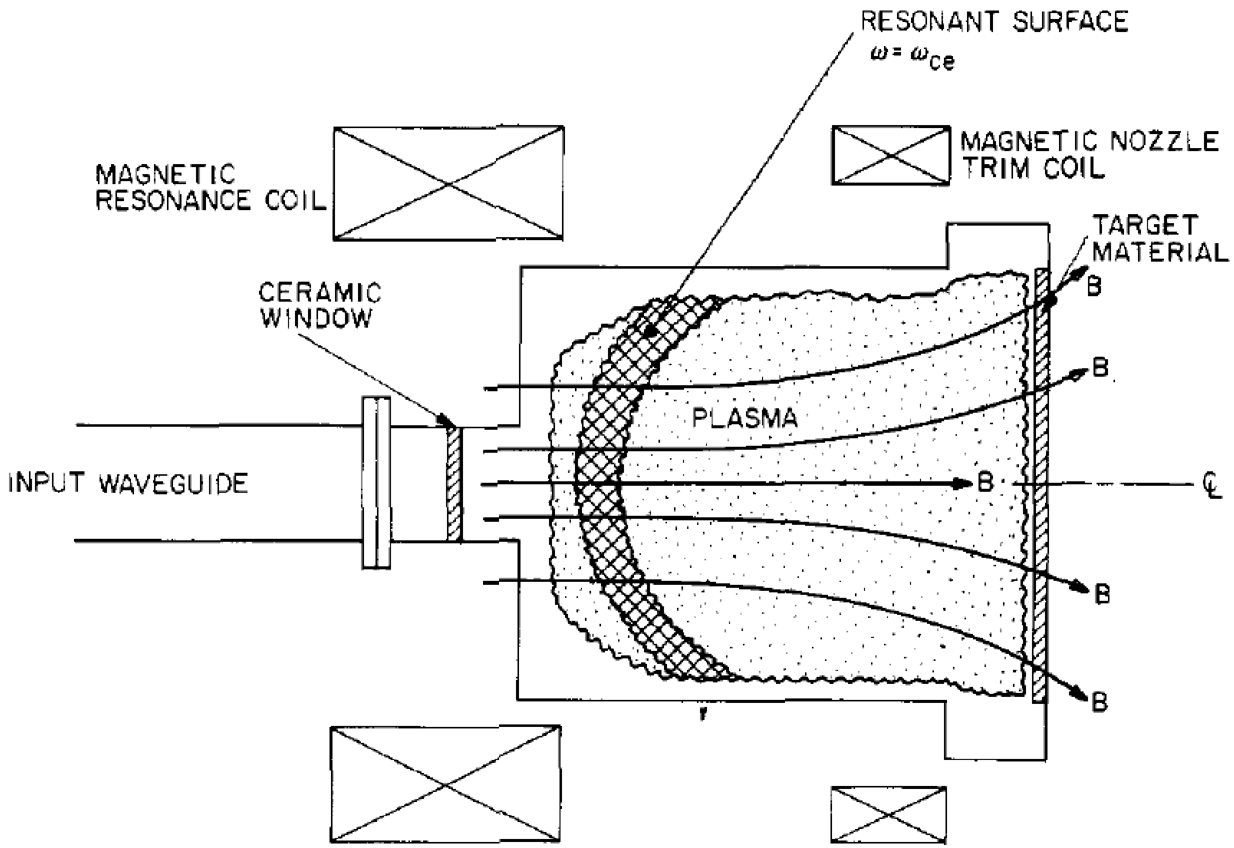

Electron cyclotron resonance (ECR) microwave systems

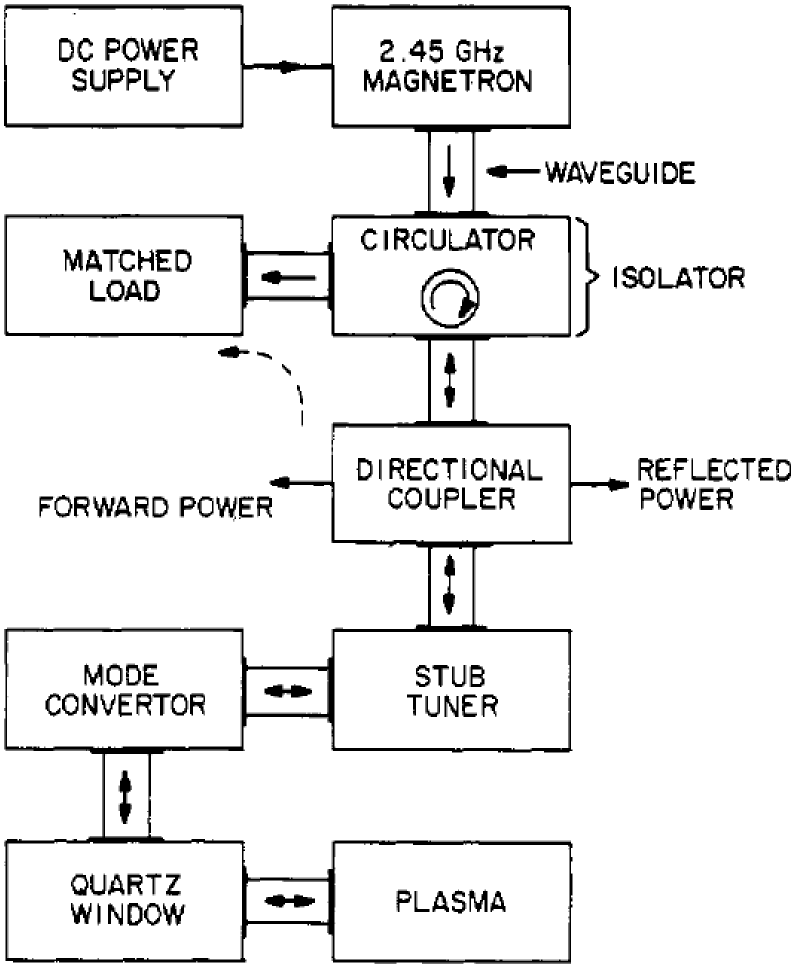

microwave systems

Immersed ECR plasma source

- **High particle fluxes on targets for diamond or other thin film deposition**
- **The ions in the plasma flux can be used for etching.**

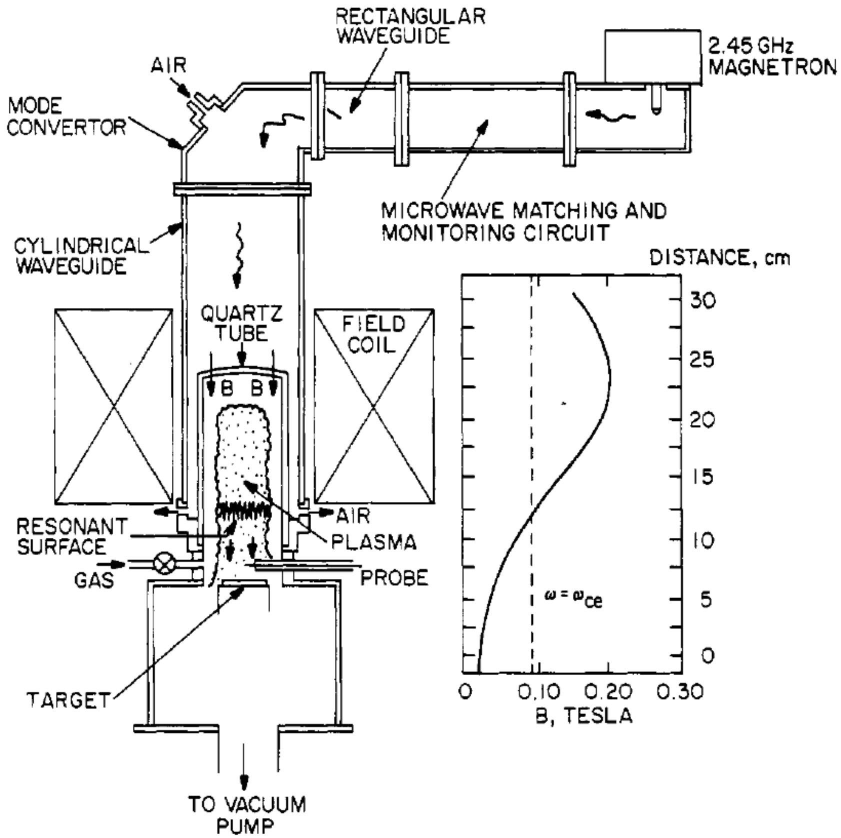

Distributed ECR system

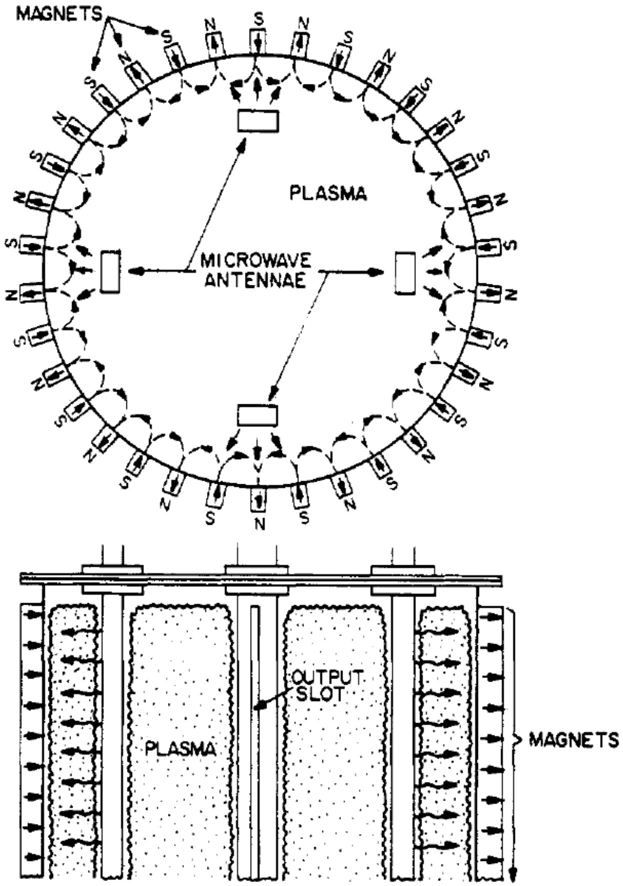

- **Function of the multipolar magnetic field at the tank boundary:**
  - **Provide a resonant surface for ECR absorption**
  - **Improve the confinement of the plasma**

Microwave plasma torch deposit a much faster rate than other types of plasma source for diamond film deposition

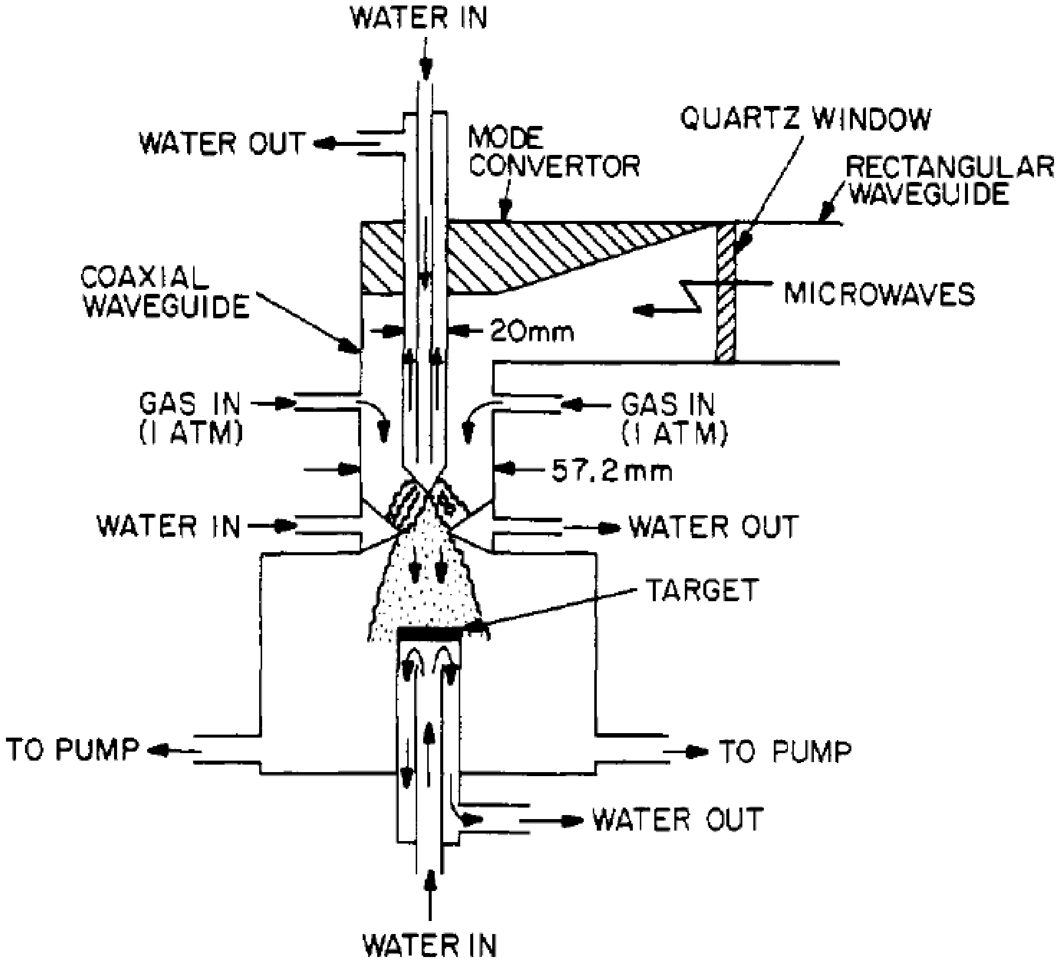

Microwave-generated plasmas have the capability of filling very large volumes with moderately high density

- **Advantages**
  - Lower neutral gas pressure, i.e., longer ion and neutral mean free paths.
  - Higher fraction ionize.
  - Higher electron density.
- **Disadvantages**
  - Lower ion bombardment energies.
  - Less control of the bombarding ion energy.
  - Difficult in tuning up and achieving efficient coupling.
  - Much more difficult and expensive to make uniform over a large area.
  - More expensive.

AC electrical discharges deliver energy to the plasma without contact between electrodes and the plasma

- DC electrical discharge – a true current in the form of a flow of ions or electrons to the electrodes.
- AC electrical discharge – the power supply interacts with the plasma by displacement current.
  - Inductive radio frequency (RF) electrical discharges
  - Capacitive RF electrical discharges
  - Microwave electrical discharges
  - Dielectric-barrier discharges (DBDs)
- Other mechanism
  - Laser produced plasma
  - Pulsed-power generated plasma

Dielectric-barrier discharges (DBDs)

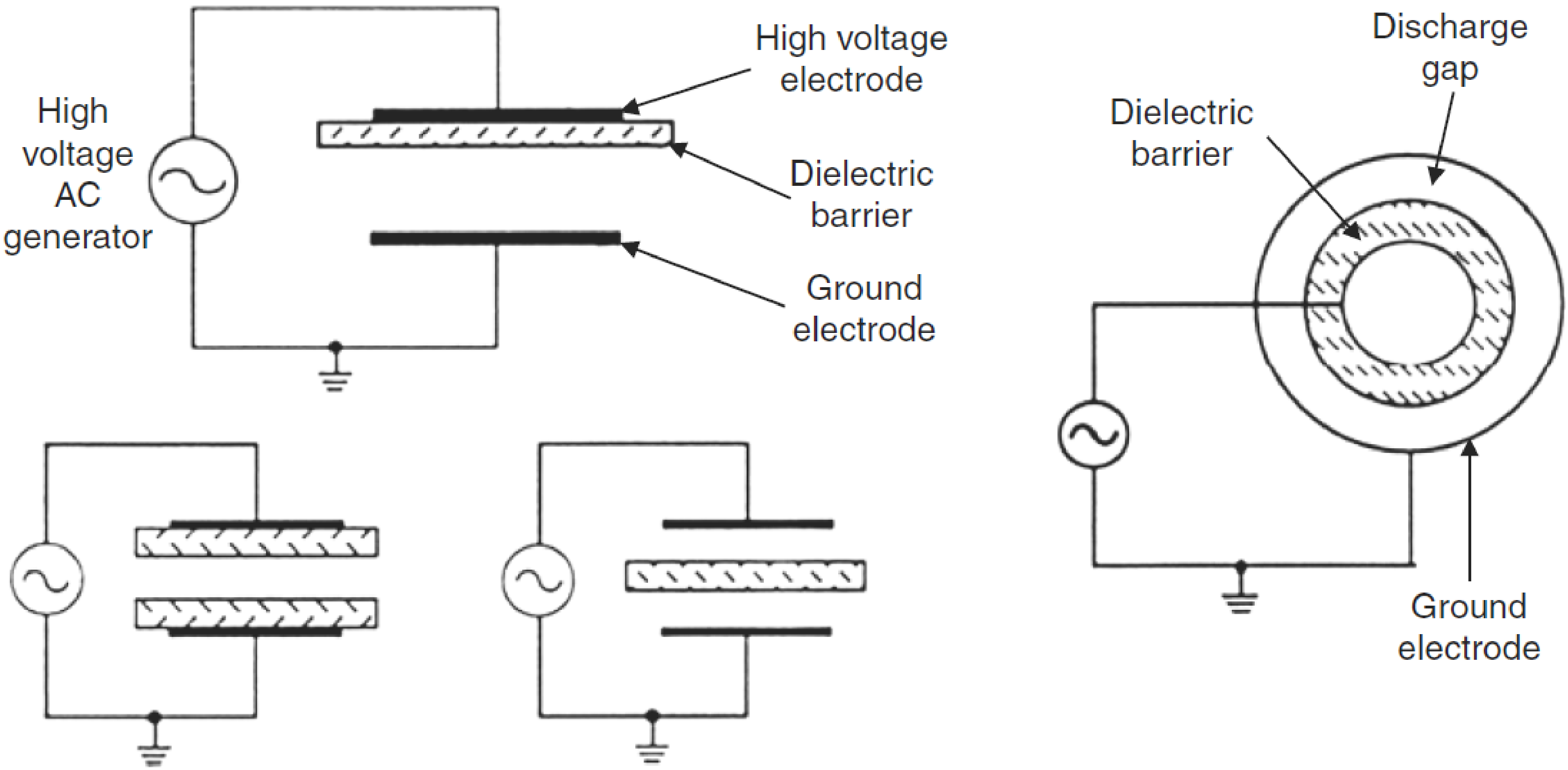

Space charge effect enhance the electric field

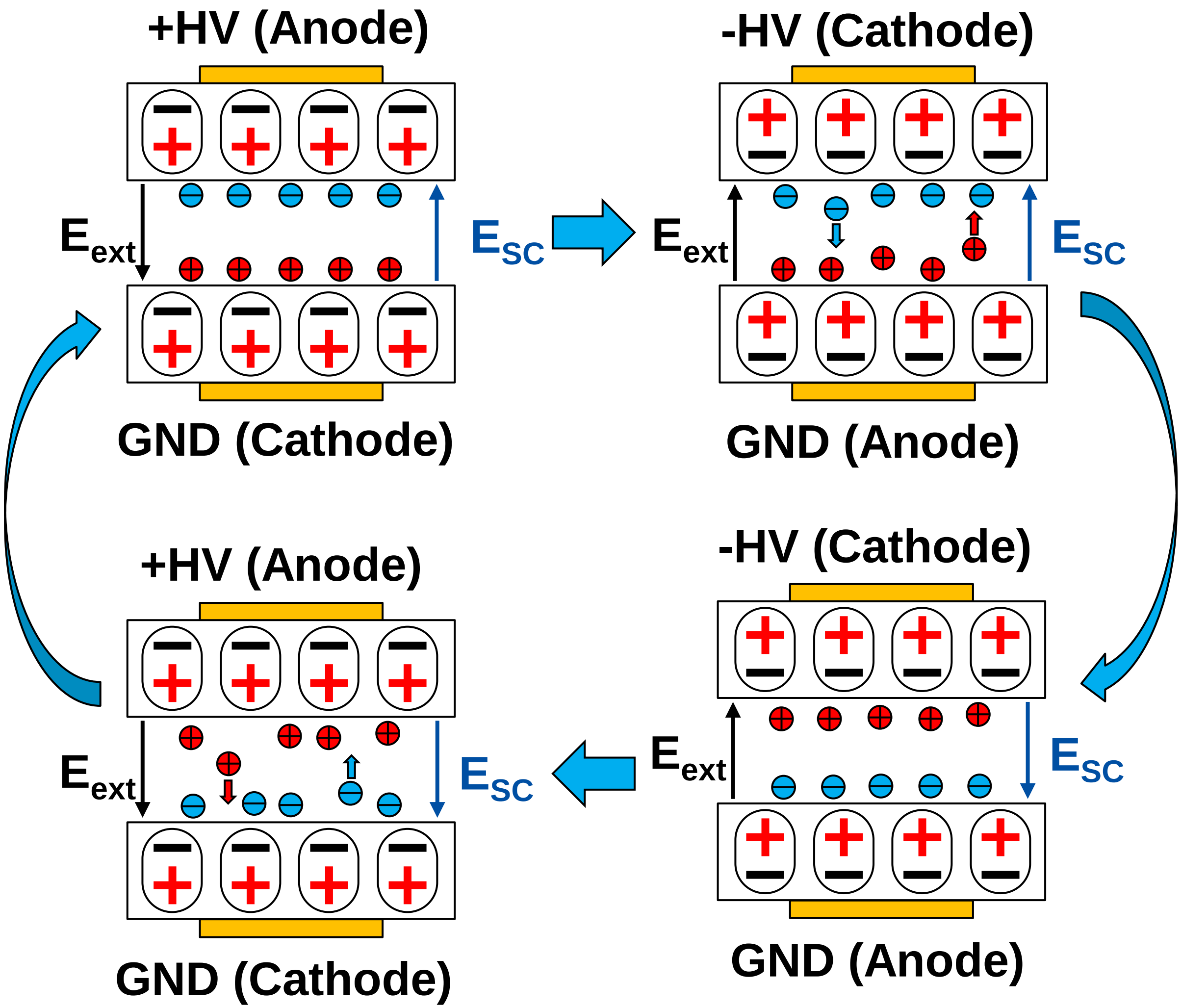

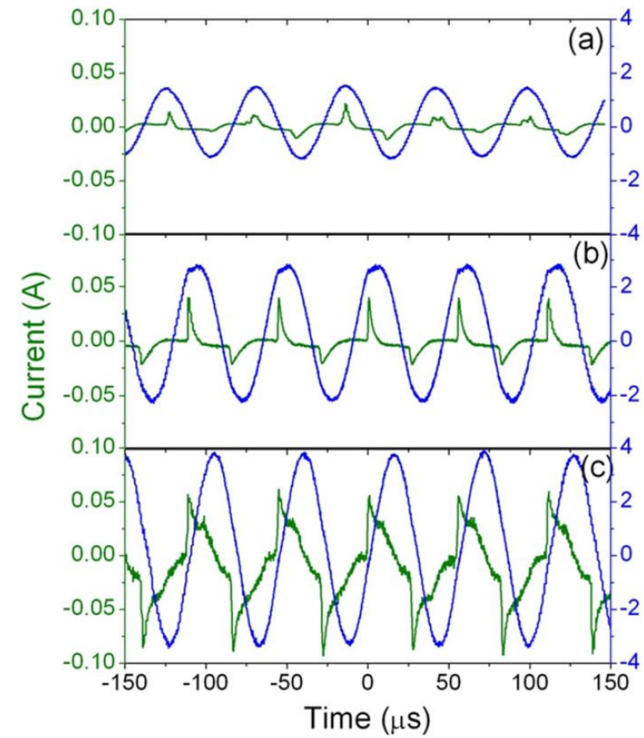

J. L. Walsh, *et al.*, J. Phys. D: Appl. Phys., **43**, 075201 (2010)

The foundation of AC discharge in plasma display panel

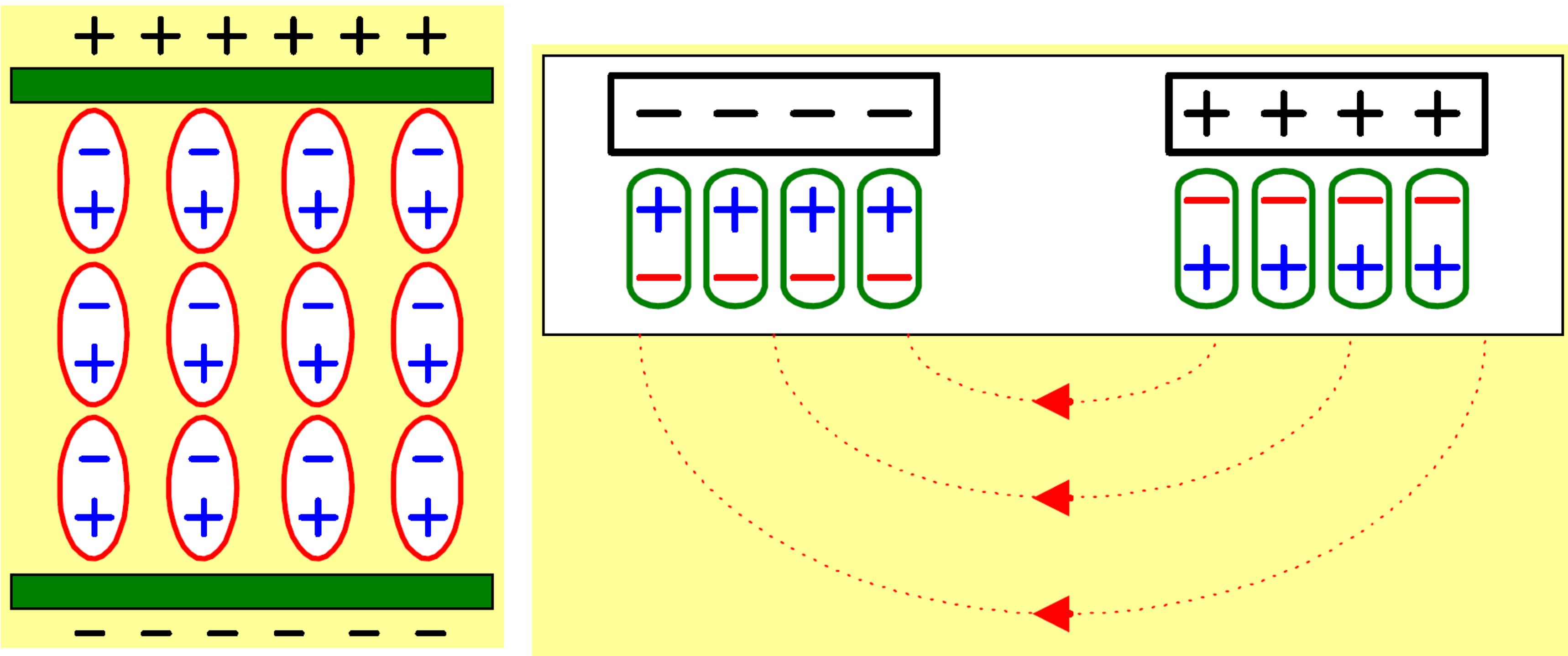

The plasma can be sustained using ac discharged in plasma display panel

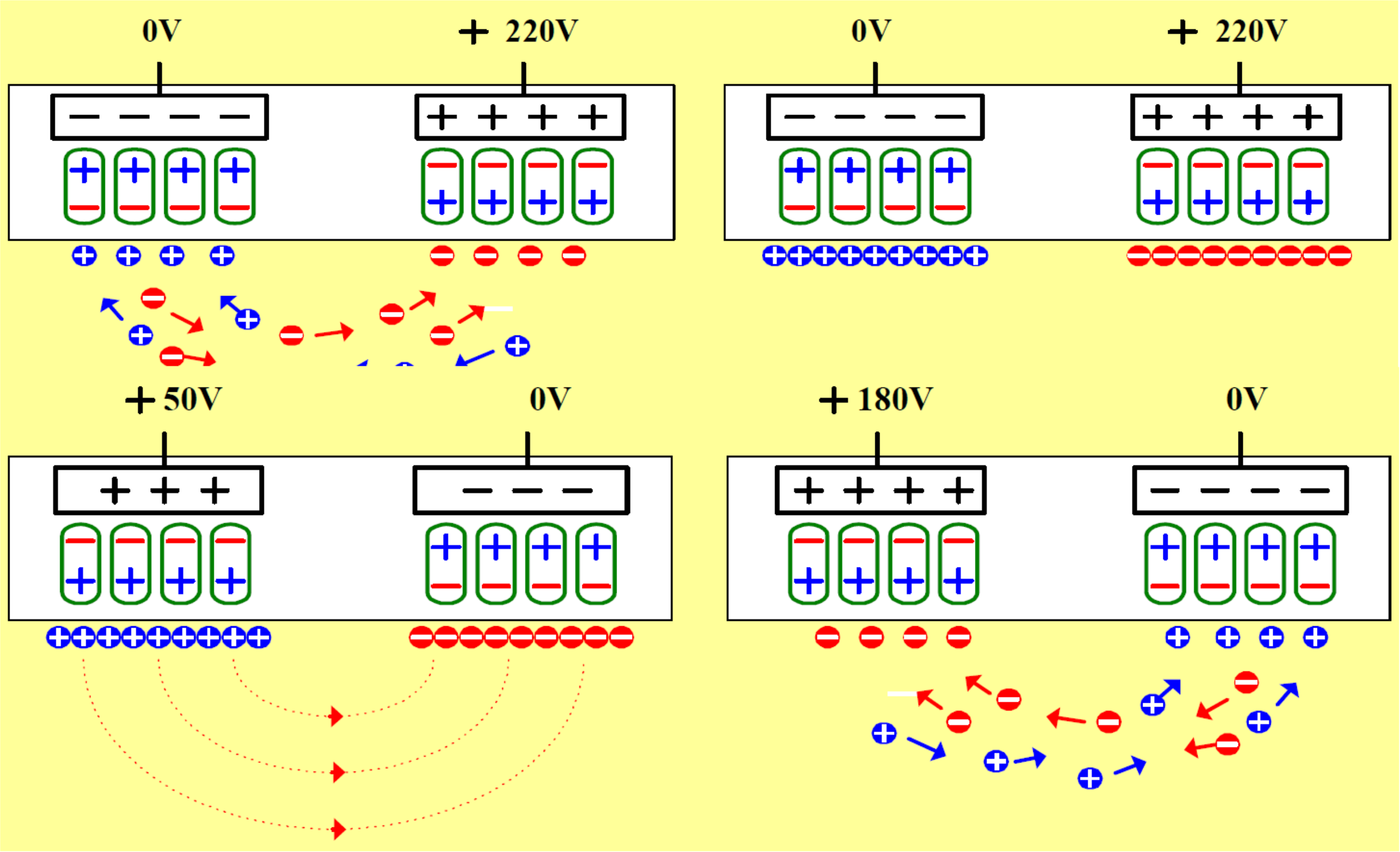

- **Wall discharge reduced the required discharge volta**

Plasma-needle discharge

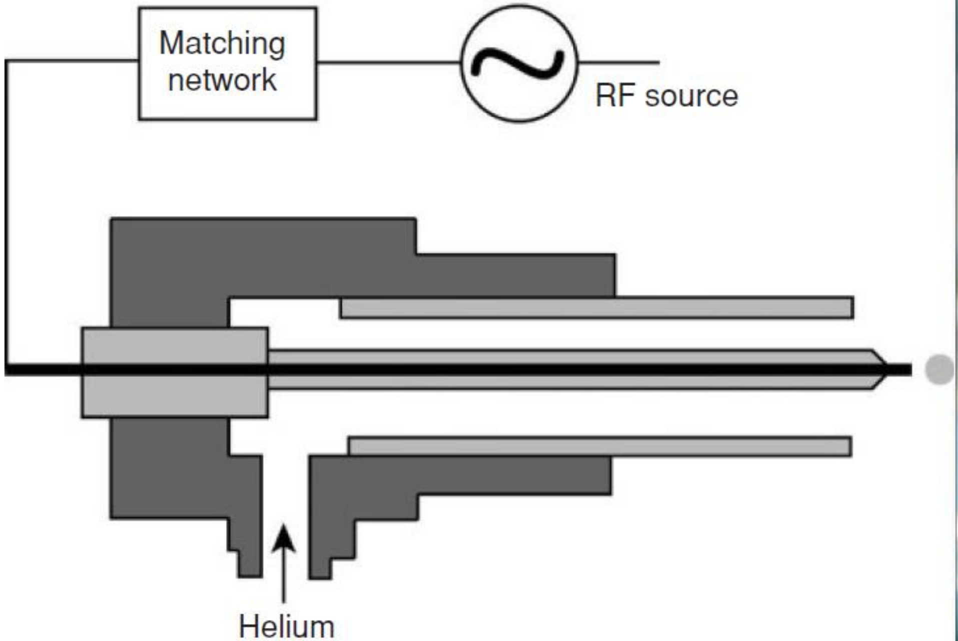

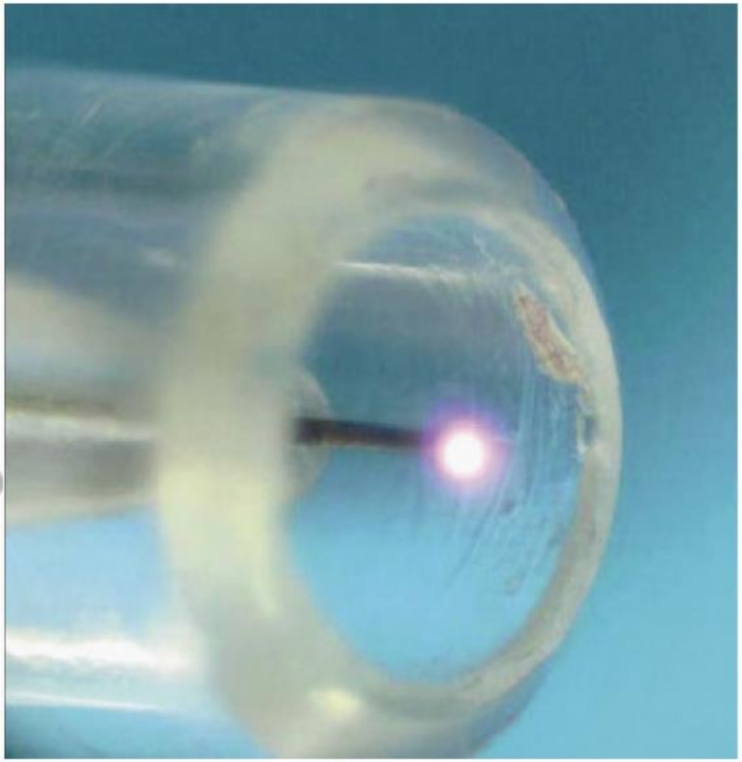

Atmospheric-pressure cold helium microplasma jets

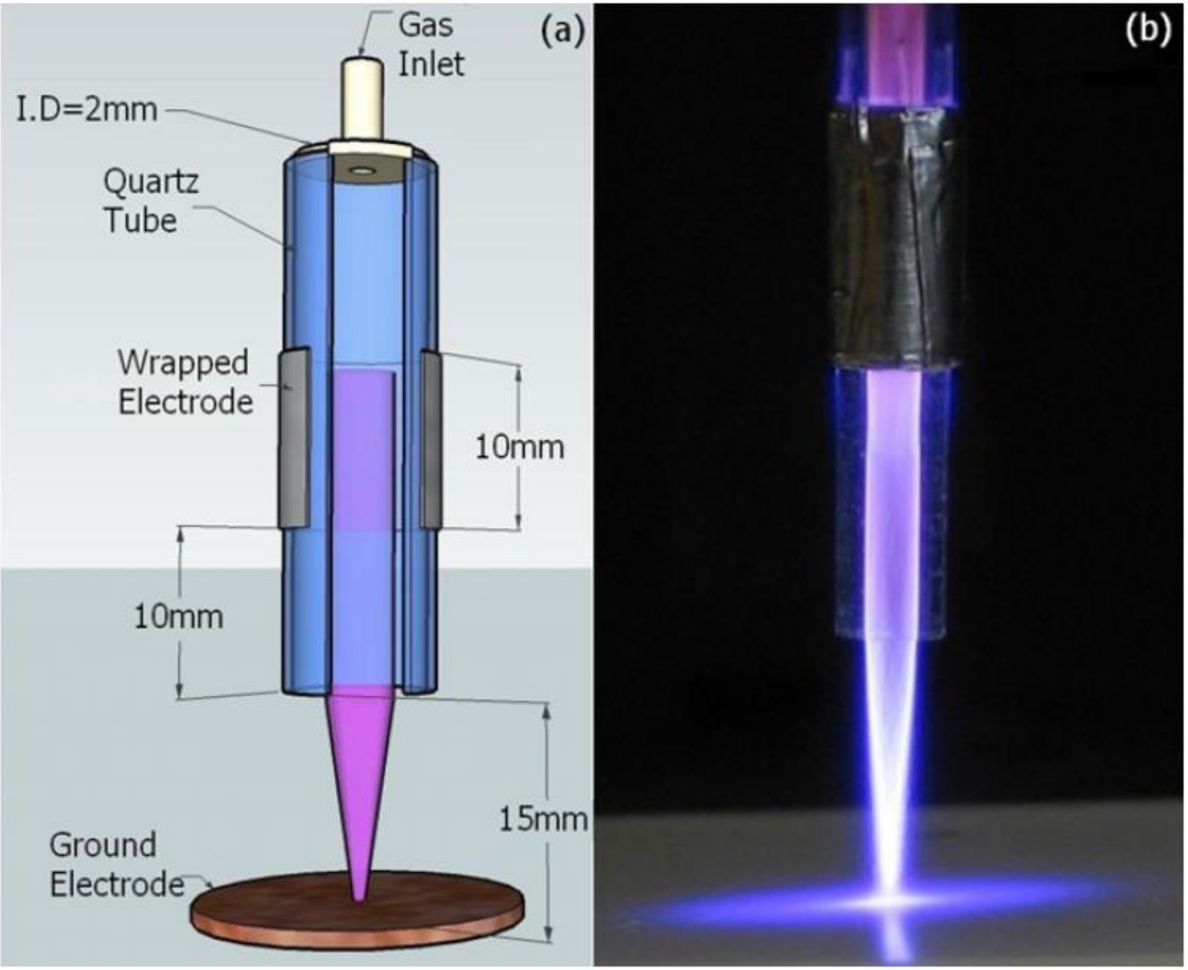

J. L. Walsh, *et al.*, J. Phys. D: Appl. Phys., **43**, 075201 (2010)

There are three different modes: chaotic, bullet, and continuous mode

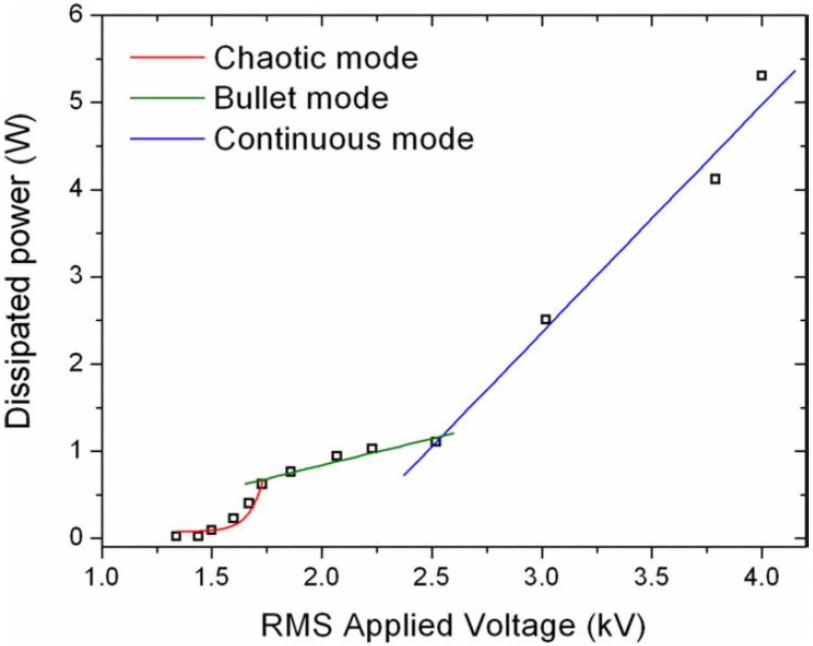

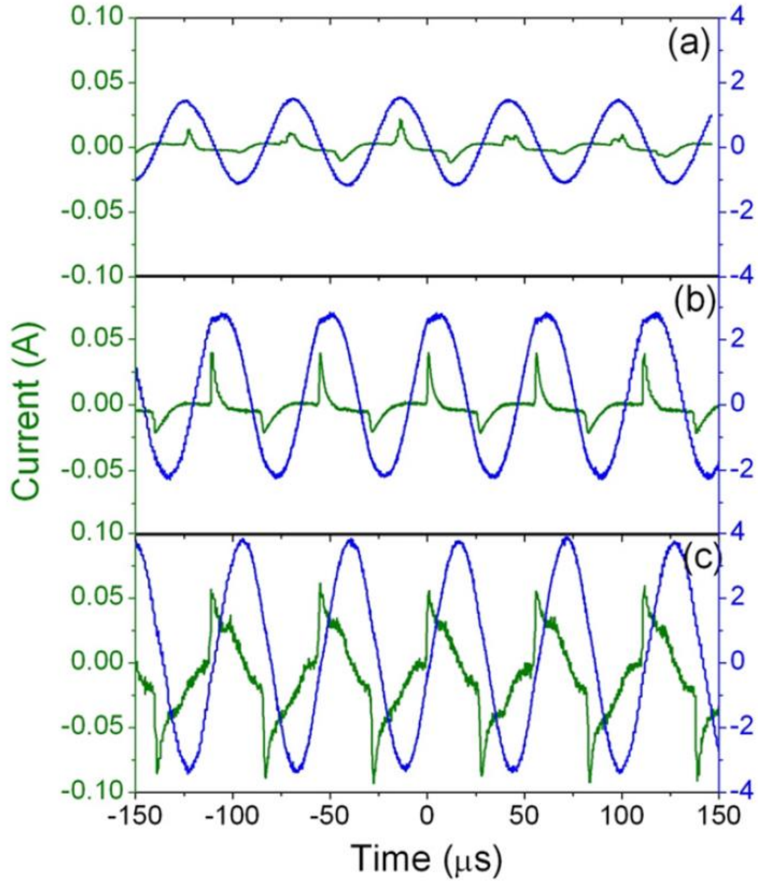

J. L. Walsh, *et al.*, J. Phys. D: Appl. Phys., **43**, 075201 (2010)

In bullet mode, the plasma jet comes out as a pulse

- **wavelength-integrated optical emission signal (350–800 nm)**
- **Images of bullet mode**

Bullet mode

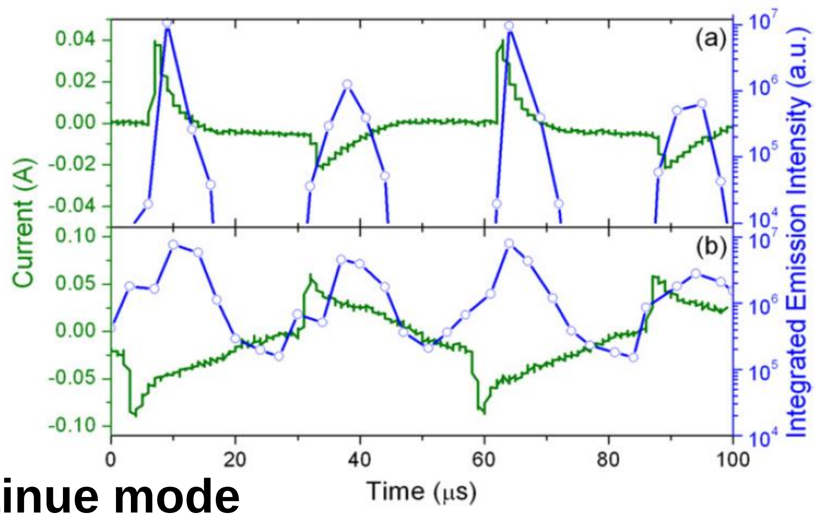

Continue mode

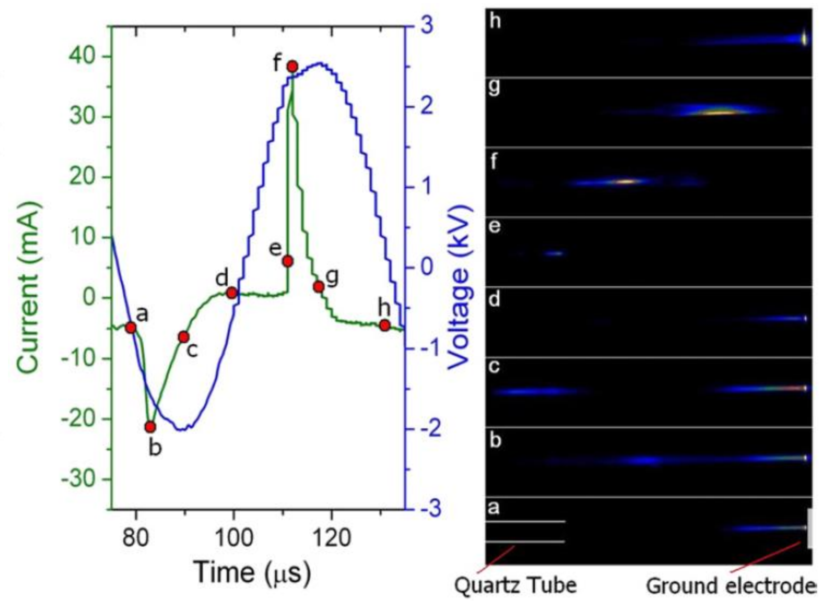

J. L. Walsh, *et al.*, J. Phys. D: Appl. Phys., **43**, 075201 (2010)

AC electrical discharges deliver energy to the plasma without contact between electrodes and the plasma

- DC electrical discharge – a true current in the form of a flow of ions or electrons to the electrodes.
- AC electrical discharge – the power supply interacts with the plasma by displacement current.
  - Inductive radio frequency (RF) electrical discharges
  - Capacitive RF electrical discharges
  - Microwave electrical discharges
  - Dielectric-barrier discharges (DBDs)
- Other mechanism
  - **Laser produced plasma**
  - Pulsed-power generated plasma

Laser is absorbed in underdense plasma through collisional process called inverse bremsstrahlung

- **Bremsstrahlung**

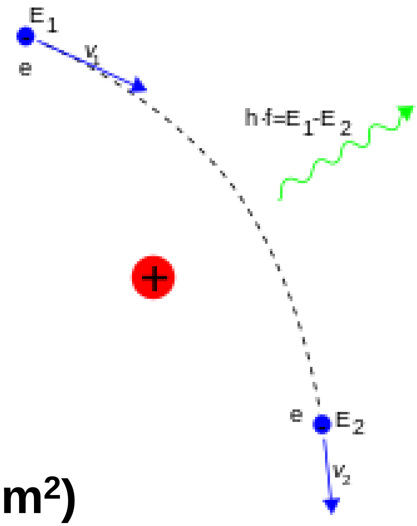

- **Inverse bremsstrahlung (For I < 10^{18} w/cm^2)**

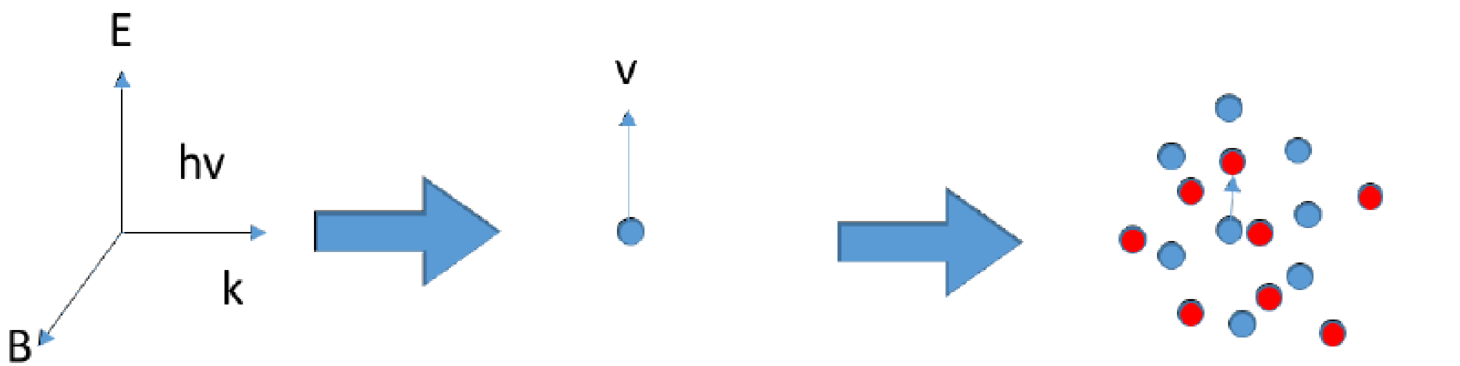

Electrons accelerated by electric fields

Electrons collide with other electrons / ions

Electric field of a high-power laser can perturb the potential of a nuclear and thus ionize the atom directly

- **For I ~ 10^{14} ~ 10^{16} w/cm^2**

$$E_{\mathrm{cutoff}} \approx I_{\mathrm{p}} + 3.17 U_{\mathrm{p}} \quad I_{\mathrm{p}}: \text{ ionization potential} \quad U_{\mathrm{p}}: \text{ ponderomotive energy}$$

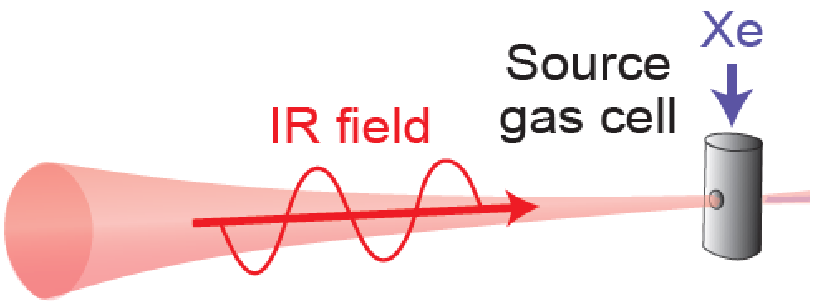

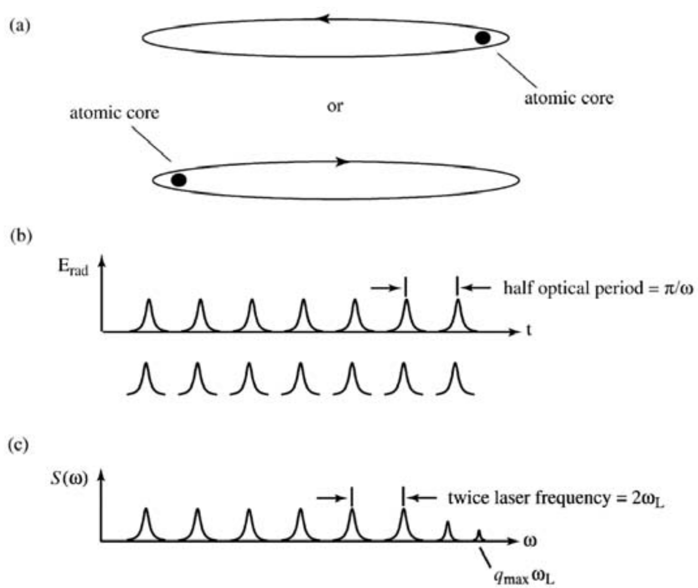

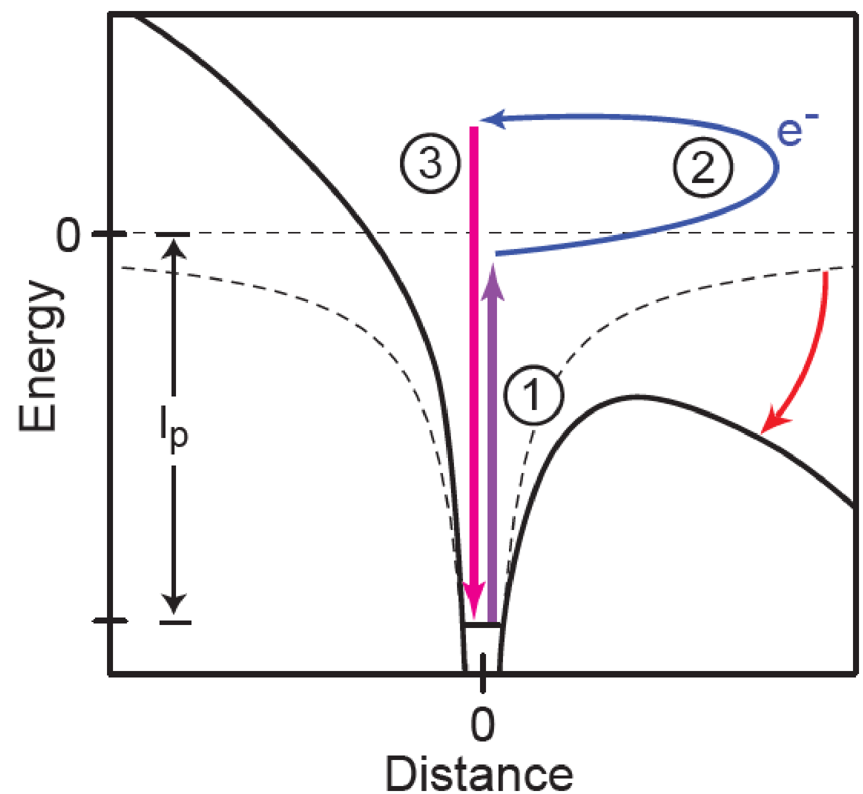

M. Krüger, etc., Appl. Sci. 9, 378 (2019)
Robert Boyd. Nonlinear optics.

Diagnostics

- Single/double Langmuir probe – n_e, T_e
- Interferometer – n_e
- Schlieren – dn_e/dx
- Faraday rotator – B
- Bdot probe – B
- Charged particle – B
- Spectroscopy – T_e, n_e
- Thomson scattering – T_e, n_e, T_i, n_i
- Faraday cup – dn_i/dt
- Retarding Potential Analyzer - v_i
- Intensified CCD – 2D image
- Framing camera – 2D image
- Streak camera – 1D image
- VISAR – shock velocity
- Neutron time of fligh (NToF)
  - Neutron yield, T_i
- Thomson parabola – e/m
- Stimulated brillouin scattering
  - Laser pulse compression

All plasmas are separated from the walls surrounding them by a sheath

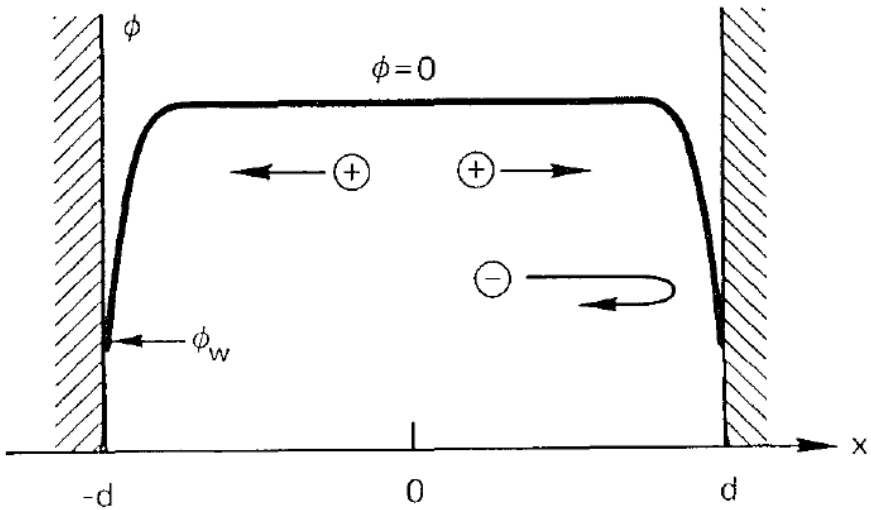

- When ions and electrons hit the wall, they recombine and are lost.
- Since electrons have much higher thermal velocities than ions, they are lost faster and leave the plasma with a net positive charge.
- Debye shielding will confine the potential variation to a layer of the order of several Debye lengths in thickness.
- A potential barrier is formed to confine electrons electrostatically.
- The flux of electrons is just equal to the flux of ions reaching the wall.

The planar sheath equation

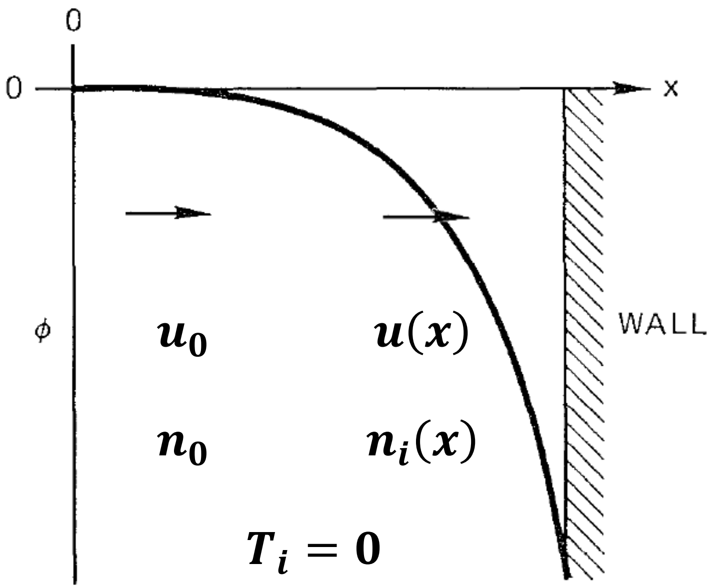

$$\frac{1}{2}mu^2 = \frac{1}{2}m{u_0}^2 - e\phi(x)$$

$$u = \left({u_0}^2 - \frac{2e\phi}{m}\right)^{1/2}$$

$$n_0 u_0 = n_i(x)u(x)$$

$$n_i(x) = n_0\left(1 - \frac{2e\phi}{m{u_0}^2}\right)^{-1/2}$$

- **Boltzmann relation:**

$$n_e(x) = n_0 \exp\left(\frac{e\phi}{KT_e}\right)$$

- **Poisson's equation:**

$$\epsilon_0 \frac{d^2\phi}{dx^2} = e(n_e - n_i)$$

$$= en_0\left[\exp\left(\frac{e\phi}{KT_e}\right) - \left(1 - \frac{2e\phi}{m{u_0}^2}\right)^{-1/2}\right]$$

$$\chi \equiv -\frac{e\phi}{KT_e}, \xi \equiv \frac{x}{\lambda_D}, M \equiv \frac{u_0}{(K\,T_e/m)^{1/2}}$$

$$\lambda_D = \left(\frac{KT_e}{4\pi n e^2}\right)^{1/2}$$

$$\chi'' = \left(1 + \frac{2\chi}{M^2}\right)^{-1/2} - e^{-\chi}$$

The Bohm sheath criterion

$$\chi'' = \left(1 + \frac{2\chi}{M^2}\right)^{-1/2} - e^{-\chi} \qquad \chi'\chi'' = \chi'\left(1 + \frac{2\chi}{M^2}\right)^{-1/2} - \chi' e^{-\chi}$$

$$\frac{d}{\mathrm{d}\xi}\left(\frac{\chi'^2}{2}\right) = \frac{\mathrm{d}\chi}{\mathrm{d}\xi}\left(1 + \frac{2\chi}{M^2}\right)^{-1/2} - \frac{\mathrm{d}\chi}{\mathrm{d}\xi} e^{-\chi} \qquad \chi_0 = 0\,, \chi_0' = 0, @\ \xi = 0$$

$$\int_{\chi_0'}^{\chi'} \mathrm{d}\left(\frac{\chi'^2}{2}\right) = \int_0^{\chi}\left(1 + \frac{2\chi}{M^2}\right)^{-1/2} \mathrm{d}\chi - \int_0^{\chi} e^{-\chi}\,\mathrm{d}\chi$$

$$\frac{1}{2}\left(\chi'^2 - \chi_0'^2\right) = M^2\left[\left(1 + \frac{2\chi}{M^2}\right)^{1/2} - 1\right] + e^{-\chi} - 1$$

- Needs to be solved numerically
- The right-hand side must be positive for all χ .

The Bohm sheath criterion - continued

$$\frac{1}{2}\left(\chi'^2-{\chi_0}'^2\right)=M^2\left[\left(1+\frac{2\chi}{M^2}\right)^{1/2}-1\right]+e^{-\chi}-1$$

- for $|\chi|\ll 1$ $$\left(1+\frac{2\chi}{M^2}\right)^{1/2}-1=1+\frac{\chi}{M^2}-\frac{1}{2}\left(\frac{\chi}{M^2}\right)^2+\cdots-1\approx\frac{\chi}{M^2}-\frac{1}{2}\left(\frac{\chi}{M^2}\right)^2$$

$$e^{-\chi}-1=1-\chi+\frac{1}{2}\chi^2+\cdots-1\approx-\chi+\frac{1}{2}\chi^2$$

$$M^2\left[\left(1+\frac{2\chi}{M^2}\right)^{1/2}-1\right]+e^{\chi}-1\approx M^2\left[\frac{\chi}{M^2}-\frac{1}{2}\left(\frac{\chi}{M^2}\right)^2\right]-\chi+\frac{1}{2}\chi^2=\frac{1}{2}\chi^2\left(-\frac{1}{M^2}+1\right)>0$$

$$M^2>1 \text{ or } \boxed{m{u_0}^2>KT_e}$$

- Ions must enter the sheath region with a velocity greater than the acoustic velocity v_s.
- There must be a finite electric field in the plasma.
- The scale of the sheath region is usually much smaller than the scale of the main plasma region in which the ions are accelerated.

The potential variation in a plasma-wall system can be divided into three parts

- **Sheath:**
  - **~Debye length, n_e is appreciable.**
  - **A dark layers where no electrons were present to excite atoms to emission.**
  - **It has been measured by the electrostatic deflection of a thin electron beam shot parallel to a wall**
- **Presheath: ions are accelerated to the required velocity u_0 by a potential drop**

$$\boxed{|\phi| \geq \frac{1}{2}\frac{KT_e}{e}\ .}$$

$$\frac{1}{2}mu_0^{\,2} = |e\phi|,\ mu_0^{\,2} > KT_e$$

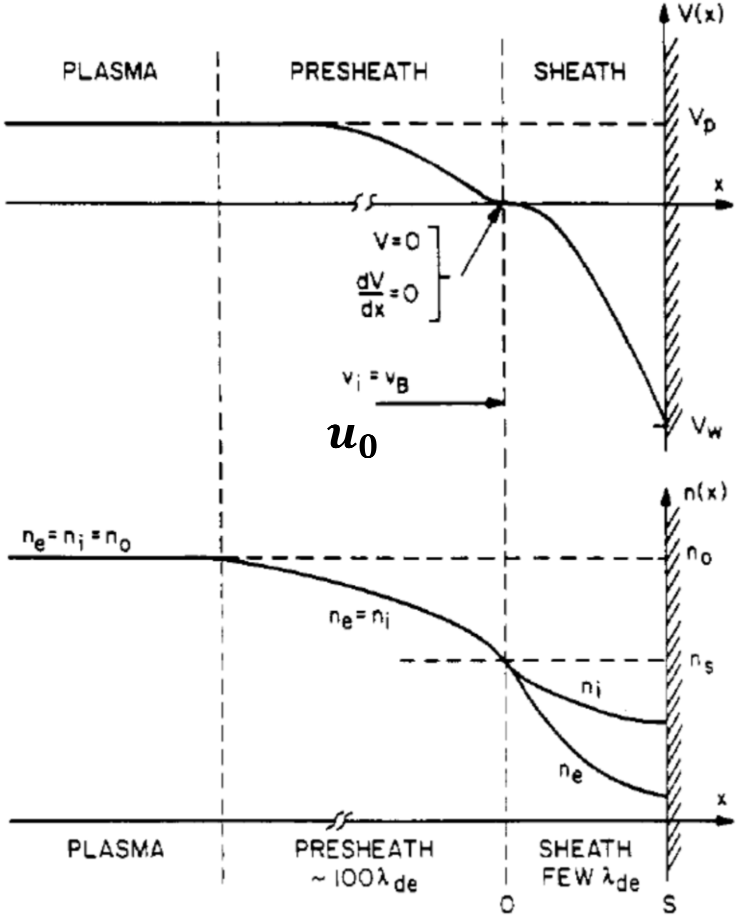

The Child-Langmuir law

- The electron density can be neglected in the region of large χ next to the wall.

$$\chi'' = \left(1+\frac{2\chi}{M^2}\right)^{-1/2} - e^{-\chi} \approx \left(1+\frac{2\chi}{M^2}\right)^{-1/2} \approx \frac{M}{(2\chi)^{1/2}}$$

$$\frac{1}{2}\left(\chi'^2 - {\chi_s}'^2\right) = \int_{\chi_s}^{\chi} \frac{M}{(2\chi)^{1/2}}\,\mathrm{d}\chi = \sqrt{2}M\left(\chi^{1/2} - {\chi_s}^{1/2}\right)$$

$n_e \approx 0 @ \xi = \xi_s,\ \chi_s << \chi$ and $\chi_s' << \chi',\ \chi'^2 = 2^{3/2}M\chi^{1/2}$

$$\frac{d\chi}{\chi^{1/4}} = 2^{3/4}M^{1/2}\mathrm{d}\xi$$

- Integrating from $\xi = \xi_s$ to $\xi_s + \frac{d}{\lambda_D} = \xi_{\text{wall}}$

$$\frac{4}{3}{\chi_w}^{3/4} = 2^{3/4}M^{1/2}\frac{d}{\lambda_D}$$

$$M = \frac{4\sqrt{2}}{9}\frac{{\chi_w}^{3/2}}{d^2}\lambda_D$$

$$\chi \equiv -\frac{e\phi}{KT_e},\ M \equiv \frac{u_0}{(KT_e/m)^{1/2}}$$

$$J = en_0u_0$$

$$\boxed{J = \frac{4}{9}\left(\frac{2e}{m}\right)^{1/2}\frac{\epsilon_0|\phi_w|^{3/2}}{d^2}}$$

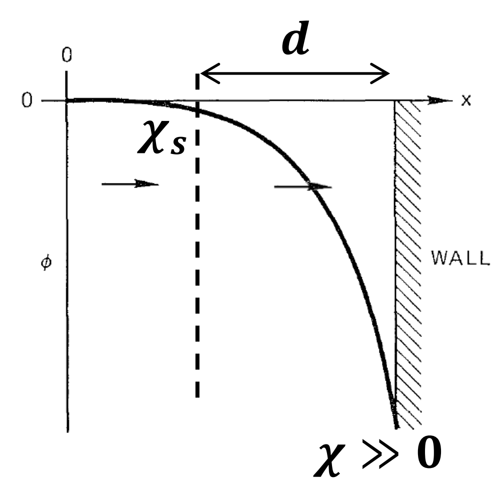

Electrostatic probes

- **The electron current can be neglected if the probe is sufficiently negative relative to the plasma to repel most electrons.**

$$mu_0^{\,2} > KT_e \qquad J = enu \qquad I = n_s eA\left(\frac{KT_e}{m}\right)^{1/2}$$

$$|\phi| \simeq \frac{1}{2}\frac{KT_e}{e}$$

$$n_s = n_0 \exp\left(\frac{e\phi}{KT_e}\right) = n_0 e^{-1/2} = 0.61 n_0$$

$$\boxed{\textbf{Bohm current: } I_B \simeq 0.5 n_0 eA\left(\frac{KT_e}{m}\right)^{1/2}}$$

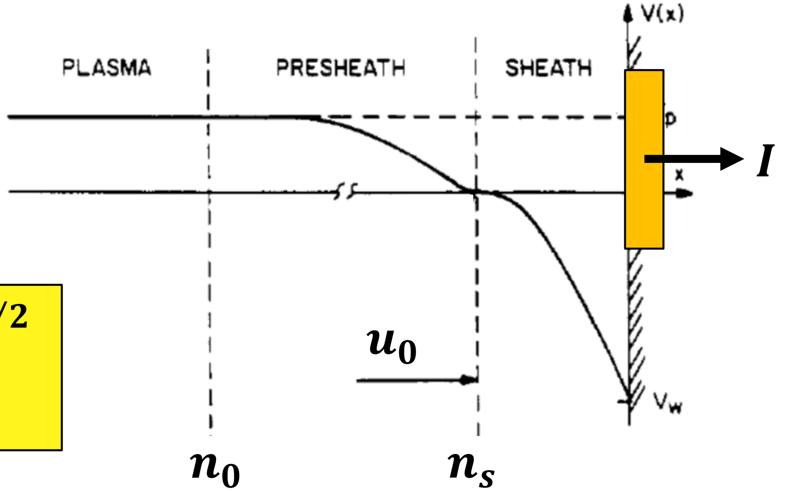

- **The plasma density can be obtained once the temperature is known.**

A plasma sheaths is formed when plasma is contact to a surface

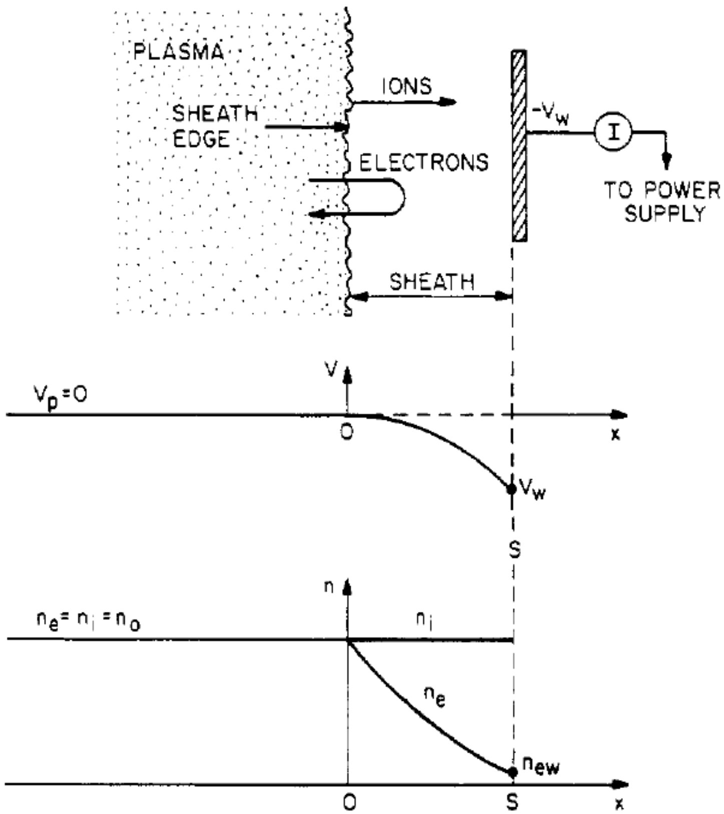

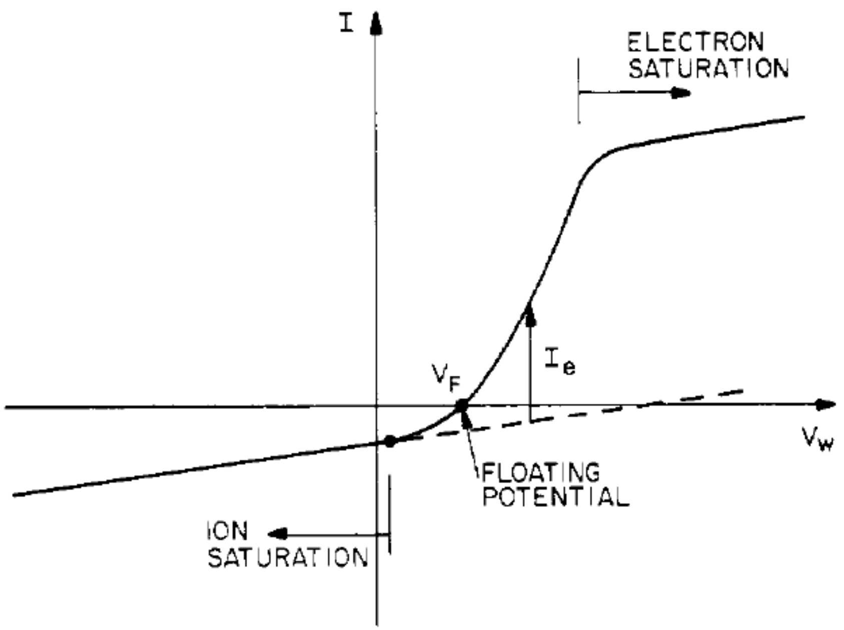

Floating voltage is determined when ion flux is balanced by electron flux

- **Wall flux of ions:**

$$\boldsymbol{\Gamma_i = \frac{1}{4} n_0 \bar{v}_i = n_0 \sqrt{\frac{8KT_i}{\pi m_i}}}$$

- **Wall flux of electrons due to random motion:**

$$\boldsymbol{n_{ew} = n_0 \exp\left(\frac{e\Phi_w}{KT_e}\right)}$$ **(Boltzman equation)**

$$\boldsymbol{\Gamma_e = \frac{1}{4} n_{ew} \bar{v}_e = n_0 \exp\left(\frac{e\Phi_w}{KT_e}\right) \sqrt{\frac{8KT_e}{\pi m_e}}}$$

- **Balance between electron and ion flux (current)**

$$\boldsymbol{I = \mathrm{eA}(\Gamma_i - \Gamma_e) = 0}$$

$$\boldsymbol{\Phi_w = -\frac{KT_e}{2e} \ln\left(\frac{m_i T_e}{m_e T_i}\right)}$$

Floating voltage can also be calculated using Bohm's velocity

- **Wall flux of ions using Bohm's velocity:**

$$u_0 = \sqrt{\frac{KT_e}{m_i}} \qquad \Gamma_i = n_s u_0$$

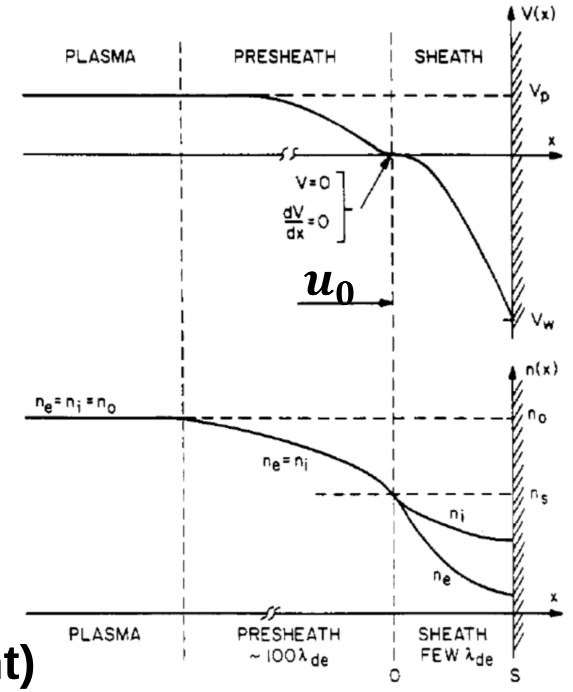

- **Wall flux of electrons due to random motion:**

$$n_{ew} = n_s \exp\left(\frac{e\Phi_w}{KT_e}\right)$$

$$\Gamma_e = \frac{1}{4} n_w \bar{v}_e = \frac{1}{4} n_s \exp\left(\frac{e\Phi_w}{KT_e}\right) \sqrt{\frac{8KT_e}{\pi m_e}}$$

- **Balance between electron and ion flux (current)**

$$I = \mathrm{eA}(\Gamma_i - \Gamma_e) = 0$$

$$\Phi_{wB} = -\frac{KT_e}{2e} \ln\left(\frac{m_i}{2\pi m_e}\right) \Leftrightarrow \Phi_w = -\frac{KT_e}{2e} \ln\left(\frac{m_i T_e}{m_e T_i}\right)$$

Electron temperature can be determined by the slope of the I-V curve between ion and electron saturation

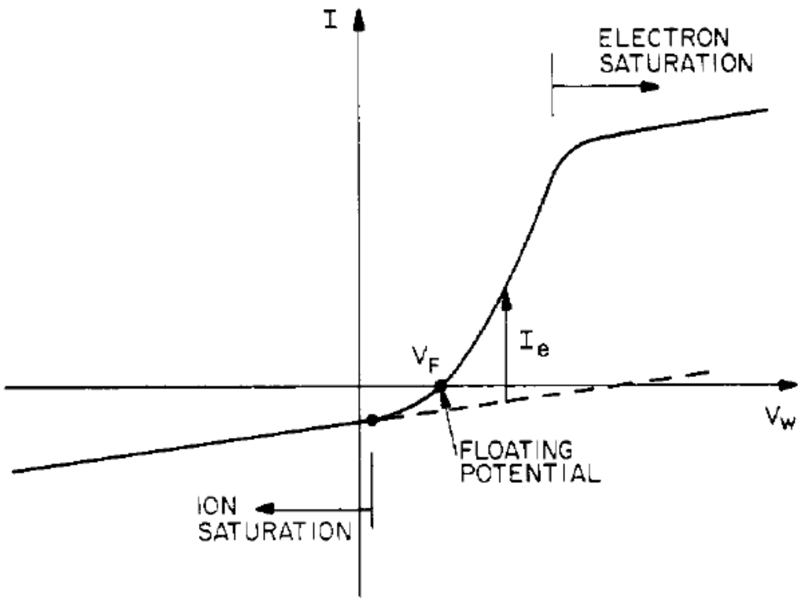

- **Ion saturation current:**

$$I_{\mathrm{is}} = \mathrm{AJ}_{\mathrm{is}} = \mathrm{eA}\Gamma_{\mathrm{is}}$$
$$= eA\frac{1}{4}n_i\bar{v}_i$$
$$= \frac{\mathrm{eA}n_i}{4}\sqrt{\frac{8KT_i}{\pi m_i}}$$

$$\boxed{n_i = \frac{4I_{\mathrm{is}}}{\mathrm{eA}}\sqrt{\frac{\pi m_i}{8KT_i}}}$$

- **Total current:** $I = I_{\mathrm{is}} + I_e = I_{\mathrm{is}} + \frac{1}{4}n_s\exp\left(\frac{\mathrm{eV}}{KT_e}\right)\bar{v}_e\mathrm{eA} \qquad V \equiv \Phi$

Assuming: $\frac{dI_{\mathrm{is}}}{dV} \ll \frac{\mathrm{dI}}{\mathrm{dV}}$

$$\frac{dI}{\mathrm{dV}} = \frac{dI_{\mathrm{is}}}{dV} + \frac{1}{4}\frac{e}{KT_e}n_s\exp\left(\frac{\mathrm{eV}}{KT_e}\right)\bar{v}_e\mathrm{eA} = \frac{dI_{\mathrm{is}}}{dV} + \frac{e}{KT_e}I_e = \frac{dI_{\mathrm{is}}}{dV} + \frac{e}{KT_e}(I - I_{\mathrm{is}})$$
$$\approx \frac{e}{KT_e}(I - I_{\mathrm{is}})$$

$$\boxed{T_e = \frac{e(I - I_{\mathrm{is}})}{\mathrm{dI/dV}}}$$

Electron temperature can be obtained alternatively by finding the slope of I-V curve in Log-Linear plot

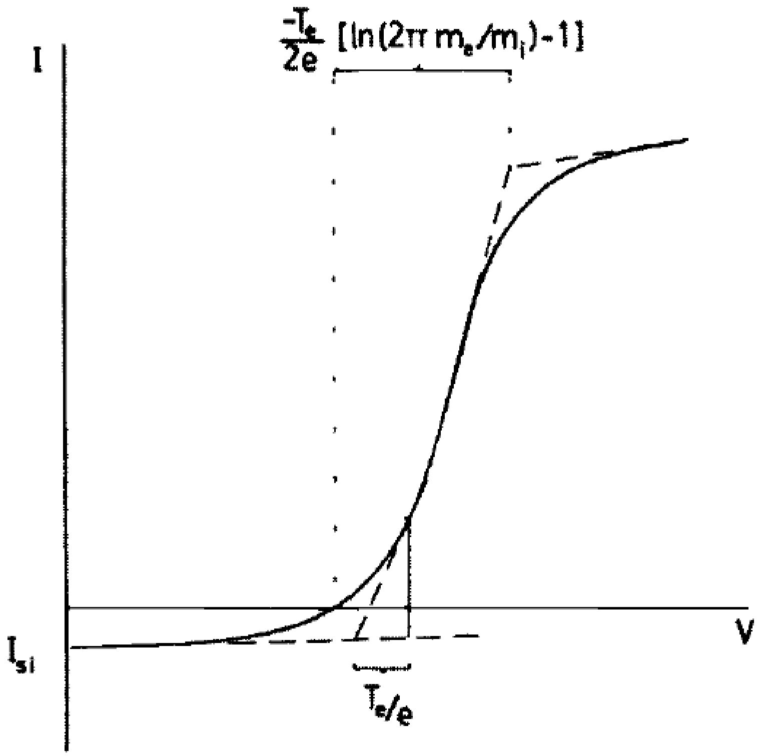

- **Electron saturation**

$$V = V_p \qquad I_{\mathrm{es}} = \frac{1}{4} n_s \exp\left(\frac{\mathrm{eV}_p}{KT_e}\right)\bar{v}_e \mathrm{eA}$$

$$I = I_e + I_{\mathrm{is}} \approx I_{\mathrm{e}} = \frac{1}{4} n_s \exp\left(\frac{\mathrm{eV}}{KT_e}\right)\bar{v}_e \mathrm{eA}$$

$$= \frac{1}{4} n_s \exp\left(\frac{\mathrm{eV} - \mathrm{eV}_p + \mathrm{eV}_p}{KT_e}\right)\bar{v}_e \mathrm{eA}$$

$$= \frac{1}{4} n_s \exp\left(\frac{\mathrm{eV}_p}{KT_e}\right)\exp\left(e\frac{V - V_p}{KT_e}\right)\bar{v}_e \mathrm{eA}$$

$$= I_{\mathrm{es}} \exp\left(e\frac{V - V_p}{KT_e}\right)$$

$$\boxed{T_e = \frac{e(V - V_p)}{K(\ln \mathrm{I}_{\mathrm{es}} - \ln \mathrm{I})}}$$

Plasma density can be obtained by finding the electron saturation current

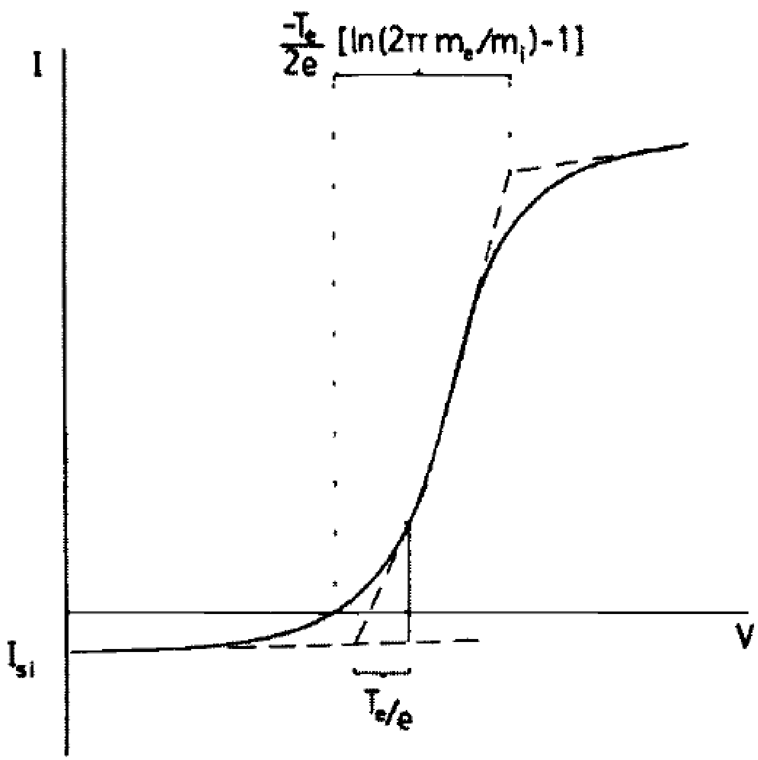

- **Electron saturation current:**

$$I_{es} = \frac{1}{4} n_s \exp\left(\frac{eV_p}{KT_e}\right) \bar{v}_e eA$$

$$= \frac{1}{4} n_0 eA \sqrt{\frac{8KT_e}{\pi m_e}}$$

$$\boxed{n_0 = \frac{4I_{es}}{eA} \sqrt{\frac{\pi m_e}{8T_e}}}$$

Two Langmuir probes can be operated simultaneously

Single Probe

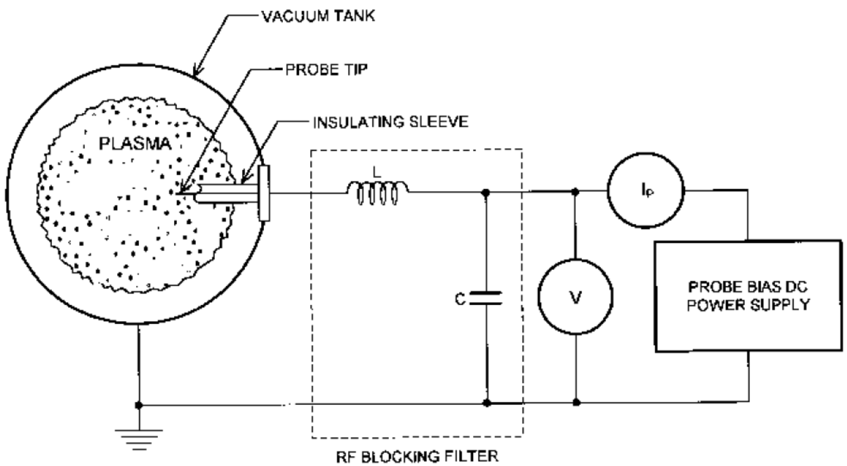

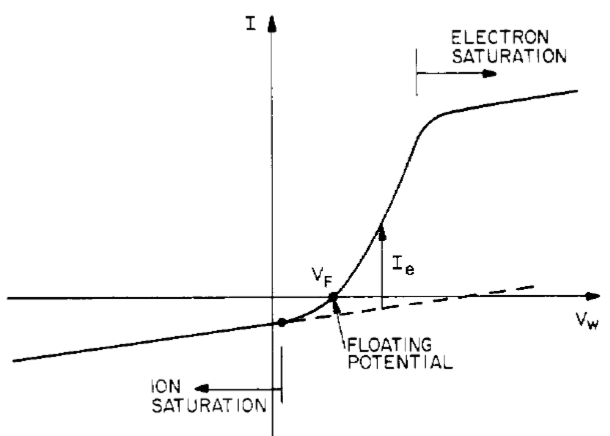

Double Probe

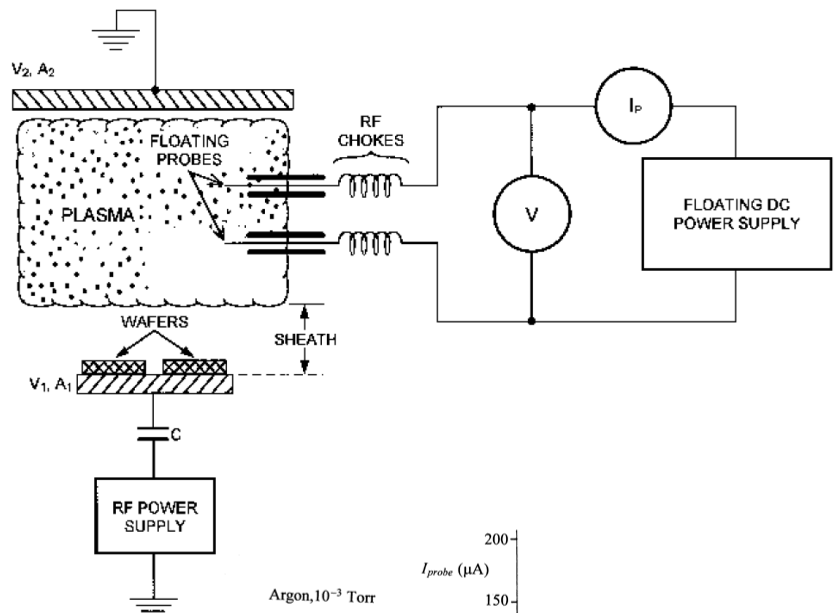

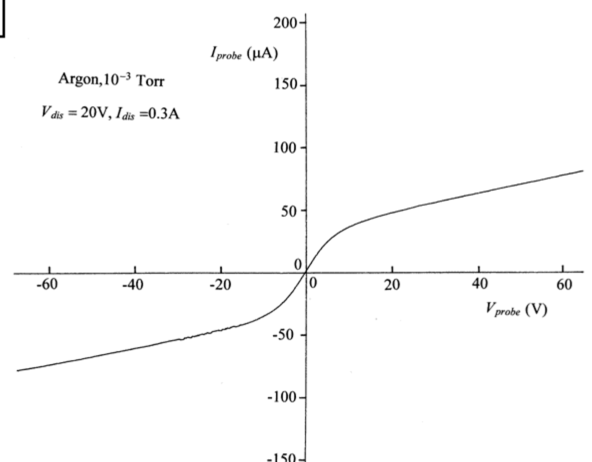

Two Langmuir probes can be operated simultaneously

Single Probe

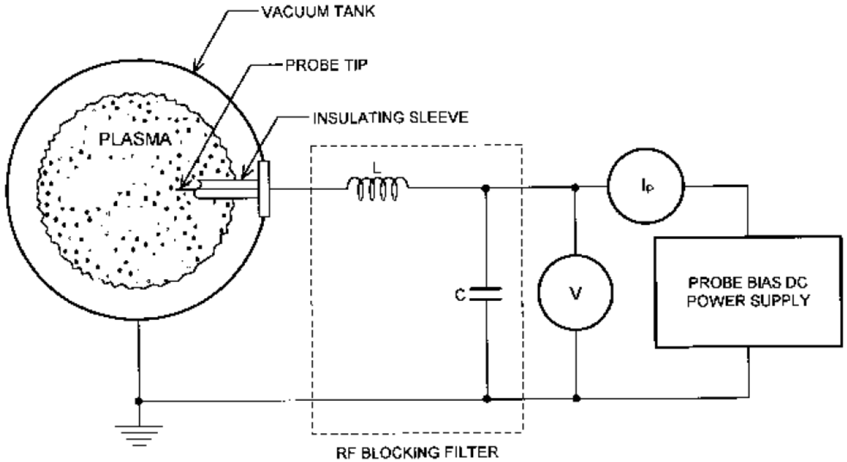

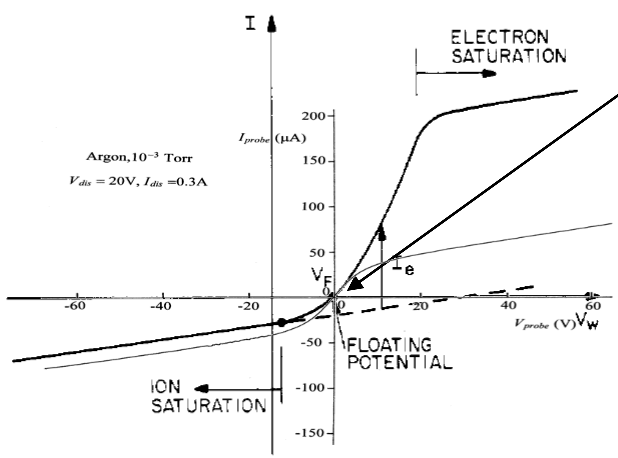

Double Probe

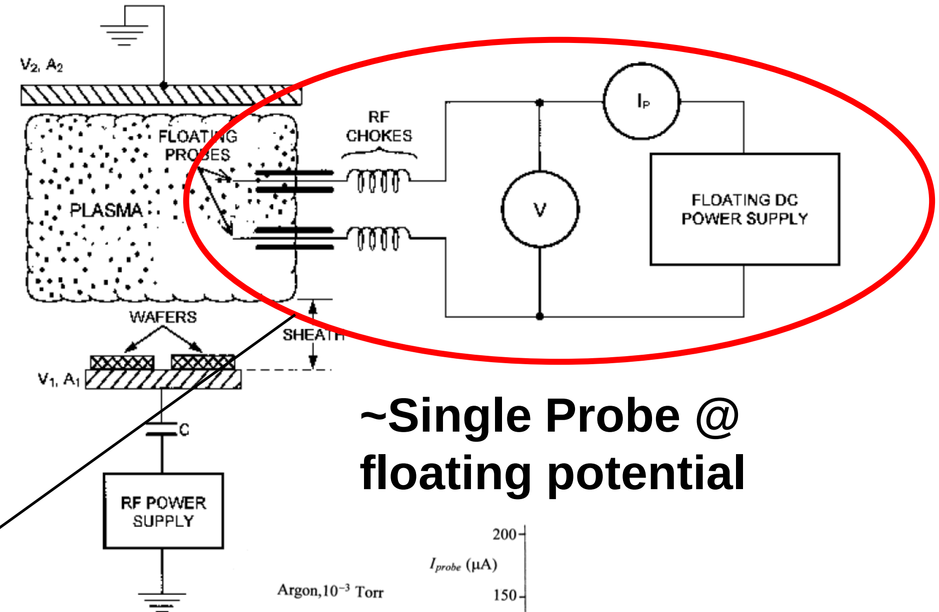

~Single Probe @ floating potential

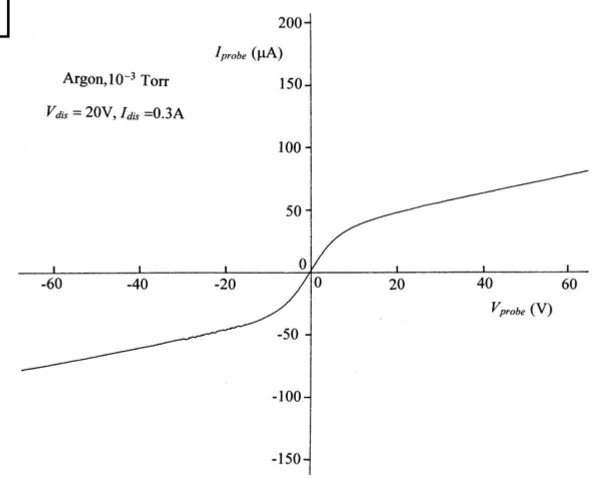

Double Langmuir probe is not disturbed by the discharge

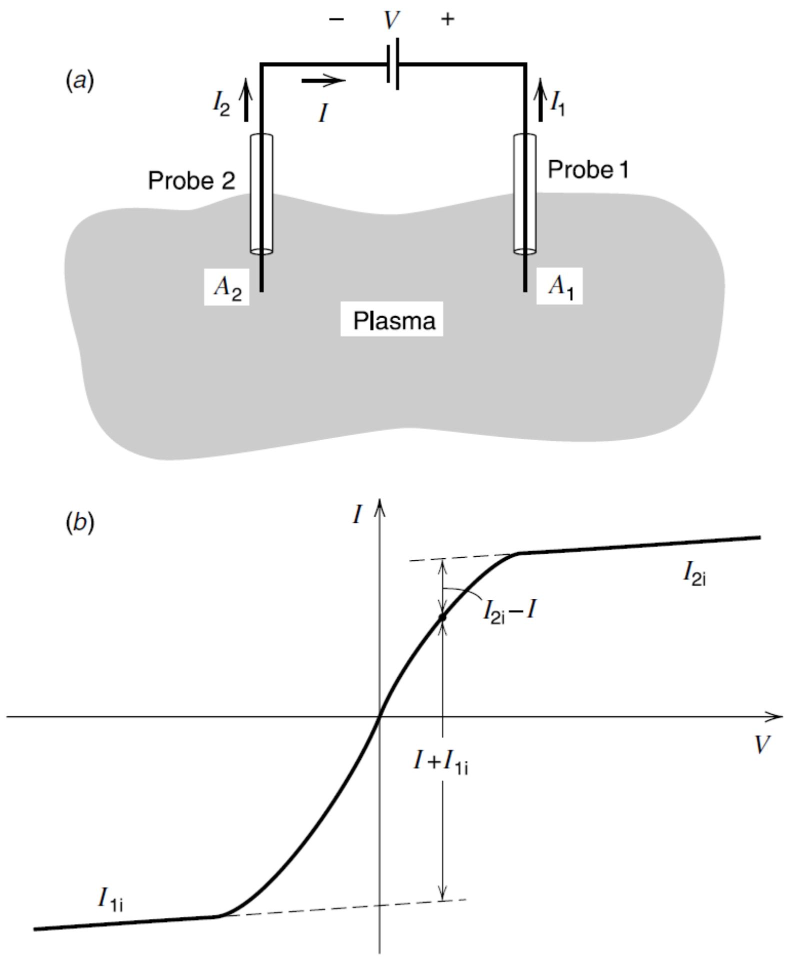

$$I = I_{1e} - I_{1i} = I_{2i} - I_{2e}$$

$$I_{1e} = A_1 \frac{\bar{v}_e e}{4} n_s \exp\left(\frac{\mathrm{eV_1}}{KT_e}\right)$$

$$I_{2e} = A_2 \frac{\bar{v}_e e}{4} n_s \exp\left(\frac{\mathrm{eV_2}}{KT_e}\right)$$

$$I_{1e} = I + I_{1i} \qquad I_{2e} = I_{2i} - I$$

$$\frac{I + I_{1i}}{I_{2i} - I} = \frac{A_1}{A_2} \exp\left(\frac{V_1 - V_2}{T_e}\right)$$

$$= \frac{A_1}{A_2} \exp\left(\frac{V}{T_e}\right)$$

$$I = I_i \tanh\left(\frac{V}{2T_e}\right) \qquad \frac{dI}{\mathrm{dV}}\Big|_{v=0} = \frac{I_i}{2T_e}$$

- **The net current never exceeds the ion saturation current, minimizing the disturbance to the discharge.**

An electromagnetic wave is described using Maxwell's equation

$$\left\{\begin{aligned} \nabla \times \vec{E} &= -\frac{\partial \vec{B}}{\partial t} \\ \nabla \times \vec{B} &= \mu_0 \vec{j} + \epsilon_0 \mu_0 \frac{\partial \vec{E}}{\partial t} \end{aligned}\right.$$

$$\nabla \times \left(\nabla \times \vec{E}\right) = -\frac{\partial}{\partial t}\left(\nabla \times \vec{B}\right) = -\frac{\partial}{\partial t}\left(\mu_0 \vec{j} + \epsilon_0 \mu_0 \frac{\partial \vec{E}}{\partial t}\right)$$

Conductivity: $\vec{j} = \overleftrightarrow{\sigma} \cdot \vec{E}$

$$\nabla \times \left(\nabla \times \vec{E}\right) = -\frac{\partial}{\partial t}\left(\nabla \times \vec{B}\right) = -\frac{\partial}{\partial t}\left(\mu_0 \overleftrightarrow{\sigma} \cdot \vec{E} + \epsilon_0 \mu_0 \frac{\partial \vec{E}}{\partial t}\right)$$

Plane wave: $\vec{E} = \vec{E} \exp\left[i\left(\vec{k} \cdot \vec{x} - \omega t\right)\right]$

$$i\vec{k} \times \left(i\vec{k} \times \vec{E}\right) = i\omega\left(\mu_0 \overleftrightarrow{\sigma} \cdot \vec{E} - i\omega\epsilon_0\mu_0\vec{E}\right)$$

Dispersion relation is determined by the determinant of the matrix of coefficient

$$-\vec{k}\times\left(\vec{k}\times\vec{E}\right) \;=\; -\left[\left(\vec{k}\cdot\vec{E}\right)\vec{k}-\left(\vec{k}\cdot\vec{k}\right)\vec{E}\right]=-\left(\vec{k}:\vec{k}\right)\vec{E}+k^2\vec{E}$$

$$\begin{aligned} i\omega\left(\mu_0\overleftrightarrow{\sigma}\cdot\vec{E}-i\omega\epsilon_0\mu_0\vec{E}\right) &= i\omega\left(\mu_0\overleftrightarrow{\sigma}\cdot\vec{E}-\frac{i\omega}{c^2}\vec{E}\right)=\frac{\omega^2}{c^2}\left[-\frac{c^2}{i\omega}\mu_0\overleftrightarrow{\sigma}\cdot\vec{E}+\vec{E}\right] \\ &= \frac{\omega^2}{c^2}\left(\overleftrightarrow{1}+\frac{i}{\omega\epsilon_0}\overleftrightarrow{\sigma}\right)\vec{E}\equiv\frac{\omega^2}{c^2}\overleftrightarrow{\varepsilon}\vec{E} \end{aligned}$$

Dielectric tensor: $\overleftrightarrow{\varepsilon}\equiv\overleftrightarrow{1}+\dfrac{i}{\omega\epsilon_0}\overleftrightarrow{\sigma}$

$$i\vec{k}\times\left(i\vec{k}\times\vec{E}\right) \;=\; i\omega\left(\mu_0\overleftrightarrow{\sigma}\cdot\vec{E}-i\omega\epsilon_0\mu_0\vec{E}\right)$$

$$\Rightarrow\quad \left(\vec{k}:\vec{k}-k^2\overleftrightarrow{1}+\frac{\omega^2}{c^2}\overleftrightarrow{\varepsilon}\right)\vec{E}=0$$

$$\det\left(\vec{k}:\vec{k}-k^2\overleftrightarrow{1}+\frac{\omega^2}{c^2}\overleftrightarrow{\varepsilon}\right)=0$$

Two mode can propagate in the plasma

$$\det\left(\vec{k}:\vec{k} - k^2\overleftrightarrow{1} + \frac{\omega^2}{c^2}\overleftrightarrow{\varepsilon}\right) = 0$$

Assuming the wave propagates along the z direction and isotropic medium:

$$\vec{k} = k\hat{z}$$

$$\overleftrightarrow{\varepsilon} = \varepsilon\overleftrightarrow{1}$$

$$\begin{pmatrix} -k^2 + \frac{\omega^2}{c^2}\varepsilon & 0 & 0 \\ 0 & -k^2 + \frac{\omega^2}{c^2}\varepsilon & 0 \\ 0 & 0 & \frac{\omega^2}{c^2}\varepsilon \end{pmatrix} = 0$$

$$\left(-k^2 + \frac{\omega^2}{c^2}\varepsilon\right)^2 \frac{\omega^2}{c^2}\varepsilon = 0$$

$$\frac{\omega^2}{c^2}\varepsilon = 0$$

$$\left(-k^2 + \frac{\omega^2}{c^2}\varepsilon\right)^2 = 0$$

Longitudinal wave **Transverse wave**

The reflective index is determined by the dielectric

- **Longitudinal wave:** $$\frac{\omega^2}{c^2}\varepsilon = 0$$

$$\begin{pmatrix} -k^2 + \frac{\omega^2}{c^2}\varepsilon & 0 & 0 \\ 0 & -k^2 + \frac{\omega^2}{c^2}\varepsilon & 0 \\ 0 & 0 & 0 \end{pmatrix} \begin{pmatrix} E_\mathrm{x} \\ E_\mathrm{y} \\ E_\mathrm{z} \end{pmatrix} = 0 = \begin{pmatrix} \left(-k^2 + \frac{\omega^2}{c^2}\varepsilon\right) E_\mathrm{x} \\ \left(-k^2 + \frac{\omega^2}{c^2}\varepsilon\right) E_\mathrm{y} \\ 0 \end{pmatrix}$$

$$E_\mathrm{x} = E_\mathrm{y} = 0$$

- **Transverse wave:** $$\left(-k^2 + \frac{\omega^2}{c^2}\varepsilon\right)^2 = 0$$

$$\begin{pmatrix} 0 & 0 & 0 \\ 0 & 0 & 0 \\ 0 & 0 & \frac{\omega^2}{c^2}\varepsilon \end{pmatrix} \begin{pmatrix} E_\mathrm{x} \\ E_\mathrm{y} \\ E_\mathrm{z} \end{pmatrix} = 0$$

$$E_\mathrm{z} = 0$$

Reflective index: $$n \equiv \frac{kc}{\omega} = \varepsilon^{1/2}$$

Conductivity tensor can be determined from equation of motion for electron

$$m_e \frac{\partial \vec{v}}{\partial t} = -e\left(\vec{E} + \vec{v} \times \vec{B}\right) \qquad \vec{v} = \vec{v}\exp\left[i\left(\vec{k}\cdot\vec{x} - \omega t\right)\right]$$

$$\begin{cases} -i\omega m_e v_x &= -eE_x - eB_0 v_y \\ -i\omega m_e v_y &= -eE_y + eB_0 v_x \\ -i\omega m_e v_z &= -eE_z \end{cases} \qquad \Omega \equiv \frac{eB_0}{m_e}$$

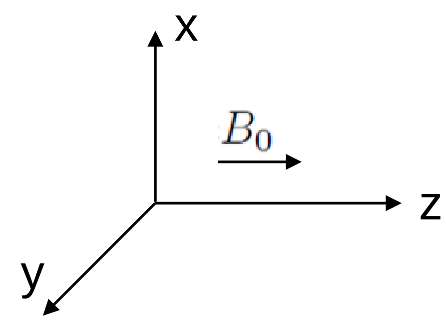

$$\begin{cases} v_x &= -\frac{ie}{\omega m_e}\frac{1}{1-\Omega^2/\omega^2}\left(E_x - i\frac{\Omega}{\omega}E_y\right) \\ v_y &= -\frac{ie}{\omega m_e}\frac{1}{1-\Omega^2/\omega^2}\left(i\frac{\Omega}{\omega}E_x + E_y\right) \\ v_z &= -\frac{ie}{\omega m_e}E_z \end{cases}$$

$$\vec{j} = -en_e\vec{v}_e \equiv \overleftrightarrow{\sigma}\vec{E}$$

$$\begin{aligned} \overleftrightarrow{\sigma} &= -en_e\left(\frac{-ie}{\omega m_e}\right)\frac{1}{1-\Omega^2/\omega^2}\begin{pmatrix} 1 & -i\frac{\Omega}{\omega} & 0 \\ i\frac{\Omega}{\omega} & 1 & 0 \\ 0 & 0 & 1-\frac{\Omega^2}{\omega^2} \end{pmatrix} \\ &= i\frac{n_e e^2}{\omega m_e}\frac{1}{1-\Omega^2/\omega^2}\begin{pmatrix} 1 & -i\frac{\Omega}{\omega} & 0 \\ i\frac{\Omega}{\omega} & 1 & 0 \\ 0 & 0 & 1-\frac{\Omega^2}{\omega^2} \end{pmatrix} \end{aligned}$$

Dielectric tensor is obtained from conductivity tensor

$$\frac{i}{\omega\epsilon_0}\overleftrightarrow{\sigma} = -\frac{n_e e^2}{\epsilon_0 m_e}\frac{1}{\omega^2}\frac{1}{1-\Omega^2/\omega^2}\begin{pmatrix} 1 & -i\frac{\Omega}{\omega} & 0 \\ i\frac{\Omega}{\omega} & 1 & 0 \\ 0 & 0 & 1-\frac{\Omega^2}{\omega^2} \end{pmatrix}$$

$$= -\frac{\omega_p^2}{\omega^2-\Omega^2}\begin{pmatrix} 1 & -i\frac{\Omega}{\omega} & 0 \\ i\frac{\Omega}{\omega} & 1 & 0 \\ 0 & 0 & 1-\frac{\Omega^2}{\omega^2} \end{pmatrix} \qquad \omega_p^2 = \frac{n_e e^2}{\epsilon_0 m_e}$$

$$= \begin{pmatrix} -\frac{\omega_p^2}{\omega^2-\Omega^2} & i\frac{\Omega}{\omega}\frac{\omega_p^2}{\omega^2-\Omega^2} & 0 \\ -i\frac{\Omega}{\omega}\frac{\omega_p^2}{\omega^2-\Omega^2} & -\frac{\omega_p^2}{\omega^2-\Omega^2} & 0 \\ 0 & 0 & -\frac{\omega_p^2}{\omega^2} \end{pmatrix}$$

$$\overleftrightarrow{\varepsilon} = \overleftrightarrow{1} + \frac{i}{\omega\epsilon_0}\overleftrightarrow{\sigma} = \begin{pmatrix} 1-\frac{\omega_p^2}{\omega^2-\Omega^2} & i\frac{\Omega}{\omega}\frac{\omega_p^2}{\omega^2-\Omega^2} & 0 \\ -i\frac{\Omega}{\omega}\frac{\omega_p^2}{\omega^2-\Omega^2} & 1-\frac{\omega_p^2}{\omega^2-\Omega^2} & 0 \\ 0 & 0 & 1-\frac{\omega_p^2}{\omega^2} \end{pmatrix}$$

Assuming the wave is on the yz plane

let $X \equiv \dfrac{\omega_{\mathrm{p}}^2}{\omega^2}$ $\qquad Y \equiv \dfrac{\Omega}{\omega}$

$$\overleftrightarrow{\varepsilon} = \begin{pmatrix} 1-\frac{X}{1-Y^2} & i\frac{XY}{1-Y^2} & 0 \\ -i\frac{XY}{1-Y^2} & 1-\frac{X}{1-Y^2} & 0 \\ 0 & 0 & 1-X \end{pmatrix}$$

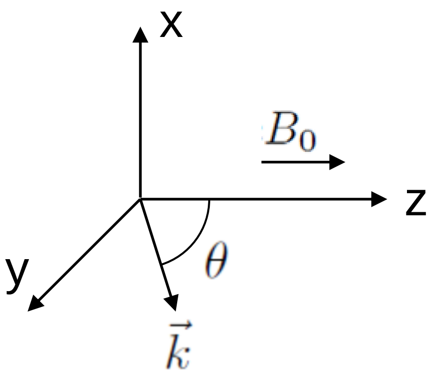

$$\vec{k} = k\,(0, \sin\theta, \cos\theta)$$

$$k_{\mathrm{i}} = 0\ ,\ k_{\mathrm{j}} = k\sin\theta\ ,\ k_{\mathrm{k}} = k\cos\theta$$

$$\vec{k}:\vec{k} = \begin{pmatrix} 0 \\ k\sin\theta \\ k\cos\theta \end{pmatrix} \cdot \begin{pmatrix} 0 & k\sin\theta & k\cos\theta \end{pmatrix} = \begin{pmatrix} 0 & 0 & 0 \\ 0 & \sin^2\theta & \sin\theta\cos\theta \\ 0 & \sin\theta\cos\theta & \cos^2\theta \end{pmatrix}$$

$$n \equiv \frac{kc}{\omega} \qquad \frac{\omega^2}{c^2}\overleftrightarrow{\varepsilon} = \frac{k^2\omega^2}{k^2c^2}\overleftrightarrow{\varepsilon} = \frac{k^2}{n^2}\overleftrightarrow{\varepsilon}$$

$$\det\left(\vec{k}:\vec{k} - k^2\overleftrightarrow{1} + \frac{\omega^2}{c^2}\overleftrightarrow{\varepsilon}\right) = 0$$

Reflective index

$$\begin{vmatrix} -k^2+\frac{k^2}{n^2}\left(1-\frac{X}{1-Y^2}\right) & i\frac{k^2}{n^2}\frac{XY}{1-Y^2} & 0 \\ -i\frac{k^2}{n^2}\frac{XY}{1-Y^2} & k^2\sin^2\theta-k^2+\frac{k^2}{n^2}\left(1-\frac{X}{1-Y^2}\right) & k^2\sin\theta\cos\theta \\ 0 & k^2\sin\theta\cos\theta & k^2\cos^2\theta-k^2+\frac{k^2}{n^2}(1-X) \end{vmatrix}=0$$

$$\begin{vmatrix} -n^2+1-\frac{X}{1-Y^2} & i\frac{XY}{1-Y^2} & 0 \\ -i\frac{XY}{1-Y^2} & -n^2\cos^2\theta+1-\frac{X}{1-Y^2} & n^2\sin\theta\cos\theta \\ 0 & n^2\sin\theta\cos\theta & -n^2\sin^2\theta+1-X \end{vmatrix}=0$$

$$n^2=1-\frac{X(1-X)}{1-X-\frac{1}{2}Y^2\sin^2\theta\pm\left[\left(\frac{1}{2}Y^2\sin^2\theta\right)^2+(1-X)^2Y^2\cos^2\theta\right]^{1/2}}$$

Wave is circular polarized propagating along the magnetic field

- **Parallel to B_0** $(\theta = 0)$

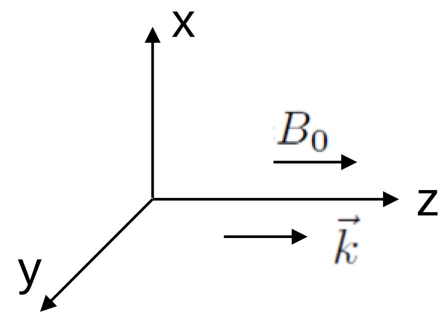

$$n^2 = 1 - \frac{X(1-X)}{1 - X \pm \left[(1-X)^2 Y^2\right]^{1/2}} = 1 - \frac{X}{1 \pm Y} = 1 - \frac{\omega_{\mathrm{p}}^2/\omega^2}{1 \pm \Omega/\omega} = 1 - \frac{\omega_{\mathrm{p}}^2}{\omega(\omega \pm \Omega)}$$

$$\begin{pmatrix} -n^2 + 1 - \frac{X}{1-Y^2} & i\frac{XY}{1-Y^2} & 0 \\ -i\frac{XY}{1-Y^2} & -n^2\cos^2\theta + 1 - \frac{X}{1-Y^2} & 0 \\ 0 & 0 & 1-X \end{pmatrix} \begin{pmatrix} E_{\mathrm{x}} \\ E_{\mathrm{y}} \\ E_{\mathrm{z}} \end{pmatrix} = 0$$

$$\left(-n^2 + 1 - \frac{X}{1-Y^2}\right) E_{\mathrm{x}} + i\frac{XY}{1-Y^2} E_{\mathrm{y}} = \frac{\mp XY}{1-Y^2} E_{\mathrm{x}} + i\frac{XY}{1-Y^2} E_{\mathrm{y}} = 0$$

$$\frac{E_{\mathrm{x}}}{E_{\mathrm{y}}} = \pm i$$ **Left hang circular (LHC) or right hang circular (RHC) polarized.**

Electric field is not necessary parallel to the propagating direction which is perpendicular to B_0

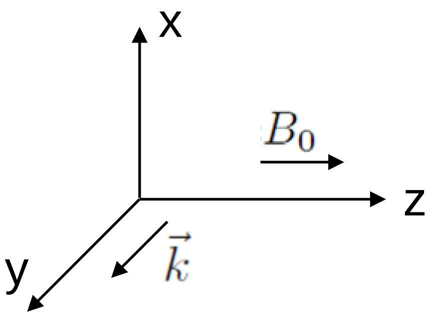

- **Perpendicular to B_0** $\left(\theta = \frac{\pi}{2}\right)$

$$n^2 = 1 - \frac{X(1-X)}{1 - X - \frac{1}{2}Y^2 \pm \frac{1}{2}Y^2} = 1 - X \text{ or } 1 - \frac{X(1-X)}{1 - X - Y^2}$$

$$\begin{pmatrix} -n^2 + 1 - \frac{X}{1-Y^2} & i\frac{XY}{1-Y^2} & 0 \\ -i\frac{XY}{1-Y^2} & 1 - \frac{X}{1-Y^2} & 0 \\ 0 & 0 & -n^2 + 1 - X \end{pmatrix} \begin{pmatrix} E_\mathrm{x} \\ E_\mathrm{y} \\ E_\mathrm{z} \end{pmatrix} = 0$$

$$n^2 = 1 - \frac{\omega_\mathrm{p}^2}{\omega^2} \qquad E_\mathrm{x} = E_\mathrm{y} = 0$$ **Ordinary wave (O-wave)**

$$n^2 = 1 - \frac{\omega_\mathrm{p}^2\left(1 - \omega_\mathrm{p}^2/\omega^2\right)}{\omega^2 - \omega_\mathrm{p}^2 - \Omega^2} \qquad \frac{E_\mathrm{x}}{E_\mathrm{y}} = -i\omega\left(\frac{\omega^2 - \omega_\mathrm{p}^2 - \Omega^2}{\omega_\mathrm{p}^2\Omega}\right) \qquad E_\mathrm{z} = 0$$

Extraordinary wave (E-wave)

The electric field of an extraordinary wave rotates elliptically

Ordinary wave (O-wave)

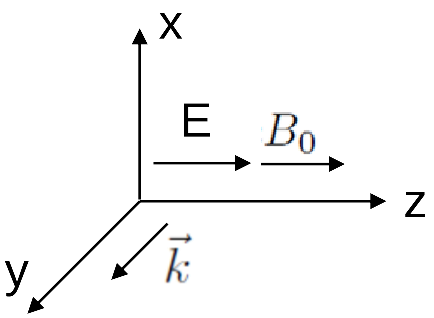

Extraordinary wave (E-wave)

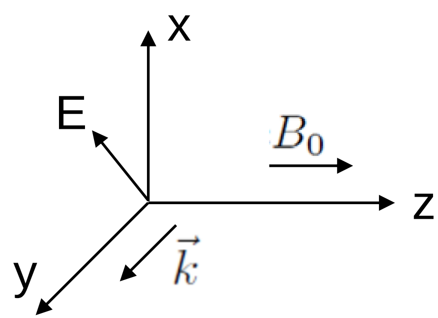

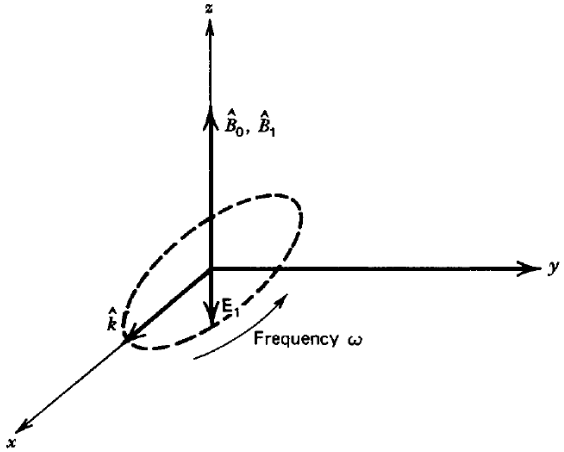

Electromagnetic wave can be used to measure the density or the magnetic field in the plasma

- **Nonmagnetized isotropic plasma (interferometer needed):**

$$n^2 = 1 - \frac{X(1-X)}{1 - X - \frac{1}{2}Y^2\sin^2\theta \pm \left[\left(\frac{1}{2}Y^2\sin^2\theta\right)^2 + (1-X)^2 Y^2\cos^2\theta\right]^{1/2}}$$

$$= 1 - X = 1 - \frac{\omega_{\mathrm{p}}^2}{\omega^2} = 1 - \frac{n_{\mathrm{e}}}{n_{\mathrm{cr}}} \qquad \left(Y \equiv \frac{\Omega}{\omega} \equiv 0\right)$$

Note: $\omega_{\mathrm{p}}^2 = \frac{n_{\mathrm{e}}e^2}{\epsilon_0 m_{\mathrm{e}}}$ $\quad n_{\mathrm{cr}} = \frac{\epsilon_0 m_{\mathrm{e}}\omega^2}{e^2}$

- **Magnetized isotropic plasma (Polarization detected needed):**

Parallel to B_0

$$n^2 = 1 - \frac{\omega_{\mathrm{p}}^2}{\omega(\omega \pm \Omega)} \qquad \frac{E_{\mathrm{x}}}{E_{\mathrm{y}}} = \pm i \qquad \Omega \equiv \frac{eB_0}{m_{\mathrm{e}}}$$

Faraday rotation: linear polarization rotation caused by the difference between the speed of LHC and RHC polarized wave.

Electromagnetic wave can be used to measure the density or the magnetic field in the plasma

- **Nonmagnetized isotropic plasma (interferometer needed):**

$$n^2 = 1 - \frac{X(1-X)}{1 - X - \frac{1}{2}Y^2\sin^2\theta \pm \left[\left(\frac{1}{2}Y^2\sin^2\theta\right)^2 + (1-X)^2 Y^2\cos^2\theta\right]^{1/2}}$$

$$= 1 - X = 1 - \frac{\omega_{\mathrm{p}}^2}{\omega^2} = 1 - \frac{n_{\mathrm{e}}}{n_{\mathrm{cr}}} \qquad \left(\boldsymbol{Y \equiv \frac{\Omega}{\omega} \equiv 0}\right)$$

Note: $\omega_{\mathrm{p}}^2 = \frac{n_{\mathrm{e}}e^2}{\epsilon_0 m_{\mathrm{e}}}$ $\qquad n_{\mathrm{cr}} = \frac{\epsilon_0 m_{\mathrm{e}}\omega^2}{e^2}$

- **Magnetized isotropic plasma (Polarization detected needed):**

Parallel to B_0

$$n^2 = 1 - \frac{\omega_{\mathrm{p}}^2}{\omega(\omega \pm \Omega)} \qquad \frac{E_{\mathrm{x}}}{E_{\mathrm{y}}} = \pm i \qquad \Omega \equiv \frac{eB_0}{m_{\mathrm{e}}}$$

Faraday rotation: linear polarization rotation caused by the difference between the speed of LHC and RHC polarized wave.

There are two main style of interferometer

Michelson interferometer

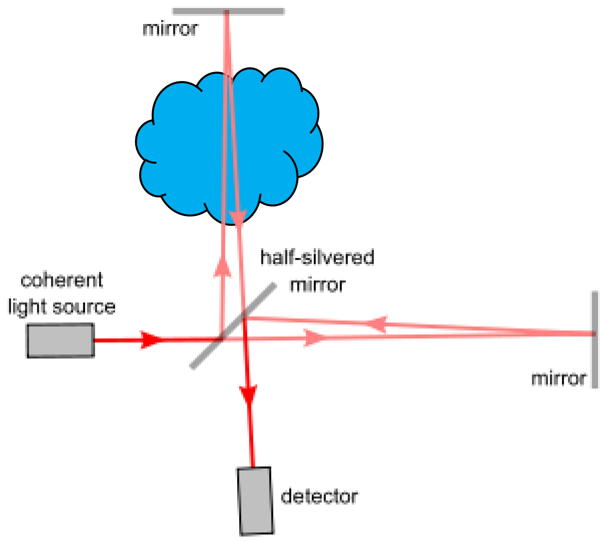

Mach-zehnder interferometer

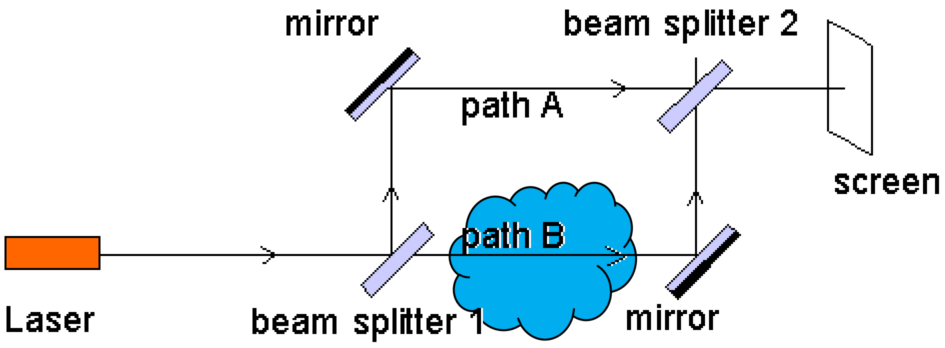

Interference pattern are due to the phase difference between two different path

$$E_1 = E_1 \exp\left(-i\omega t\right)$$

$$E_2 = E_2 \exp\left(-i\omega t + i\phi\right)$$

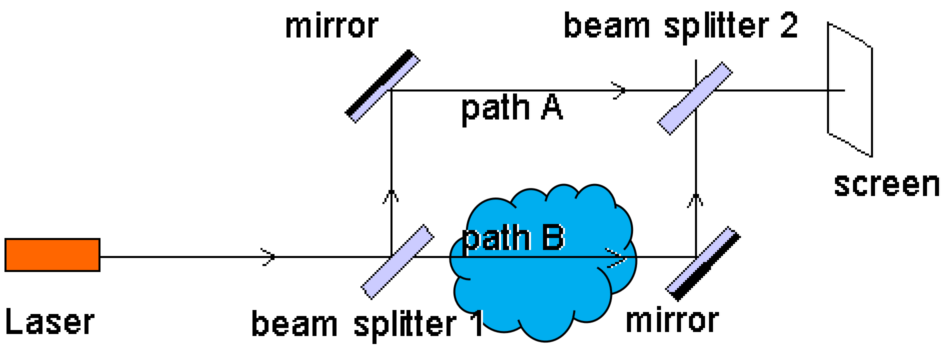

$$E = E_1 + E_2 = \left[E_1 + E_2 \exp\left(i\phi\right)\right] \exp\left(-i\omega t\right)$$

$$\begin{aligned} I &= |E|^2 = E^* E = \left[E_1 + E_2 \exp\left(-i\phi\right)\right] \exp\left(i\omega t\right) \left[E_1 + E_2 \exp\left(i\phi\right)\right] \exp\left(-i\omega t\right) \\ &= E_1^2 + E_2^2 + E_1 E_2 \exp\left(i\phi\right) + E_1 E_2 \exp\left(-i\phi\right) \\ &= E_1^2 + E_2^2 + 2E_1 E_2 \cos\phi \\ &= \left(E_1^2 + E_2^2\right)\left(1 + \frac{2E_1E_2}{E_1^2 + E_2^2}\cos\phi\right) \end{aligned}$$

The intensity on screen depends on the phase different between two paths

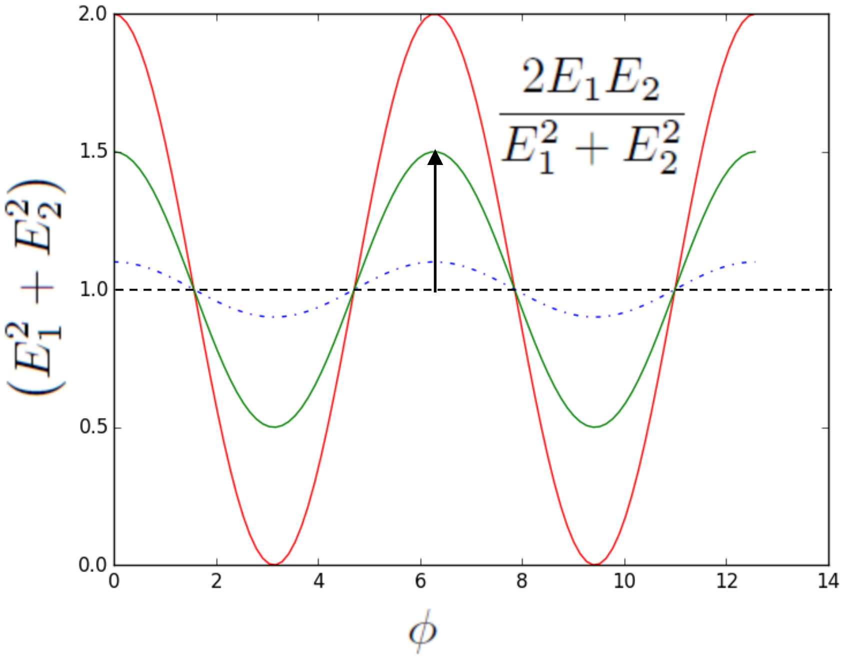

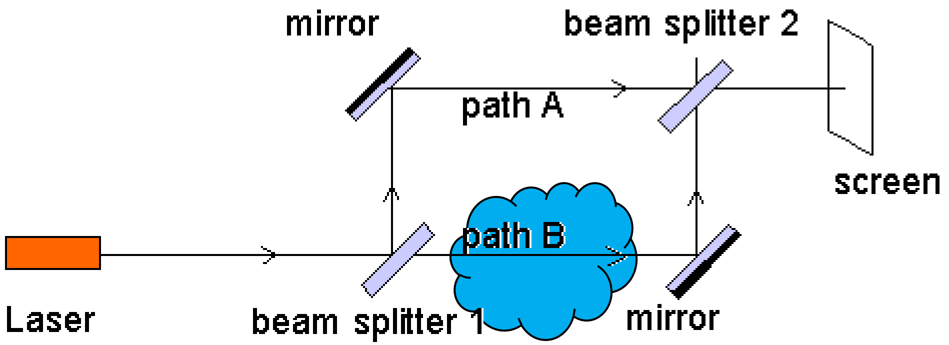

$$I = (E_1^2+E_2^2)\left(1+\frac{2E_1E_2}{E_1^2+E_2^2}\cos\phi\right)$$

The phase different depends on the line integral of the electron density along the path

$$\phi = \int k dl = \int n \frac{\omega}{c} dl$$

$$n^2 = 1 - \frac{n_e}{n_{cr}} \qquad n_{cr} = \frac{\epsilon_0 m_e \omega^2}{e^2}$$

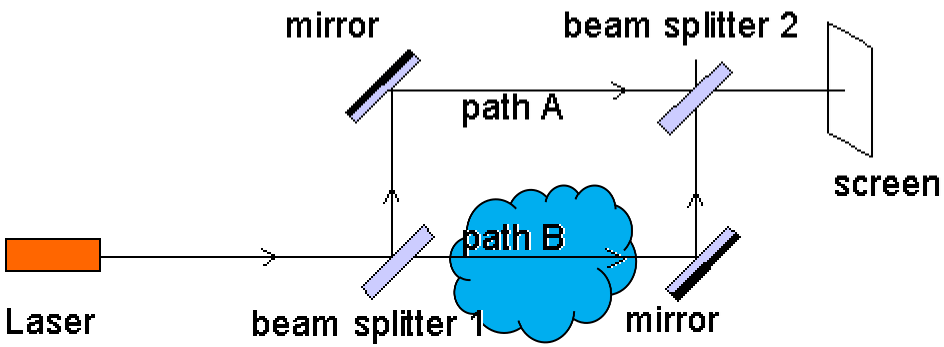

$$\begin{aligned}
\Delta\phi &= \int (k_{\text{plasma}} - k_0)\, dl = \frac{\omega}{c}\int (n-1)\, dl \\
&= \frac{\omega}{c}\int \left(\sqrt{1 - \frac{n_e}{n_c}} - 1\right) dl \approx \frac{\omega}{c}\int \left(1 - \frac{1}{2}\frac{n_e}{n_c} - 1\right) dl \\
&= -\frac{\omega}{2 c n_c}\int n_e dl
\end{aligned}$$

Note that $n_e << n_{cr}$ **is assumed,** $\sqrt{1 - \frac{n_e}{n_{cr}}} \approx 1 - \frac{1}{2}\frac{n_e}{n_{cr}}$

The phase is determined by comparing to the pattern without the phase shift

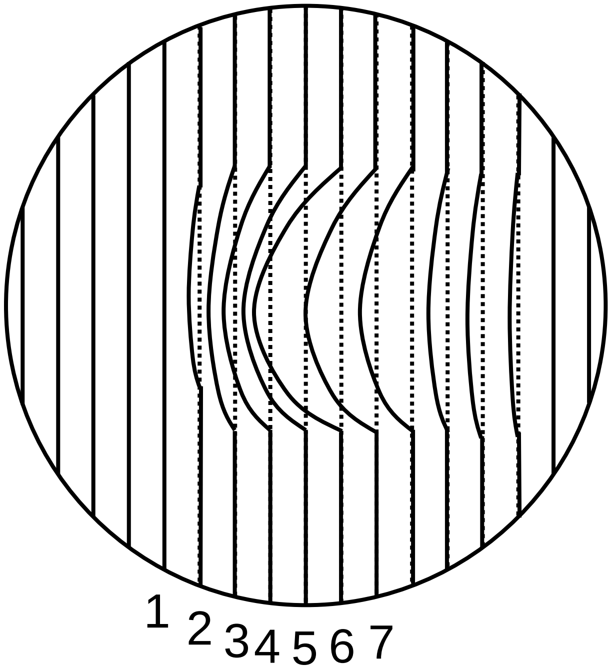

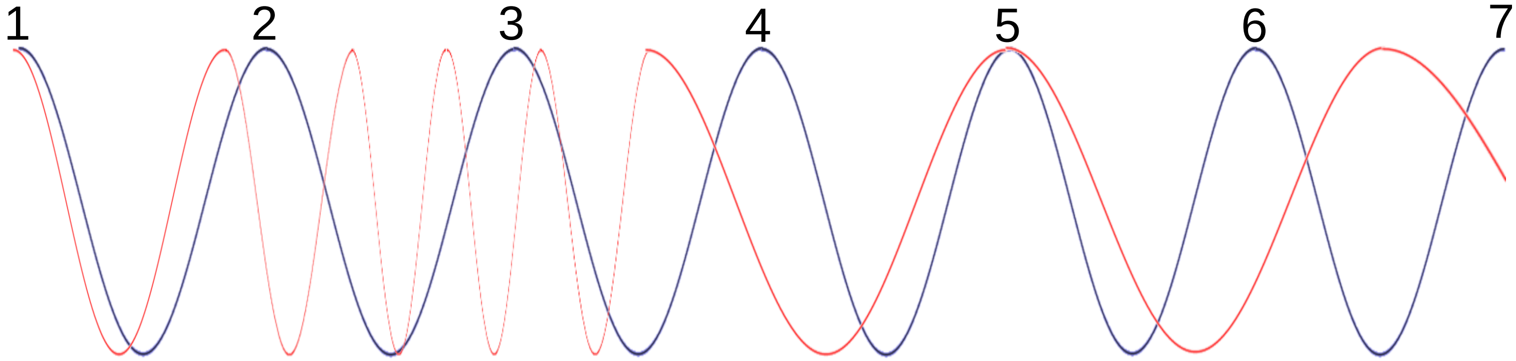

Fourier transform can be used to retrieve the data from the interferometer image

$$\mathrm{I}(x,y) = I_0(x,y) + m(x,y)\cos[2\pi\nu_0 x + \phi(x,y)] \qquad cos(x) = \frac{e^{ix}+e^{-ix}}{2}$$

$$= I_0(x,y) + \frac{1}{2}m(x,y)\left(e^{i[2\pi\nu_0 x+\phi(x,y)]} + e^{-i[2\pi\nu_0 x+\phi(x,y)]}\right)$$

$$= I_0(x,y) + \frac{1}{2}m(x,y)e^{i\phi(x,y)}e^{i2\pi\nu_0 x} + \frac{1}{2}m(x,y)e^{-i\phi(x,y)}e^{-i2\pi\nu_0 x}$$

$$= I_0(x,y) + c(x,y)e^{i2\pi\nu_0 x} + c^*(x,y)e^{-i2\pi\nu_0 x}$$

$$c(x,y) \equiv \frac{1}{2}m(x,y)e^{i\phi(x,y)} \qquad \phi(x,y) = \tan^{-1}\left(\frac{\mathrm{Im}[c(x,y)]}{\mathrm{Re}[c(x,y)]}\right)$$

$$\hat{g}(f_x,y) \equiv \mathrm{FT}[g(x,y)]$$

$$\hat{g}(f_x-\nu_0,y) = \mathrm{FT}\left[g(x,y)e^{i2\pi\nu_0 x}\right]$$

$$\hat{I}(f_x,y) = \hat{I}_0(f_x,y) + \hat{c}(f_x-\nu_0,y) + \hat{c}^*(f_x+\nu_0,y)$$

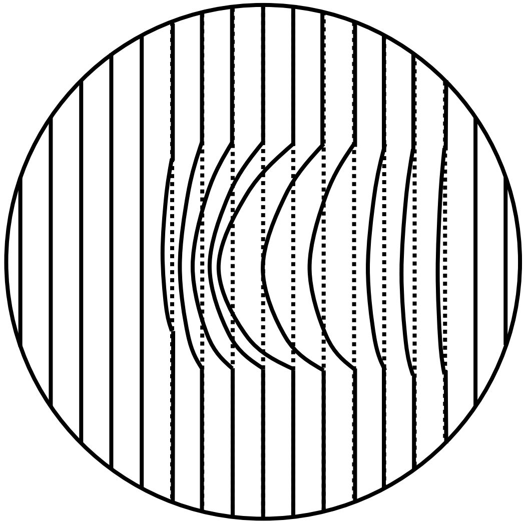

Basic knowledge of Fourier transform

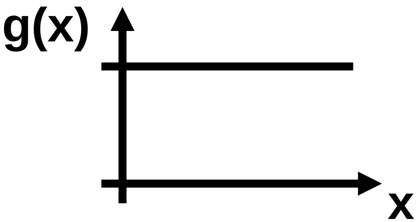

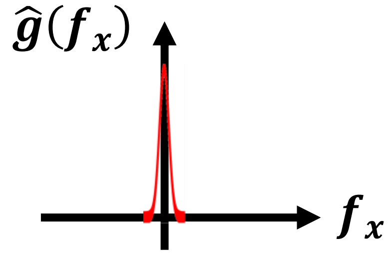

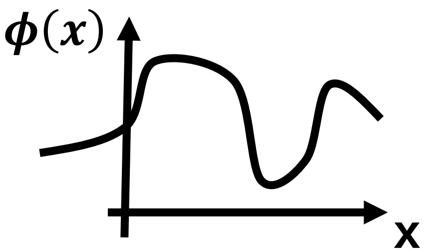

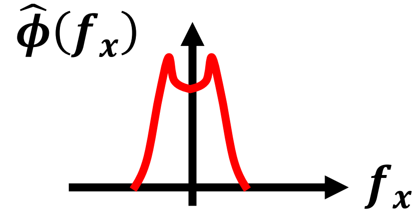

$$\mathrm{h}(x) = \phi(x) \times e^{-\mathrm{i}2\pi\nu_0 x}$$

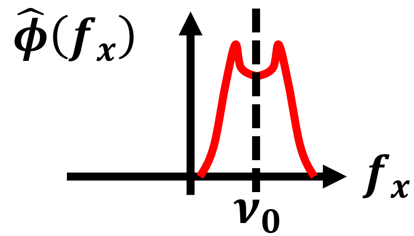

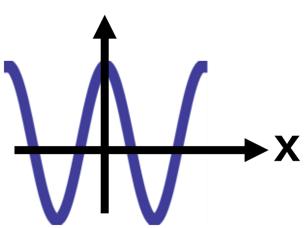

$$\mathrm{g}(x) = cos(2\pi\nu_0 x) = \frac{e^{\mathrm{i}2\pi\nu_0 x} + e^{-\mathrm{i}2\pi\nu_0 x}}{2}$$

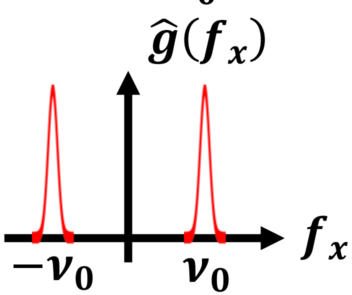

Procedure of retrieving data

$$\mathrm{I}(x) = I_0(x) + m(x)\cos[2\pi\nu_0 x + \phi(x)]$$
$$\equiv \cos[2\pi\nu_0 x + \phi(x)]$$
$$= c^*(x,y)e^{\mathrm{i}2\pi\nu_0 x} + c(x,y)e^{-\mathrm{i}2\pi\nu_0 x}$$

$$\hat{I}(f_x) = \hat{c}(f_x - \nu_0) + \hat{c}^*(f_x + \nu_0)$$

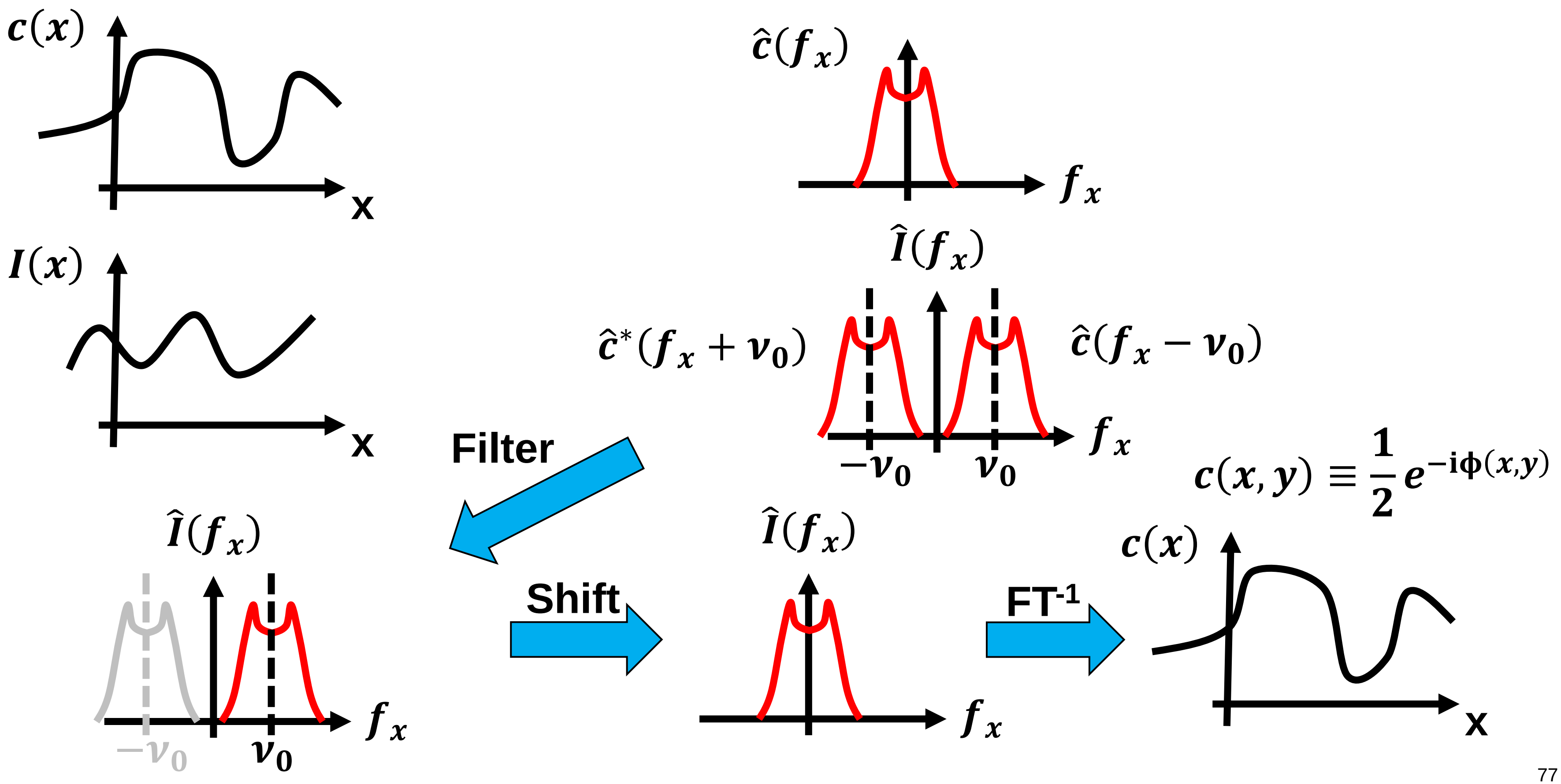

Example of retrieving data from 1D interferometer

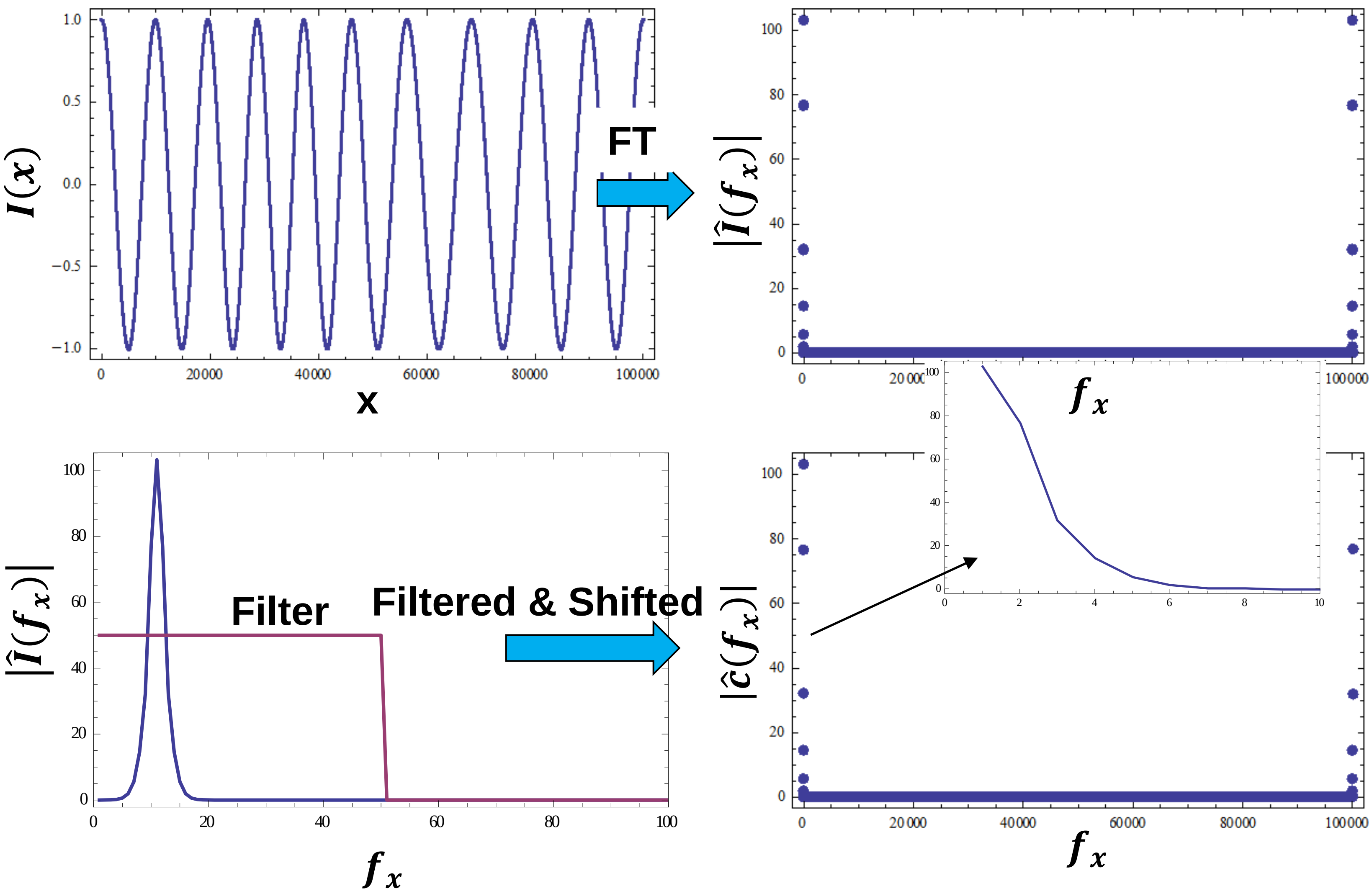

The retrieved data need to be modified if the phase change is too much

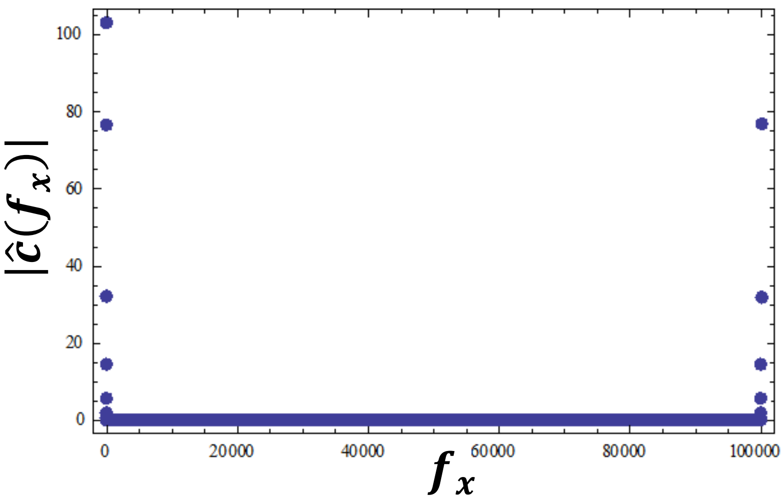

FT^{-1}& $\phi(x) = tan^{-1}\left(\frac{Im[c(x)]}{Re[c(x)]}\right)$

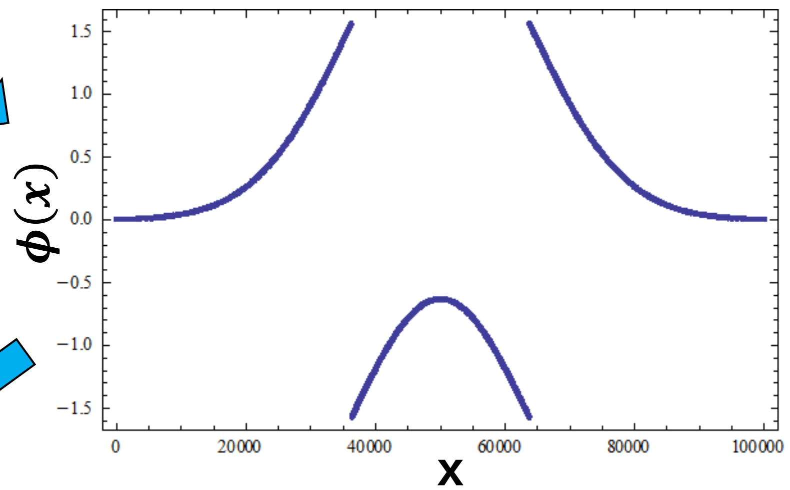

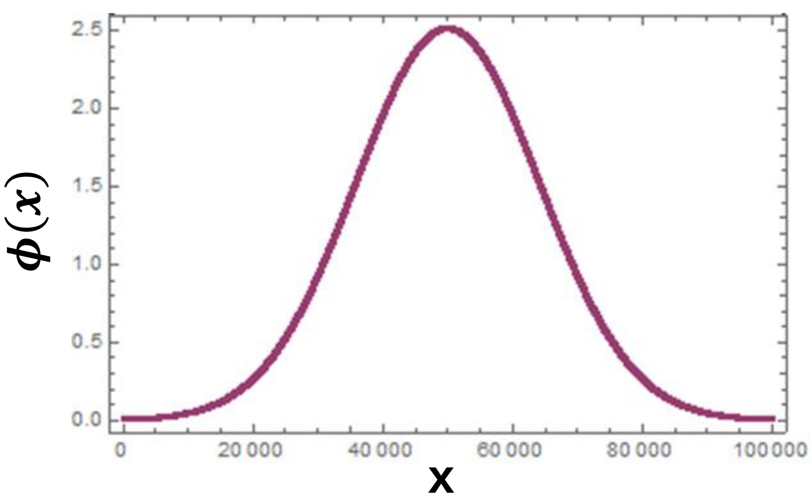

The final phase difference needs to be determined manually since it may exceeds 2π

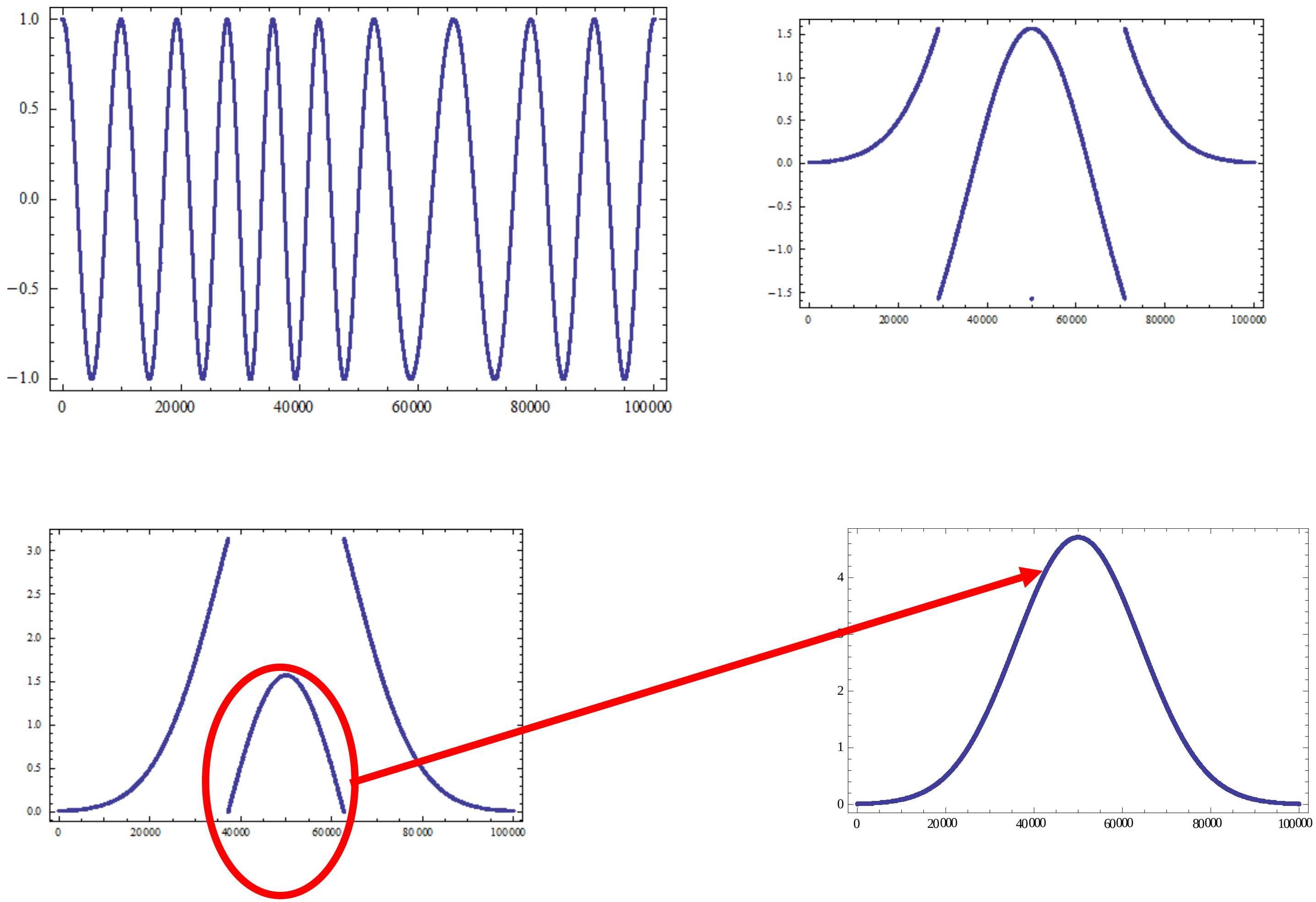

Example of retrieving data from 2D interferometer

$$\mathbf{I}(x,y) = \cos[2\pi \nu_0 x + \phi(x,y)]$$

$$\hat{I}(f_x, y) = \hat{c}(f_x - \nu_0, y) + \hat{c}^*(f_x + \nu_0, y)$$

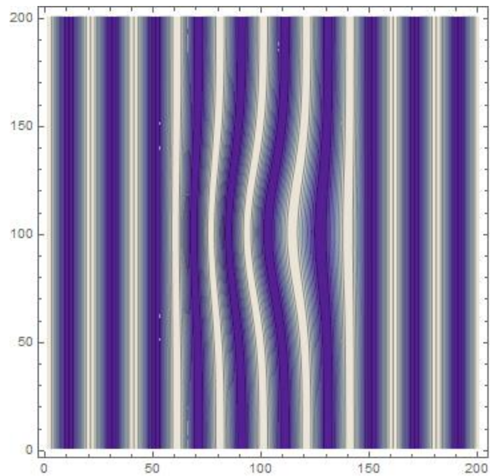

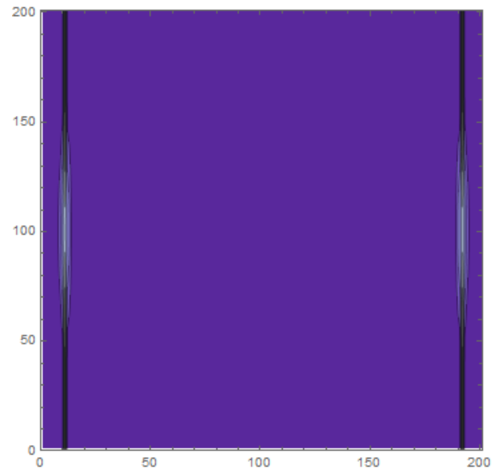

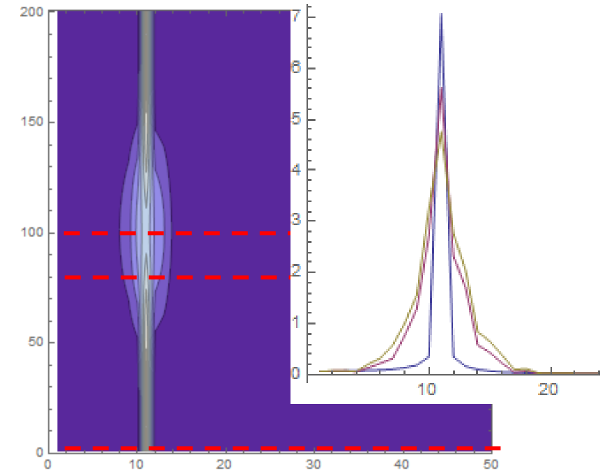

Filter

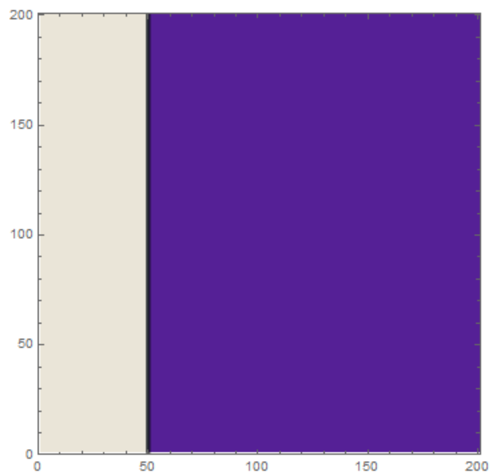

Filtered & Shifted

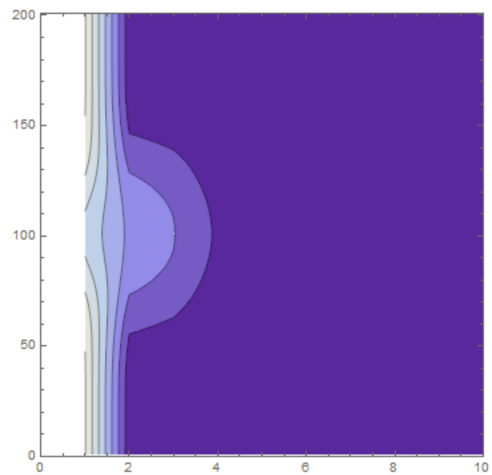

Retrieved data

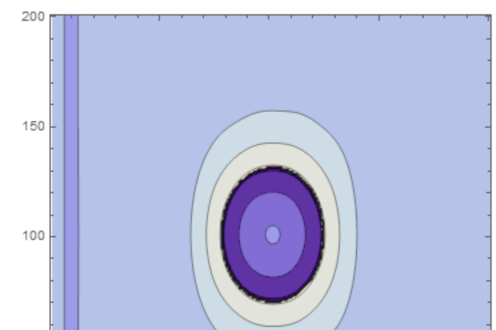

FT^{-1} &

$$\phi(x,y) = -\tan^{-1}\left(\frac{\mathrm{Im}[c(x,y)]}{\mathrm{Re}[c(x,y)]}\right)$$

The retrieved data may need to be modified if the phase change is too large

Retrieved data

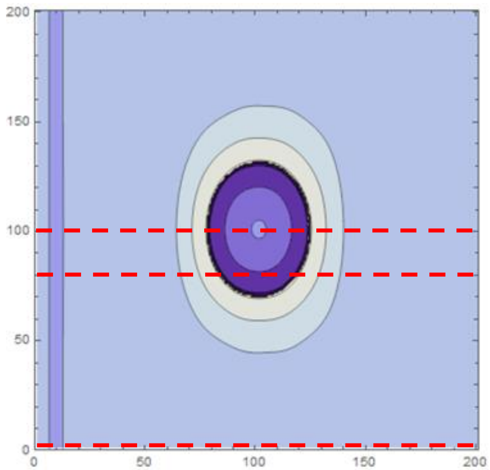

1D profile

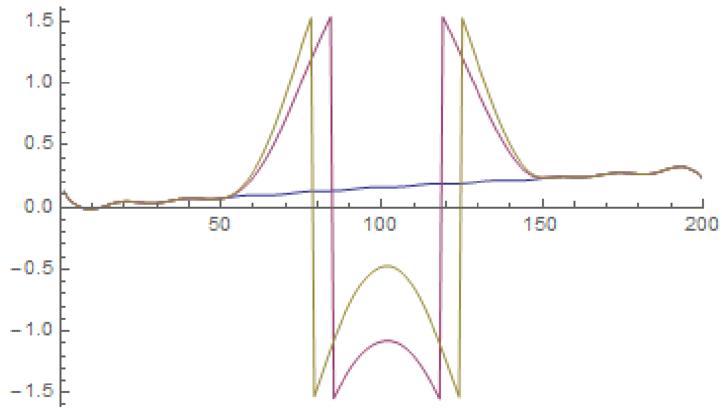

Modified result

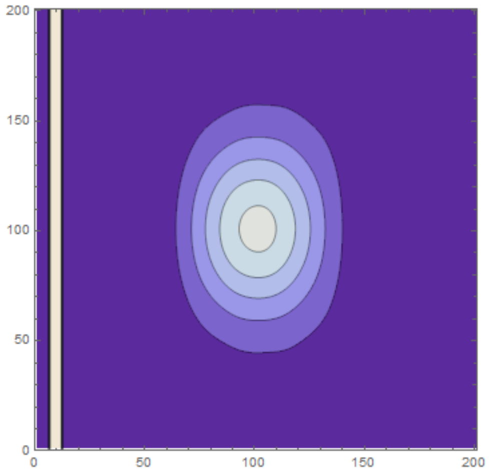

- **Noise came from low spatial resolution.**

Schlieren imaging system can detect density gradient

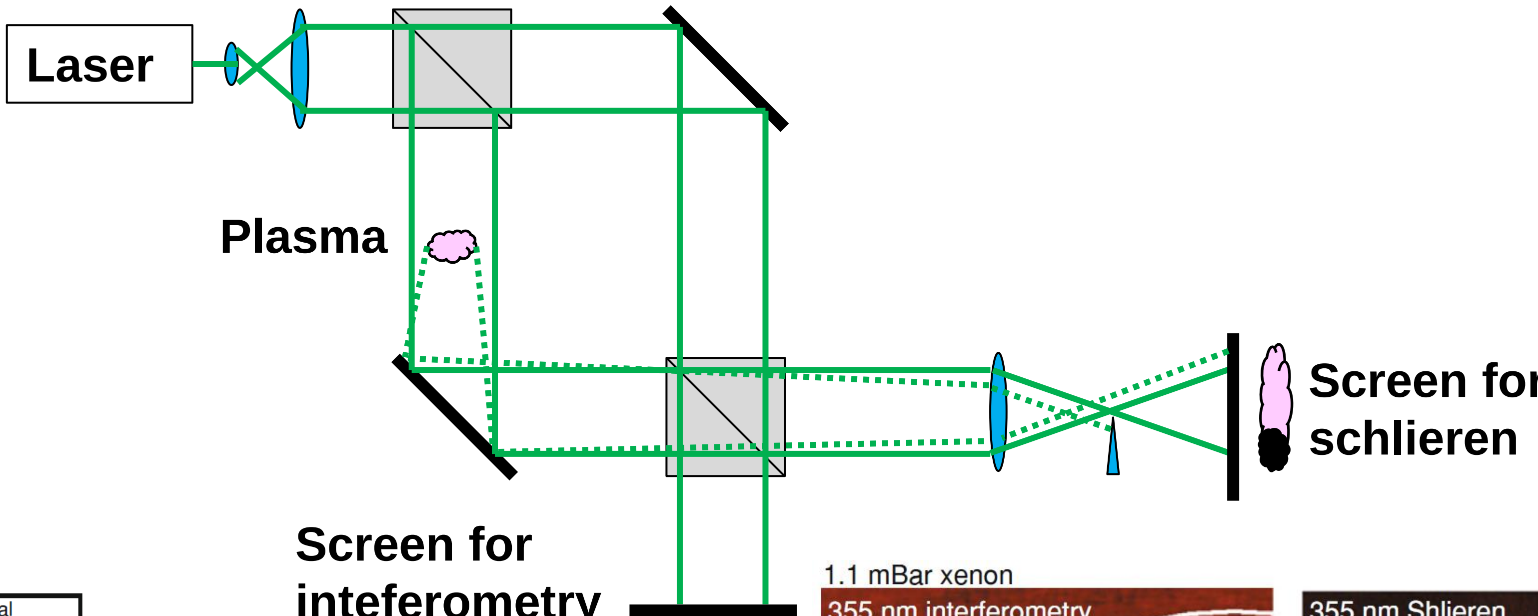

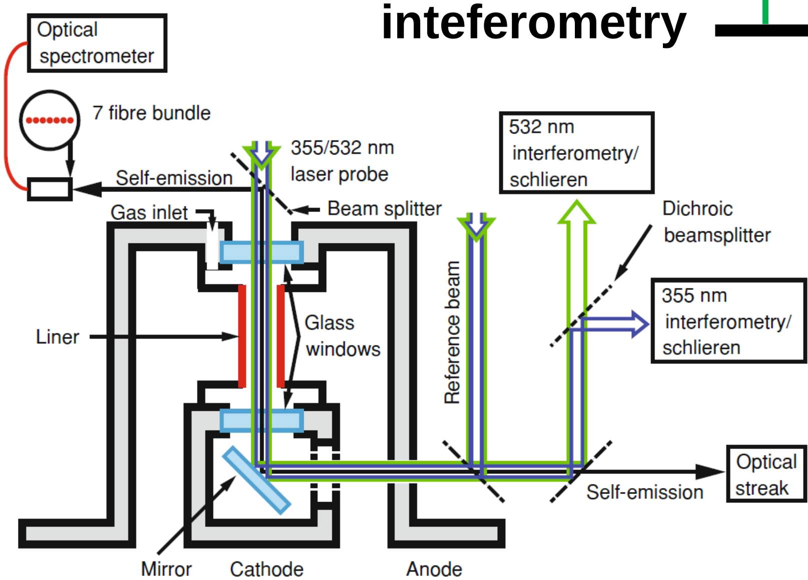

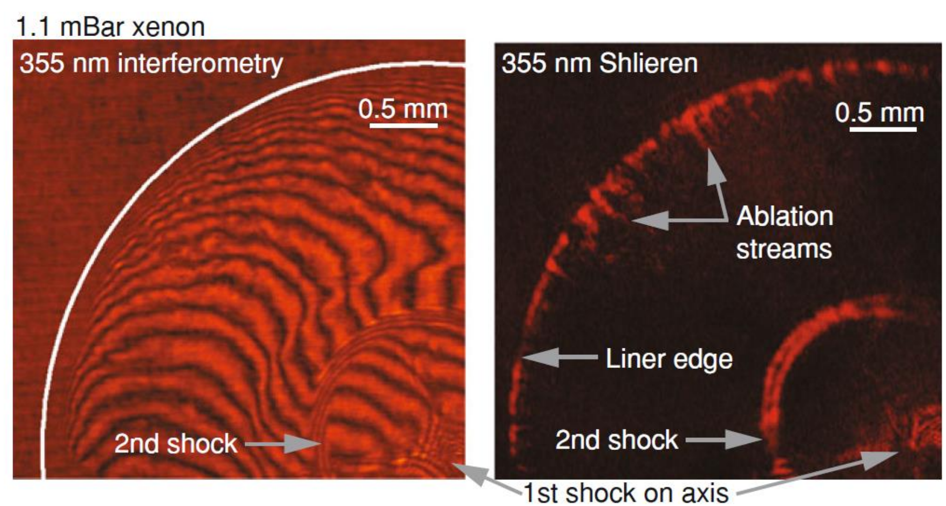

G. C. Burdiak, Cylindrical liner z-pinches as drivers for converging strong shock experiments

Angular filter refractometry (AFR) maps the refraction of the probe beam at TCC to contours in the image plane

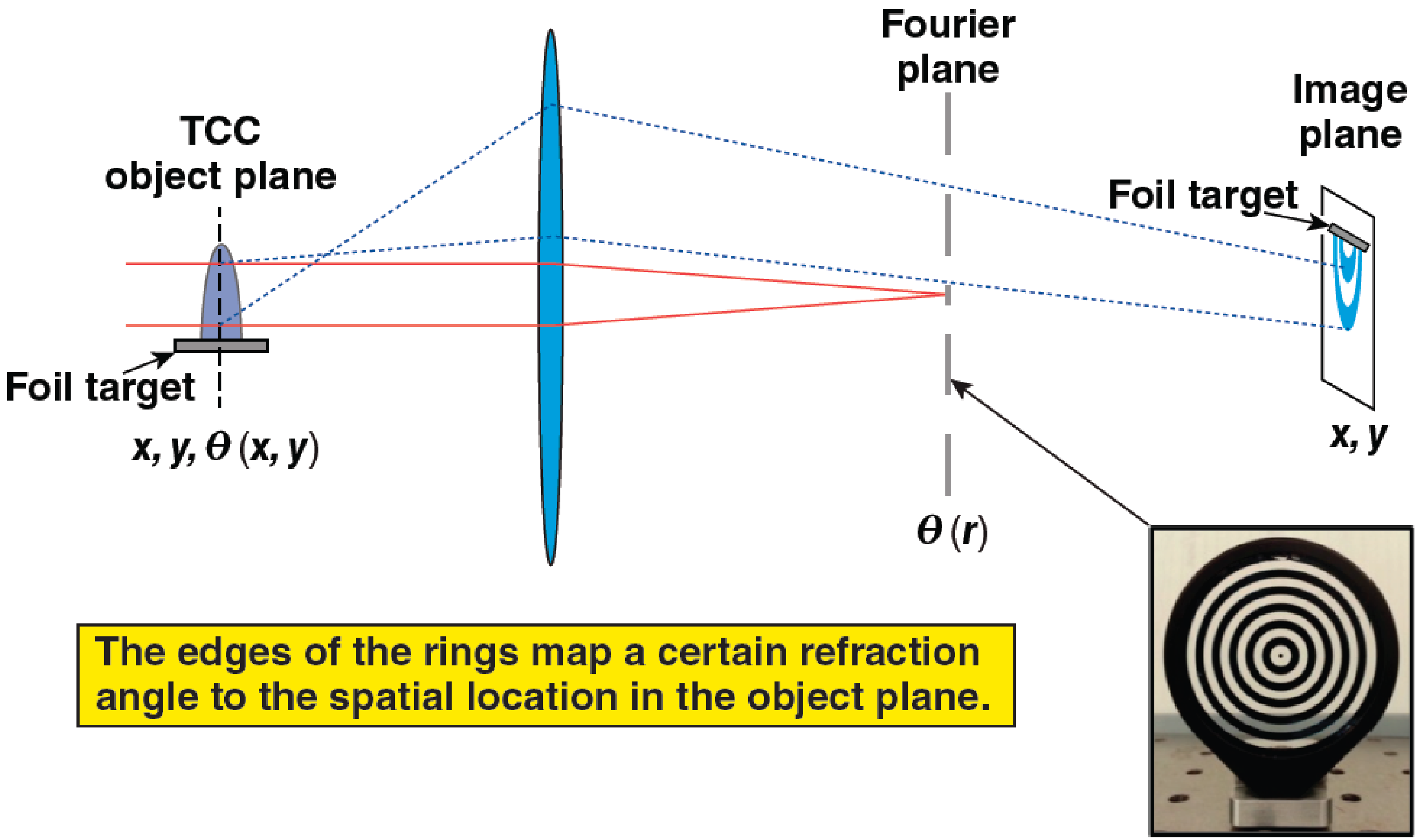

The edges of the rings map a certain refraction angle to the spatial location in the object plane.

Angular spectrum of plane waves can be used for diagnostic

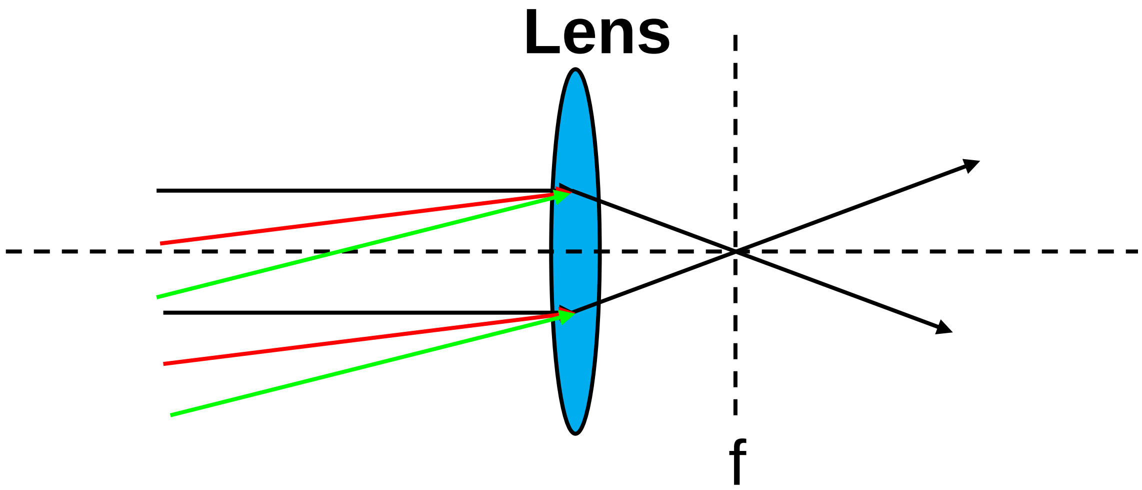

Angular spectrum of plane waves can be used for diagnostic

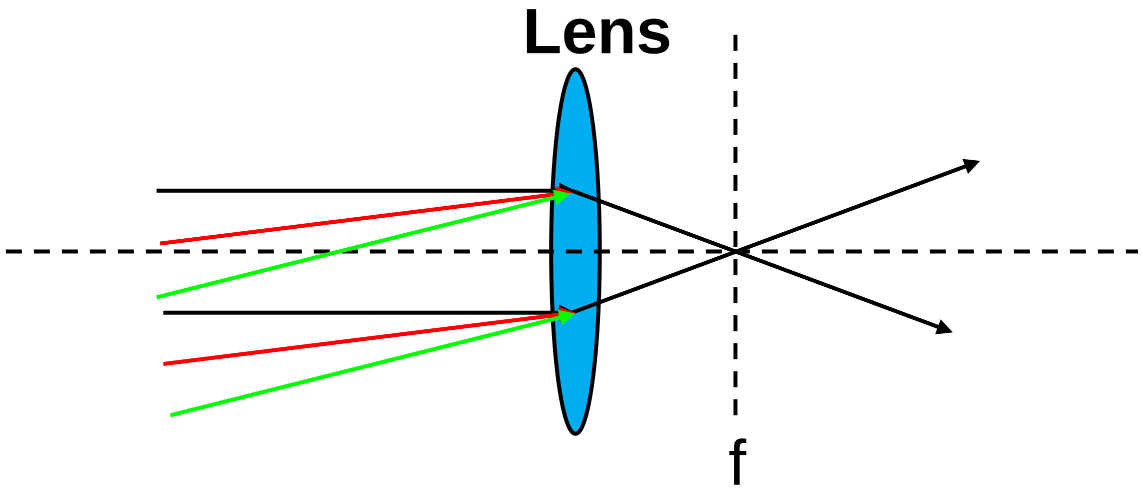

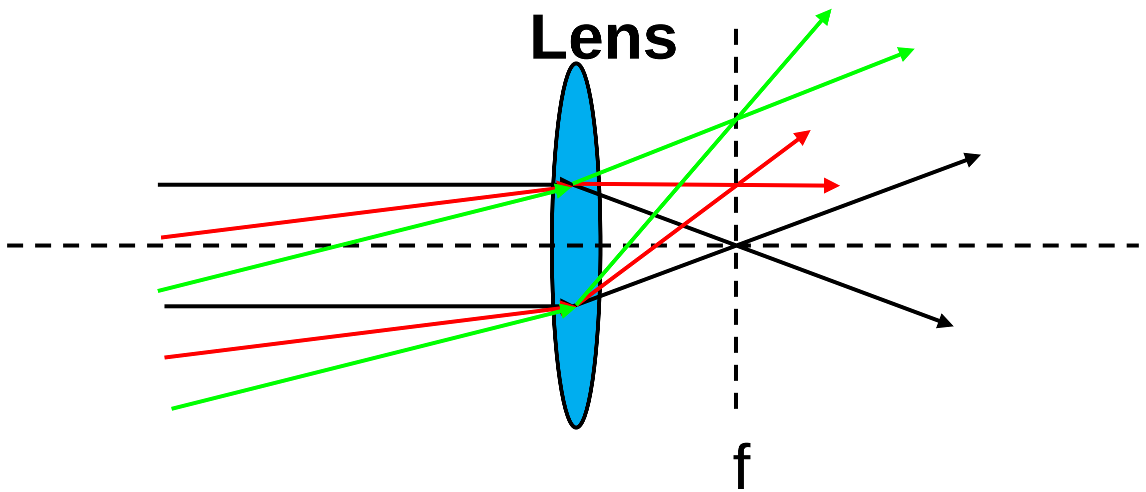

Rays with different angles go through different focal points on the focal points

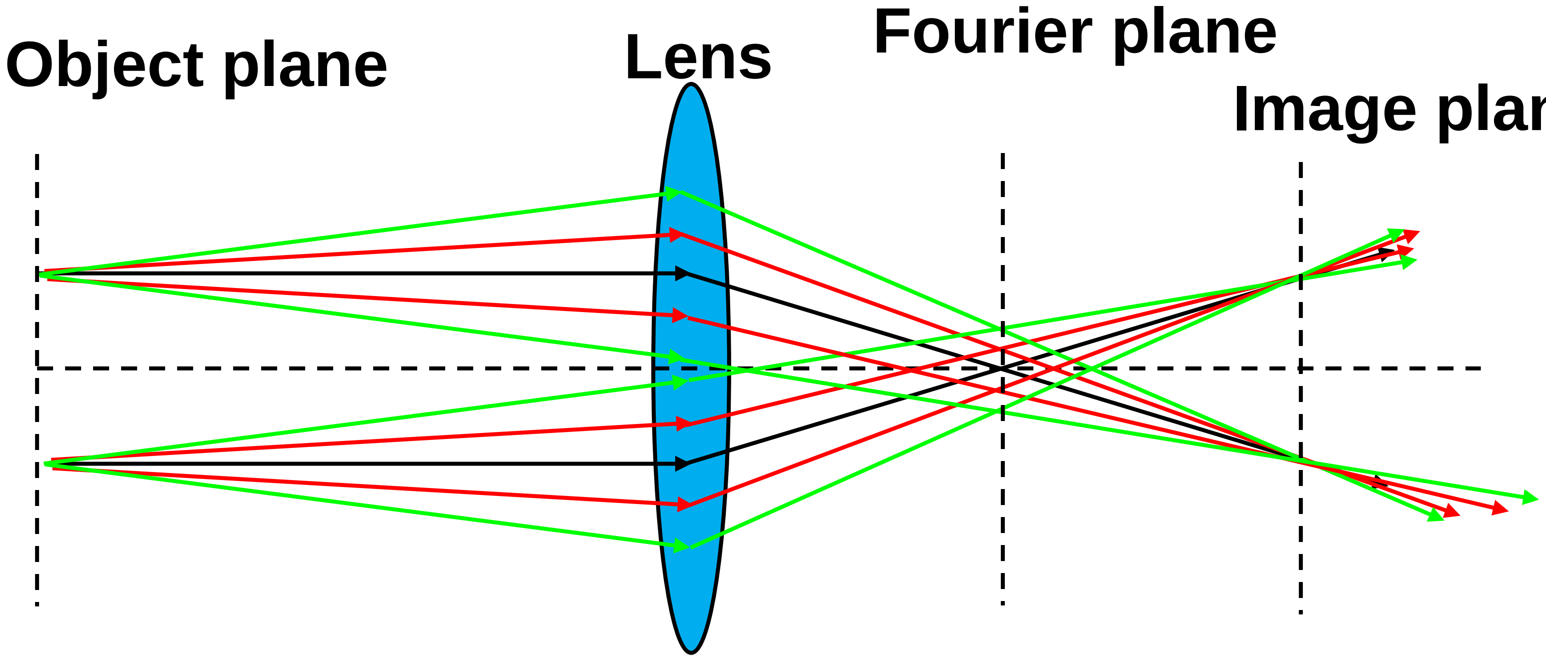

Rays with different angles can be selected by blocking different focal points

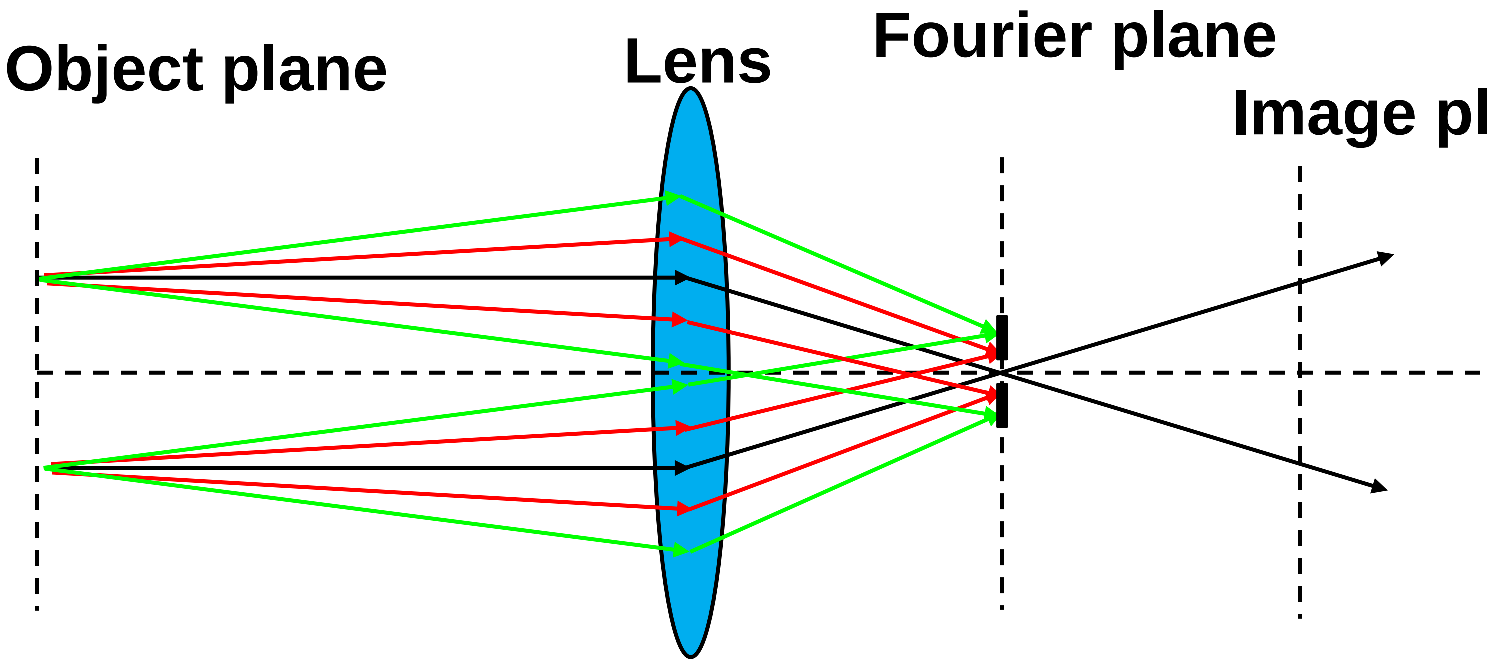

Rays with different angles go through different focal points on the focal points

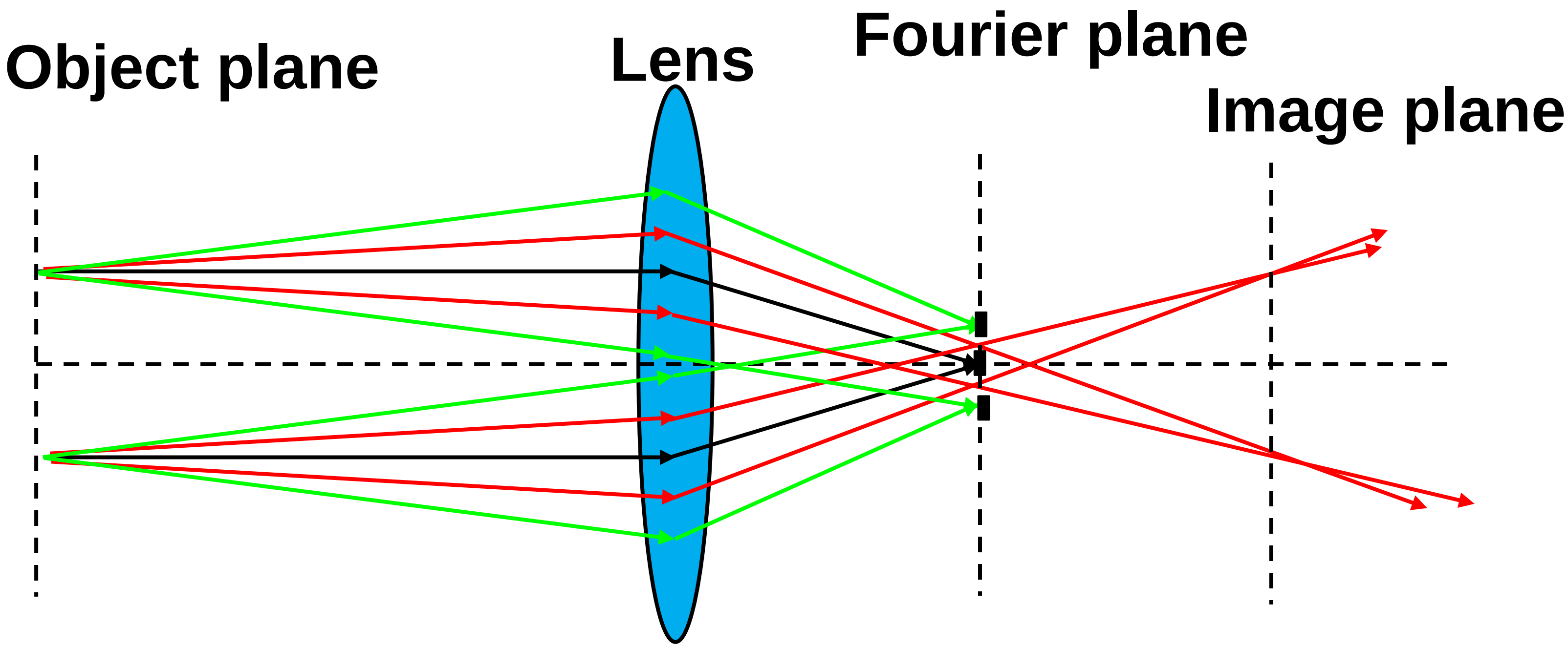

Rays with different angles go through different focal points on the focal points

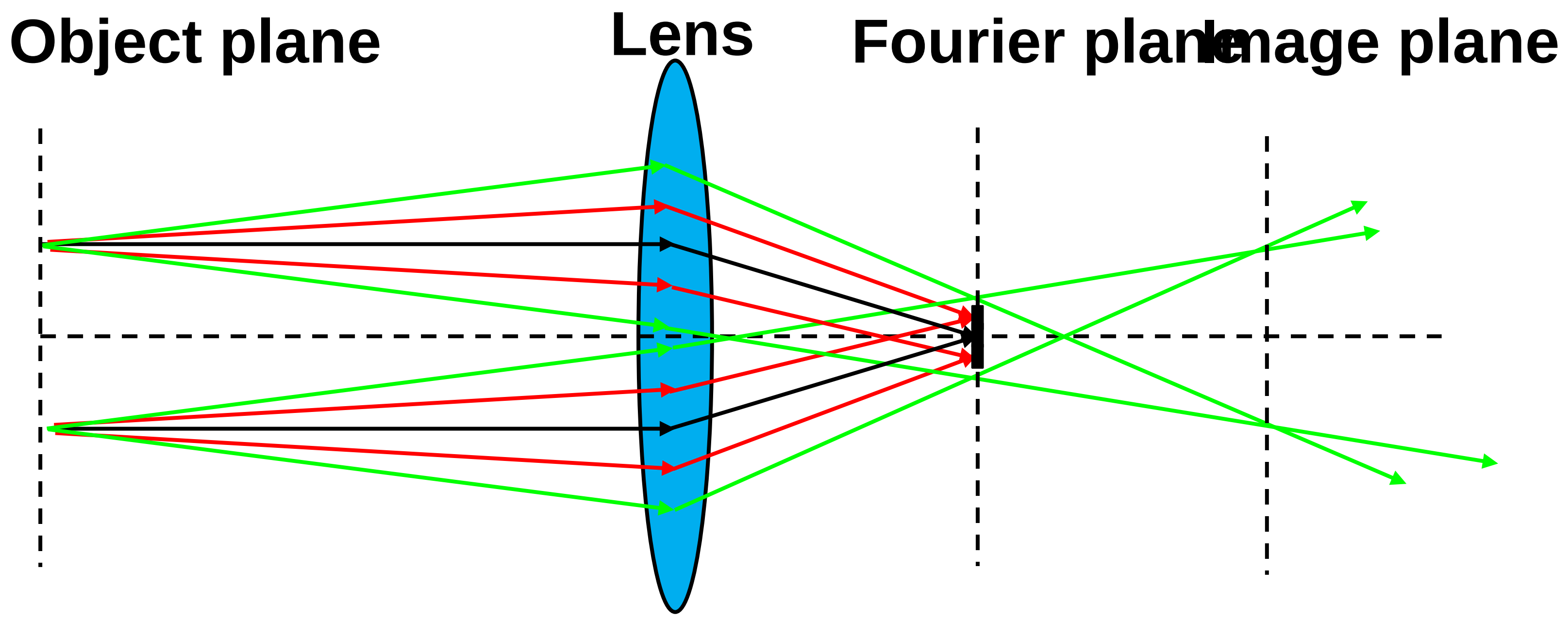

Angular filter refractometry (AFR) maps the refraction of the probe beam at TCC to contours in the image plane

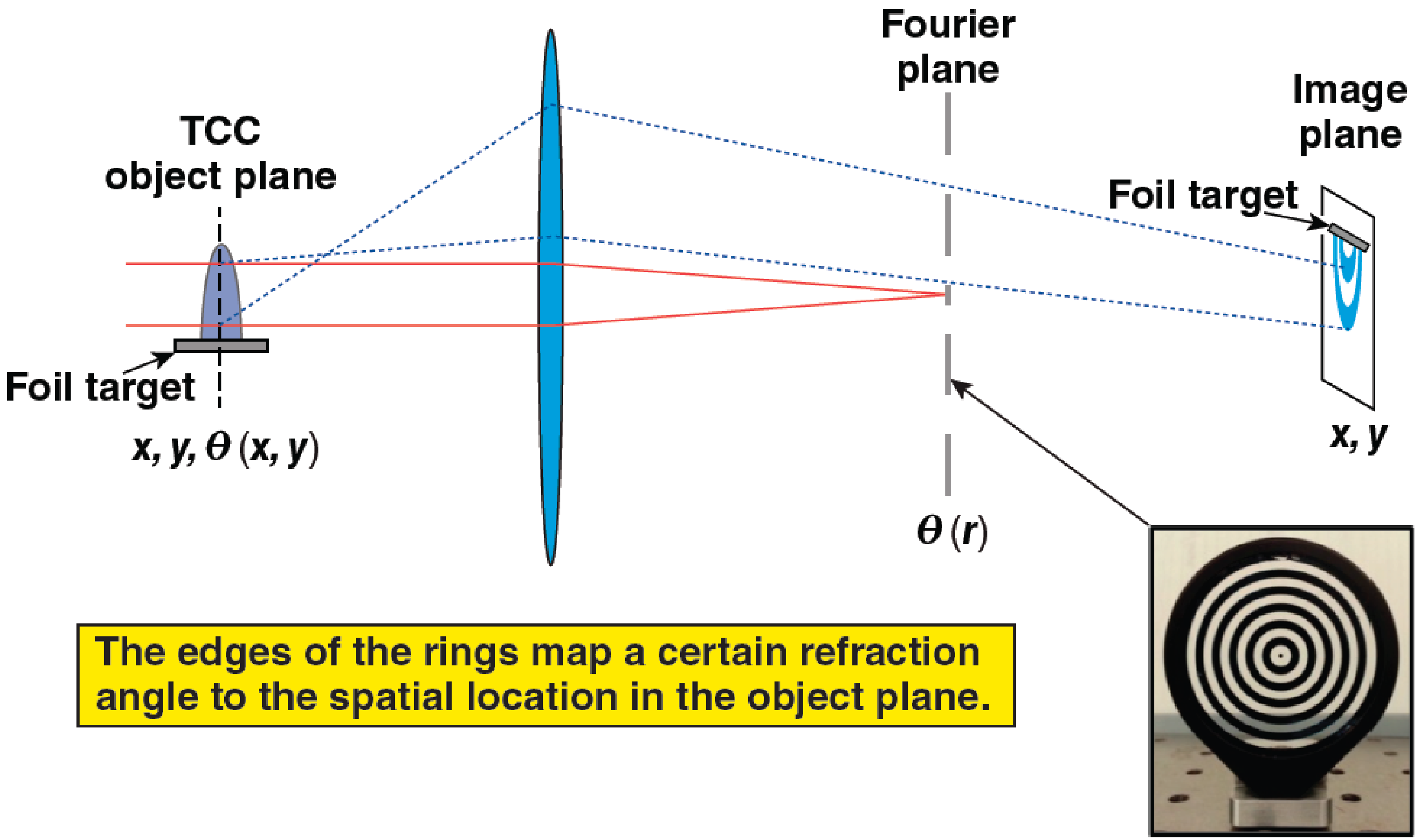

The edges of the rings map a certain refraction angle to the spatial location in the object plane.

Channeling of multi-kilojoule high-intensity laser beams in an inhomogeneous plasma was observed using AFR

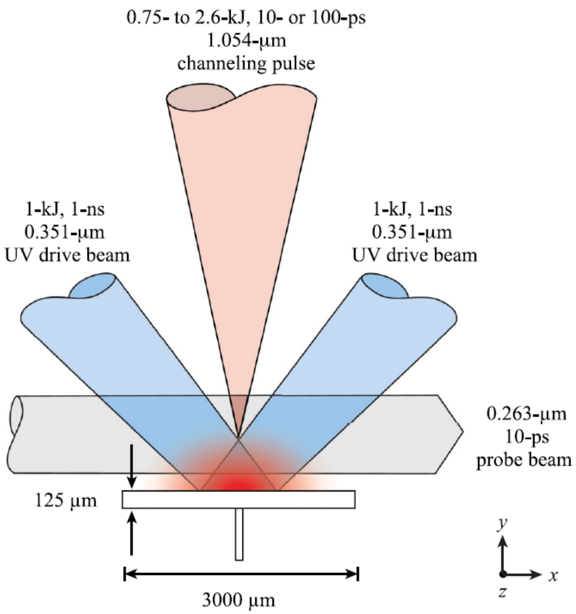

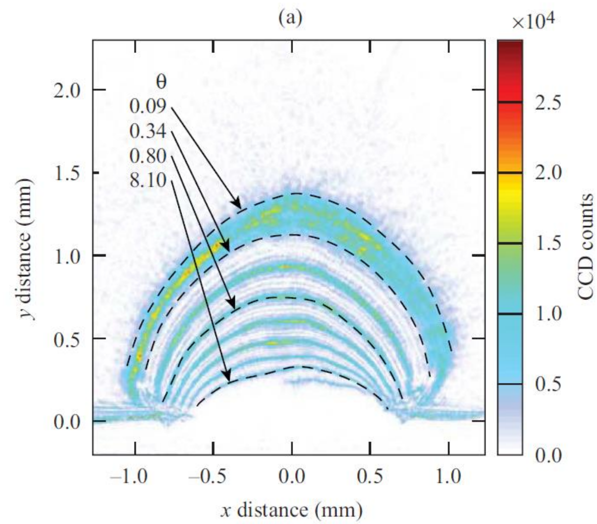

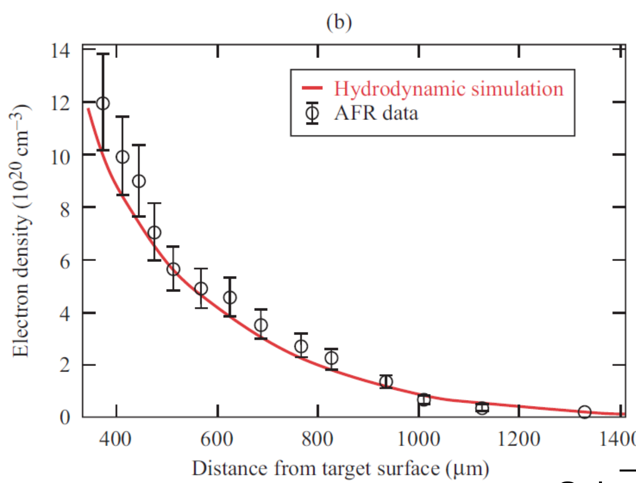

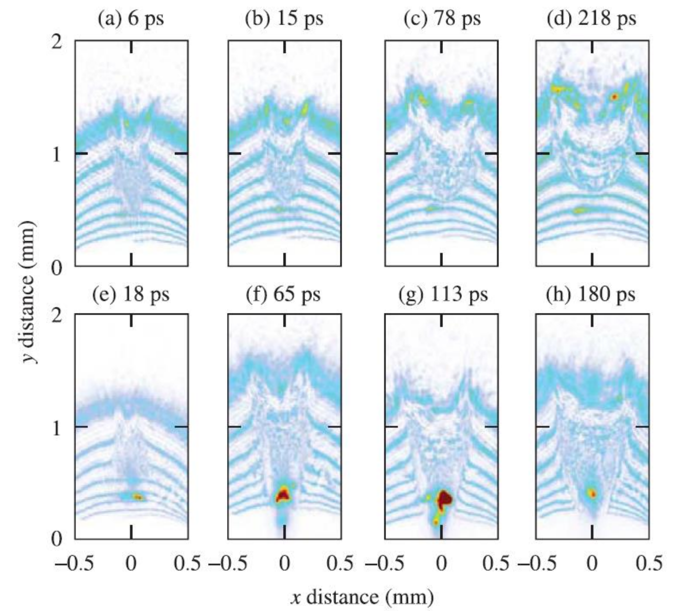

S. Ivancic *et al.*, Phys. Rev. E 91 , 051101 (2015)

Electromagnetic wave can be used to measure the density or the magnetic field in the plasma

- Nonmagnetized isotropic plasma (interferometer needed):

$$n^2 = 1 - \frac{X(1-X)}{1 - X - \frac{1}{2}Y^2\sin^2\theta \pm \left[\left(\frac{1}{2}Y^2\sin^2\theta\right)^2 + (1-X)^2 Y^2\cos^2\theta\right]^{1/2}}$$

$$= 1 - X = 1 - \frac{\omega_p^2}{\omega^2} = 1 - \frac{n_e}{n_{cr}} \qquad \left(Y \equiv \frac{\Omega}{\omega} \equiv 0\right)$$

Note: $\omega_p^2 = \frac{n_e e^2}{\epsilon_0 m_e}$ $\quad n_{cr} = \frac{\epsilon_0 m_e \omega^2}{e^2}$

- **Magnetized isotropic plasma (Polarization detected needed):**

Parallel to B_0

$$n^2 = 1 - \frac{\omega_p^2}{\omega(\omega \pm \Omega)} \qquad \frac{E_x}{E_y} = \pm i \qquad \Omega \equiv \frac{eB_0}{m_e}$$

Faraday rotation: linear polarization rotation caused by the difference between the speed of LHC and RHC polarized wave.

Circular polarization

$$E_{\mathrm{x}} = E_0 \exp\left(-i\omega t\right)$$

$$E_{\mathrm{y}} = iE_{\mathrm{x}} = iE_0 \exp\left(-i\omega t\right) = E_0 \exp\left(i\frac{\pi}{2}\right) \exp\left(-i\omega t\right) = E_0 \exp\left[-i\left(\omega t - \frac{\pi}{2}\right)\right]$$

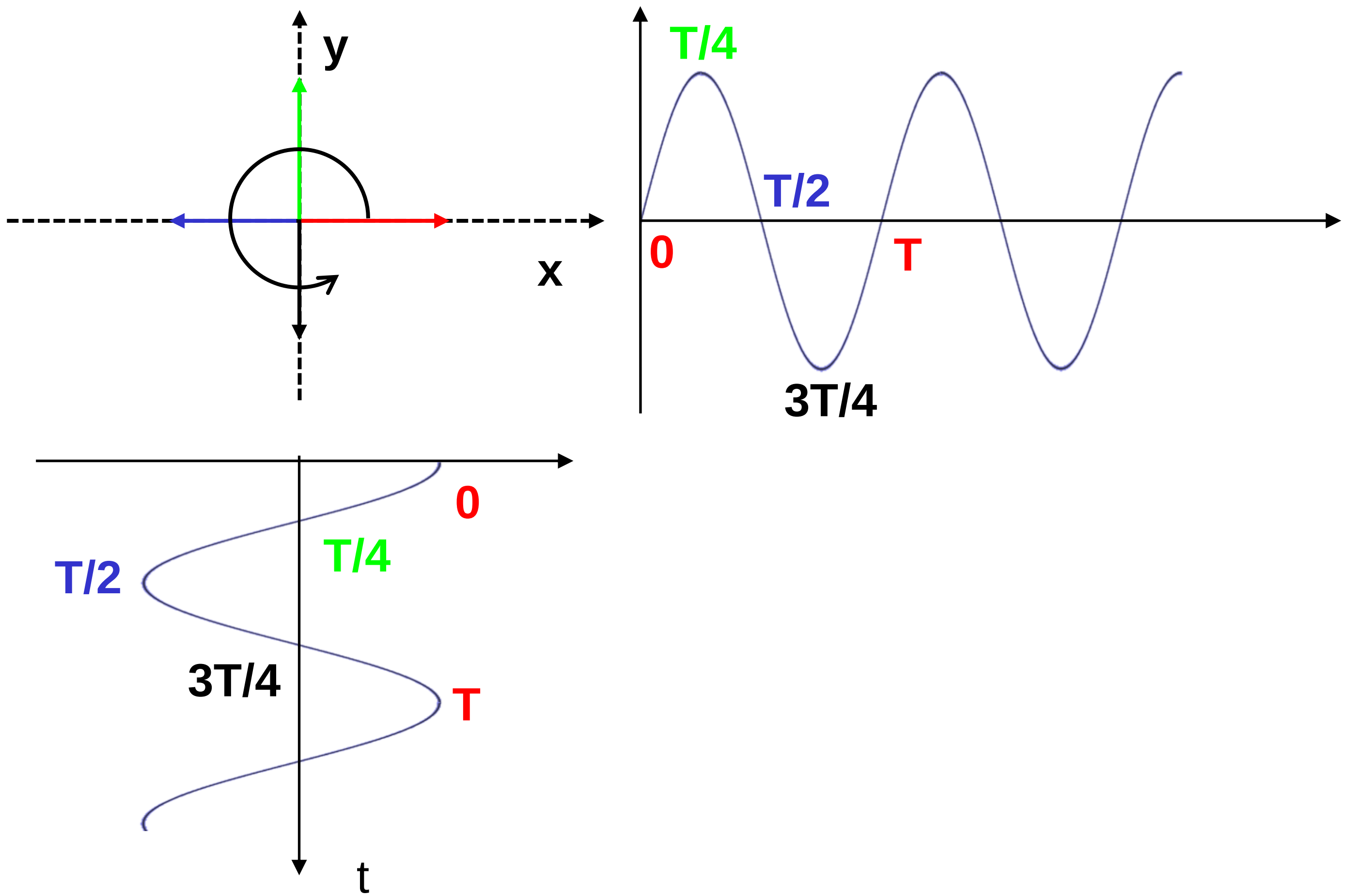

Linear polarization rotates as the wave propagates with different speed in LHC and RHC polarization

$$\vec{E} = E_0\hat{x} = \frac{E_0}{2}\left[(\hat{x}+i\hat{y}) + (\hat{x}-i\hat{y})\right] \qquad \vec{E}(z) = \vec{E}\exp(i\phi) \qquad \phi_{\mathrm{R}} \neq \phi_{\mathrm{L}}$$

$$\vec{E}(z) = \frac{E_0}{2}\left[(\hat{x}+i\hat{y})e^{i\phi_R} + (\hat{x}-i\hat{y})e^{i\phi_L}\right] \qquad \bar{\phi} \equiv \frac{\phi_{\mathrm{R}}+\phi_{\mathrm{L}}}{2} \quad , \quad \Delta\phi = \frac{\phi_{\mathrm{R}}-\phi_{\mathrm{L}}}{2}$$

$$= \frac{E_0}{2}\left[\hat{x}\left(e^{i\phi_R}+e^{i\phi_L}\right) + \hat{y}i\left(e^{i\phi_R}-e^{i\phi_L}\right)\right]$$

$$= \frac{E_0}{2}\left[\hat{x}\left(e^{i\left(\bar{\phi}+\frac{\Delta\phi}{2}\right)} + e^{i\left(\bar{\phi}-\frac{\Delta\phi}{2}\right)}\right) + \hat{y}i\left(e^{i\left(\bar{\phi}+\frac{\Delta\phi}{2}\right)} - e^{i\left(\bar{\phi}-\frac{\Delta\phi}{2}\right)}\right)\right]$$

$$= E_0 e^{i\bar{\phi}}\left[\hat{x}\left(\frac{e^{i\frac{\Delta\phi}{2}}+e^{-i\frac{\Delta\phi}{2}}}{2}\right) + \hat{y}i\left(\frac{e^{i\frac{\Delta\phi}{2}}-e^{-i\frac{\Delta\phi}{2}}}{2}\right)\right]$$

$$= E_0 e^{i\bar{\phi}}\left[\hat{x}\cos\left(\frac{\Delta\phi}{2}\right)\mathrm{Cos}+\hat{y}\sin\left(\frac{\Delta\phi}{2}\right)\right]$$

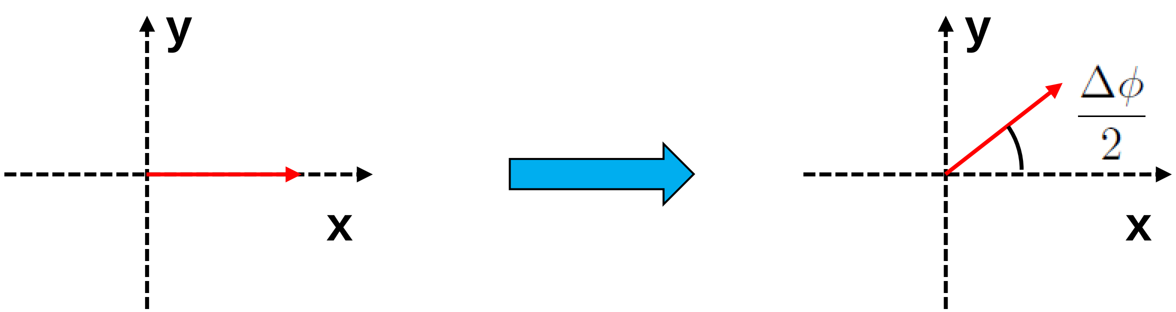

The rotation angle of the polarization depends on the linear integral of magnetic field and electron density

$$\phi = \int k dl = \int n \frac{\omega}{c} dl \qquad \alpha = \frac{\Delta\phi}{2} = \frac{\omega}{2c}\int (n_{\rm R} - n_{\rm L})\, dl$$

$$n_{\rm R} = \sqrt{1 - \frac{X}{1+Y}} \sim 1 - \frac{1}{2}\frac{X}{1+Y} \qquad X, Y << 1$$

$$n_{\rm L} \sim 1 - \frac{1}{2}\frac{X}{1-Y} \qquad \frac{X}{1 \pm Y} << 1$$

$$n_{\rm R} - n_{\rm L} \sim \frac{X}{2}\left(\frac{1}{1-Y} - \frac{1}{1+Y}\right) = \frac{XY}{1-Y^2} \sim XY$$

$$\begin{aligned} \alpha &\sim \frac{\omega}{2c}\int XY dl = \frac{\omega}{2c}\int \frac{\omega_{\rm p}^2}{\omega^2}\frac{\Omega}{\omega} dl = \frac{1}{2c}\int \frac{n_{\rm e}}{n_{\rm cr}}\frac{eB}{m_{\rm e}} dl \\ &= \frac{e}{2cm_{\rm e}n_{\rm cr}}\int n_{\rm e} B dl \end{aligned}$$

The rotation angle of the polarization depends on the linear integral of magnetic field and electron density

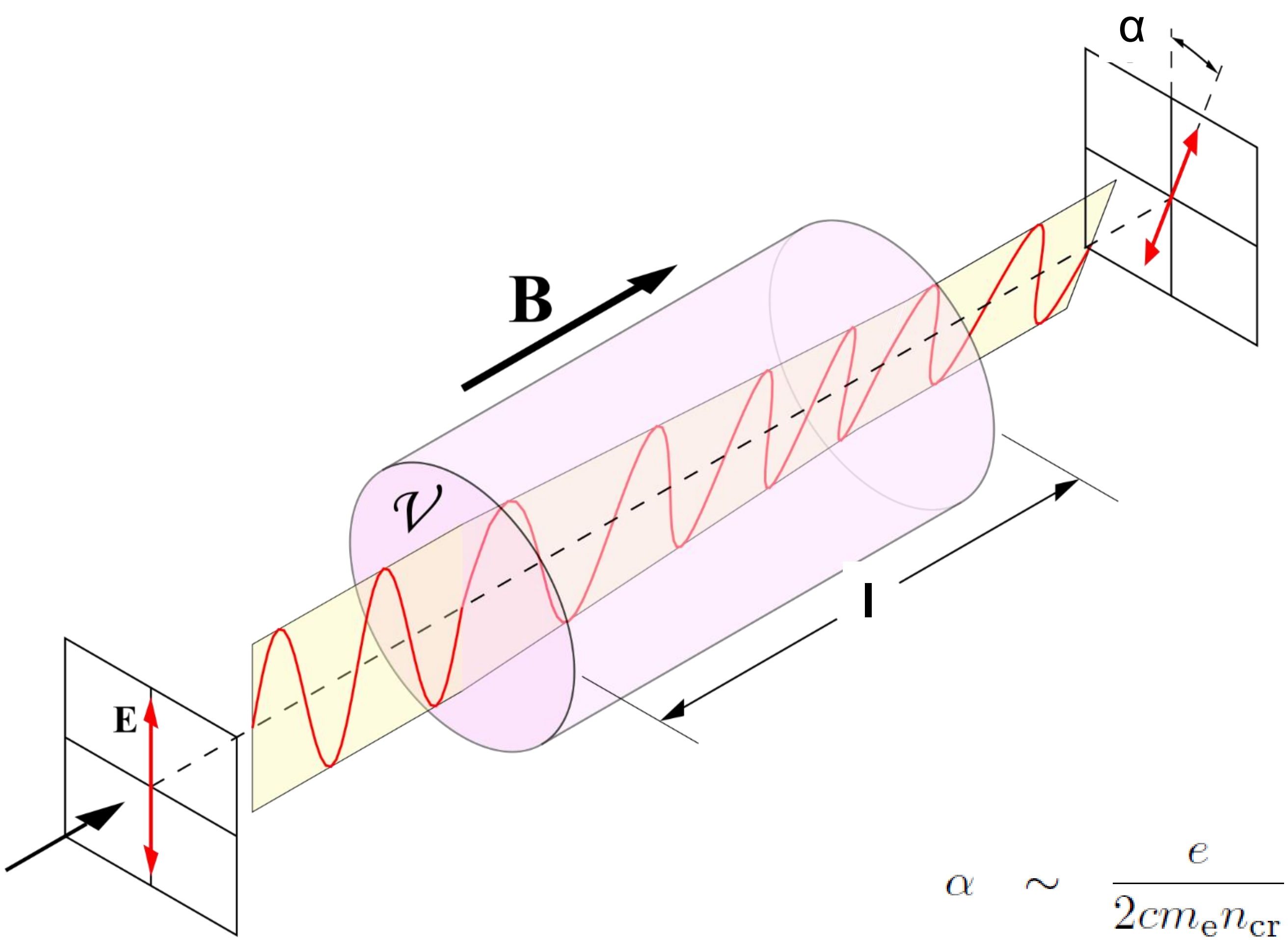

$$\alpha \sim \frac{e}{2cm_{\mathrm{e}}n_{\mathrm{cr}}} \int n_{\mathrm{e}} B dl$$

Magnetic field can be generated when the temperature and density gradients are not parallel to each other

$$\frac{\partial \vec{B}}{\partial t} = \nabla \times \left[\underbrace{\vec{u} \times \vec{B}}_{\text{Convection term}} + \underbrace{\frac{1}{\sigma \mu_0} \nabla \times \vec{B}}_{\text{Diffusion term}} + \underbrace{\frac{\nabla p_e}{n_e e}}_{\text{self generated field}} - \underbrace{\frac{1}{\mu_0} \left(\frac{\nabla \times \vec{B}}{n_e e} \times \vec{B} \right)}_{\text{Hall term}} \right]$$

$$\nabla \times \frac{\nabla p_e}{n_e e} = -\frac{k_B}{e} \frac{\nabla n_e \times \nabla T_e}{n_e}$$

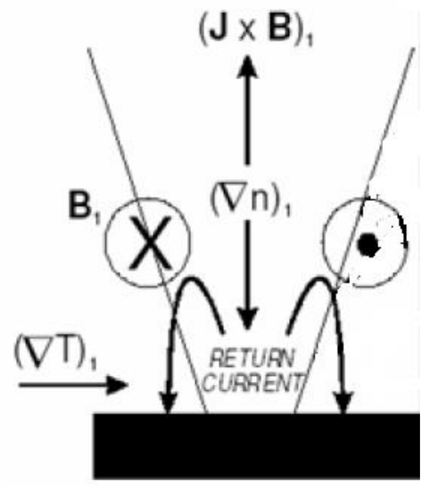

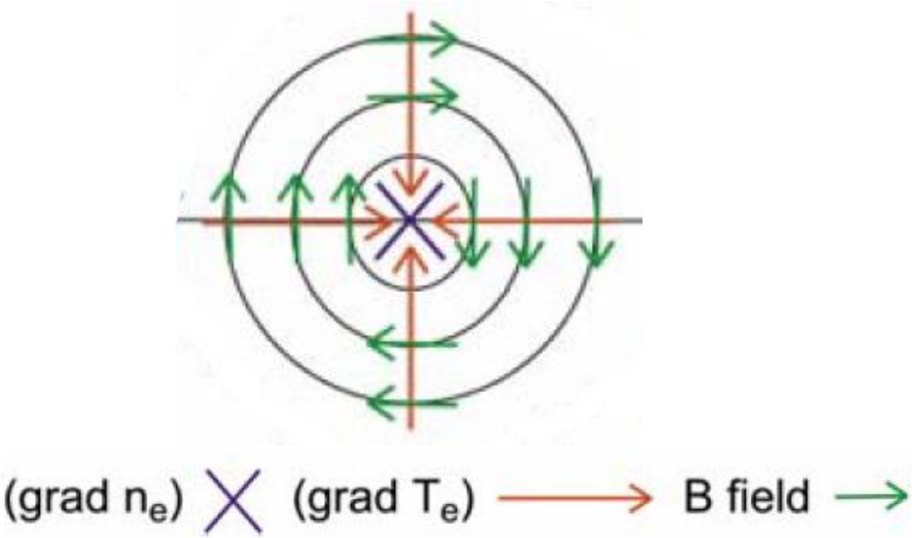

P M Nilson *et al.*, Central Laser Facility Annual Report 2004/2005

Polarimetry diagnostic can be used to measure the magnetic field

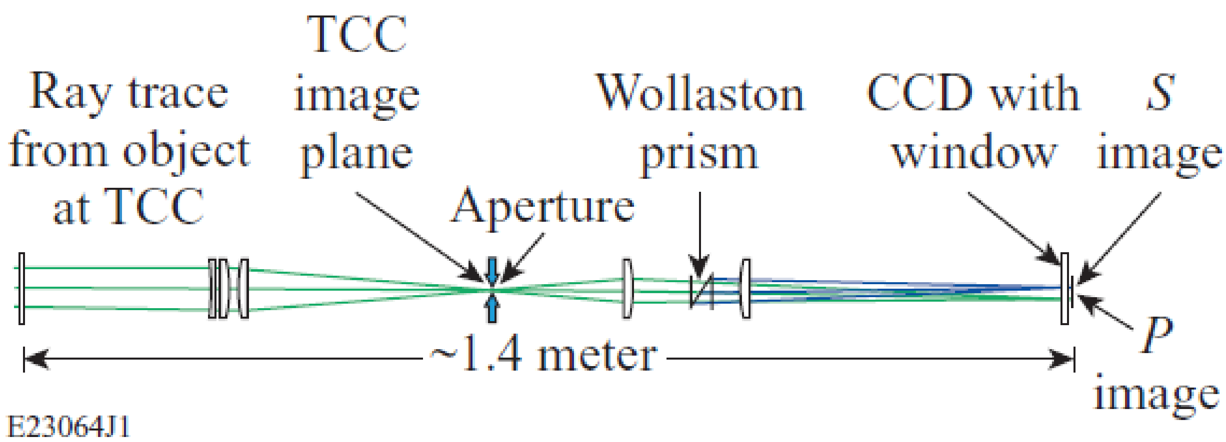

Wollaston prism

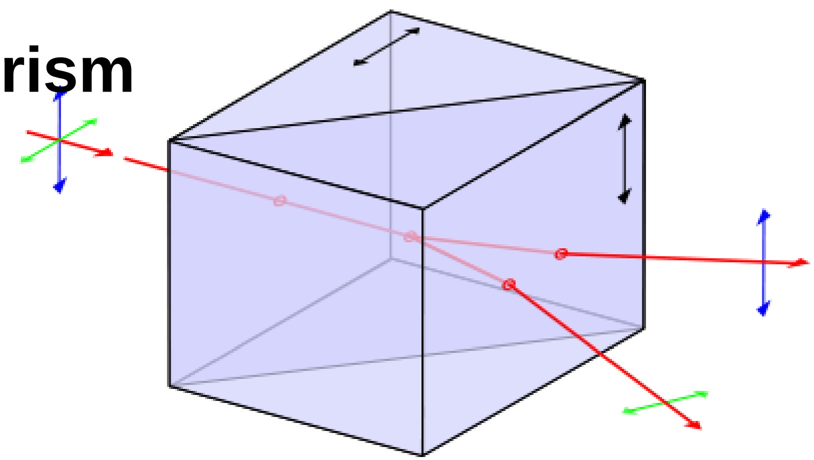

A. Davies *et al.*, Rev. Sci. Instrum. **85**, 11E611 (2014)

Self-generated field was suggested when multi-kilojoule high-intensity laser beams illuminated on an inhomogeneous plasma

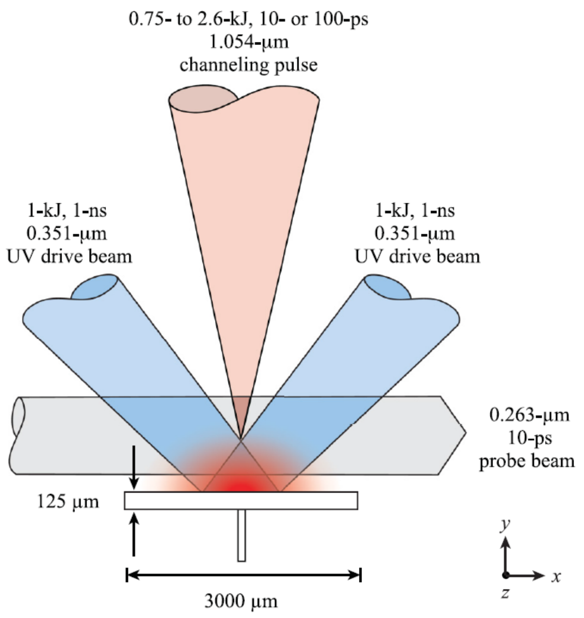

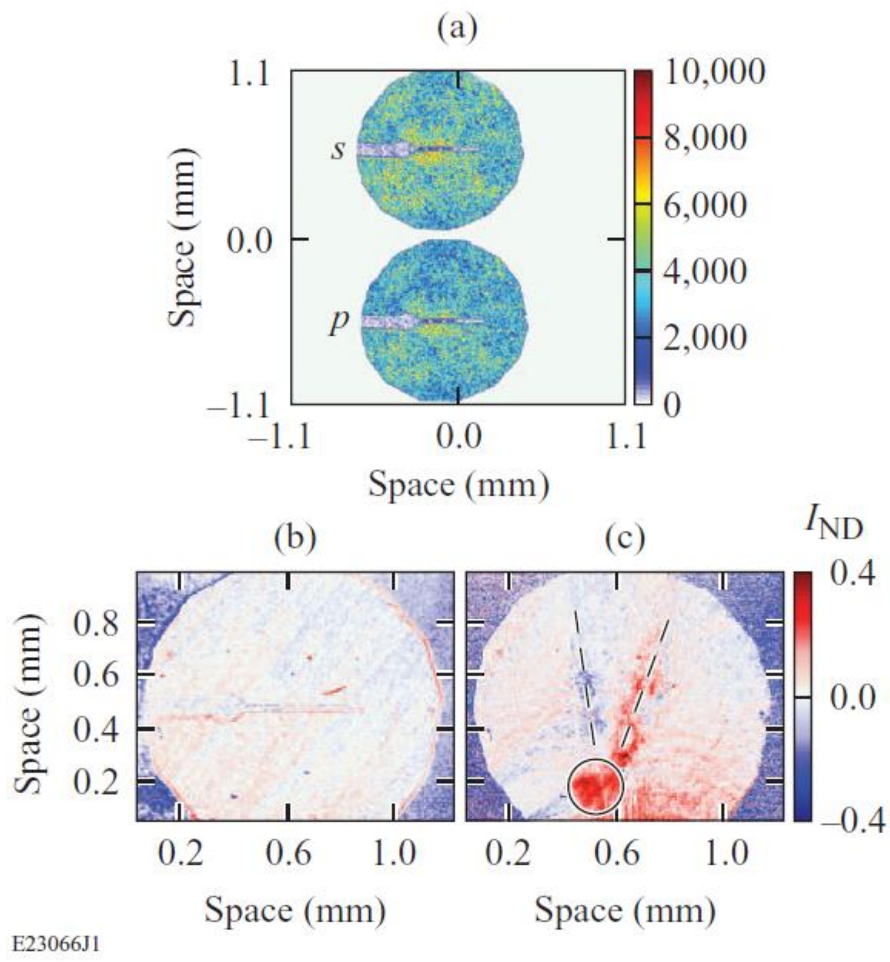

The magnetic field can be measured by measuring the deflected angle of charged particles

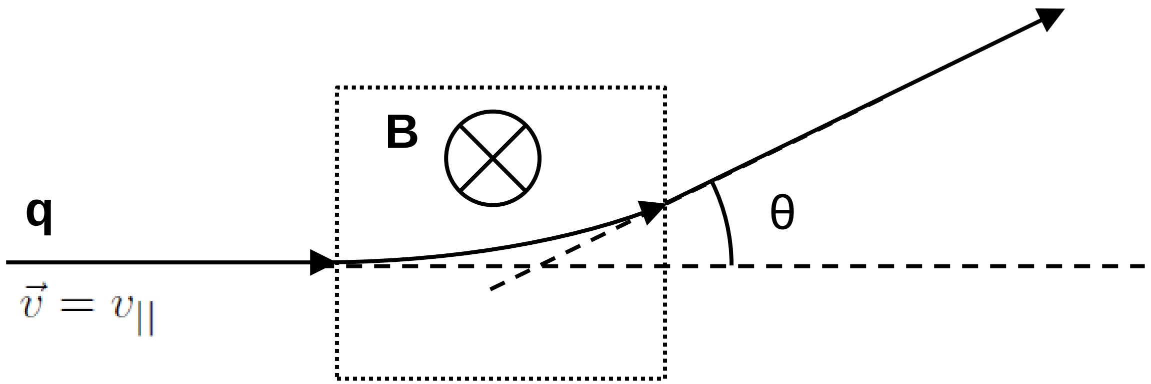

$$F_{\perp} = q\vec{v} \times \vec{B} = qv_{||}B = m\frac{dv_{\perp}}{dt}$$

$$v_{\perp} = \int \frac{qv_{||}B}{m}dt = \frac{qv_{||}}{m}\int Bdt\frac{dx}{dx} = \frac{qv_{||}}{m}\int \frac{B}{v_{||}}dx = \frac{q}{m}\int Bdx$$

$$\tan\theta = \frac{v_{\perp}}{v_{||}} = \frac{q}{mv_{||}}\int Bdx = \frac{q}{\sqrt{2mE}}\int Bdx$$

$$\int Bdx = \frac{\sqrt{2mE}}{q}\tan\theta$$

Magnetic field was measured using protons

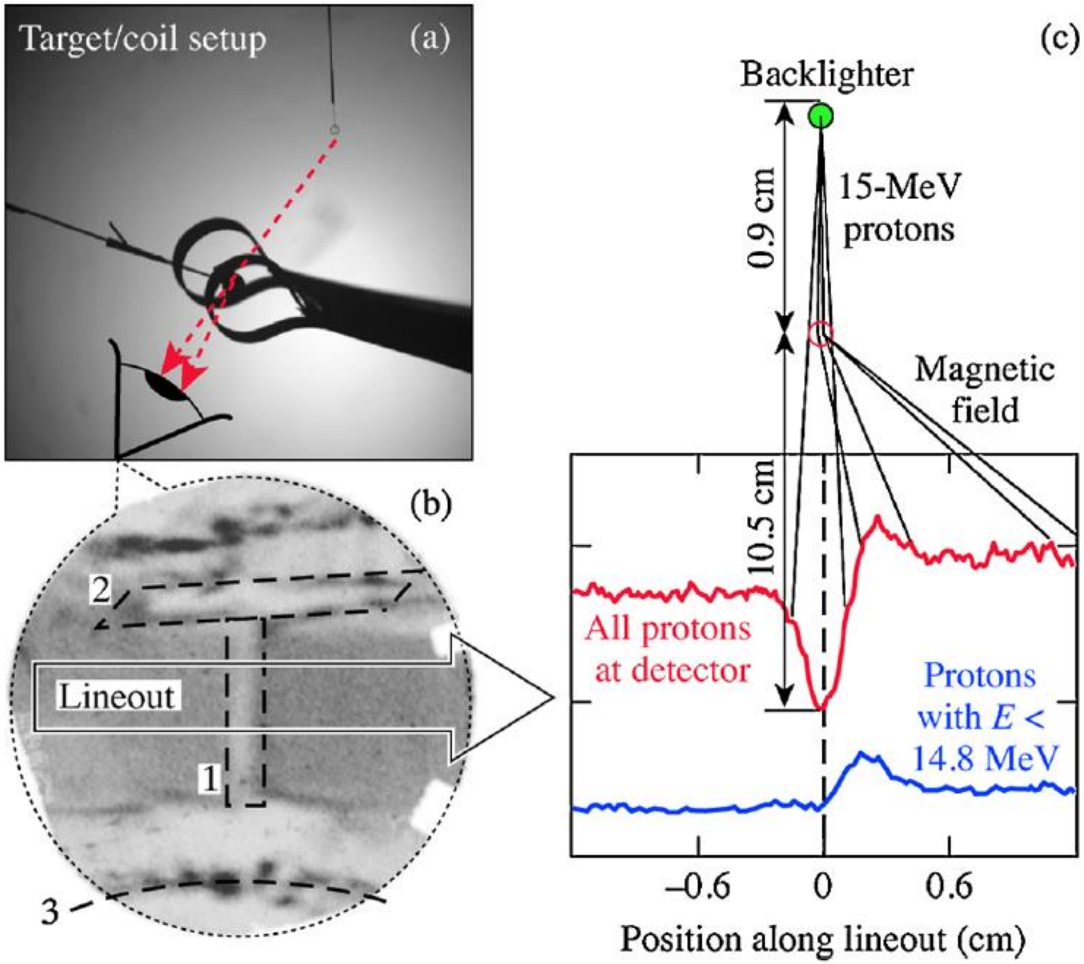

O. V. Gotchev *et al.*, Phys. Rev. Lett. **103**, 215004 (2009)

Protons can be generated from fusion product or copper foil illuminated by short pulse laser

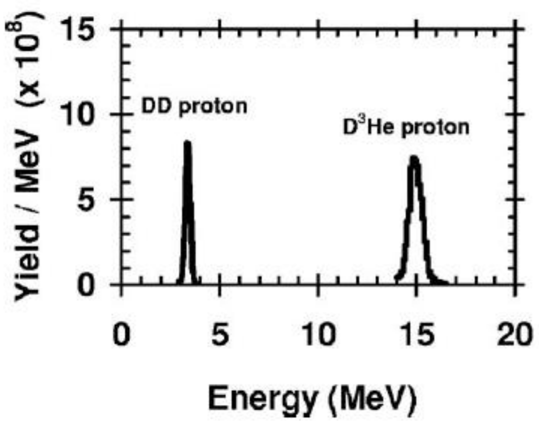

$$D + D \longrightarrow T(1.01\text{MeV}) + p(3.02\text{MeV})$$

$$D + \text{He}^3 \longrightarrow \text{He}^4(3.6\text{MeV}) + p(14.7\text{MeV})$$

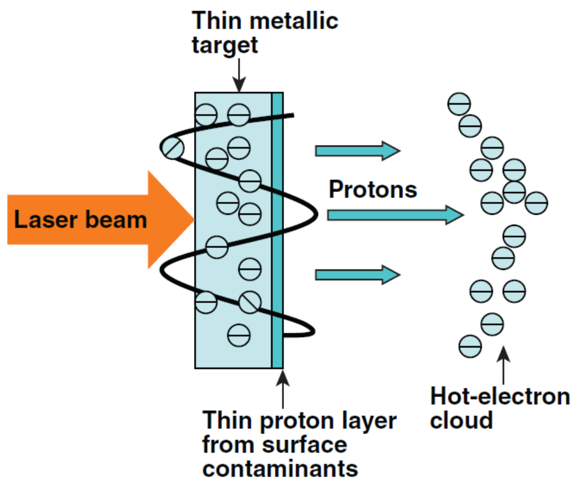

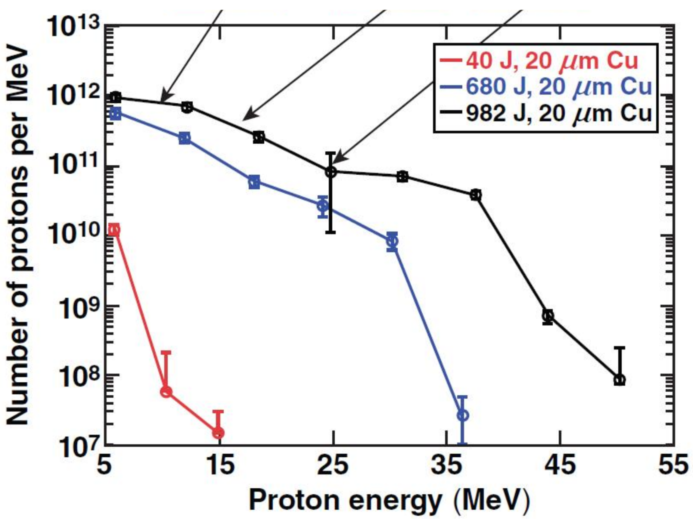

Target normal sheath acceleration (TNSA)

C. K. Li *et al.*, Rev. Sci. Instrum. **77**, 10E725 (2006)
L. Gao, PhD Thesis

Protons can leave tracks on CR39 or film

CR 39

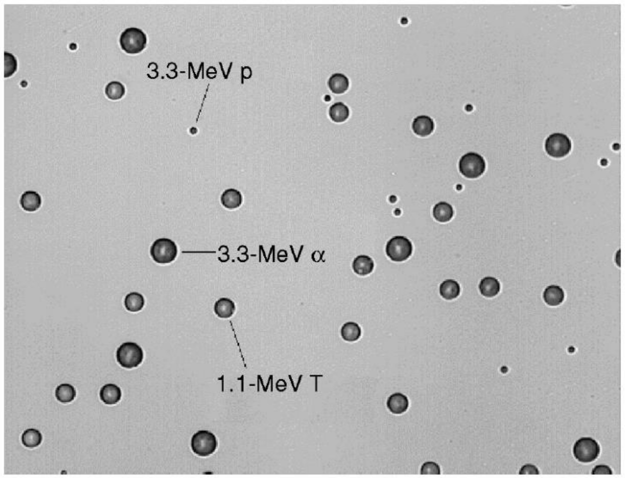

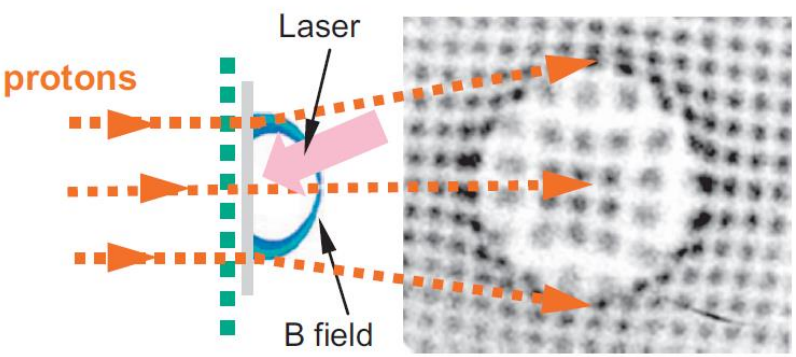

Radiochromic film pack

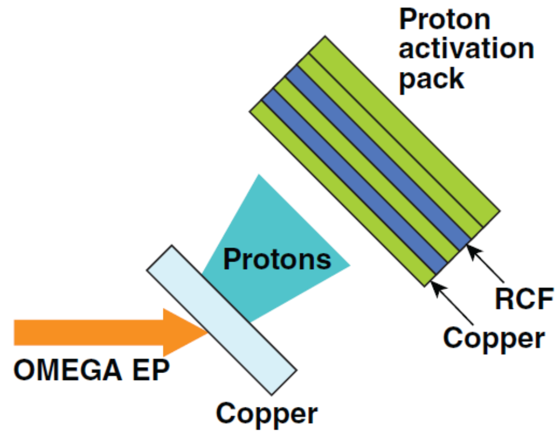

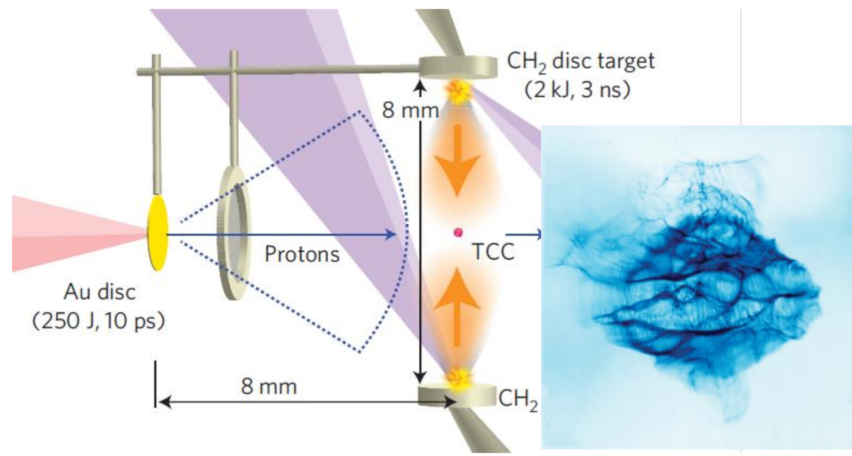

F. H. Seguin *et al.*, Rev. Sci. Instrum. **74**, 975 (2003)
C. K. Li *et al.*, Phys. Plasmas **16**,056304 (2009)
L. Gao, PhD Thesis
N. L. Kugland et al., Nature Phys. B, 809 (2012)

Time dependent magnetic field can be measured using B-dot probe

$$B = B(t)$$

$$\nabla \times \vec{E} = -\frac{\partial \vec{B}}{\partial t}$$

$$\int d\vec{A}\nabla \times \vec{E} = \oint \vec{E} d\vec{l} = V = -\int d\vec{A}\frac{\partial}{\partial t}\vec{B}$$

$$V \sim -A\frac{\partial B}{\partial t}$$

$$B = -\int \frac{V}{A} dt \sim -\frac{1}{A}\int V dt$$

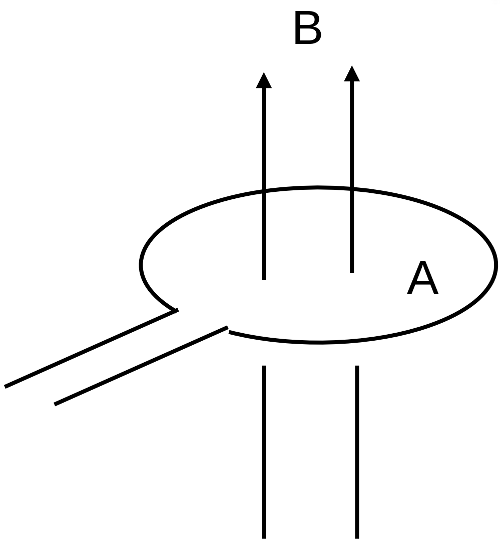

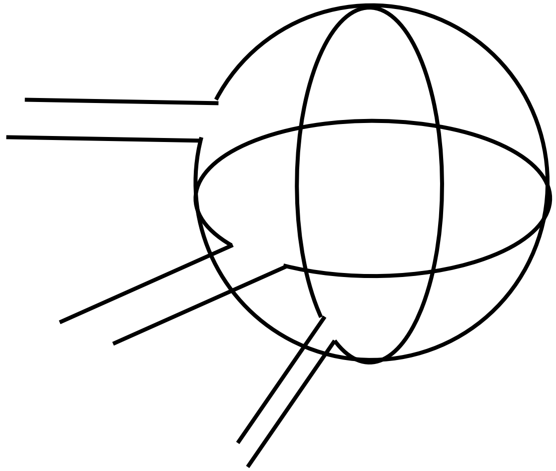

A Thomson parabola uses parallel electric and magnetic fields to deflect particles onto parabolic curves that resolve q/m

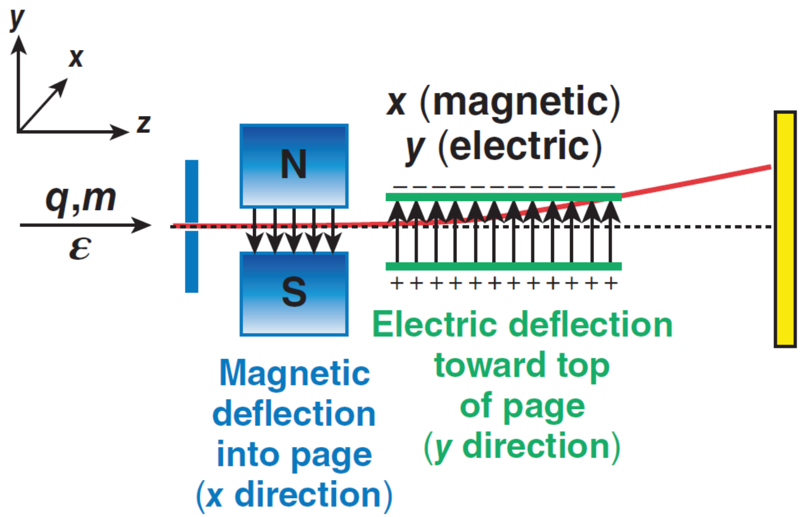

- Deflection caused by magnetic field ~*q*/*p*
- Deflection caused by electric field ~*q*/*KE*
- Ion traces form parabolic curves on detector plane

$$y = \frac{mc^2 E}{qLB^2} x^2$$

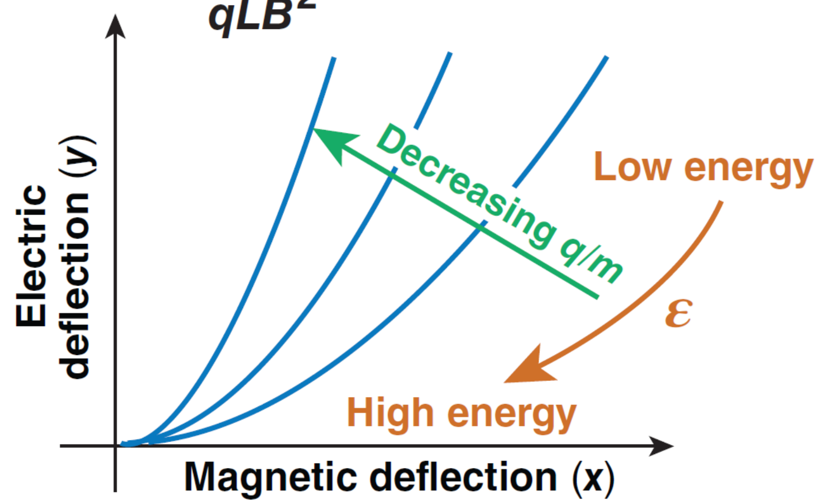

$$\tan \Delta\theta_x = \Delta\theta_x = \frac{qBL}{c\sqrt{2\,m\varepsilon}}$$

y deflection

$$\varepsilon = \frac{q^2 B^2 L^2}{c^2 2m \Delta\theta_x^2}$$

$$F_\perp = qE$$

$$\Delta m V_y = qE\tau = \frac{qEL}{V}$$

$$\tan\theta_y \sim \theta_y = \frac{\Delta m V_y}{mV} = \frac{qEL}{2\varepsilon}$$

E16717b

Faraday cup

A faraday cup measures the flux of charge particles

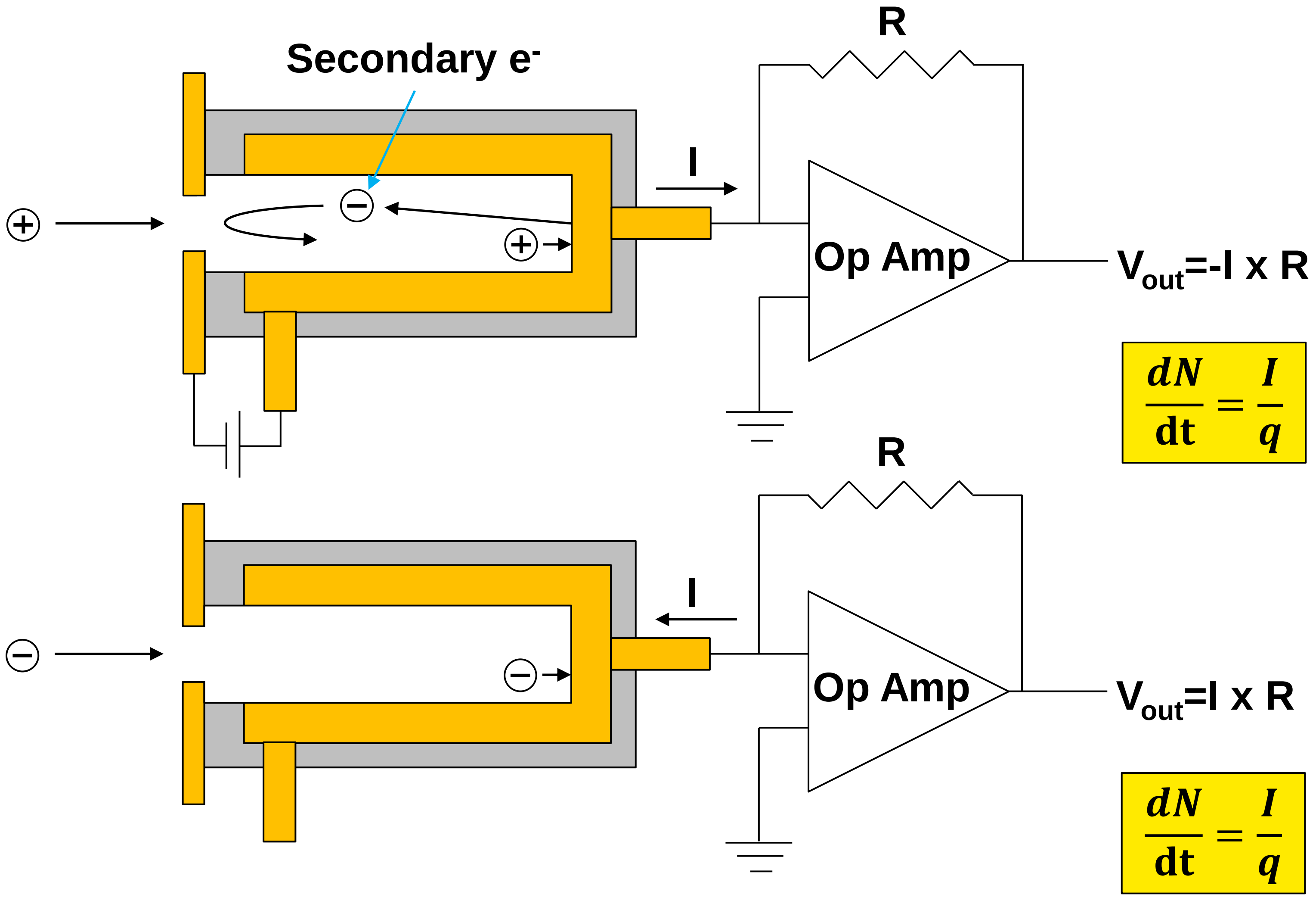

Retarding potential analyzer measures the energy / velocity distribution function

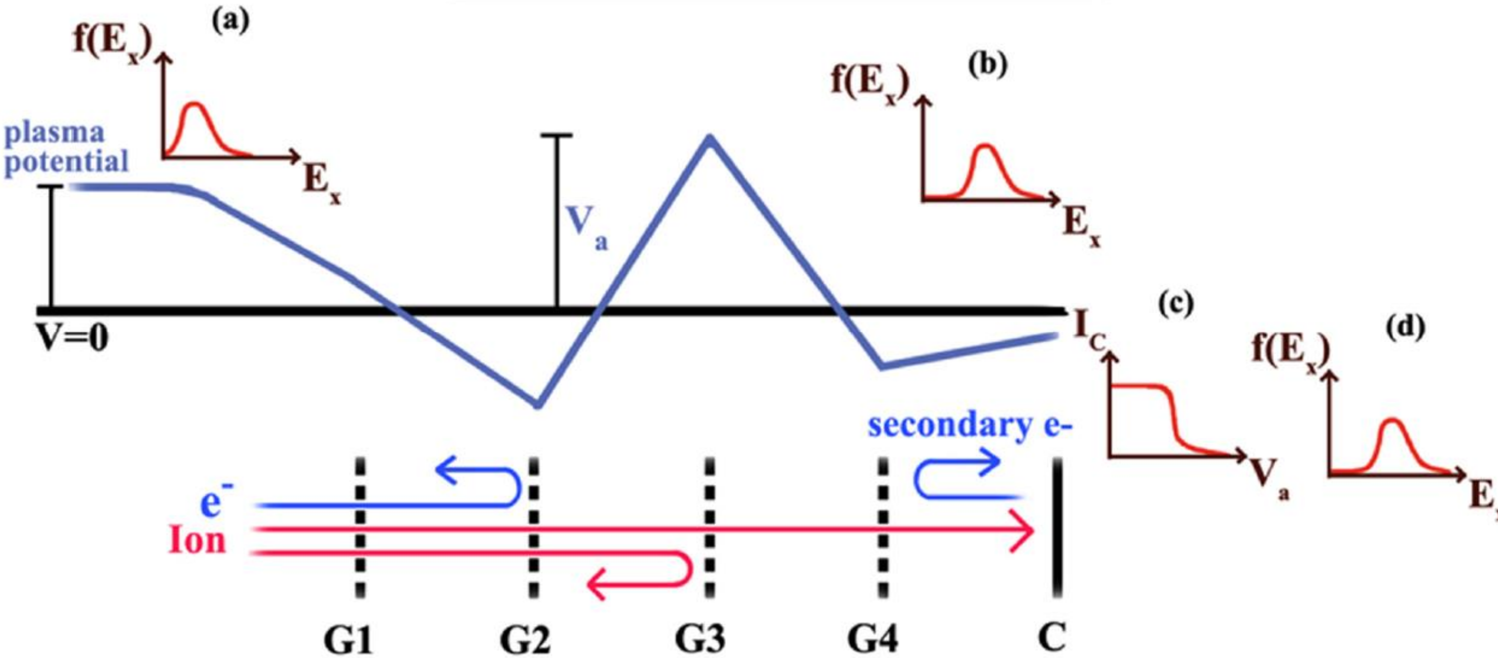

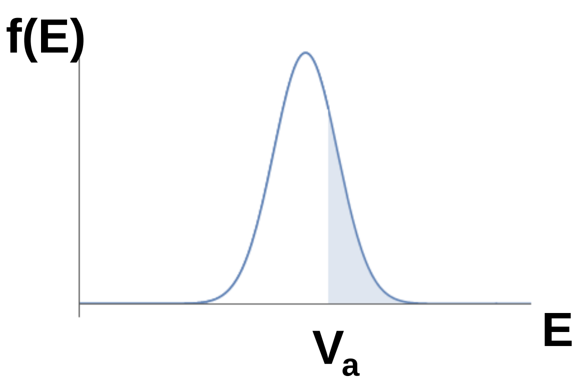

H.-K. Fang, 2015 NCKU Ph. D. Thesis, Ion measurements of ionosphere plasma in space plasma operation chamber

The photon energy spectrum provides valuable information

- Plasma conditions can be determined from the photon spectrum
  - visible light: absorption and laser-plasma interactions
  - x rays: electron temperature, density, plasma flow, material mixing
- There are three basic tools for determining the spectrum detected
  - filtering
  - grating spectrometer
  - Bragg spectrometer

Spectrum can be obtained using grating

- **Grating is used to disperse the light**

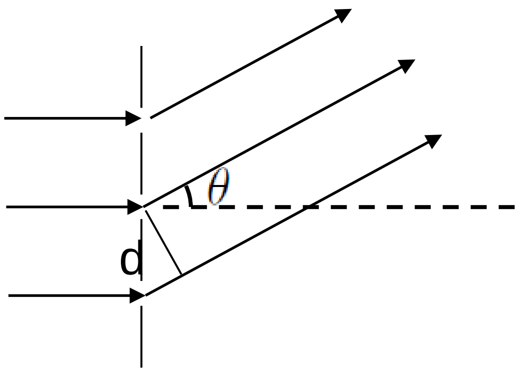

$$d \sin \theta = m\lambda$$

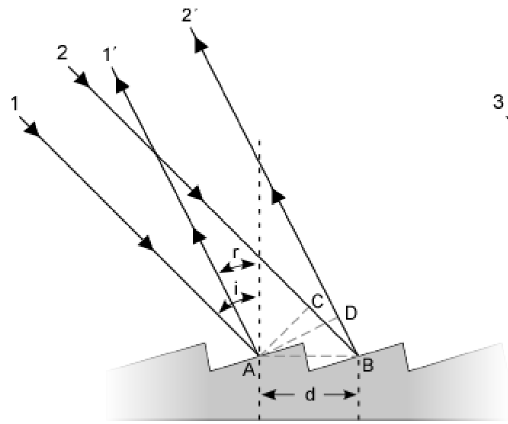

nλ = d(sin(i) + sin (r))

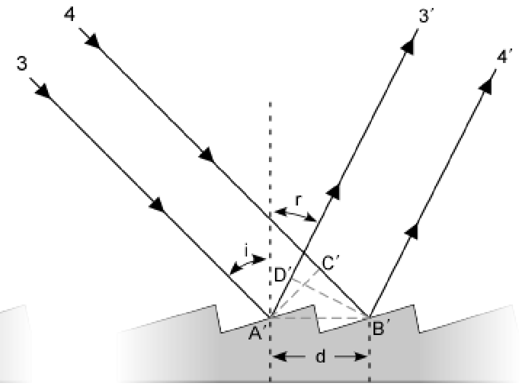

nλ = d(sin(i) - sin (r))

- **Bragg condition in the crystal is used for X-ray.**

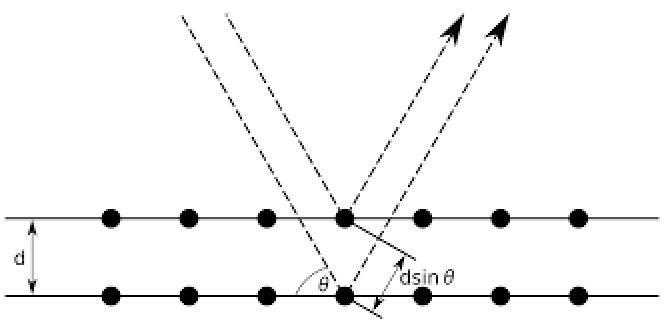

$$2d \sin \theta = m\lambda$$

Temperature and density can be obtained from the emission

Line emission

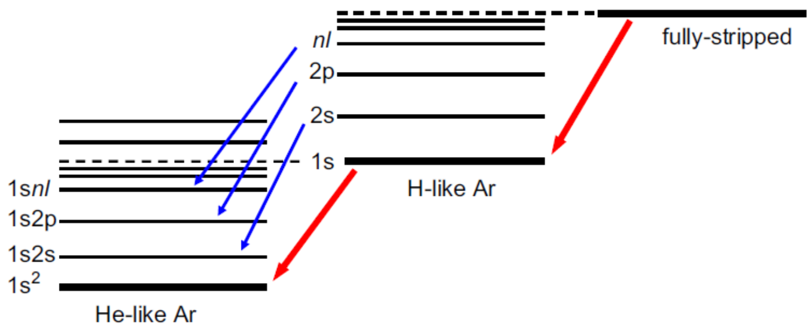

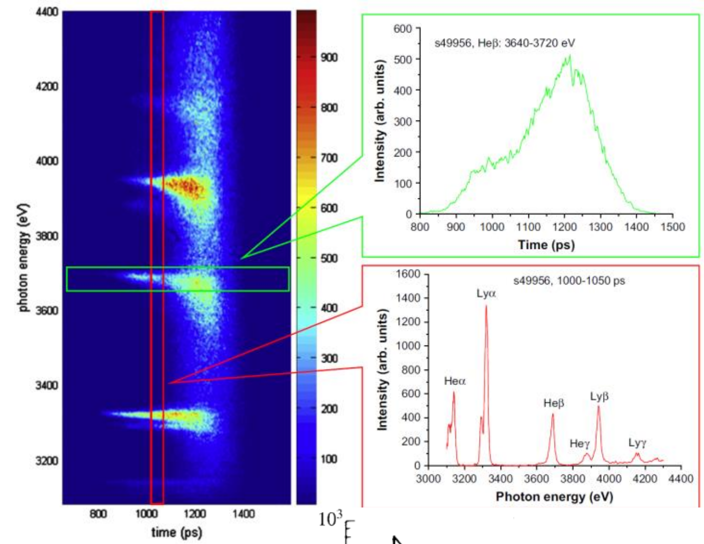

Bremsstrahlung emission

$$\eta_\nu = \frac{16\pi}{3\sqrt{6\pi}} \frac{e^6}{m_e^2 c^3} \frac{Z_i^2 n_e}{\sqrt{k_B T_e / m_e} A m_p} \exp\left(-\frac{h\nu}{k_B T_e}\right)$$

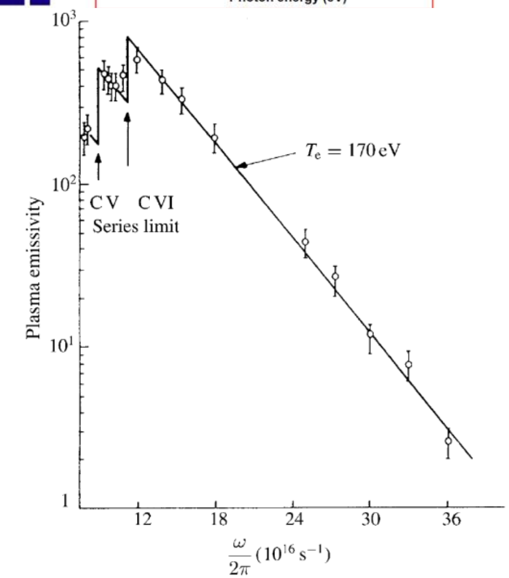

R. Florido *et al.*, High Energy Dens. Phys. **6**, 70 (2010)

Information of x-ray transmission or reflectivity over a surface can be obtained from the Center for X-Ray Optics

- **http://henke.lbl.gov/optical_constants/**

CXRO
THE CENTER FOR X-RAY OPTICS

X-Ray Database
Nanomagnetism
X-Ray Microscopy
EUV Lithography
EUV Mask Imaging
Reflectometry
Zoneplate Lenses
Coherent Optics
Nanofabrication
Optical Coatings
Engineering
Education
Publications
Contact

BERKELEY LAB

The Center for X-Ray Optics is a multi-disciplined research group within Lawrence Berkeley National Laboratory's (LBNL)

X-Ray Interactions With Matter

Introduction
Access the atomic scattering factor files.
Look up x-ray properties of the elements.
The index of refraction for a compound material.
The x-ray attenuation length of a solid.
X-ray transmission
- Of a solid.
- Of a gas.

X-ray reflectivity
- Of a thick mirror.
- Of a single layer.
- Of a bilayer.
- Of a multilayer.

The diffraction efficiency of a transmission grating.
Related calculations:
- Synchrotron bend magnet radiation.

Other x-ray web resources.
X-ray Data Booklet

Reference

B.L. Henke, E.M. Gullikson, and J.C. Davis. *X-ray interactions: photoabsorption, scattering, transmission, and reflection at E=50-30000 eV, Z=1-92*, Atomic Data and Nuclear Data Tables Vol. **54** (no.2), 181-342 (July 1993).

A band pass filter is obtained by combing a filter and a mirror

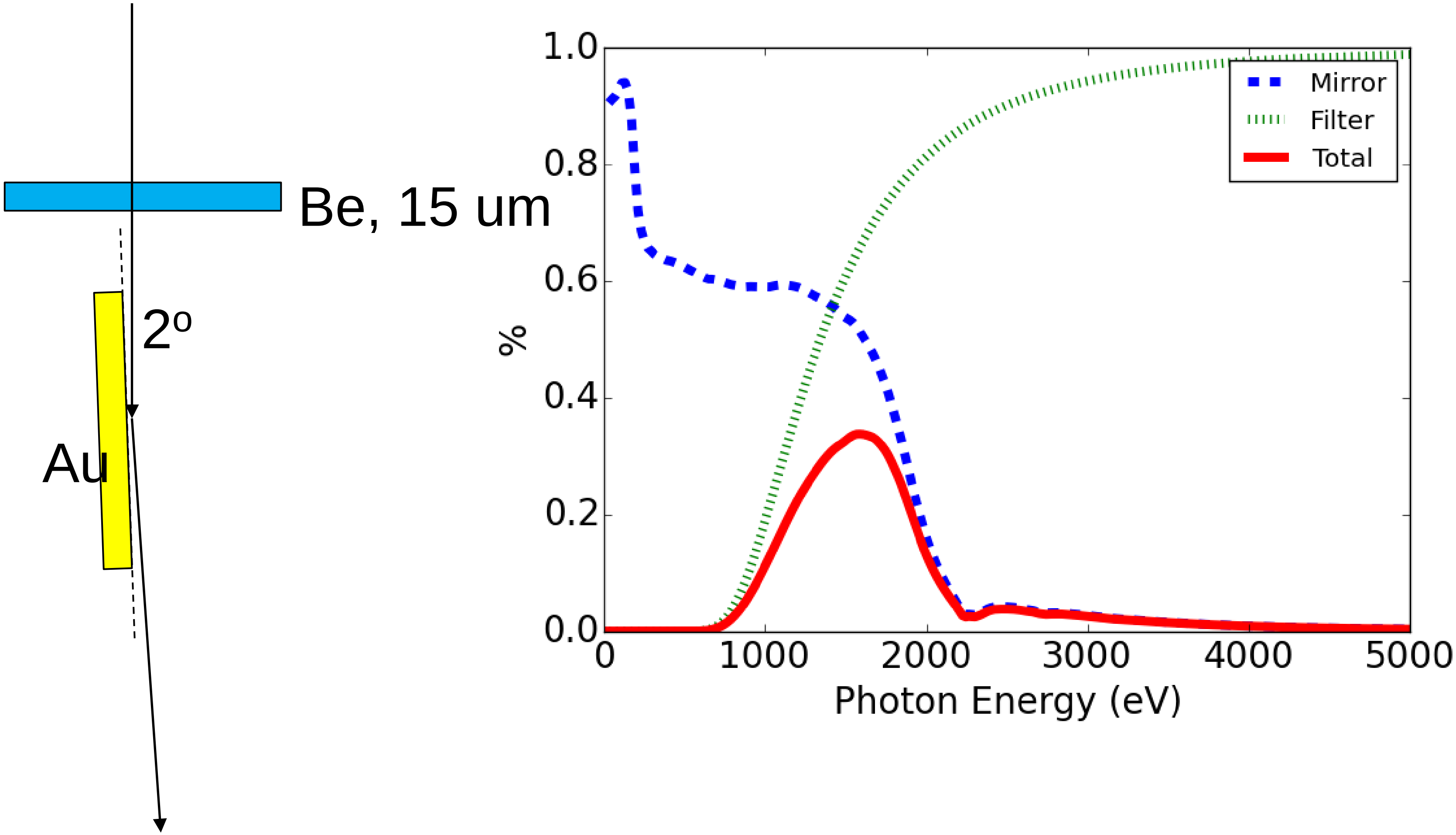

X rays can not be concentrated by lenses

- **X-ray refractive indices are less than unity,** $n \lesssim 1$
- **For those with lower refractive indices, the absorption is also strong**
- **X-ray mirrors can be made through**
  - **Bragg reflection**
  - **External total reflection with a small grazing angle**

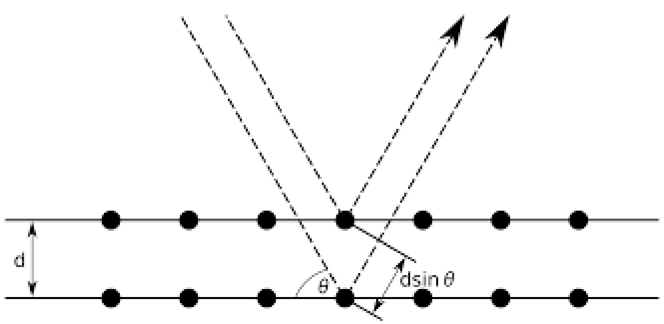

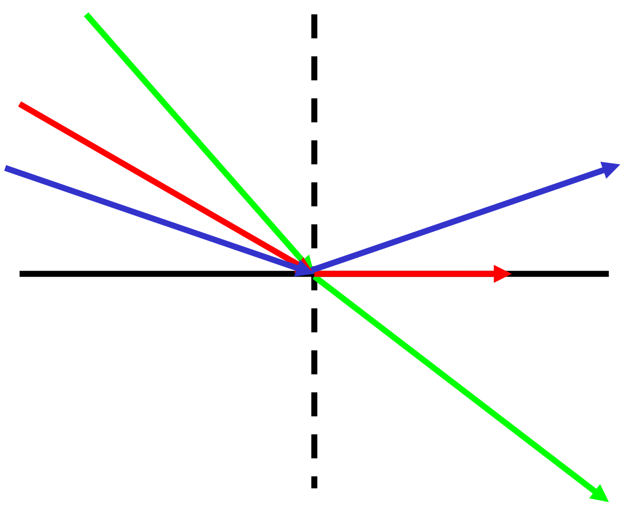

The simplest imaging device is a pinhole camera

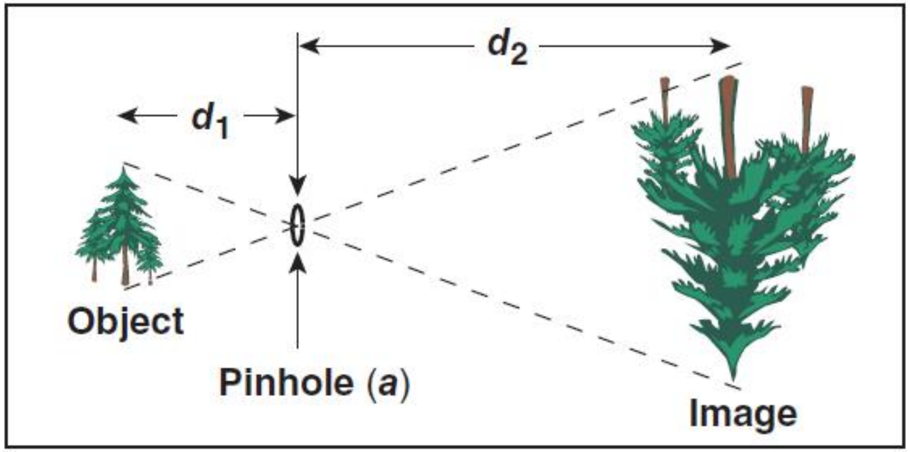

Kodak Brownie camera

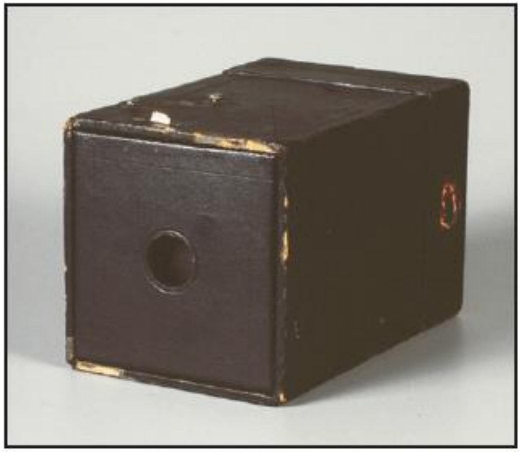

- Magnification = $\dfrac{d_2}{d_1}$
- Infinite depth of field (variable magnification)
- Pinhole diameter determines
  - resolution $\sim a$
  - light collection: $\Delta\Omega = \dfrac{\pi}{4}\dfrac{a^2}{d_1^2}$

Imaging optics (e.g., lenses) can be used for higher resolutions with larger solid angles.

E13982a

http://hedpschool.lle.rochester.edu/1000_proc2013.php

2D images can be taken using charge injection device (CID) or charge coupled device (CCD)

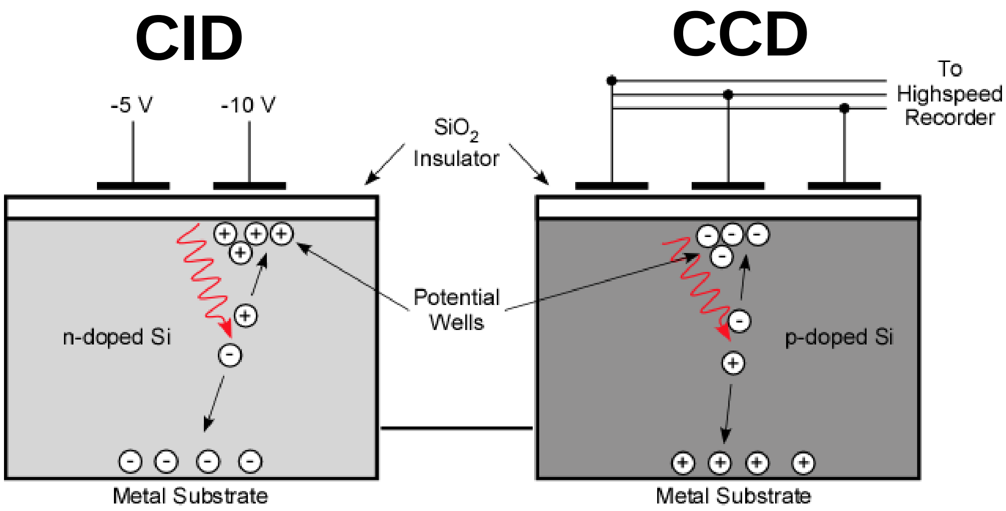

- **Color mask is used for color image**

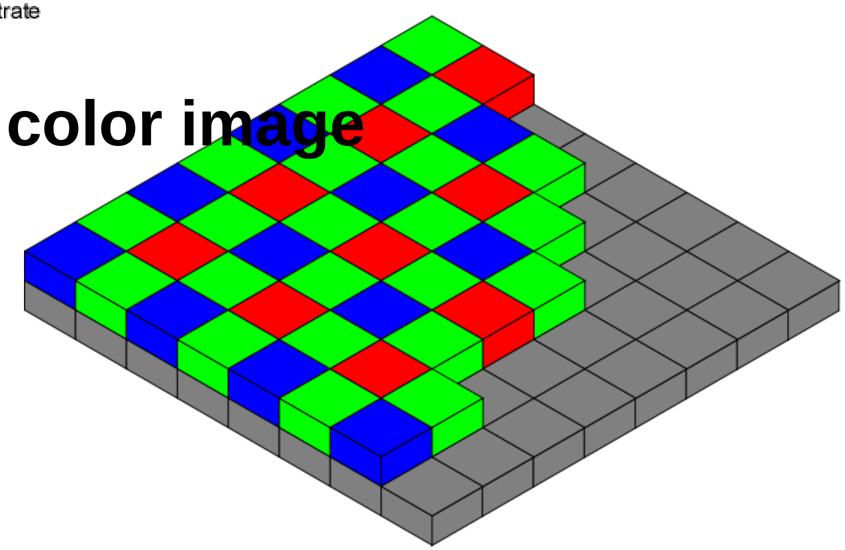

http://people.whitman.edu/~dunnivfm/FAASICPMS_Ebook/CH2/2_2_9.html
https://en.wikipedia.org/wiki/Charge-coupled_device

Charges are transferred along the array for readout in CCD

CCD readout:

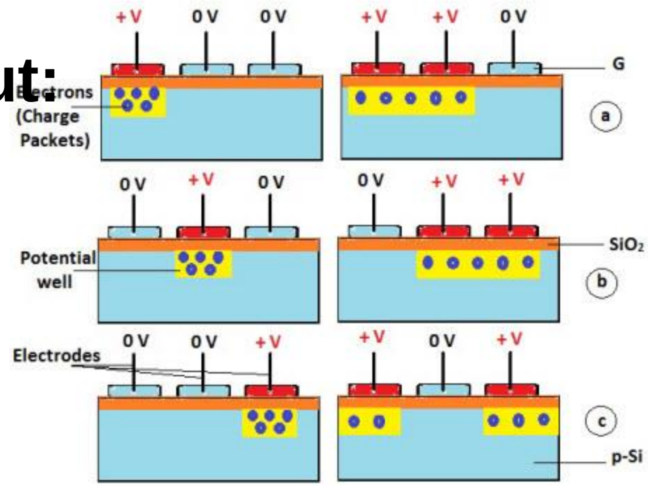

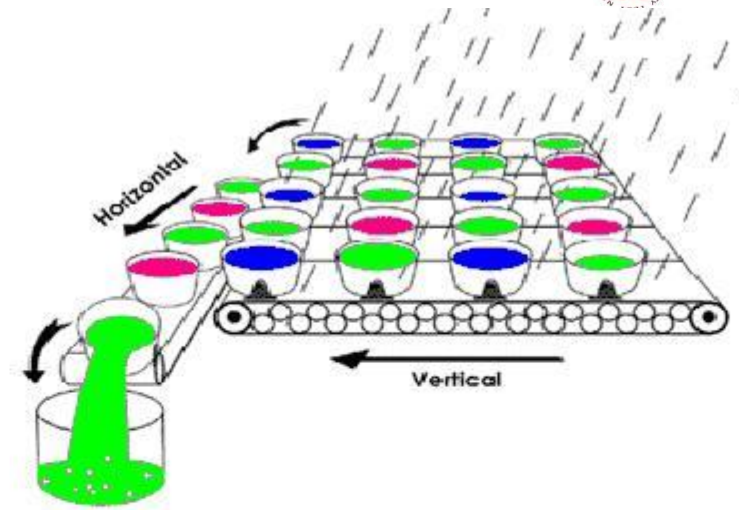

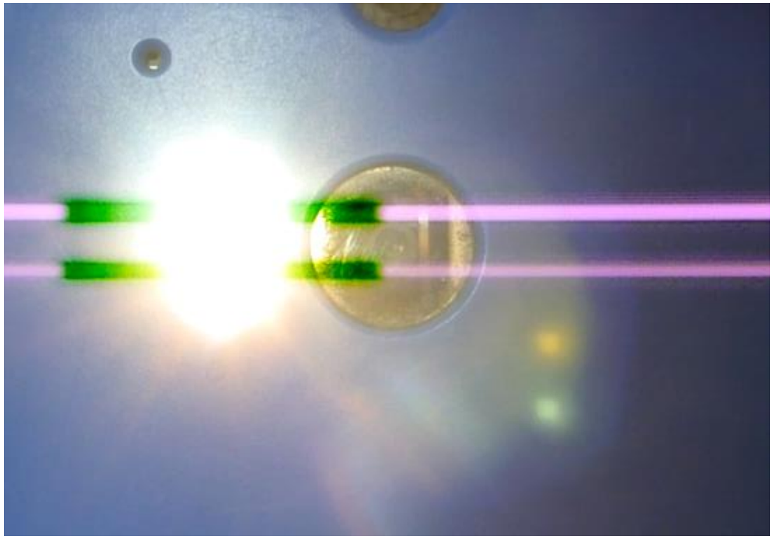

https://www.elprocus.com/know-about-the-working-principle-of-charge-coupled-device/
http://www.siliconimaging.com/ARTICLES/CMOS%20PRIMER.htm

Signal is readout individually in CMOS sensor

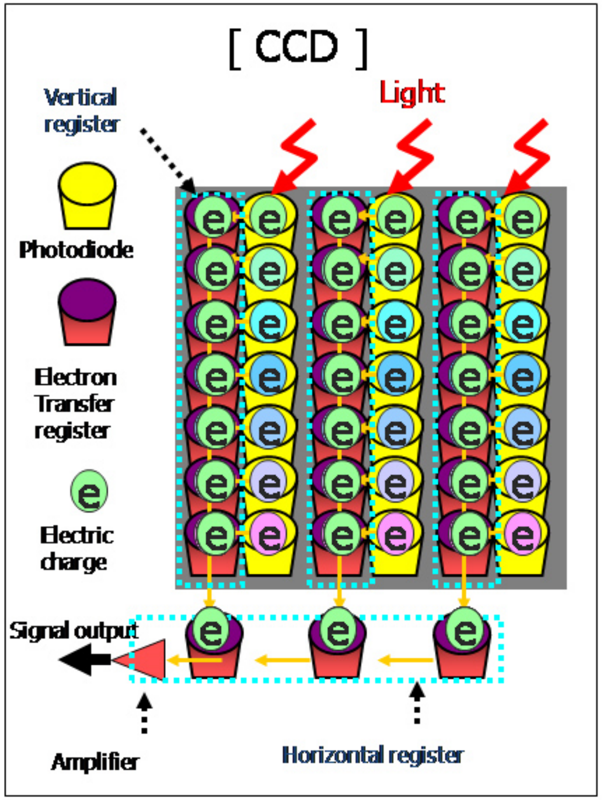

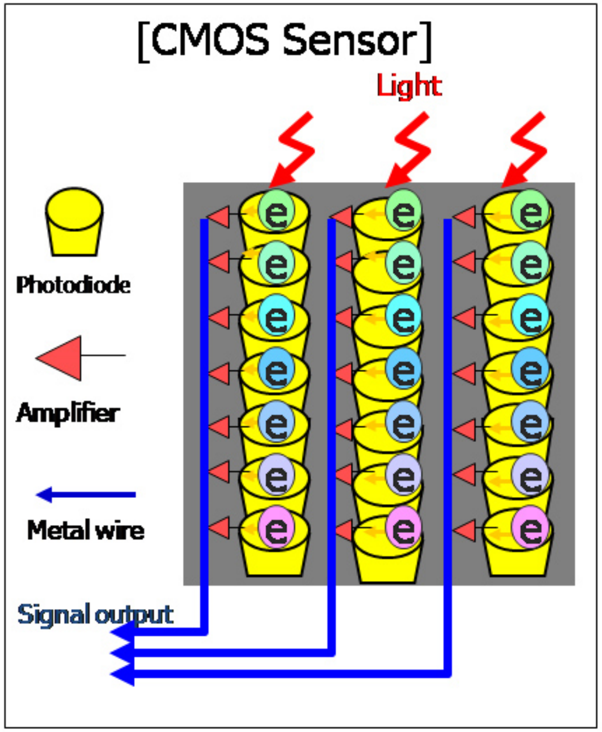

The number of electrons can be increased through photomultipliers or microchannel plate (MCP)

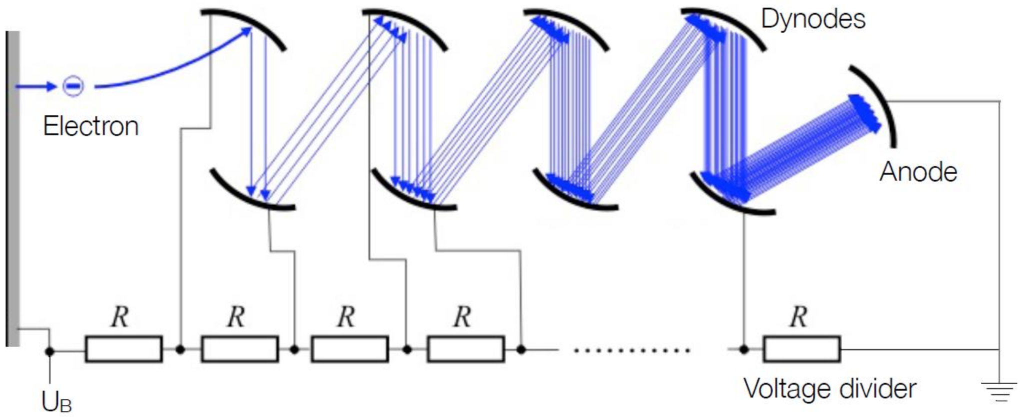

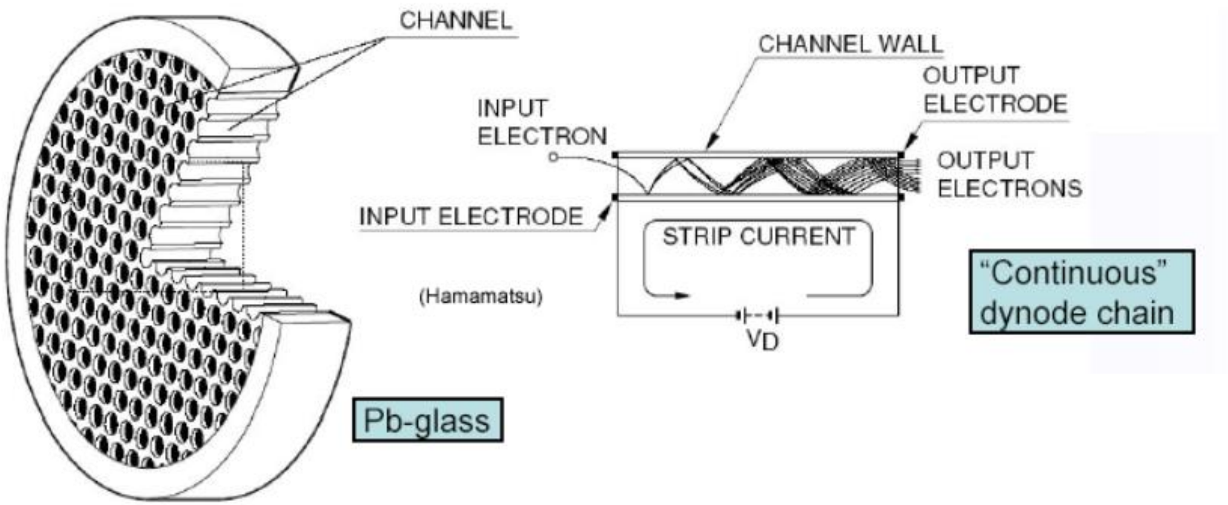

http://www.kip.uni-heidelberg.de/~coulon/Lectures/DetectorsSoSe10/

X-rays are imaged using photocathode, MCP, phosphor, and CCD

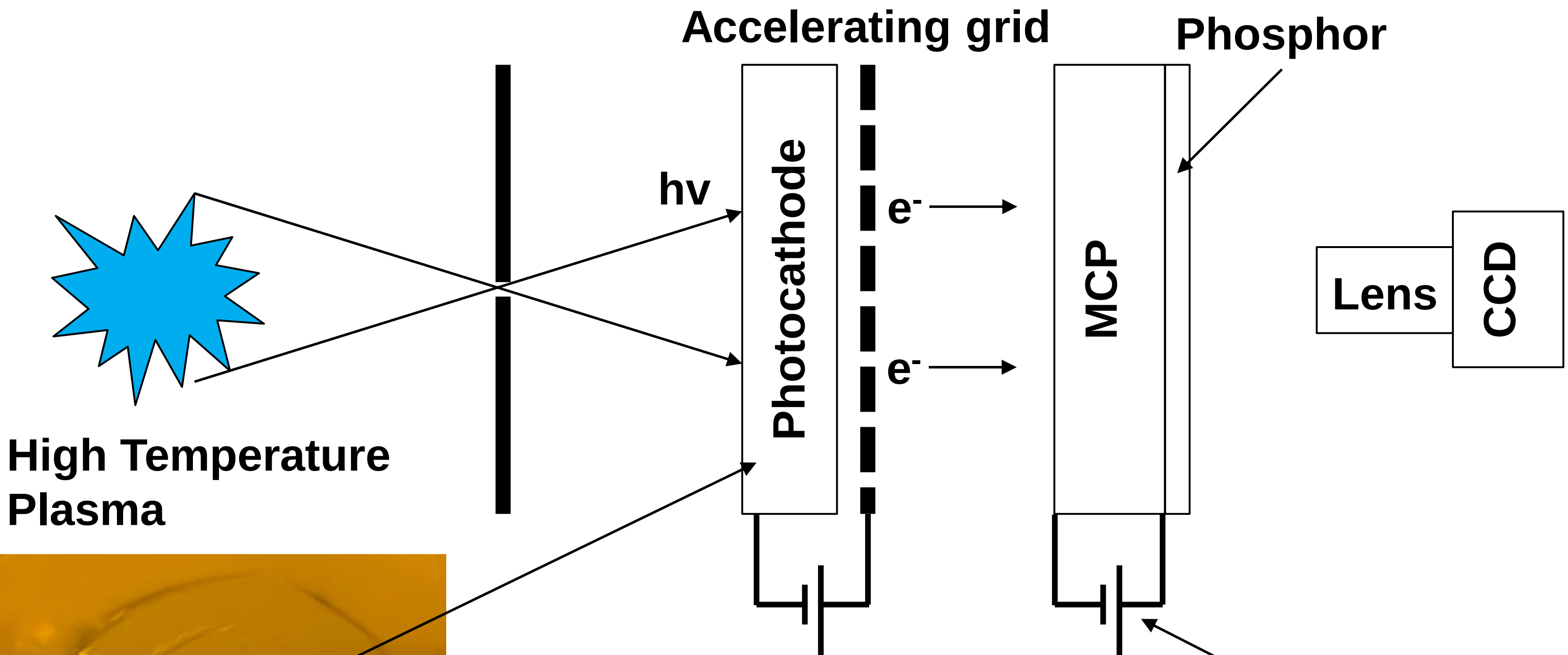

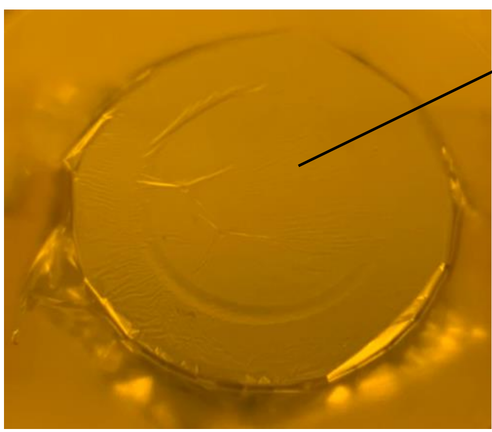

- CsI is used right now.
- Prof. Chou @ Photonics, NCKU is developing 50nm Au foil for us.

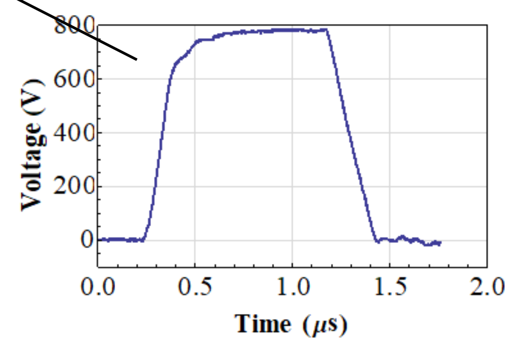

- **Images can be gated using fast high voltage pulses.**

A negative high-voltage pulse is used in our x-ray pinhole camera

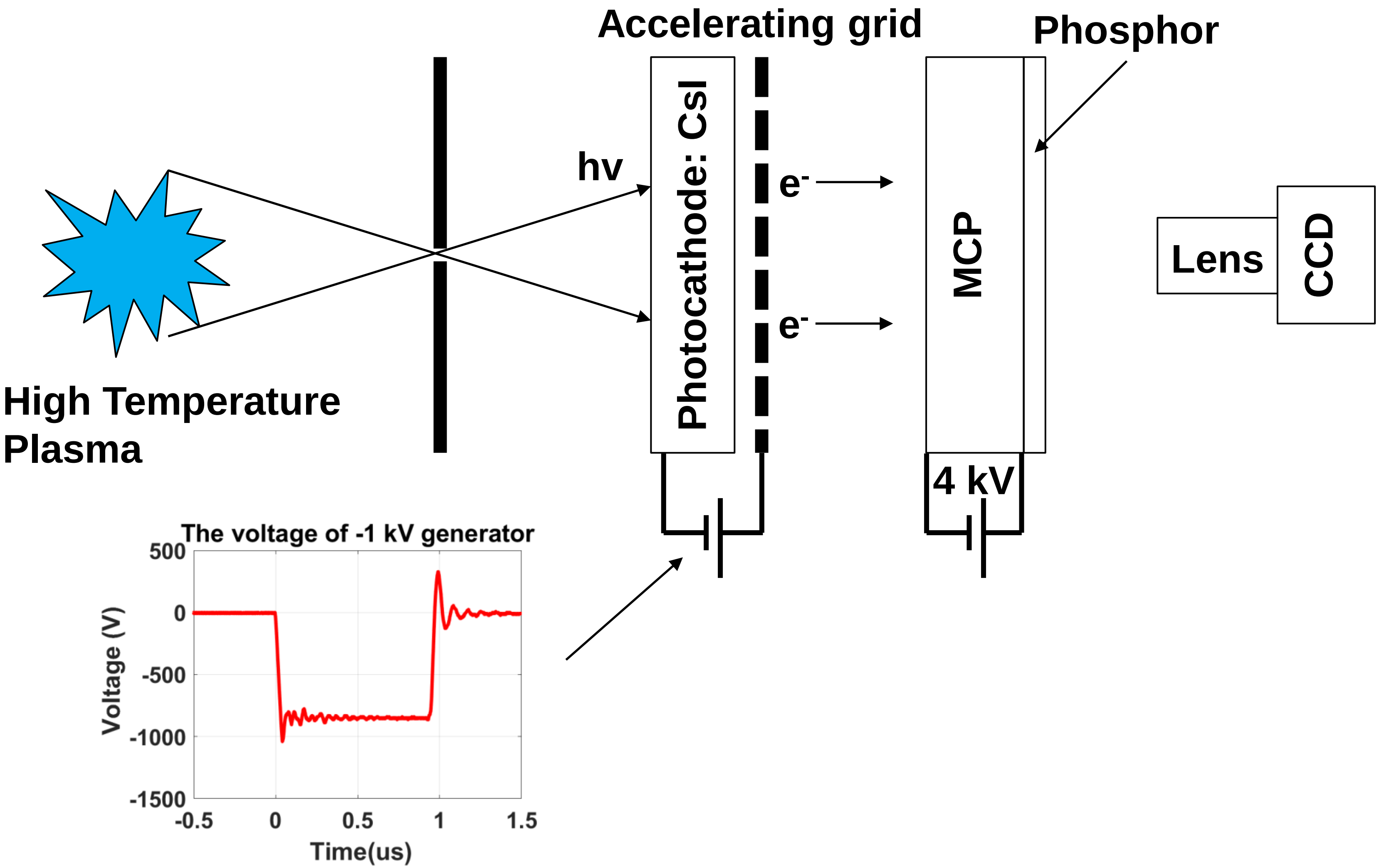

- **The x-ray camera with a shutter opening time of ≤ 10 ns will be built.**

A pinhole camera was designed and was built

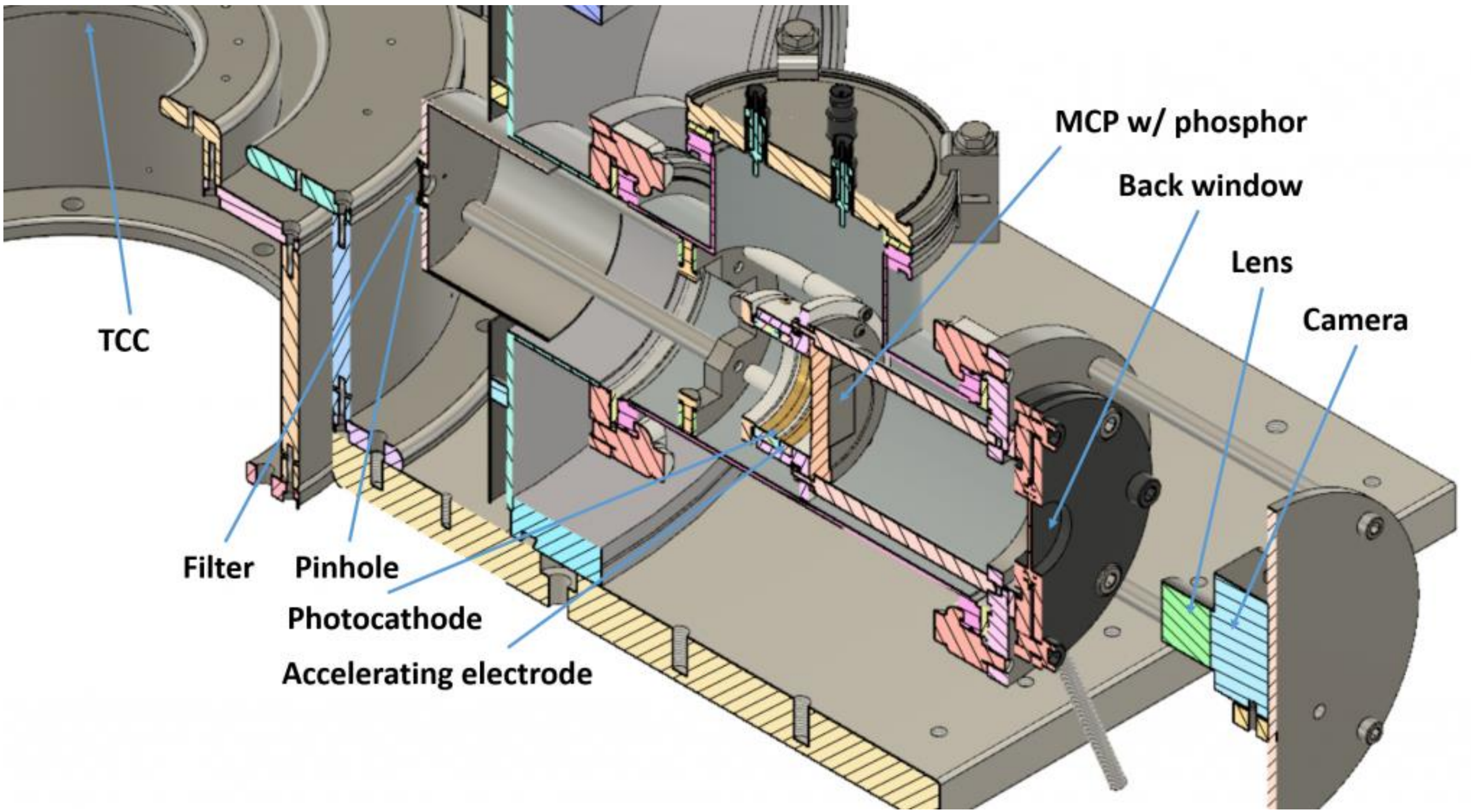

Electronic detectors provide rapid readout

- Electronic detectors are typically semiconductors or ionization-based stacks (e.g., photomultipliers)

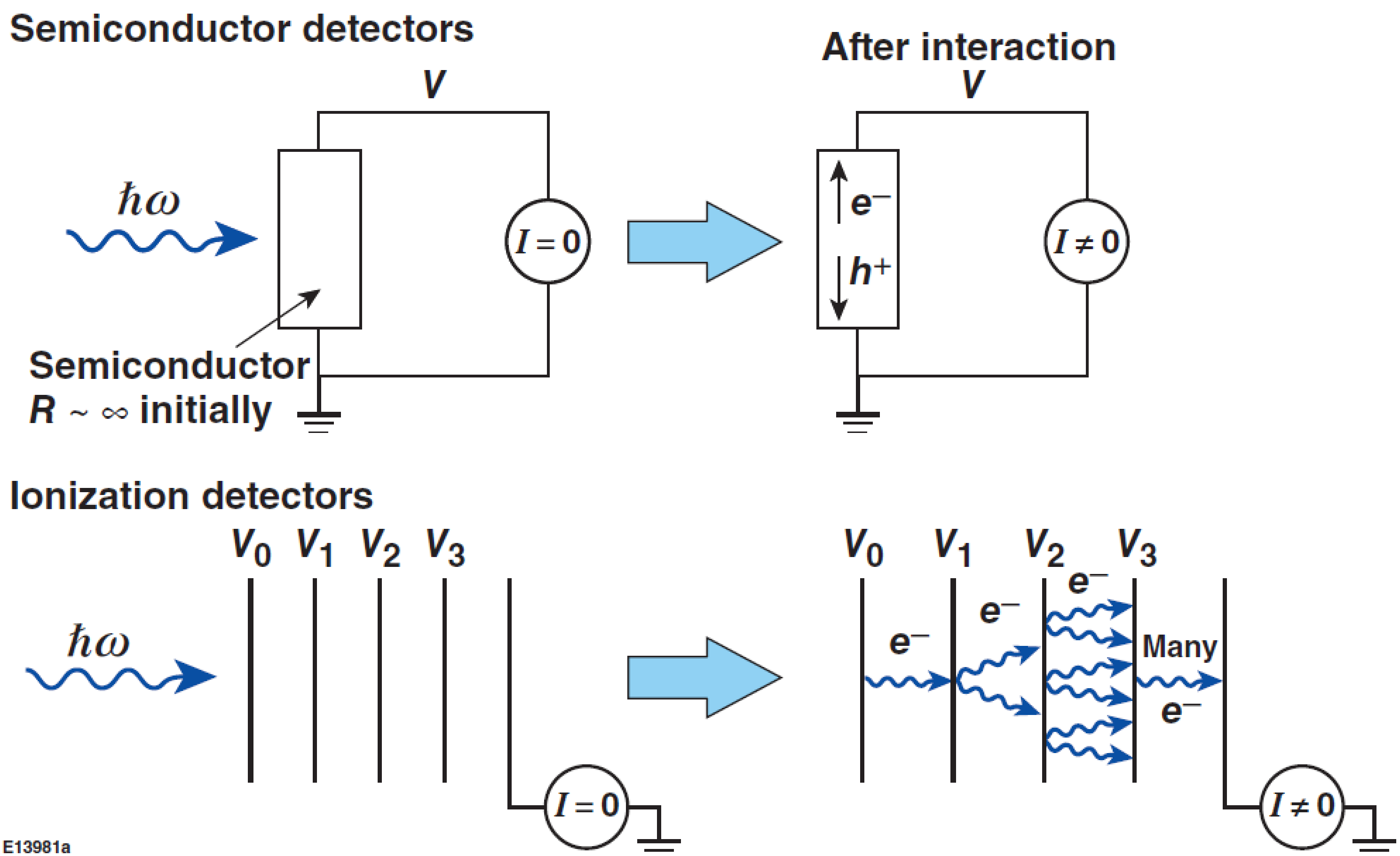

http://hedpschool.lle.rochester.edu/1000_proc2013.php

A framing camera provides a series of time-gated 2-D images, similar to a movie camera

- The building block of a framing camera is a gated microchannel-plate (MCP) detector
- An MCP is a plate covered with small holes, each acts as a photomultiplier

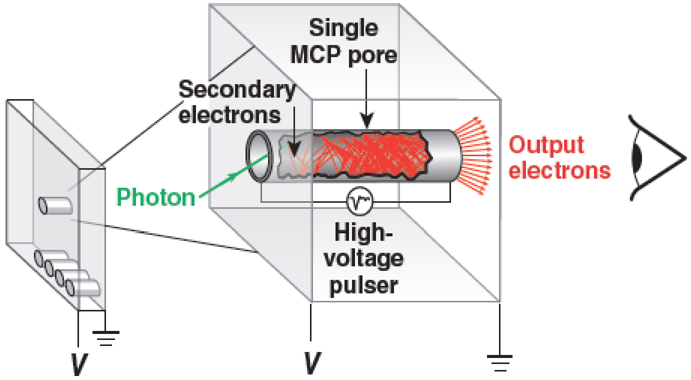

Multiple electrons are produced each time an electron or photon hits the wall

- A voltage pulse is sent down the plate, gating the detector

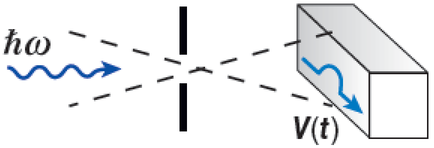

The detector is only on when the voltage pulse is present

E13986b

http://hedpschool.lle.rochester.edu/1000_proc2013.php

A framing camera detector consists of a microchannel plate (MCP) in front of a phosphor screen

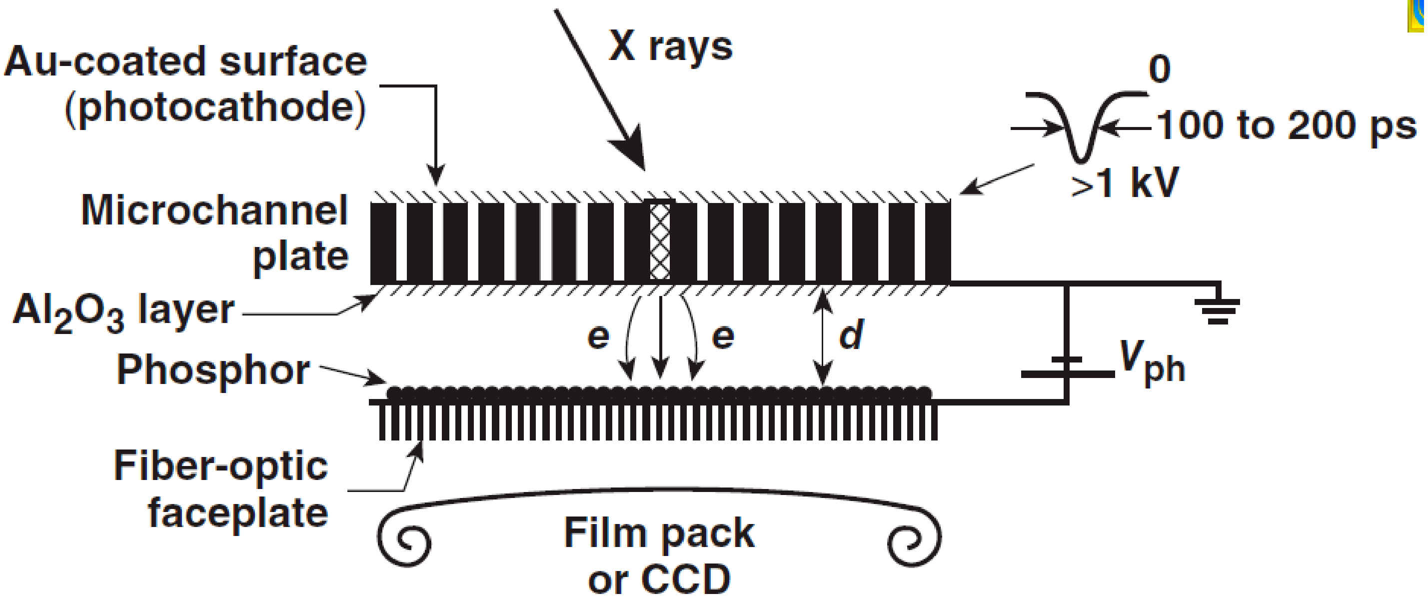

- Electrons are multiplied through MCP by voltage V_c
- Images are recorded on film behind phosphor
- Insulating Al_2O_3 layer allows for V_{ph} to be increased, thereby improving the spatial resolution of phosphor

E7795b

http://hedpschool.lle.rochester.edu/1000_proc2013.php

Two-dimensional time-resolved images are recorded using x-ray framing cameras

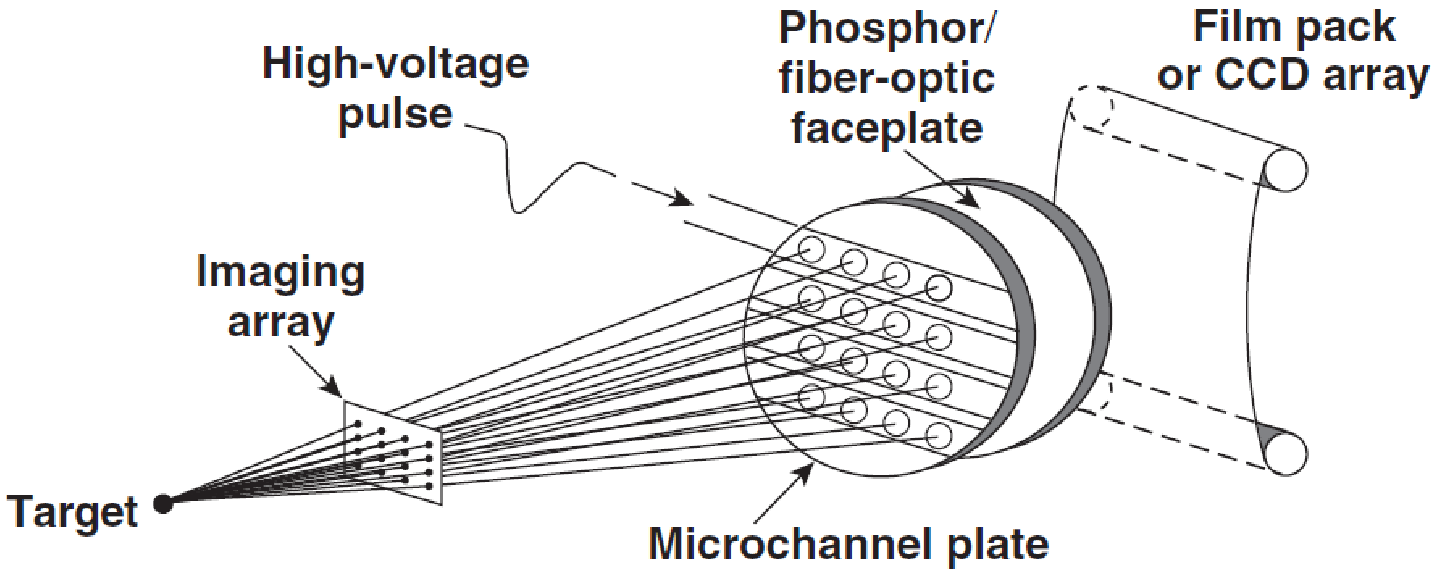

- Temporal resolution = 35 to 40 ps
- Imaging array: Pinholes: 10- to 12-μm resolution, 1 to 4 keV
- Space-resolved x-ray spectra can be obtained by using Bragg crystals and imaging slits

E7105b

http://hedpschool.lle.rochester.edu/1000_proc2013.php

X-ray framing cameras for recording two-dimensional time-resolved images will be built by the end of 2021

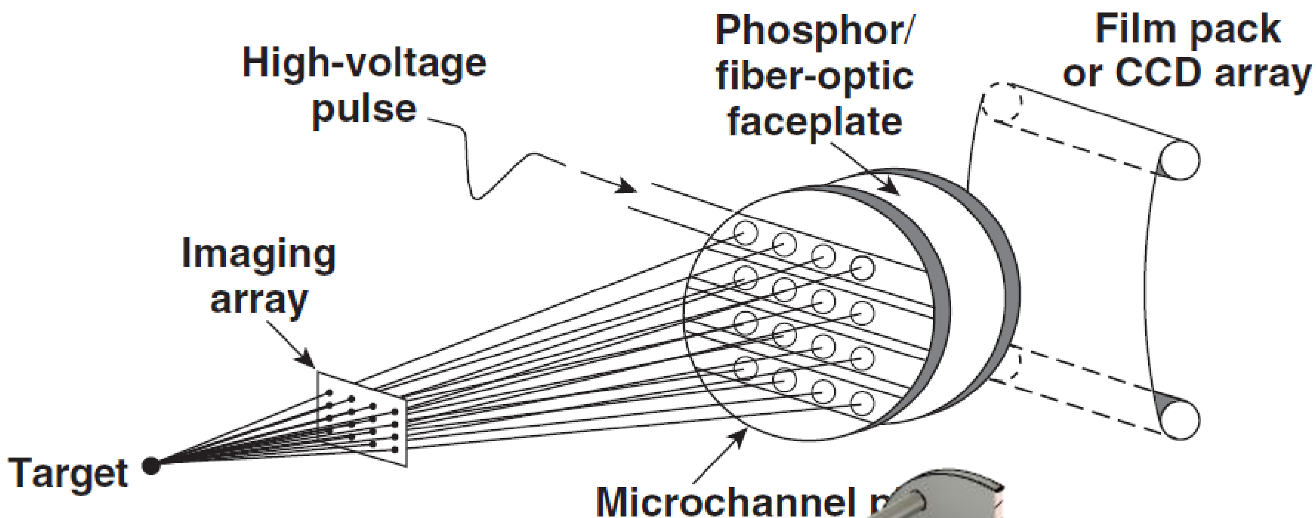

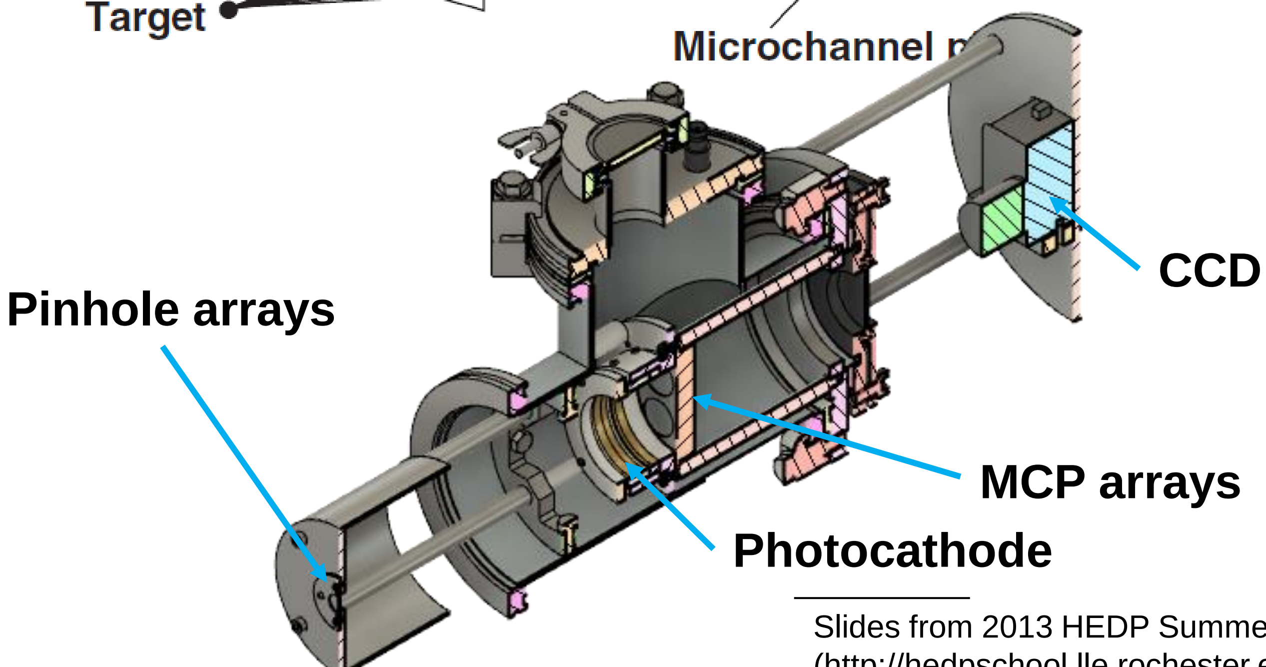

Slides from 2013 HEDP Summer School (http://hedpschool.lle.rochester.edu/1000_proc2013.php)

Each pinhole camera will be triggered separately

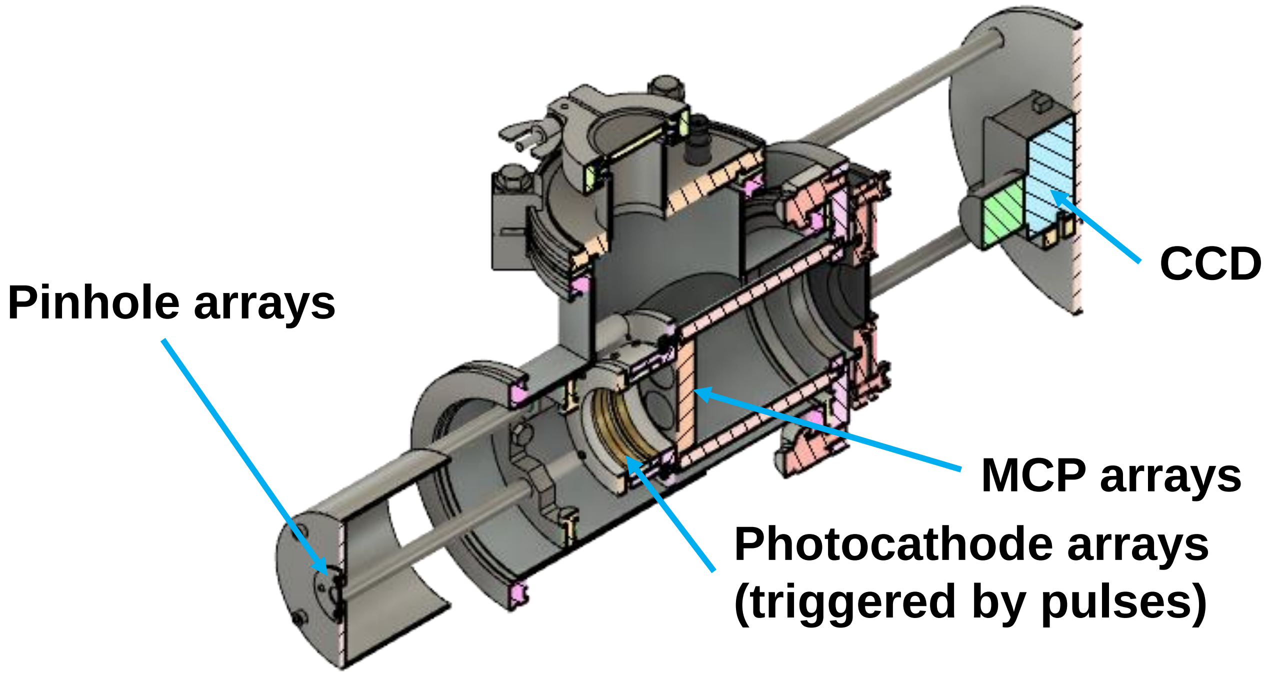

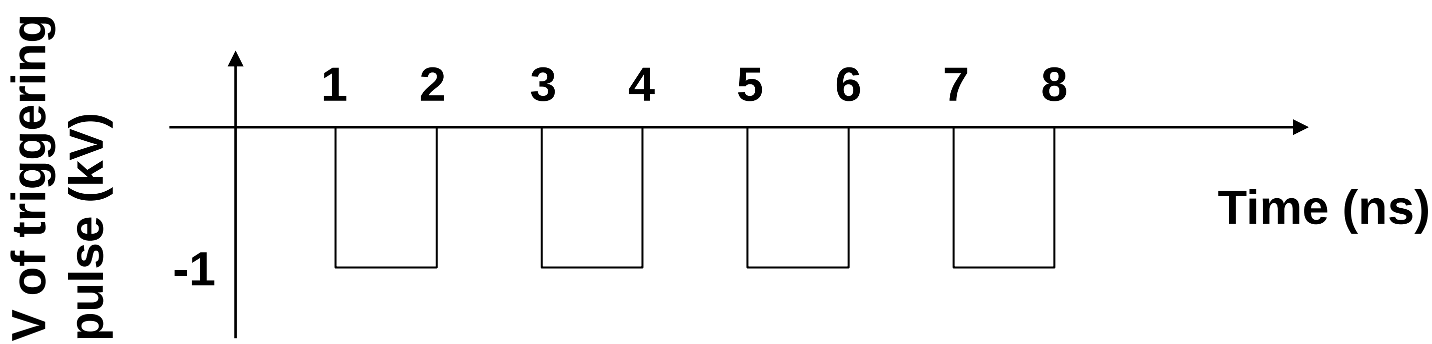

A streak camera provides temporal resolution of 1-D data

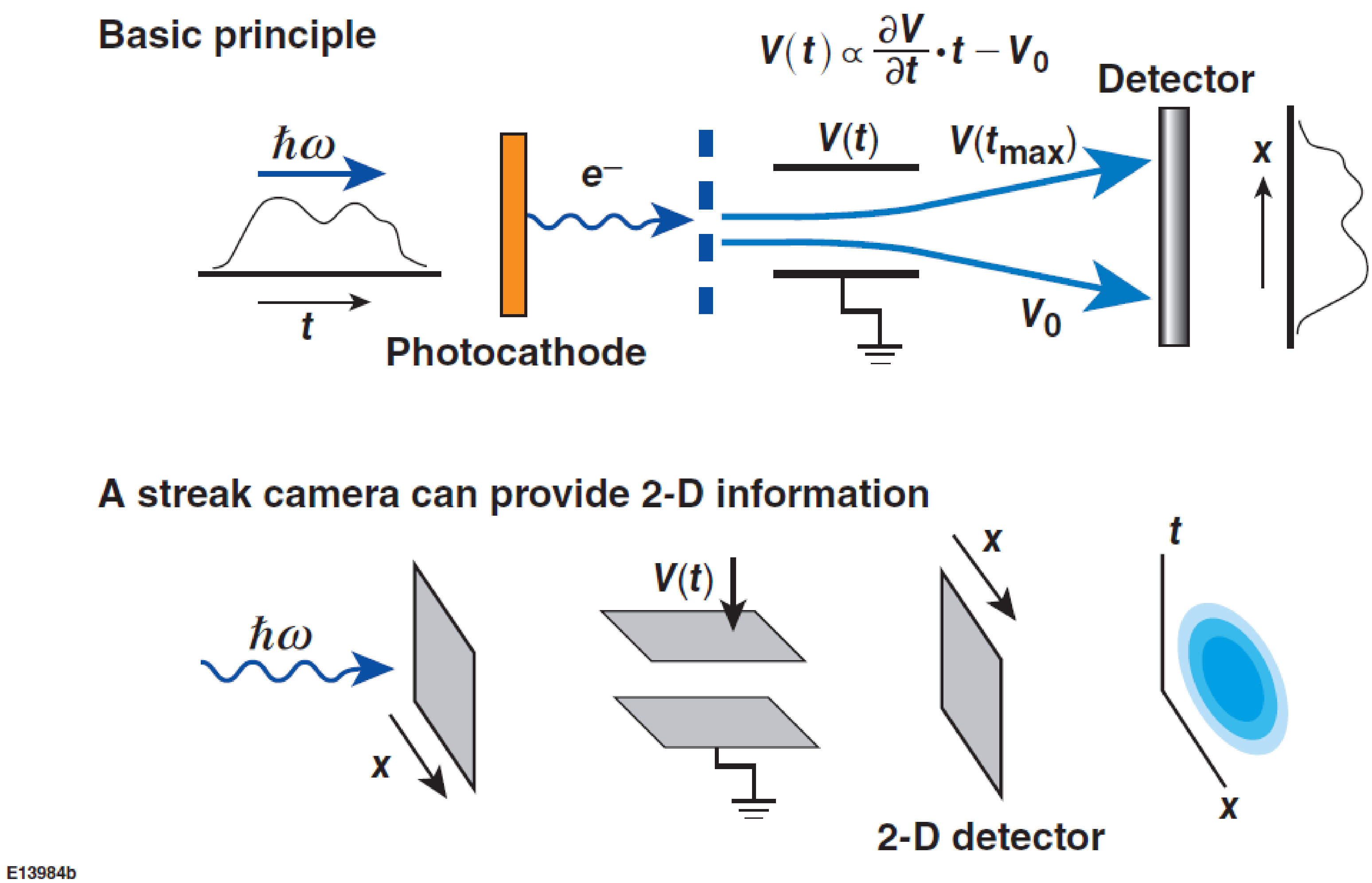

http://hedpschool.lle.rochester.edu/1000_proc2013.php

A temporal resolution higher than 15 ps is expected

Imaging system
- **Visible light: regular lens**
- **X rays: pinhole**

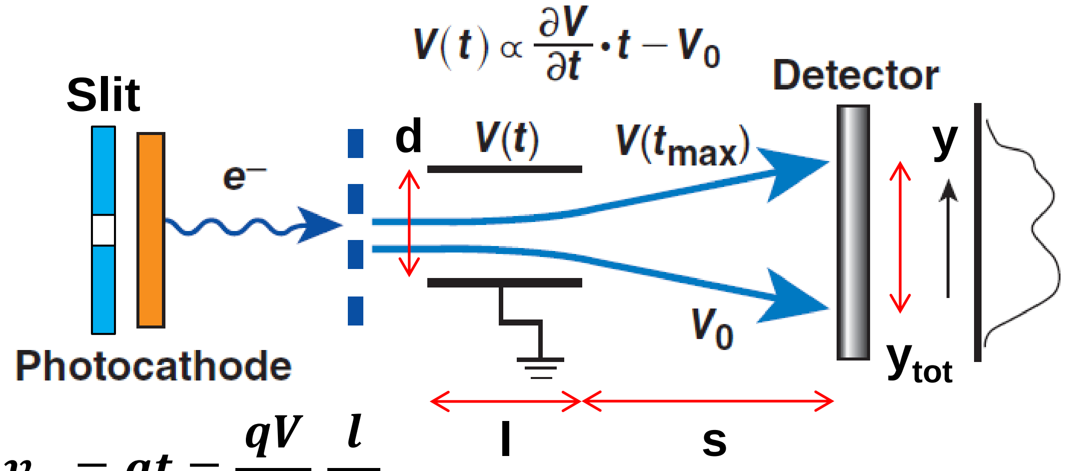

$$a = \frac{F}{m} = \frac{\mathrm{qE}}{m} = \frac{qV}{md} \qquad v_\perp = at = \frac{qV}{md}\frac{l}{v_{||}}$$

$$y = s\,\mathrm{Tan}\theta = s\frac{V_\perp}{V_{||}} = \frac{1}{2E_k}\frac{l}{d}sqV = \frac{1}{2E_k}\frac{l}{d}sq(V_0 + V't)$$

- **Let d=10 mm, l=20 mm, s=50 mm, E_k=1 keV, V=-200 ~ 200 V**

$$V' \equiv \frac{V_{\mathrm{tot}}}{t_{\mathrm{tot}}} = 0.06\,\mathrm{kV/ns} \qquad y_{\mathrm{tot}} = 15\mathrm{mm} \qquad y_{\mathrm{tot}} = 15\mathrm{mm}$$

- **Temporal resolution:**

$$\delta\mathrm{t} = \delta\mathrm{y}\frac{2E_k d}{lsqV'} = 15\ \mathrm{ps} \quad \mathrm{for} \quad \delta\mathrm{y} = 45\mu\mathrm{m}$$

- **δt will be adjusted by changing E_k.**

A streak camera with temporal resolution of 15 ps has been developed

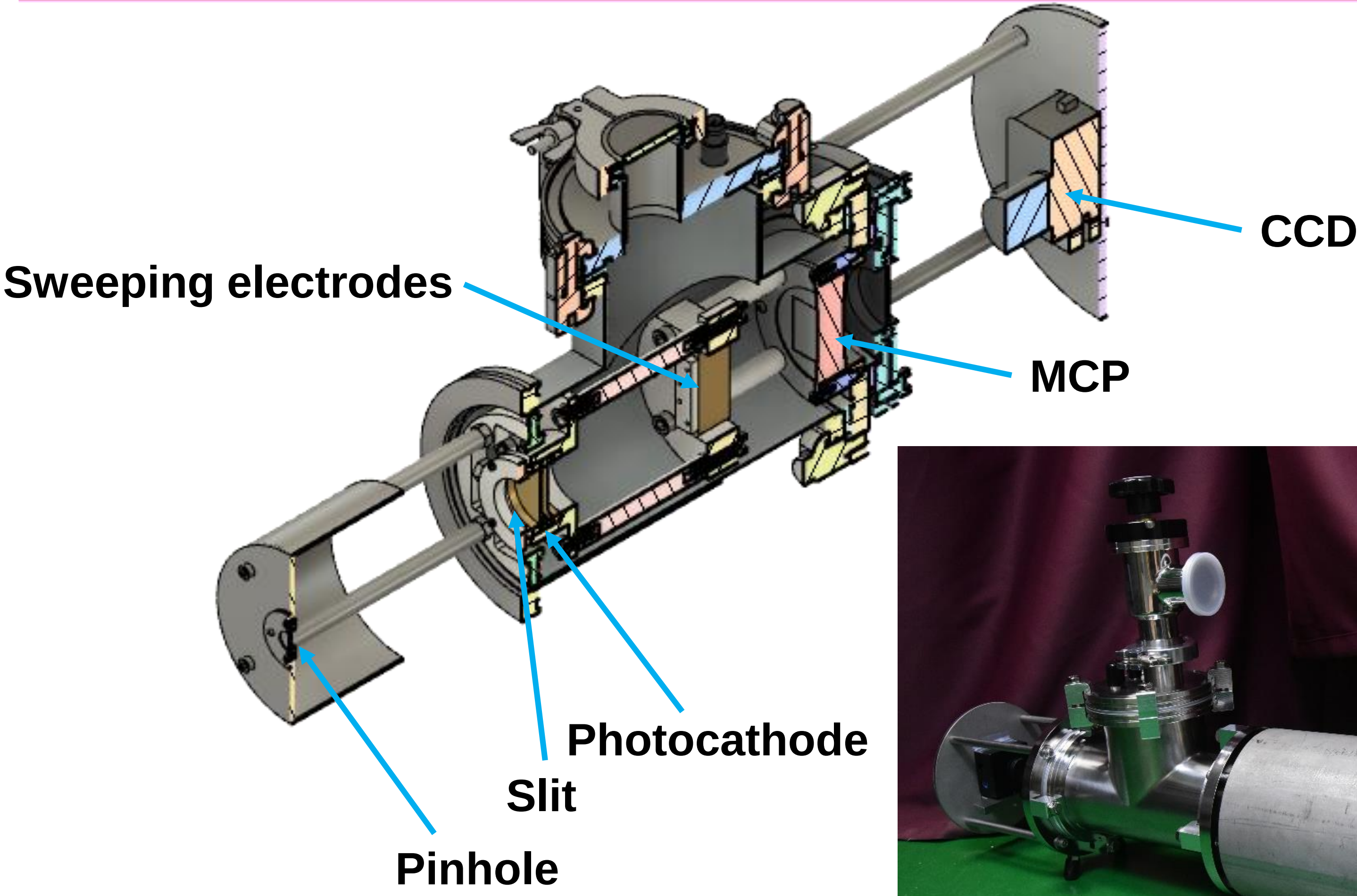

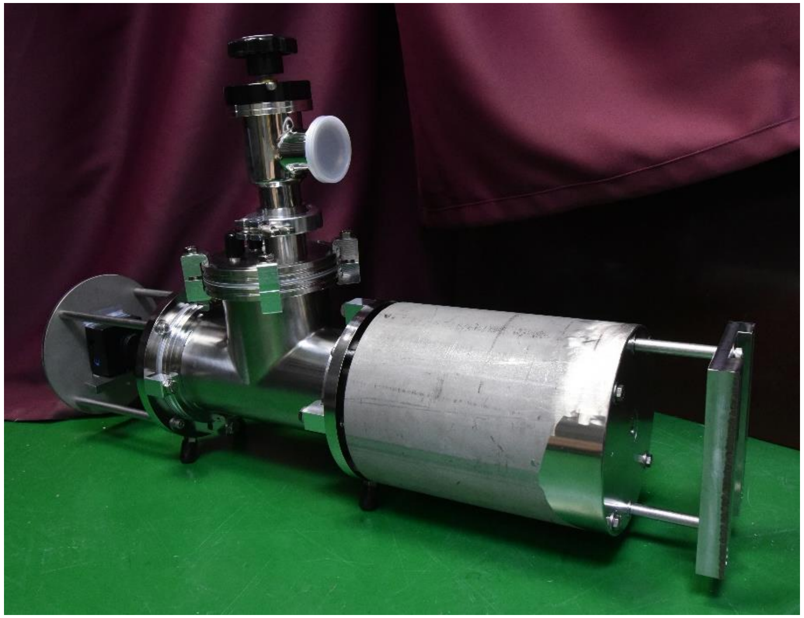

Shell trajectories can be measured using framing camera or streak camera

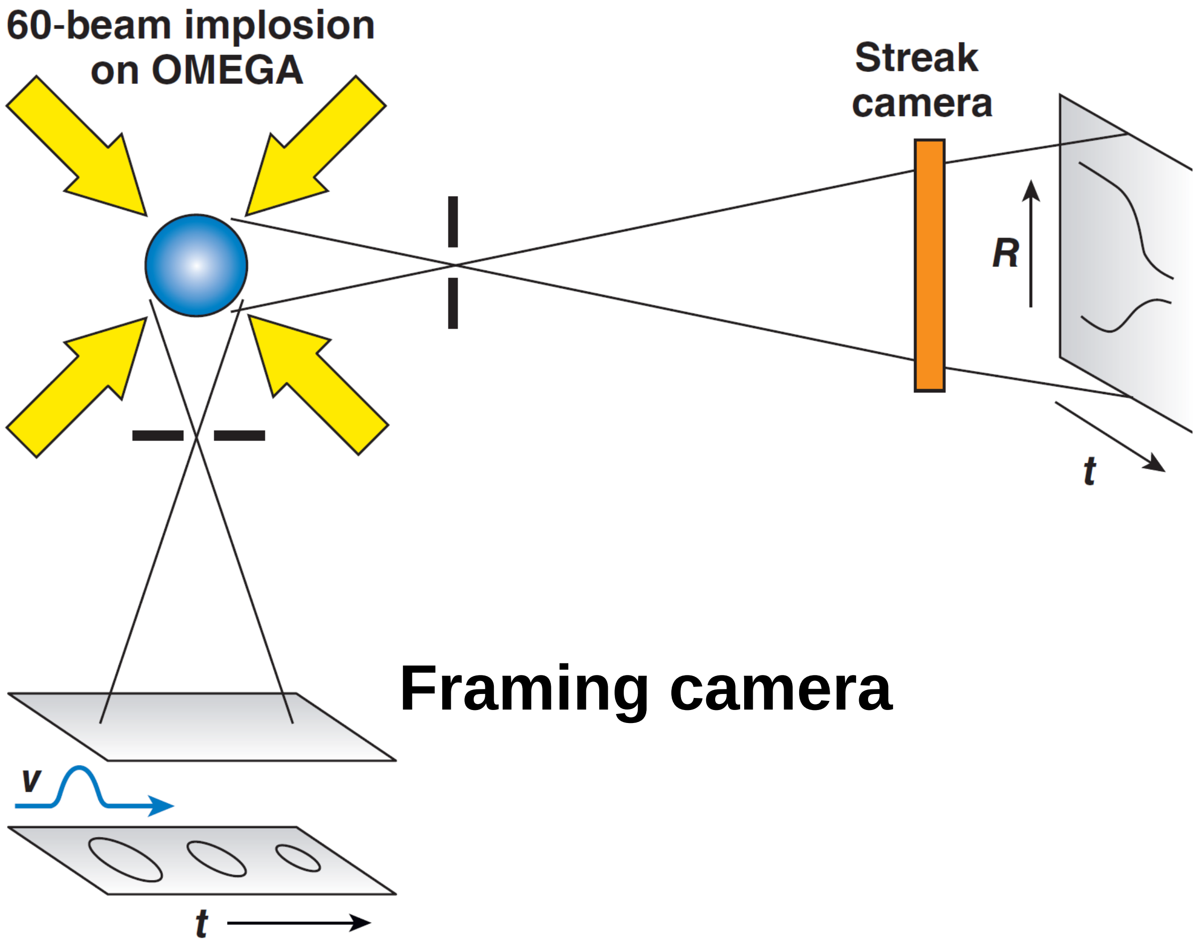

Comparison of images from framing camera versus streak camera

Framing-camera image
6× magnification

Shot 13377

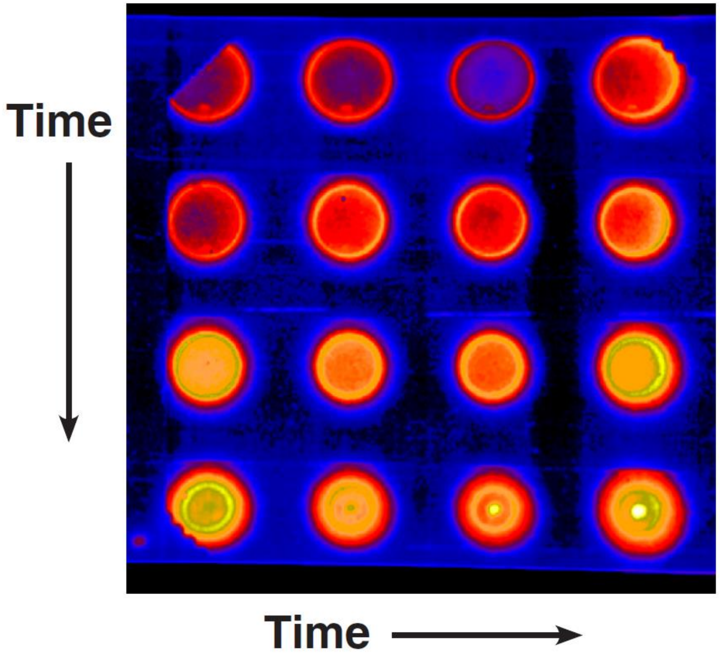

Streak-camera image

Shot 13377

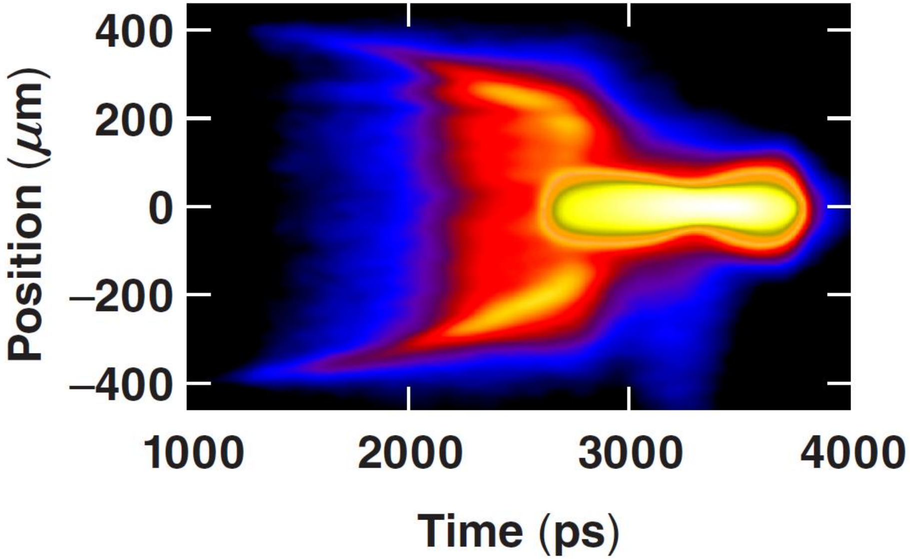

The optical density can be measured using the absorption of a backlighter

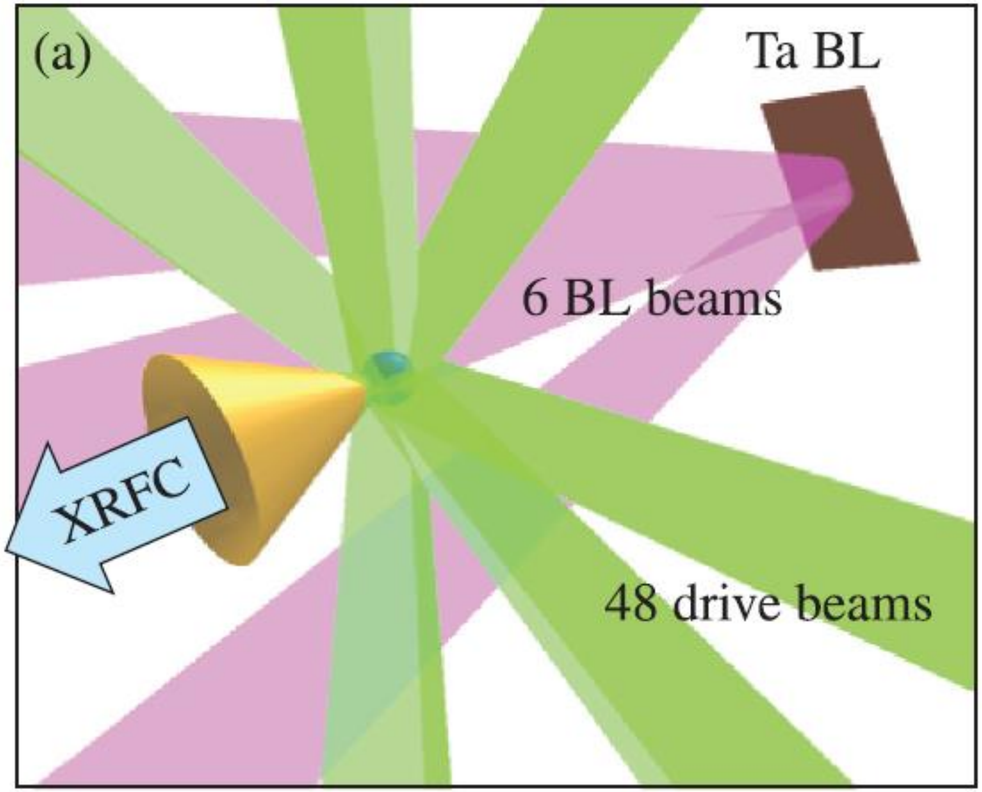

$$I = \int I(\varepsilon)\exp(-\mu(\varepsilon)\rho\delta)d\varepsilon$$

$$I = I_{\mathrm{BL}}\exp(-\bar{\mu}\rho\delta)$$

$$\ln I = \ln I_{BL} - \mu\rho r$$

G. Fiksel *et al.*, Phys. Plasmas **19**, 062704 (2012)

Shock velocities are measured using time-resolved Velocity Interferometer System for Any Reflector (VISAR)

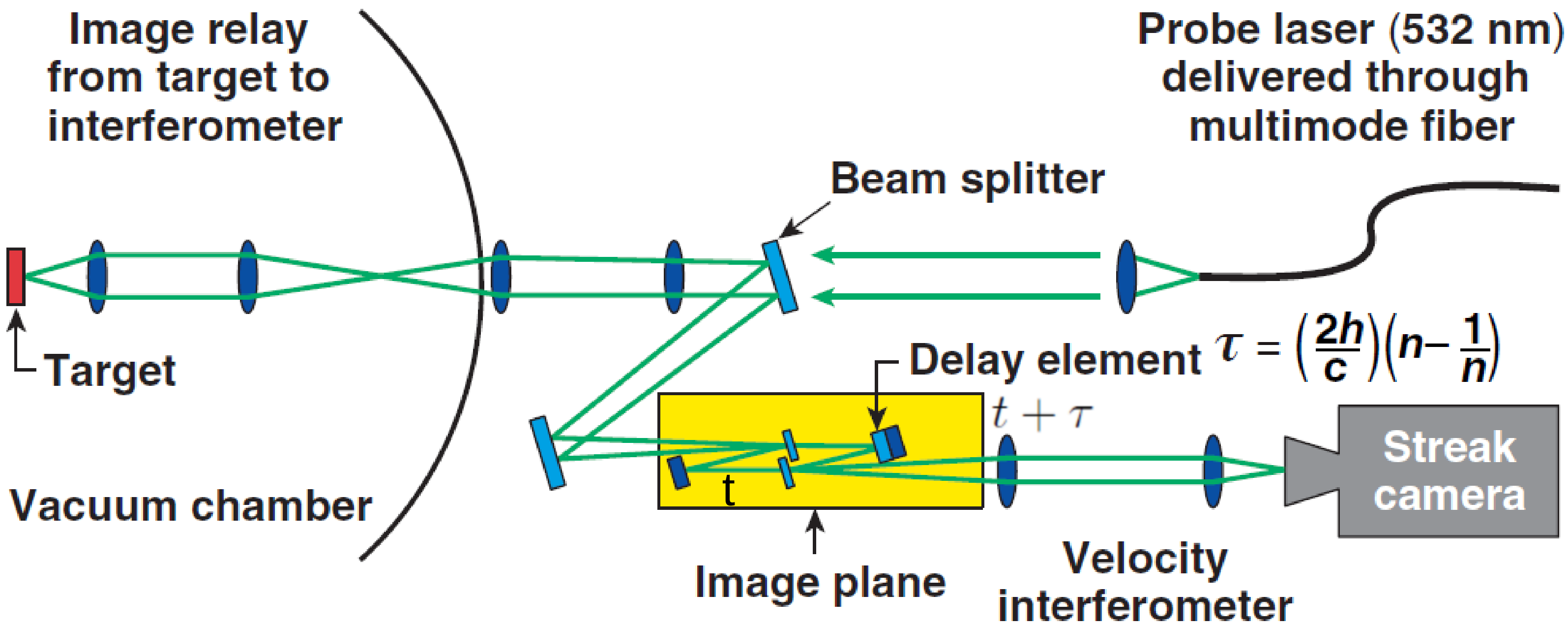

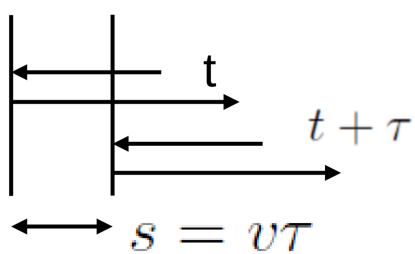

$$\Delta\phi = \frac{v\tau}{\lambda} \propto v$$

http://hedpschool.lle.rochester.edu/1000_proc2013.php

Neutron average temperature is obtained using Neutron Time of Flight (NToF)

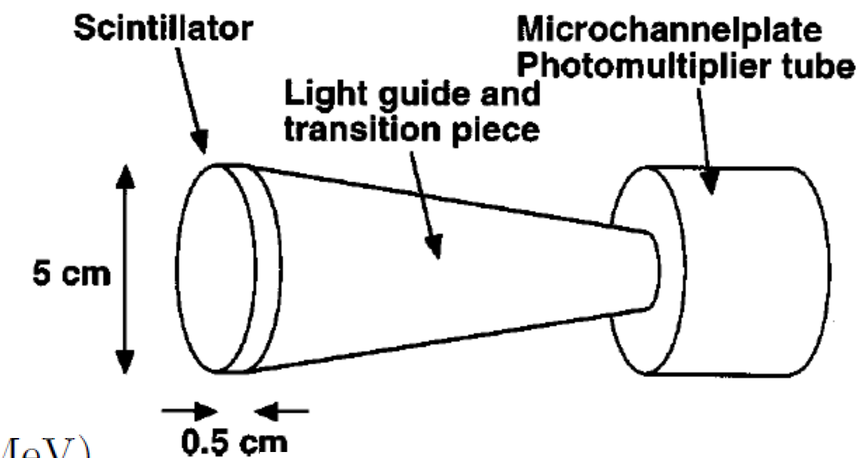

$$D + D \longrightarrow He^3\,(0.82\ \mathrm{MeV}) + n\,(2.45\ \mathrm{MeV})$$

$$D + T \longrightarrow He^4\,(3.5\ \mathrm{MeV}) + n\,(14.1\ \mathrm{MeV})$$

$$s = vt \qquad v = \frac{s}{t}$$

$$f\,(v) = \sqrt{\left(\frac{m}{2\pi kT}\right)} \exp\left(-\frac{mv^2}{2kT}\right)$$

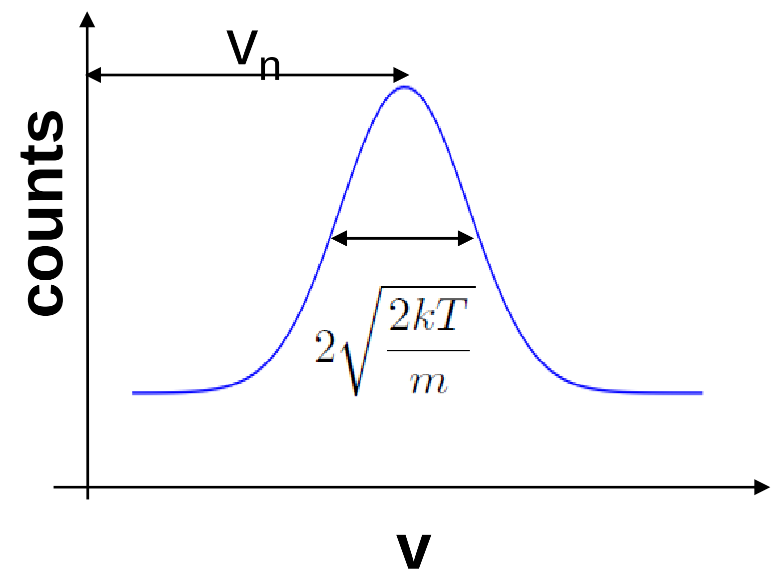

The OMEGA Facility is carrying out ICF experiments using a full suite of target diagnostics

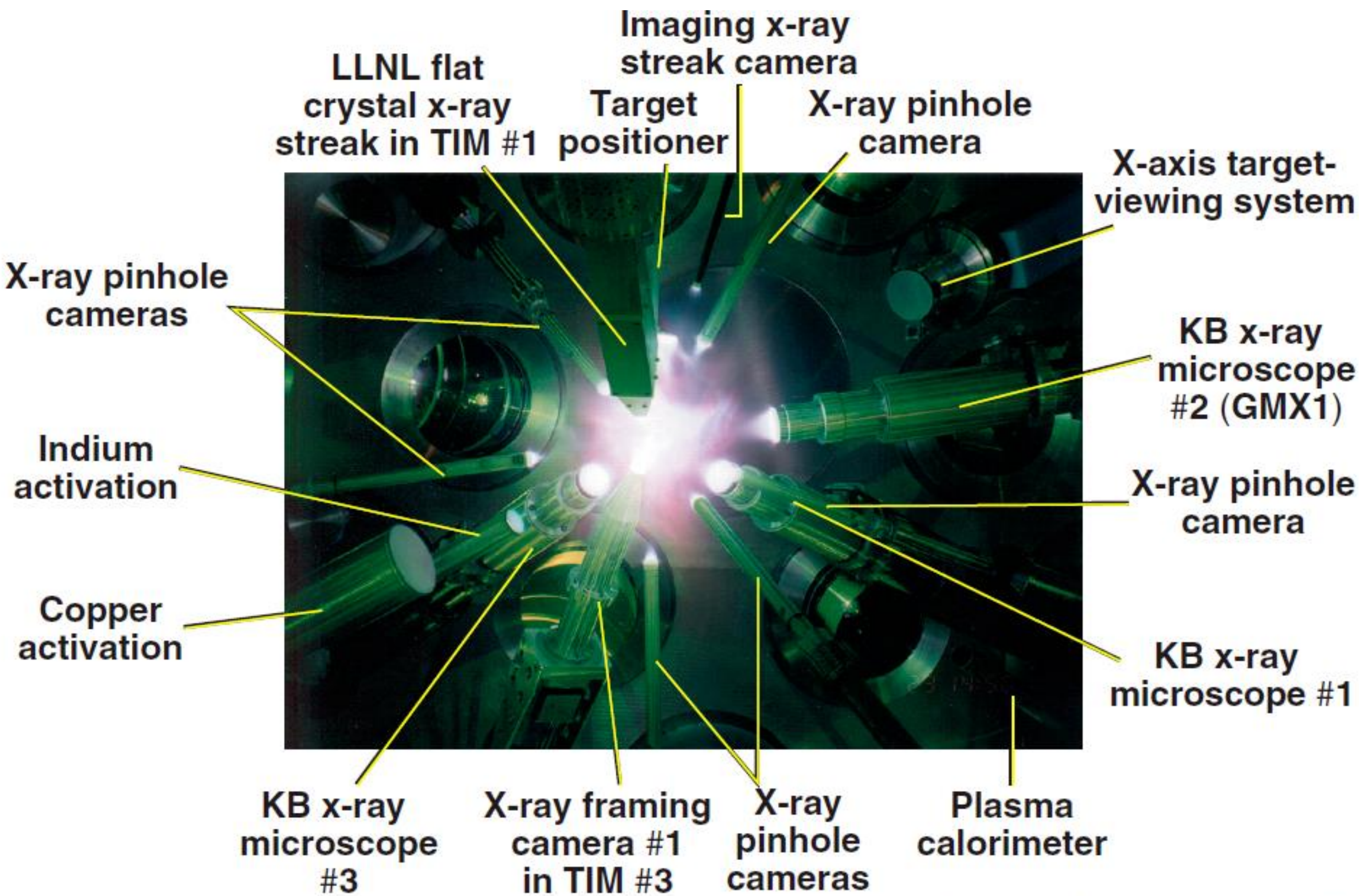

E8012b

Photo taken from port H11B

A suit of diagnostics in the range of (soft) x-ray are being built

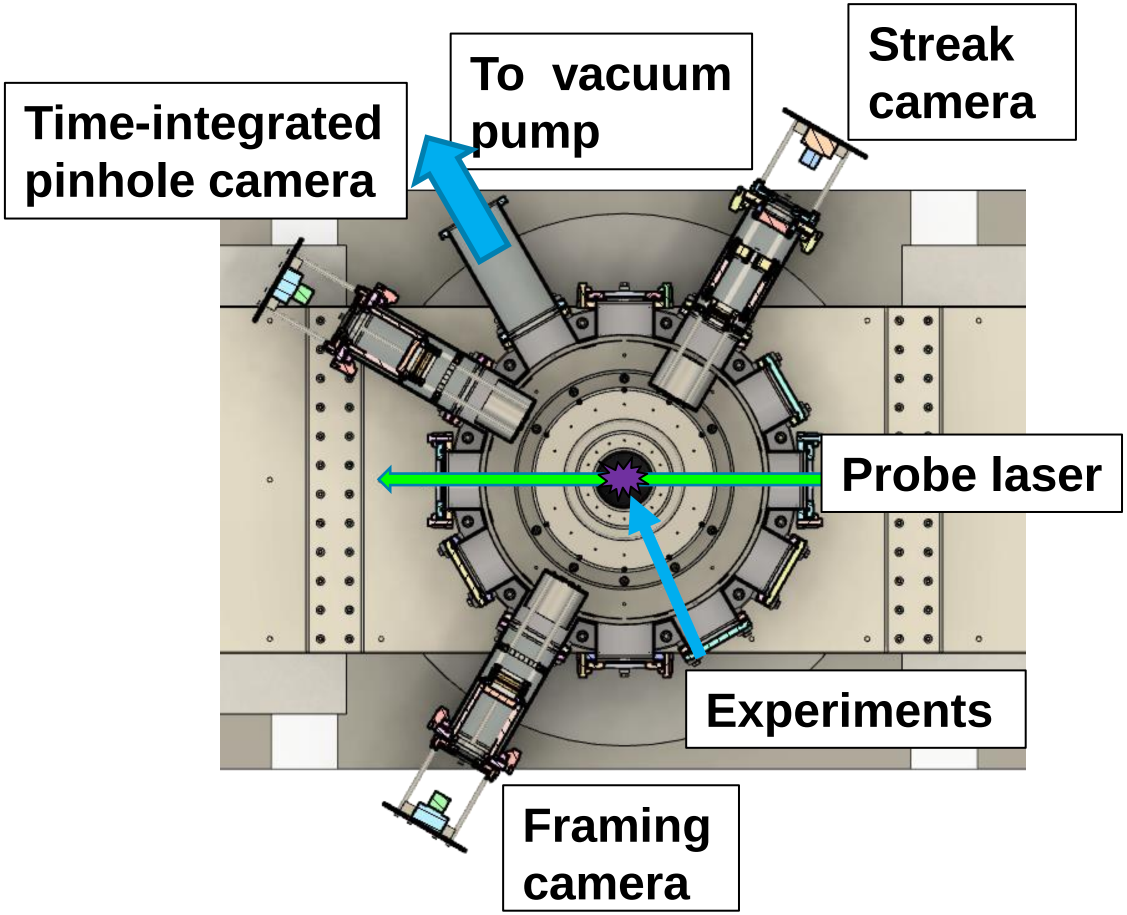

- CsI are used as the photocathode for all x-ray imaging system.
- Au photocathode may be used in the future.

- **Pinhole camera:**
  - Magnification: 1x
  - Exposure time: 1 us
- **Streak camera:**
  - Magnification: 1x
  - Temporal resolution: 15 ps
- **Framing camera:**
  - Magnification: 0.3x
  - Temporal resolution: ~ns using 4 individual MCPs
- **Laser probing:**
  - For interferometer, schlieren, shadowgraphy, Thomson scattering.
  - Temporal resolution: ~300 ps using stimulated brillouin scattering (SBS) pulse compression in water

Varies diagnostics were integrated to the system

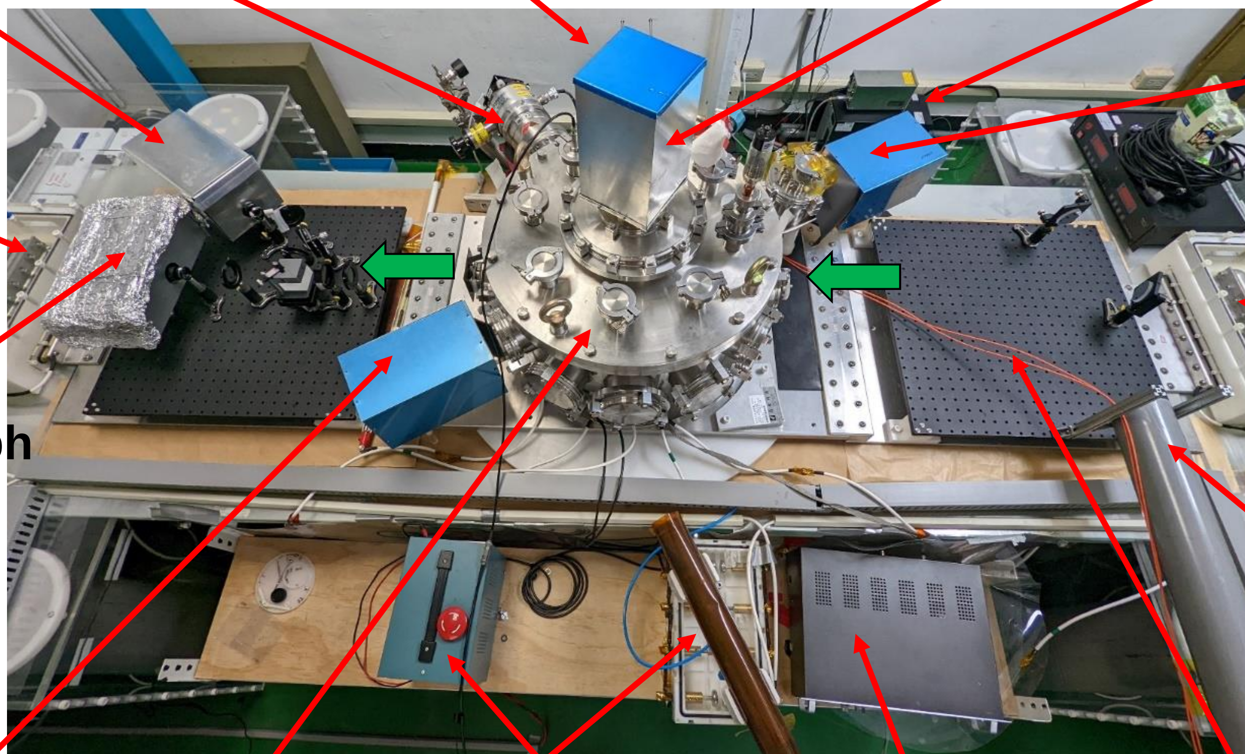

Time-resolved imaging system with temporal resolution in the order of nanoseconds was implemented

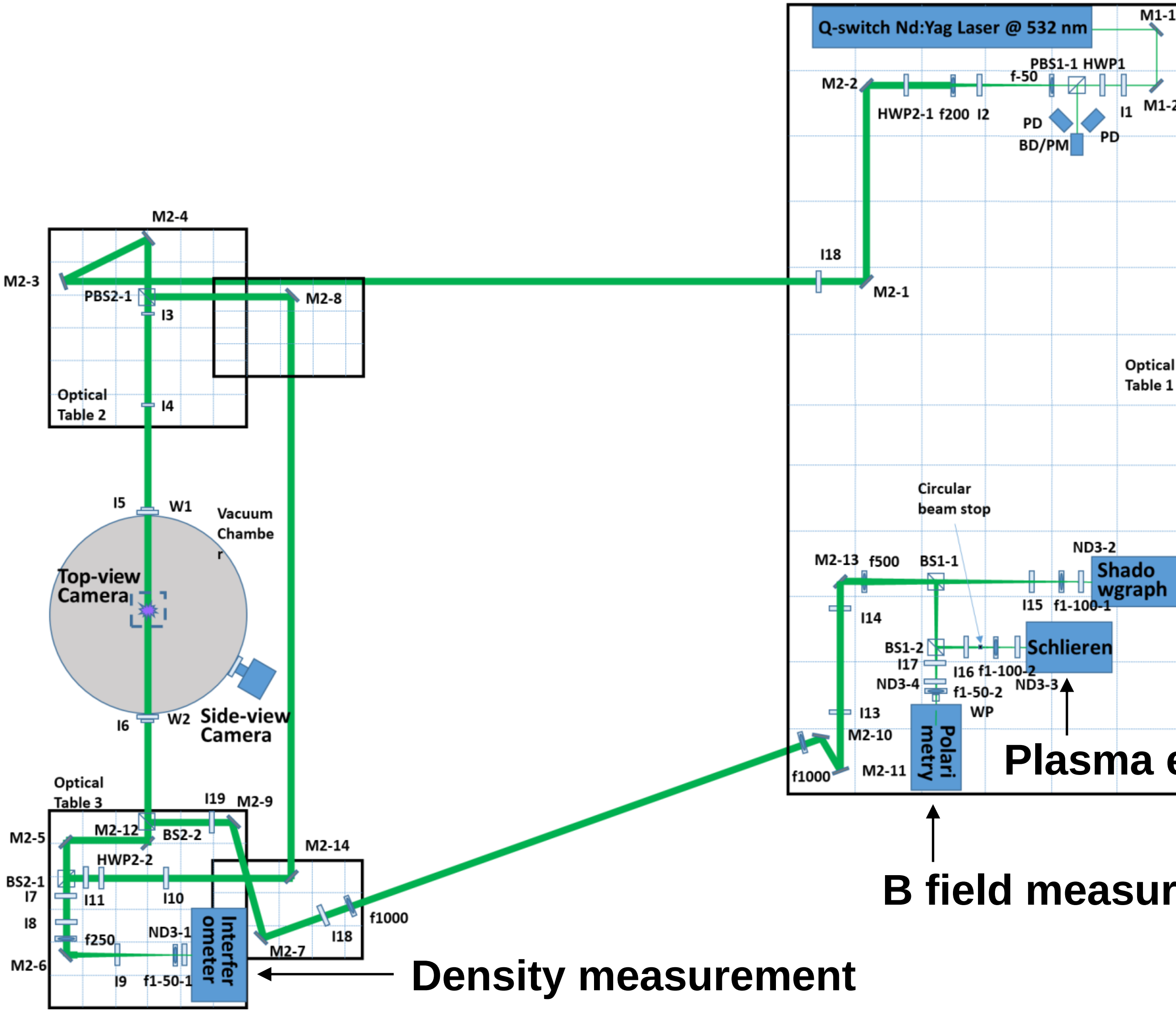

Plasma edge detection

B field measurement

Density measurement

A peak current of ~135 kA with a rise time of ~1.6 us is provided by the pulsed-power system

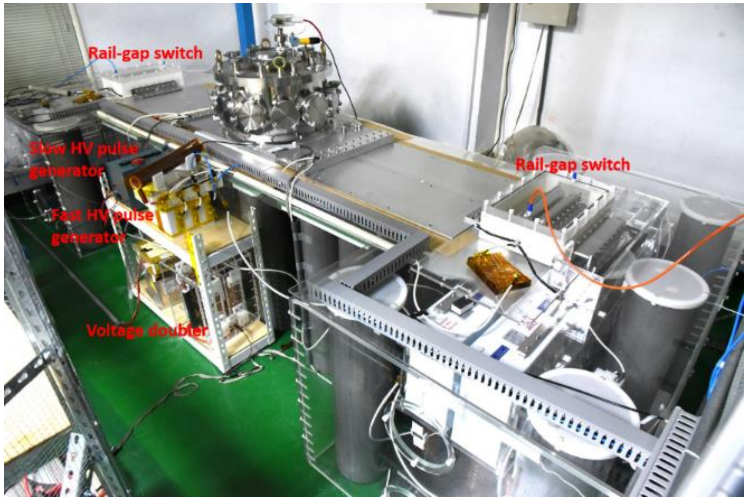

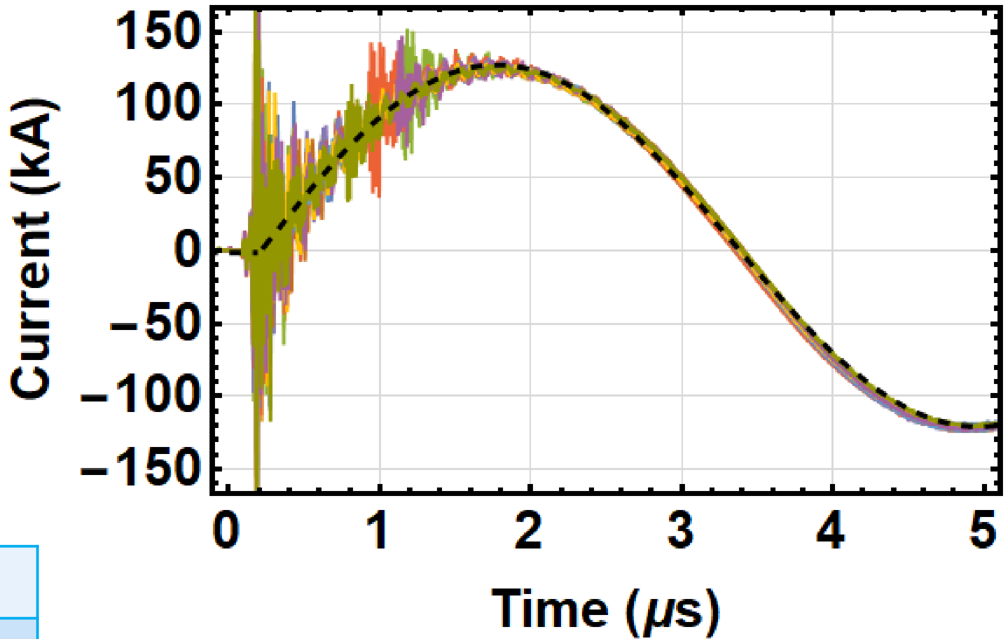

Capacitance (μF)	5
V_{charge} (kV)	20
Energy (kJ)	1
Inductance (nH)	204 ± 4
Rise time (quarter period, ns)	1592 ± 3
I_{peak} (kA)	135 ± 1

- EUV generation using discharged-produced plasma:
  - PP-PP-002 Chenghan Du
  - PP-PP-003 Jia-Kai Liu

A plasma jet can be generated by a conical-wire array due to the nonuniform z-pinch effect

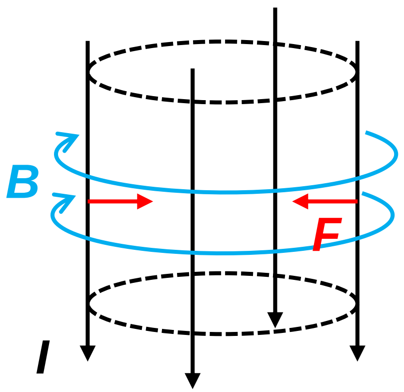

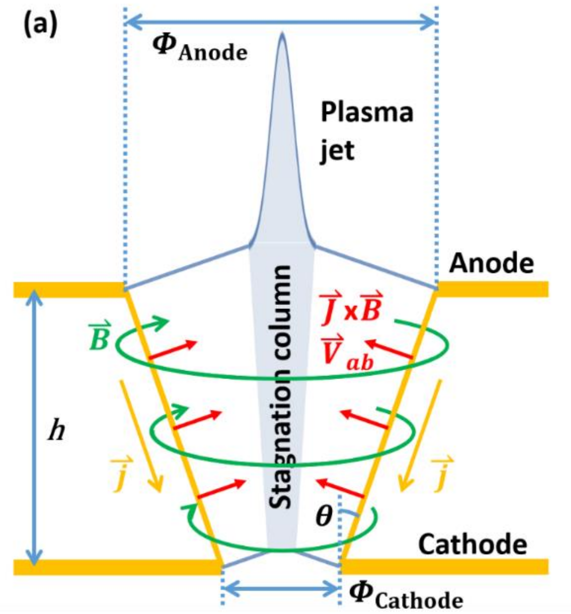

$$V_{\mathrm{j}} = V_{\mathrm{ab}} \frac{1 + \cos\theta}{\sin\theta}$$

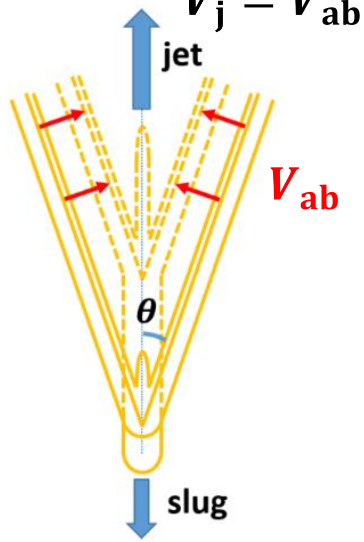

1. **Wire ablation : corona plasma is generated by wire ablations.**
2. **Precursor : corona plasma is pushed by the $\vec{J} \times \vec{B}$ force and accumulated on the axis forming a precursor.**
3. **Plasma jet is formed by the nonuniform z-pinch effect due to the radius difference between the top and the bottom of the array.**

D. J. Ampleforda, et al., Phys. Plasmas 14, 102704 (2007)
G. Birkhoff, et al., J. Applied Physics 19, 563 (1948)

Our conical-wire array consists of 4 tungsten wires with an inclination angle of 30° with respect to the axis

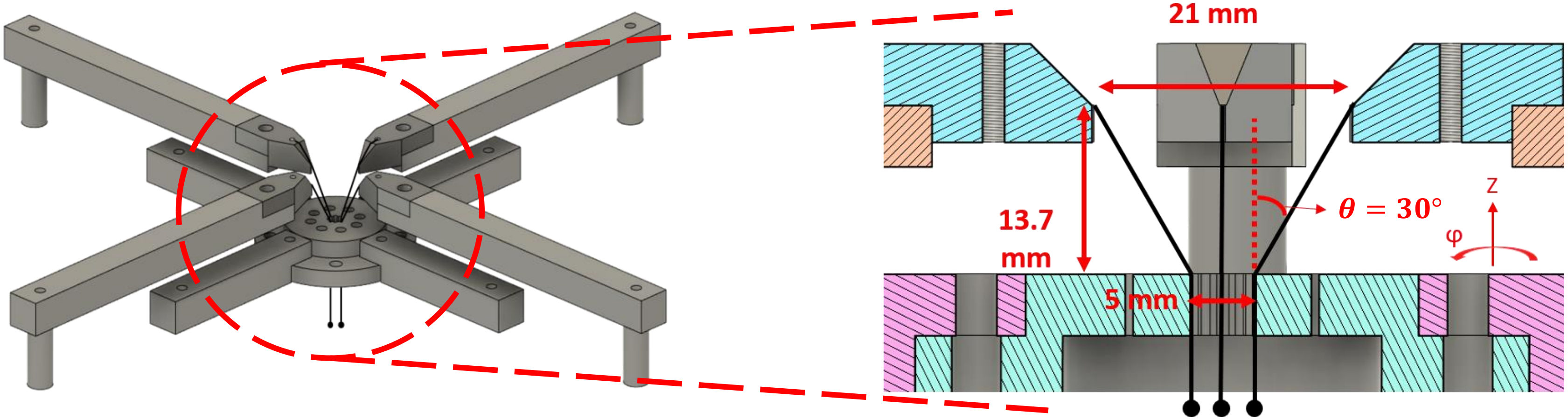

- **Conical-wire array**

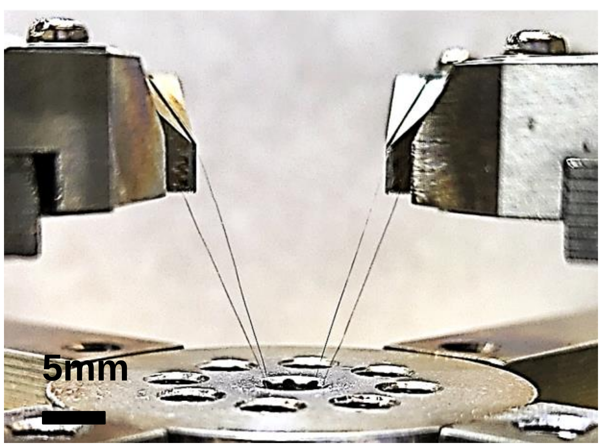

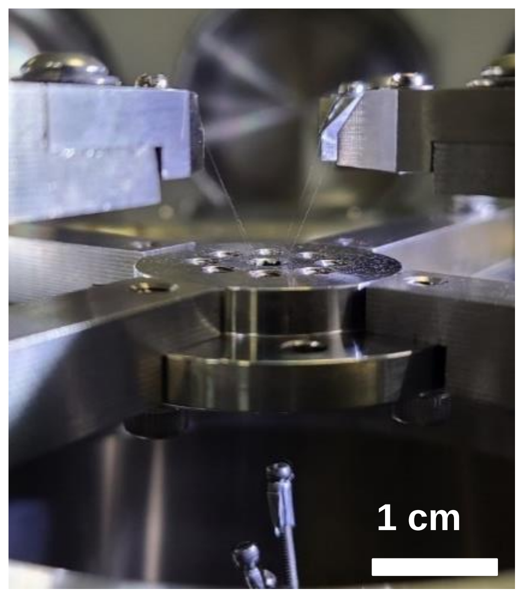

- **Material : Tungsten.**
- **Number of wires : 4.**
- **Diameter : 20 μm.**

Y.-C. Lin, NCKU Master Thesis 2021

Self-emission of the plasma jet in the UV to soft x-ray regions was captured by the pinhole camera

- Image in UV/soft x ray

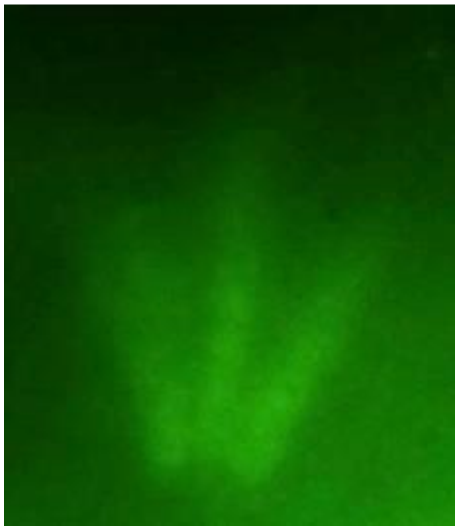

(Brightness is increased by 40 %.)

- Pinhole diameter: 0.5 mm, i.e., spatial resolution: 1 mm.

- Image in visible light

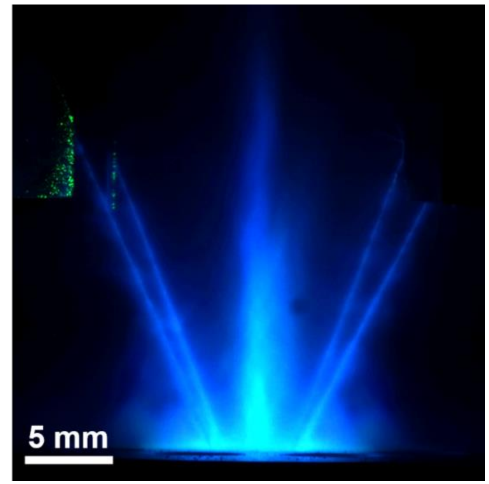

(Enhanced by scaling the intensity range linearly from 0 − 64 to 0 − 255.)

Y.-C. Lin, NCKU Master Thesis 2021

Plasma jet propagation was observed using laser diagnostics

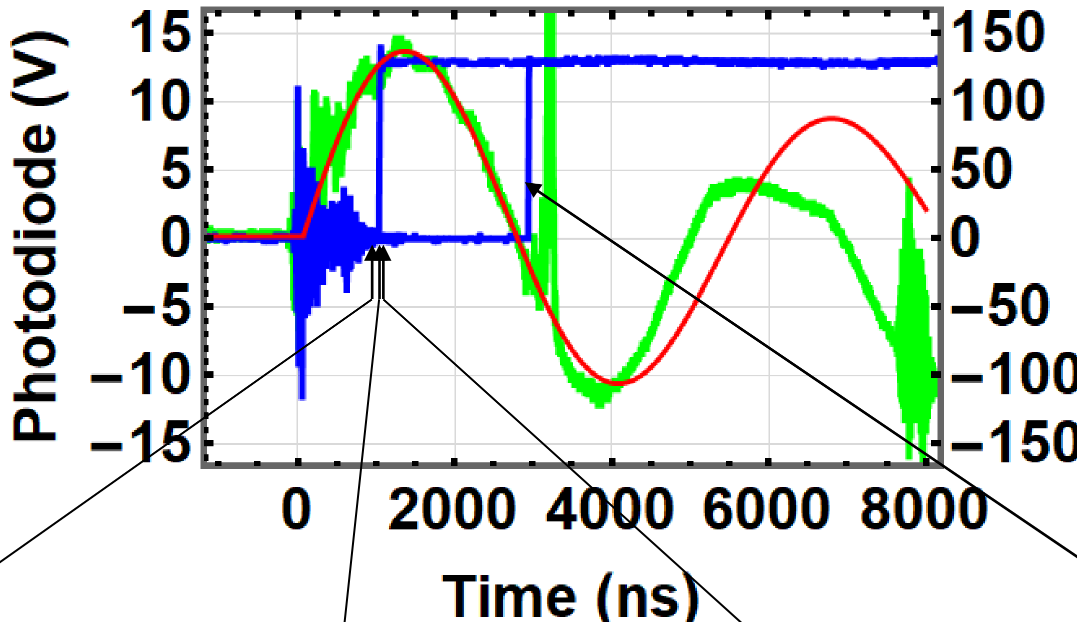

- **Shadowgraph images:**

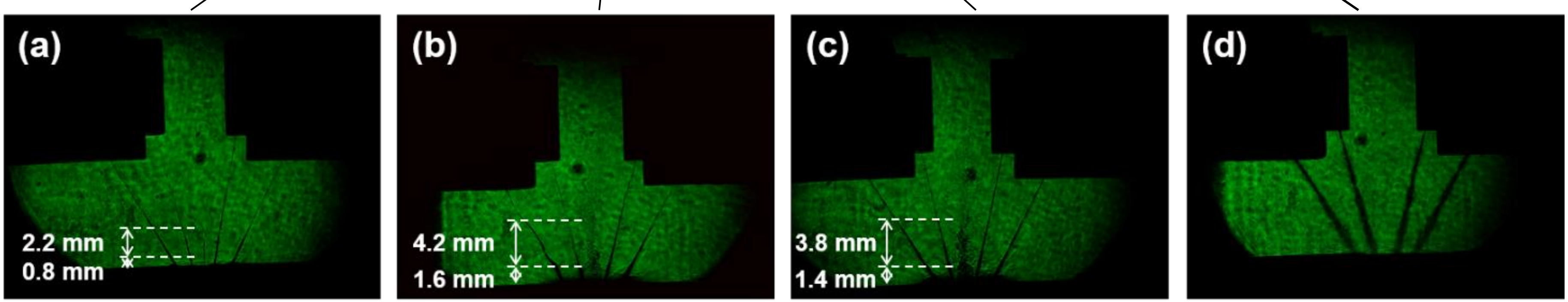

930 ± 20 ns | **975 ± 2 ns** | **985 ± 3 ns** | **2945 ± 2 ns**

Length of the plasma jet at different time was obtained by the Schlieren images at different times

- **Shadowgraph images:**

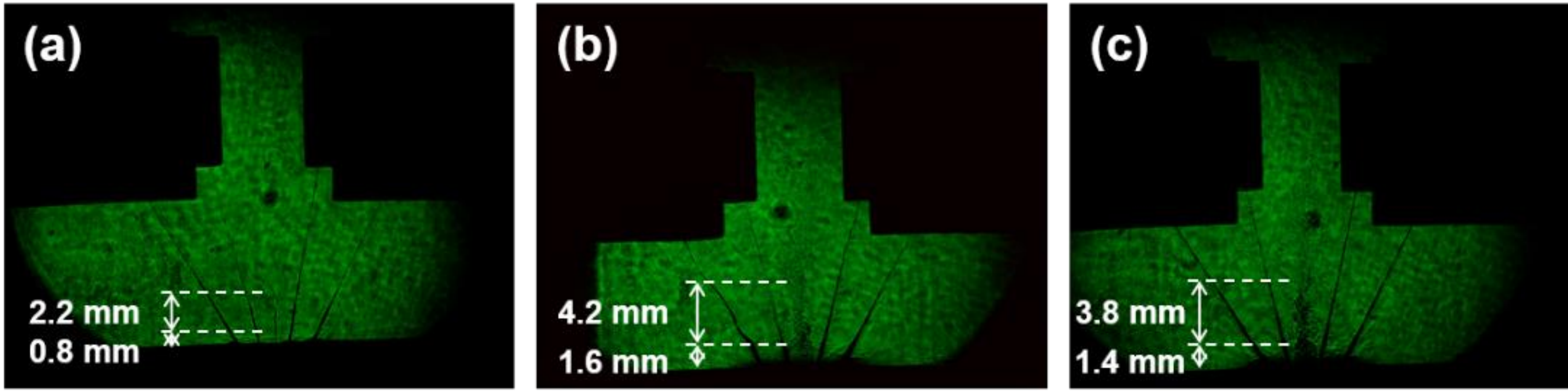

- **Schlieren images:**

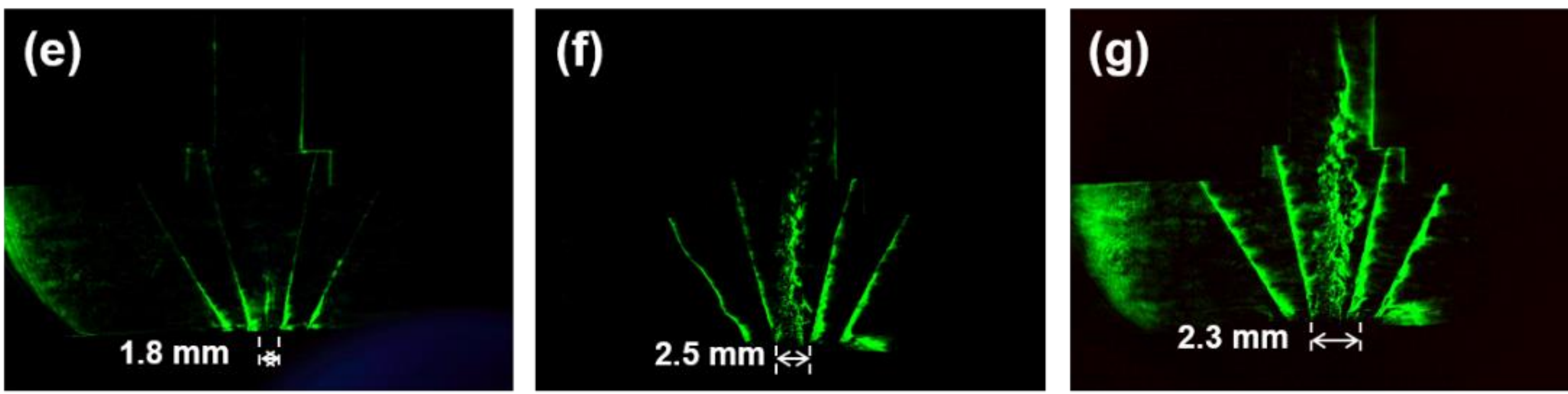

930 ± 20 ns 975 ± 2 ns 985 ± 3 ns

The measured plasma jet speed is 170 ± 70 km/s with the corresponding Mach number greater than 5

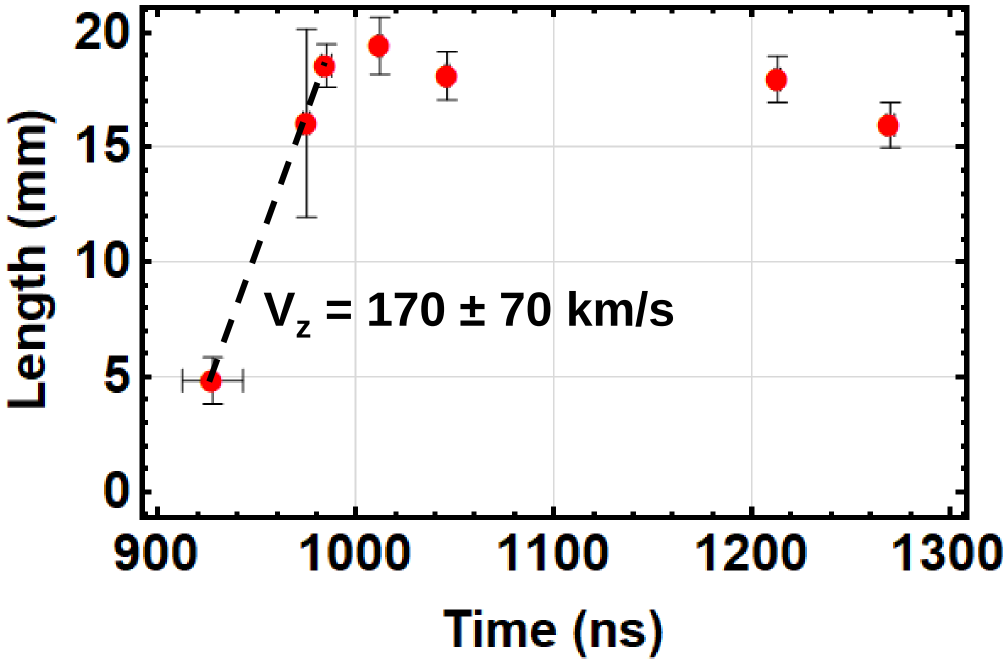

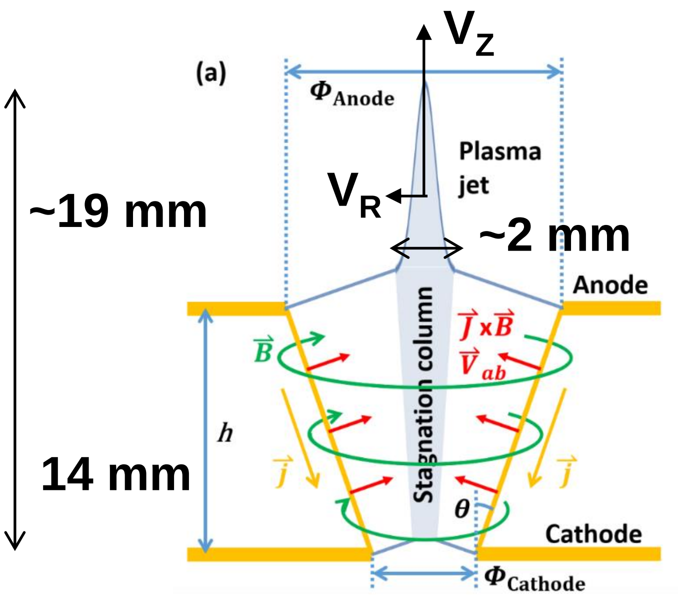

$$M = \frac{V_Z}{V_R} \geq \frac{Z}{r} \approx \frac{(19 - 14)\ \mathrm{mm}}{\frac{2\ \mathrm{mm}}{2}} = 5$$

$$V_{\mathrm{ab}} = V_{\mathrm{j}} \frac{\sin\theta}{1 + \cos\theta} = 50\ \pm 20\ \mathrm{km/s}$$

Plasma disk can be formed when two head-on plasma jets collide with each other

- **Astronomers Find a ‘Break’ in One of the Milky Way’s Spiral Arms.**

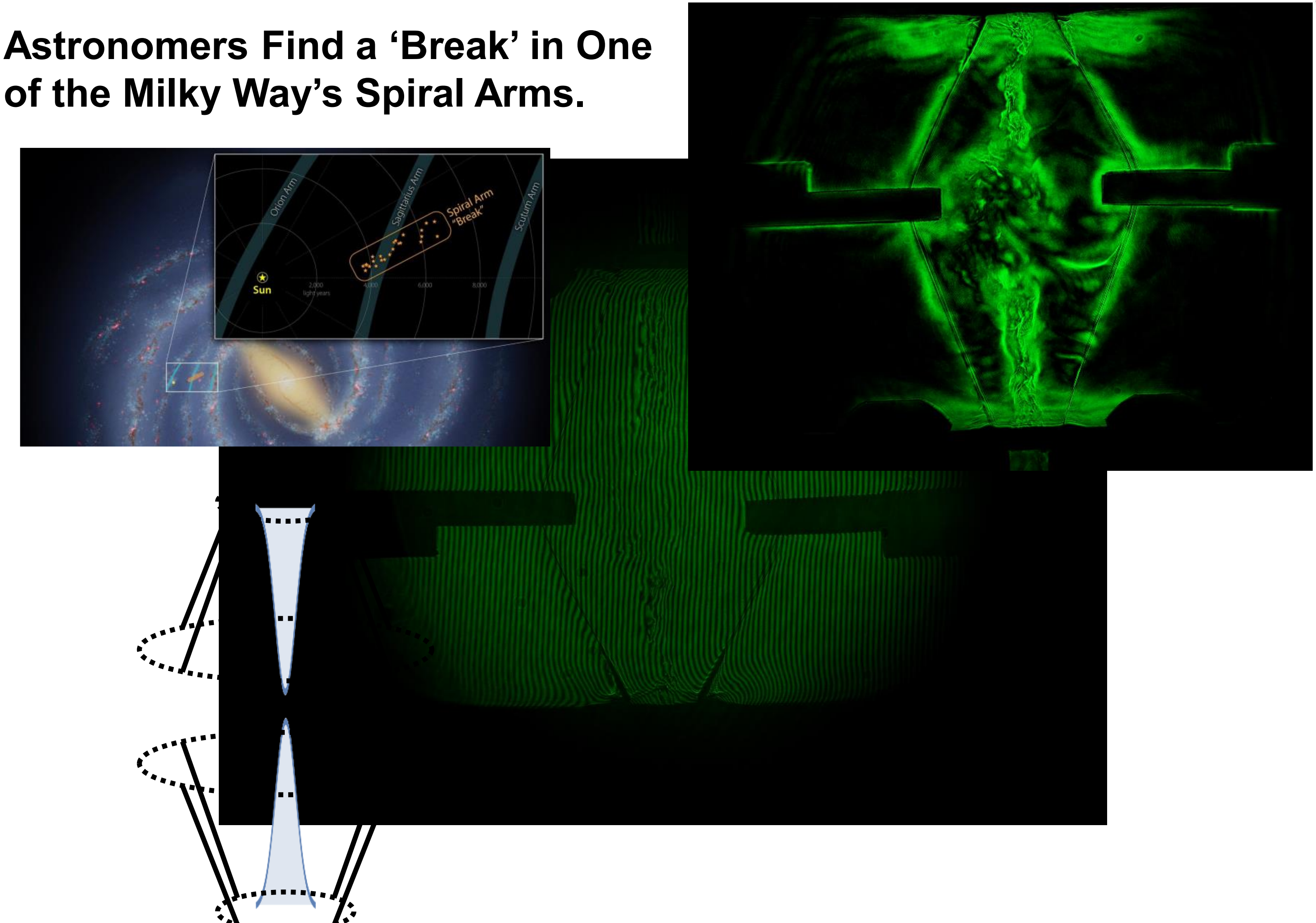

Energetic charged particles losses most of its energy right before it stops

Momentum transfer:

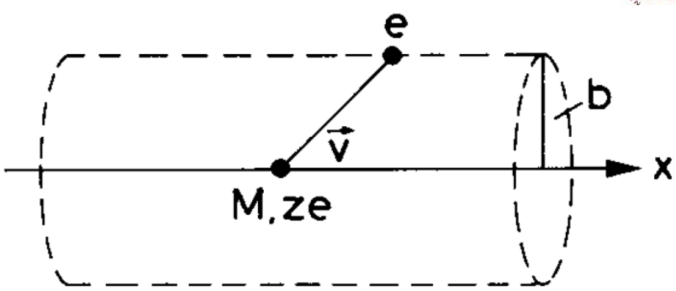

$$\Delta p_\perp = \int F_\perp dt = \int F_\perp \frac{dt}{dx} dx = \int F_\perp \frac{dx}{v}$$

$$= \int_{-\infty}^{\infty} \frac{ze^2}{(x^2+b^2)} \cdot \frac{b}{\sqrt{x^2+b^2}} \cdot \frac{1}{v}\, dx = \frac{ze^2 b}{v} \left[\frac{x}{b^2\sqrt{x^2+b^2}} \right]_{-\infty}^{\infty} = \frac{2ze^2}{bv}$$

$\Delta p_{||}$: averages to zero

$$\Delta E(b) = \frac{\Delta p^2}{2m_e} \qquad N_e = n \cdot (2\pi b) \cdot db\, dx$$

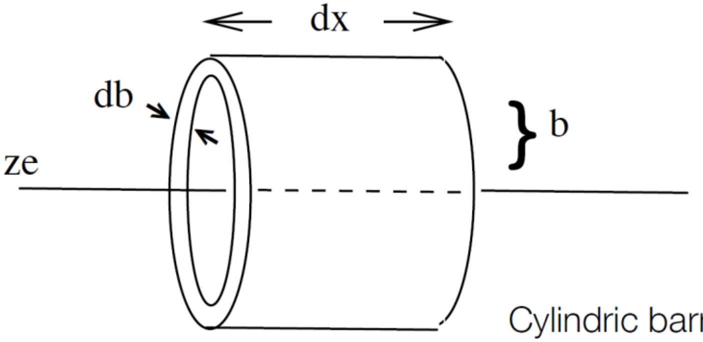

Cylindric barrel with N_e electrons

$$-dE(b) = \frac{\Delta p^2}{2m_e} \cdot 2\pi n b\, db\, dx$$

$$-\frac{dE}{dx} = \frac{4\pi\, n\, z^2 e^4}{m_e v^2} \cdot \int_{b_{\min}}^{b_{\max}} \frac{db}{b} = \frac{4\pi\, n\, z^2 e^4}{m_e v^2} \ln \frac{b_{\max}}{b_{\min}}$$

http://www.kip.uni-heidelberg.de/~coulon/Lectures/DetectorsSoSe10/

Proton therapy takes the advantage of using Bragg peak

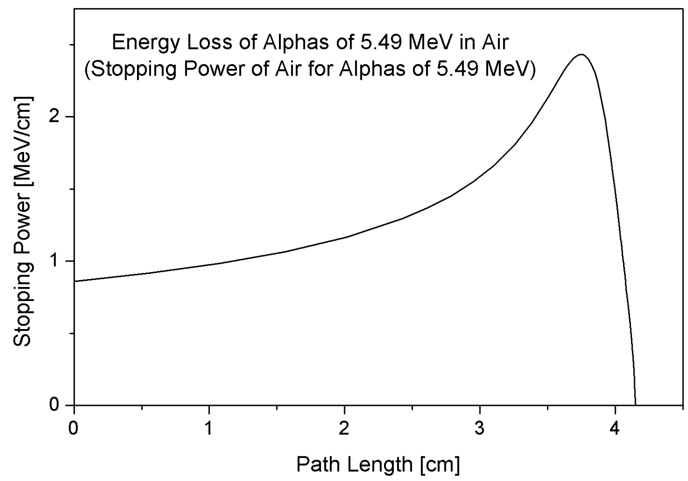

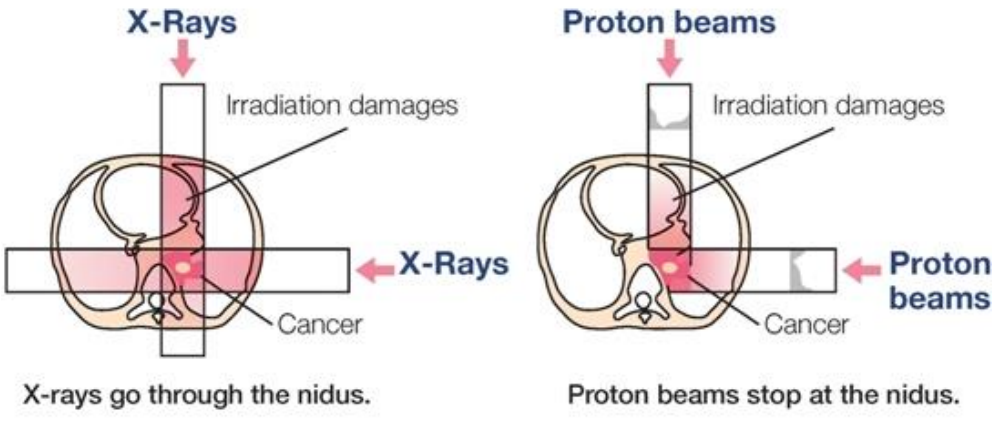

http://www.shi.co.jp/quantum/eng/product/proton/proton.html

There are two suggested website for getting the information of proton stopping power in different materials

http://www.nist.gov/pml/data/star/

http://www.srim.org/

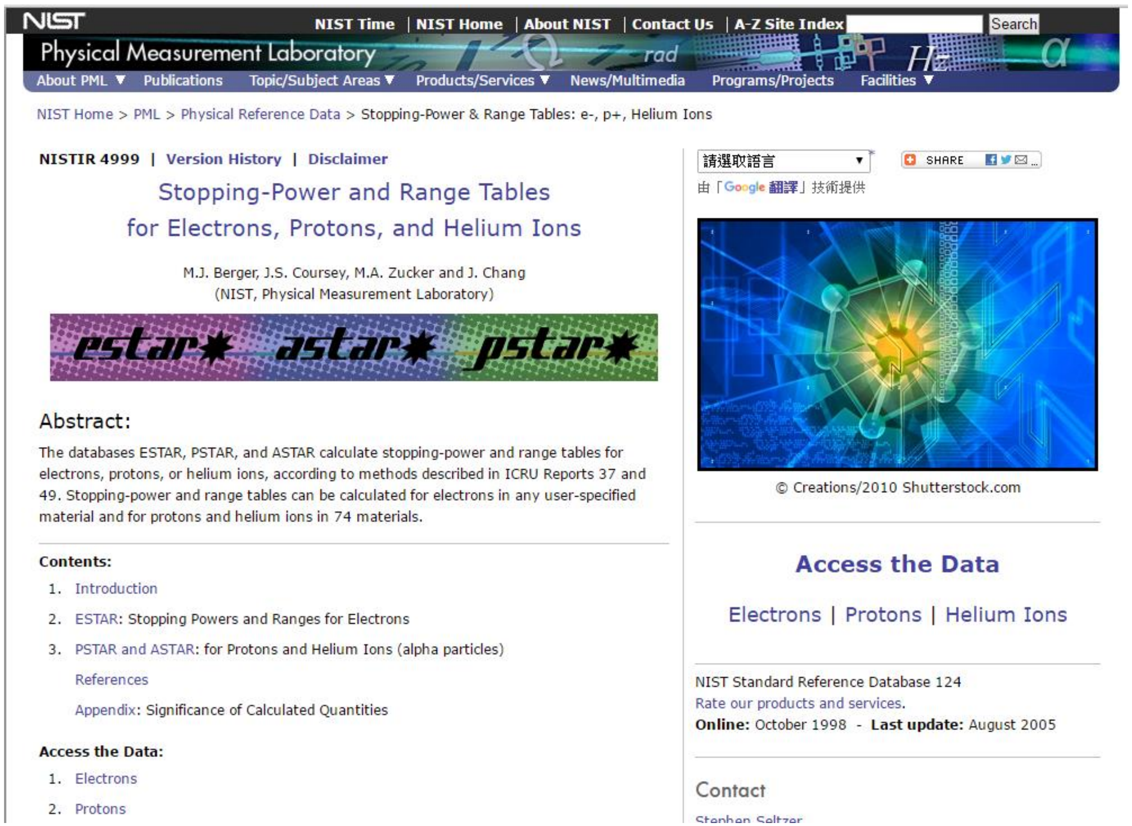

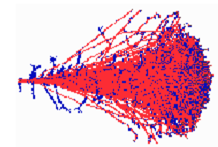

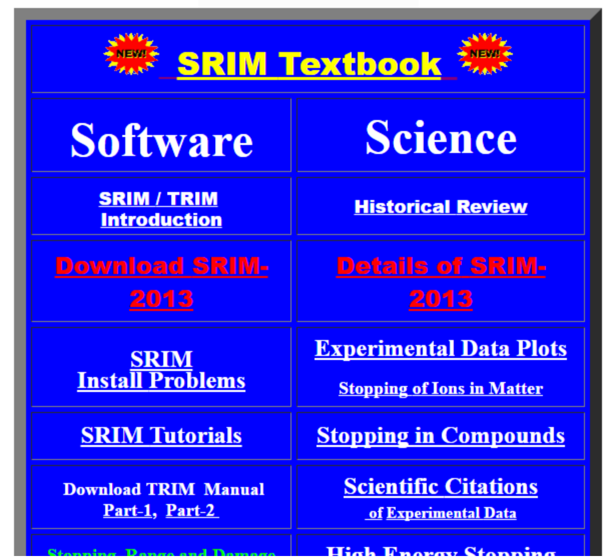

The thickness of a filter can be decided from the range data from NIST website

COPPER

To download data in spreadsheet (array) form, choose a delimiter and use the checkboxes in the table heading. After downloading, save the output by using your browser's `Save As` feature.

Delimiter:
- space
- | (vertical bar)
- tab (some browsers may use spaces instead)
- newline

Download data | Reset

$$\frac{dE}{\rho dx} \qquad \rho x$$

(required) Kinetic Energy (MeV)	Stopping Power (MeV cm^2/g)			Range		
	Electronic	Nuclear	Total	CSDA (g/cm^2)	Projected (g/cm^2)	Detour Factor Projected / CSDA
1.000E-03	3.490E+01	4.408E+00	3.931E+01	4.116E-05	5.620E-06	0.1365
1.500E-03	4.274E+01	4.231E+00	4.697E+01	5.267E-05	8.301E-06	0.1576
2.000E-03	4.935E+01	4.049E+00	5.340E+01	6.263E-05	1.101E-05	0.1759
2.500E-03	5.518E+01	3.876E+00	5.906E+01	7.152E-05	1.374E-05	0.1921
3.000E-03	6.045E+01	3.718E+00	6.416E+01	7.964E-05	1.647E-05	0.2068
4.000E-03	6.980E+01	3.440E+00	7.324E+01	9.419E-05	2.194E-05	0.2329
5.000E-03	7.804E+01	3.207E+00	8.124E+01	1.071E-04	2.739E-05	0.2556
6.000E-03	8.548E+01	3.010E+00	8.849E+01	1.189E-04	3.280E-05	0.2758
7.000E-03	9.233E+01	2.840E+00	9.517E+01	1.298E-04	3.817E-05	0.2940
8.000E-03	9.871E+01	2.692E+00	1.014E+02	1.400E-04	4.347E-05	0.3106
9.000E-03	1.047E+02	2.561E+00	1.073E+02	1.496E-04	4.872E-05	0.3258
1.000E-02	1.104E+02	2.445E+00	1.128E+02	1.587E-04	5.391E-05	0.3398

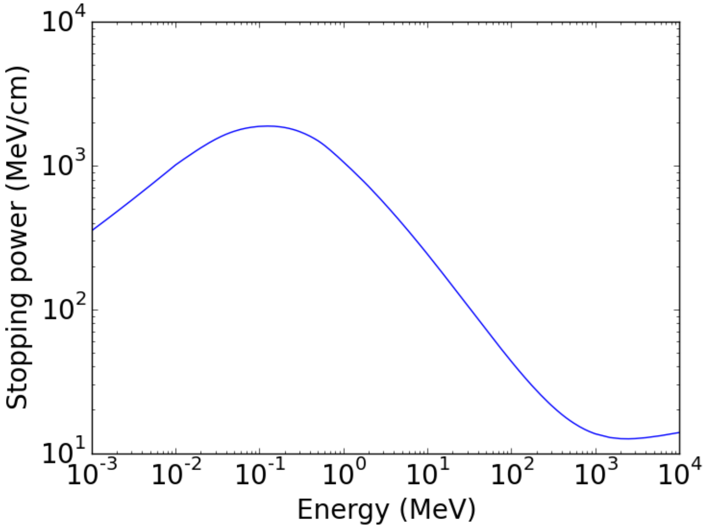

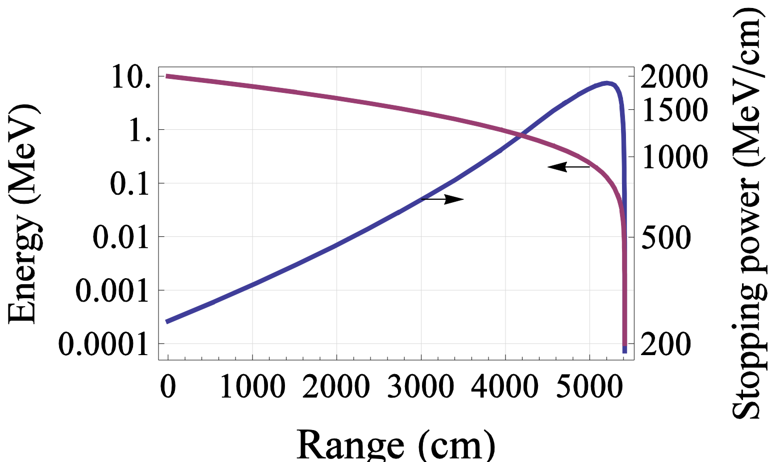

$$\frac{dE}{dx} = f(E) \Rightarrow x = \int_{E_i}^{E_f} \frac{dE}{f(E)}$$

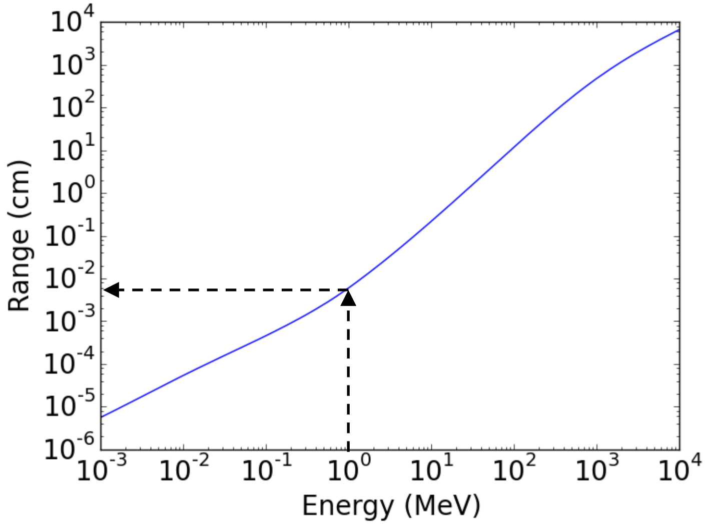

Proton therapy takes the advantage of using Bragg peak

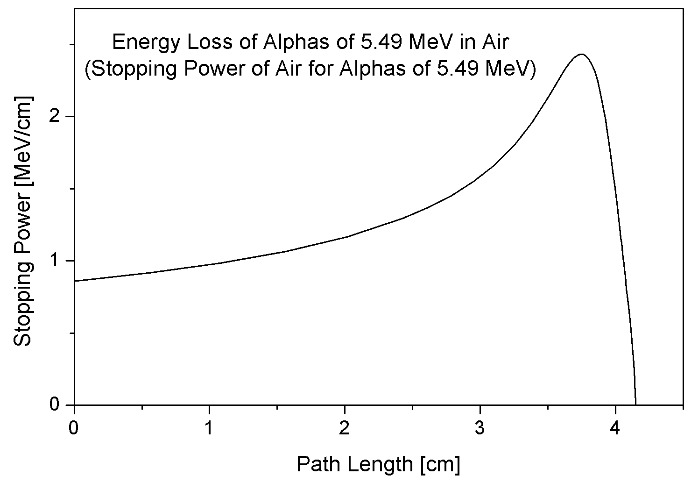

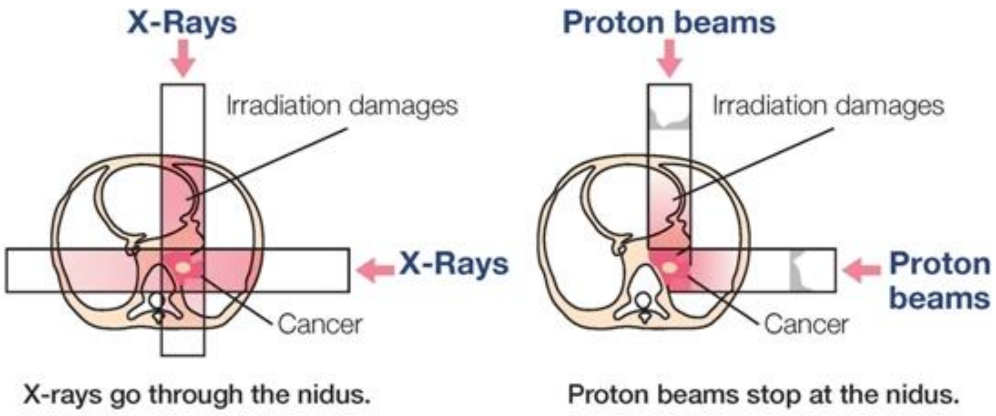

http://www.shi.co.jp/quantum/eng/product/proton/proton.html

Saha equation gives the relative proportions of atoms of a certain species that are in two different states of ionization in thermal equilibrium

$$\frac{n_{r+1} n_e}{n_r} = \frac{G_{r+1} g_e}{G_r} \frac{(2\pi m_e K T)^{3/2}}{h^3} \exp\left(-\frac{\chi_r}{KT}\right)$$

- **n_{r+1}, n_r: Density of atoms in ionization state r+1, r (m^{-3})**
- **n_e: Density of electrons (m^{-3})**
- **G_{r+1}, G_r: Partition function of ionization state r+1, r**
- **g_e=2: Statistical weight of the electron**
- **m_e: Mass of the electron**
- **χ_r: Ionization potential of ground level of state r to reach to the ground level of state r+1**
- **T: Temperature**
- **h: Planck's constant**
- **K: Boltzmann constant**

Supplement to Ch. 6 of Astrophysics Processes by Hale Bradt
(http://homepages.spa.umn.edu/~kd/Ast4001-2015/NOTES/n052-saha-bradt.pdf)

Some backgrounds of quantum mechanics

- **Planck blackbody function:**

$$u(\nu,T)=\frac{8\pi h\nu^3}{c^3}\frac{1}{e^{h\nu/KT}-1}\left(W/m^3\,\mathrm{Hz}\right)$$

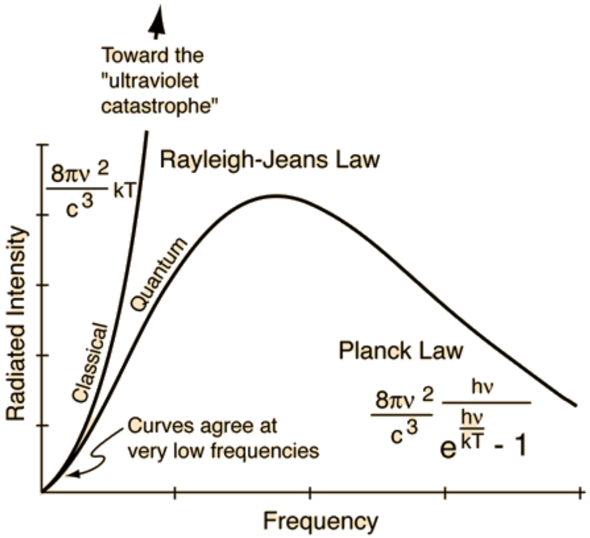

- **Boltzmann formula:**
  - **g_i, g_j: statistical weight**

$$\frac{n_i}{n_j}=\frac{g_i e^{-\epsilon_i/KT}}{g_j e^{-\epsilon_j/KT}}=\frac{g_i}{g_j}e^{-h\nu_{ij}/KT}\qquad \frac{g_i}{g_j}=\frac{2J_i+1}{2J_j+1}$$

(J: angular momenta quantum number)

  - **Number in the i^th state to the total atom:**

$$\frac{n_i}{n}=\frac{n_i}{\Sigma n_j}\equiv\frac{g_i e^{-\epsilon_i/KT}}{G}\qquad G\equiv\Sigma g_j e^{-\epsilon_j/KT}$$

G: partition function of statistical weight for the atom, taking into account all its excited states.

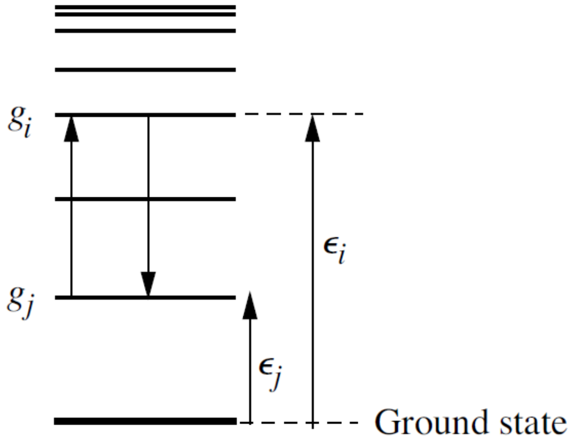

http://hyperphysics.phy-astr.gsu.edu/hbase/mod6.html

Einstein coefficient

- **Probability of electron energy transition:**
  - **Excitation (↑):** $P_{\text{ji}} = B_{\text{ji}} u(\nu, T)$
  - **De-excitation (↓):** $P_{\text{ij}} = A_{\text{ij}} + B_{\text{ij}} u(\nu, T)$
- **In thermal equilibrium:**

$$n_i\left(A_{\text{ij}} + B_{\text{ij}} u\right) = n_j B_{\text{ji}} u$$

$$\frac{g_i}{g_j} e^{-x}\left(A_{\text{ij}} + B_{\text{ij}} u\right) = B_{\text{ji}} u \qquad x \equiv \frac{\text{h}\nu}{\text{KT}}$$

$$u = a(e^x - 1)^{-1} \qquad a \equiv \frac{8\pi \text{h}\nu^3}{c^3}$$

$$a\left(e^x B_{\text{ji}} - \frac{g_i}{g_j} B_{\text{ij}}\right) = (e^x - 1)\frac{g_i}{g_j} A_{\text{ij}}$$

- **The Einstein coefficients are independent of T or v.**

$$x \to 0, e^x \to 1 \qquad x \to \infty, e^x \to \infty$$

$$\frac{B_{\text{ij}}}{B_{\text{ji}}} = \frac{g_j}{g_i} \qquad aB_{\text{ji}} = \frac{g_i}{g_j} A_{\text{ij}} \quad \frac{A_{\text{ij}}}{B_{\text{ij}}} = \frac{8\pi h\nu^3}{c^3}$$

- **Photoexcitation:**

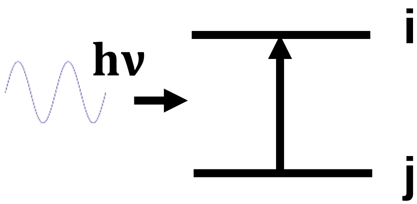

- **Induced radiation:**

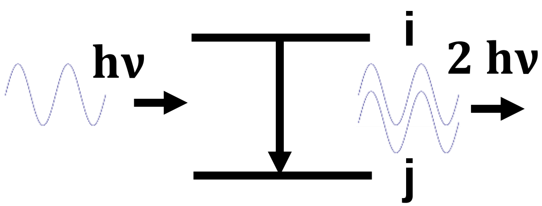

- **Spontaneous radiation:**

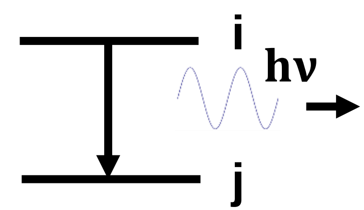

Saha equation is derived using the transition between different ionization states

- **Required photon energy for transition (1) from the ground state of r ionization state to the ground state of r+1 ionization state:**

$$\mathbf{h\nu = \chi_r + \frac{p^2}{2m}}$$

Energy of the free electron

- **Required photon energy for transition (1) from the energy level k of r ionization state to the energy level j of r+1 ionization state:**

$$\mathbf{h\nu = \chi_r + \epsilon_{r+1,j} - \epsilon_{r,k} + \frac{p^2}{2m}}$$

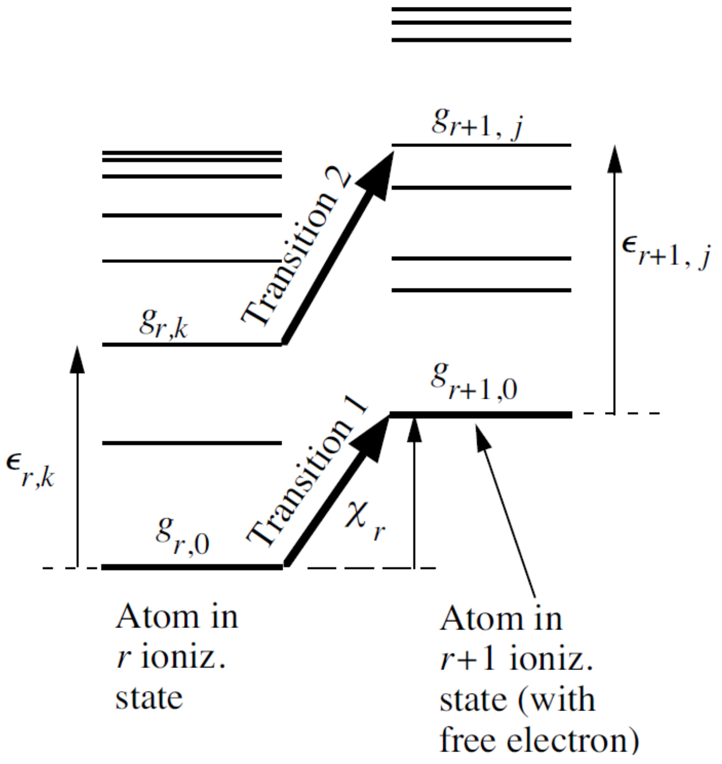

Saha equation is derived using the transition between different ionization states

- **Photoionization:**

$$R_{\mathrm{pi}} = n_{r,k} u(\nu) B_{r,k\to r+1,j}$$

- **Induced radiation:**

$$R_{\mathrm{ir}} = n_{r+1,j} n_{e,p}(p) u(\nu) B_{r+1,j\to r,k}$$

- **Spontaneous emission:**

$$R_{\mathrm{sr}} = n_{r+1,j} n_{e,p}(p) A_{r+1,j\to r,k}$$

- **In thermal equilibrium:**

$$n_{r+1,j} n_{e,p} A_{r+1,j\to r,k} + n_{r+1,j} n_{e,p} u B_{r+1,j\to r,k} = n_{r,k} u B_{r,k\to r+1,j}$$

- **Einstein coefficients:**

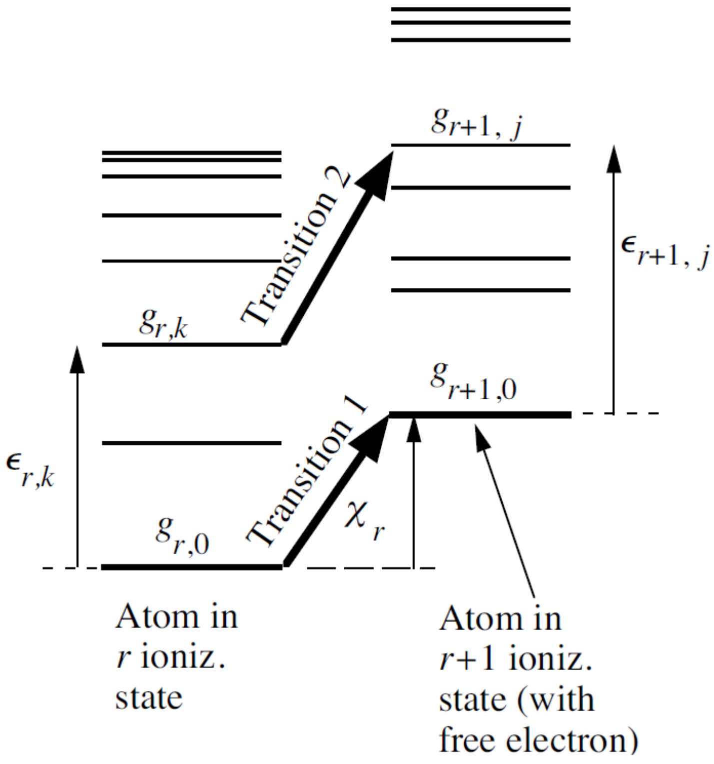

$$\frac{B_{r,k\to r+1,j}}{B_{r+1,j\to r,k}} = \frac{g_{r+1,j}}{g_{r,k}} \frac{g_e 4\pi p^2}{h^3}$$

$$\frac{A_{r+1,j\to r,k}}{B_{r+1,j\to r,k}} = \frac{8\pi h \nu^3}{c^3}$$

Saha equation - continued

$$n_{r+1,j}n_{e,p}A_{r+1,j\to r,k} + n_{r+1,j}n_{e,p}uB_{r+1,j\to r,k} = n_{r,k}uB_{r,k\to r+1,j}$$

$$n_{r+1,j}n_{e,p}\frac{A_{r+1,j\to r,k}}{B_{r+1,j\to r,k}} + n_{r+1,j}n_{e,p}u = n_{r,k}u\frac{B_{r,k\to r+1,j}}{B_{r+1,j\to r,k}}$$

$$\frac{n_{r+1,j}n_{e,p}}{n_{r,k}} = \left(\frac{A_{r+1,j\to r,k}}{uB_{r+1,j\to r,k}} + 1\right)^{-1}\frac{B_{r,k\to r+1,j}}{B_{r+1,j\to r,k}}$$

$$\frac{B_{r,k\to r+1,j}}{B_{r+1,j\to r,k}} = \frac{g_{r+1,j}}{g_{r,k}}\frac{g_e 4\pi p^2}{h^3}$$

$$n_{e,p}(p) = \frac{n_e 4\pi p^2}{(2\pi \mathrm{mKT})^{3/2}}\exp\left(-\frac{p^2}{2\mathrm{mKT}}\right)$$

$$\frac{A_{r+1,j\to r,k}}{B_{r+1,j\to r,k}} = \frac{8\pi h\nu^3}{c^3}$$

$$\frac{n_{r+1,j}n_e}{n_{r,k}} = \frac{(2\pi \mathrm{mKT})^{3/2}}{4\pi p^2}\exp\left(\frac{p^2}{2\mathrm{mKT}}\right)\left[\frac{c^3}{8\pi h\nu^3}\left(e^{\mathrm{h\nu/KT}} - 1\right)\frac{8\pi h\nu^3}{c^3} + 1\right]^{-1}\frac{g_{r+1,j}}{g_{r,k}}\frac{g_e 4\pi p^2}{h^3}$$

$$\frac{n_{r+1,j}n_e}{n_{r,k}} = \frac{(2\pi \mathrm{mKT})^{3/2}}{h^3}\frac{g_{r+1,j}g_e}{g_{r,k}}\exp\left[\frac{1}{\mathrm{KT}}\left(\frac{p^2}{2m} - \mathrm{h\nu}\right)\right]$$

Saha equation - continued

$$\frac{n_{r+1,j}n_e}{n_{r,k}} = \frac{(2\pi \mathrm{mKT})^{3/2}}{h^3}\frac{g_{r+1,j}g_e}{g_{r,k}}\exp\left[\frac{1}{\mathrm{KT}}\left(\frac{p^2}{2m} - \mathrm{h\nu}\right)\right]$$

$$\frac{n_{r+1,j}n_e}{n_{r,k}} = \frac{(2\pi \mathrm{mKT})^{3/2}}{h^3}\frac{g_{r+1,j}g_e}{g_{r,k}}\exp\left[\frac{1}{\mathrm{KT}}\left(\frac{p^2}{2m} - \chi_r - \epsilon_{r+1,j} + \epsilon_{r,k} - \frac{p^2}{2m}\right)\right]$$

$$\frac{n_{r+1,j}n_e}{n_{r,k}} = \frac{(2\pi \mathrm{mKT})^{3/2}}{h^3}\frac{g_{r+1,j}\exp\left(\frac{\epsilon_{r+1,j}}{\mathrm{KT}}\right)g_e}{g_{r,k}\exp\left(\frac{\epsilon_{r,k}}{\mathrm{KT}}\right)}\exp\left(-\frac{\chi_r}{\mathrm{KT}}\right)$$

$$\frac{n_{r,k}}{n_r} = \frac{g_{r,k}e^{-\epsilon_{r,k}/\mathrm{KT}}}{G_r} \qquad G_r = \Sigma g_{r,k}e^{-\epsilon_{r,k}/\mathrm{KT}}$$

$$\frac{n_{r+1,j}}{n_{r+1}} = \frac{g_{r+1,j}e^{-\epsilon_{r+1,j}/\mathrm{KT}}}{G_{r+1}} \qquad G_{r+1} = \Sigma g_{r+1,j}e^{-\epsilon_{r+1,j}/\mathrm{KT}}$$

$$\boxed{\frac{n_{r+1}n_e}{n_r} = \frac{G_{r+1}g_e}{G_r}\frac{(2\pi m_e KT)^{3/2}}{h^3}\exp\left(-\frac{\chi_r}{KT}\right)}$$

Saha equation – example: hydrogen plasma of the sun

- Photosphere of the sun – hydrogen atoms in an optically thick gas in thermal equilibrium at temperature T=6400 K.
  - Neutral hydrogen (r state / ground state)

$$G_r = \Sigma g_{r,k} = g_{r,0} + g_{r,1}\exp\left(-\frac{\epsilon_{r,1}}{KT}\right) + \cdots = 2 + 8\exp\left(-\frac{10.2\text{eV}}{0.56\text{eV}}\right) + \cdots$$
$$= 2 + 9.8 \times 10^{-8} + \cdots \approx 2$$

  - Ionized state (r+1 state)

$$G_{r+1} = \Sigma g_{r+1,j} = g_{r+1,0} + g_{r+1,1}\exp\left(-\frac{\epsilon_{r+1,1}}{KT}\right) + \cdots \approx 1$$

  - Other information: $g_e = 2$ $\chi_r = 13.6\text{eV}; KT = 0.56\text{eV}$ $n_{r+1} = n_e$

$$\frac{{n_{r+1}}^2}{n_r} = 2.41 \times 10^{21}\,\frac{1 \times 2}{2}(6400)^{3/2}\exp\left(-\frac{13.6}{0.56}\right) = 3.5 \times 10^{16} m^{-3}$$

It is mostly neutral in the photosphere of the sun

- Assuming 50 % ionization:

$$n_{r+1} = n_r = 3.5 \times 10^{16} m^{-3} \qquad n = n_{r+1} + n_r = 7 \times 10^{16} m^{-3}$$

- At lower densities n at the same temperature, there should be fewer collisions leading to recombination and thus the plasma to be more than 50 % ionization.

- In the photosphere of the sun:

$$\rho \sim 3 \times 10^{-4}\,\mathrm{kg}/m^3 \to n = 2 \times 10^{23} m^{-3} \gg 7 \times 10^{16} m^{-3}$$

$\Rightarrow$ Less than 50 % ionization

- Use the total number density to estimate the ionization percentage:

$$n_{r+1} + n_r = 2 \times 10^{23}$$

$$\frac{n_{r+1}}{n_r} = 4 \times 10^{-4} @ 6400K$$